In vitro induction of cell death pathways by *Artemisia afra* extract and isolation of an active compound, isoalantolactone.

Luanne Venables

Submitted in fulfilment of the requirements for the degree of *Philosophiae Doctor* in the Faculty of Science at the Nelson Mandela Metropolitan University.

December 2013

Promoter: Prof M. van de Venter (Nelson Mandela Metropolitan University)

Co-promoter: Dr E.D. Goosen (Rhodes University)

DECLARATION

I, Luanne Venables (student number: 204004039), hereby declare that the thesis for *Philosophiae Doctor (PhD)* is my own work and that it has not previously been submitted for assessment or completion of any postgraduate qualification to another University or for another qualification.

Luanne Venables.

In accordance with Rule G4.6.3,

4.6.3 A treatise/dissertation/thesis must be accompanied by a written declaration on the part of the candidate to the effect that it is his/her own work and that it has not previously been submitted for assessment to another University or for another qualification. However, material from publications by the candidate may be embodied in a treatise/dissertation/thesis.

ACKNOWLEDGEMENTS:

I would like to thank the following people:

To my parents, John and Val Spies, it has been 10 years of studying and I cannot remember one day where you did not show interest and pride. Without your support, my dream of completing this PhD would not have been possible. Although it has been tough, knowing that you are always there for me means the world to me. Through your love, kindness, guidance and strength you have shown me the type of person I hope I am; loving, kind and strong.

To my husband, Dal, your patience with me deserves an award. You have had to bear the brunt of experiments not working, late nights in the lab, trips all over the place and my computer giving me problems. Your work ethic and ability to meet deadlines with a smile on your face has been so encouraging to me. Your patience, encouragement and quiet strength has enabled me to get through some of the toughest times.

To my incredible sister, Tamsyn, although you are far away, knowing that you are always there to listen to me, there when I need a laugh or a cry means so much to me. Although you have your own pressures and studies to deal with, you always remembered to give me a call and remind me that I can do this. You deserve all the happiness in this world.

To my friends, you have filled my life with laughter and love and without all of you I would have gone insane. Thanks for the shoulders that I could lean on and the ears that listened.

To all my family, thank you for all your love and support.

To my promoter, Prof Maryna van de Venter (a.k.a. Tannie), my PhD has been one of the best times of my life because you made it possible for me to grow as an independent and confident researcher. Your encouragement, open door policy and numerous cups of tea has made it all that much easier. Thank you for enabling me to join you at International conferences where I have not only been motivated, but also seen parts of the world that I never thought I would. You are not only my PhD promoter, but my mentor and friend.

To Dr Leonie Goosen, you have taught me so much about chemistry that I thought I would never know. Thank you for all that you have done for me in the lab, organising NMR, IR and CD experiments. It made my life easier. Your patience teaching me all about sesquiterpene lactones and different analytical techniques will always be remembered with fondness.

To Dr Trevor Koekemoer, what would I have done without you in Pigeon Valley and in the lab, always there to lend a helping hand and to give great advice. I really appreciate it.

To the lab rats, my lab friends, you have made coming in everyday so enjoyable, entertaining me with stories and events. We have had some very good times.

To Mrs Louise Hamilton of InnoVenton for GC/EI-MS analysis of my compound.

To Mrs Susan Cooper and Prof Dirk Lang of UCT for assisting me at late notice with confocal microscopy. It was a pleasure working at your facility.

To the Central Analytical Facility at the University of Stellenbosch for CD spectroscopy.

To the NMMU and NRF, for personal financial support.

To the NRF and ALC, for funding of the project.

Finally, I thank God everyday for the gift of my talents, knowledge and understanding and for the gift of love and life.

CONTENTS:

LIST OF FIGURES:

LIST OF TABLES:

ABSTRACT:

Artemisia afra is one of the oldest, most well known and widely used traditional medicinal plants in South Africa. It is used to treat many different medical conditions, particularly respiratory and inflammatory ailments. There is no reported evidence of its use for the treatment of cancer but due to its reported cytotoxicity, an investigation of the mode of cell death induced by an ethanol *A. afra* extract using two cancer cell lines was done. IC_{50} values of 18.21 and 31.88 µg/mL of ethanol extracts were determined against U937 and HeLa cancer cells, respectively. An IC_{50} value of the aqueous extract was greater than 250 µg/mL. The ethanol extract was not cytotoxic against confluent control cell lines, Chang Liver and Vero cells. The effect of the cytotoxic ethanol *A. afra* extract on U937 and HeLa cells and their progression through the cell cycle, apoptosis and mitochondrial membrane potential was investigated. After 12 hours of treatment with *A. afra* a delay in G2/M phase of the cell cycle was evident. Apoptosis was confirmed using the TUNEL assay for DNA fragmentation, as well as fluorescent staining with annexin V-FITC. Apoptosis was evident with the positive control and *A. afra* treatment at 24 and 48 hours. JC-1 staining showed a decrease in mitochondrial membrane potential at 24 hours. It was deduced that *A. afra* ethanol extract induces caspase-dependent apoptosis in a mitochondrial dependent manner.

Plants harbour many compounds that are not only useful to the plants but also to mankind. Many metabolites have been isolated from *A. afra* and their biological activity characterised. Due to observed apoptosis induction, isolation of cytotoxic compounds was done and a new sesquiterpene lactone from *A. afra* was isolated. Structural elucidation of the compound was done by IR, 1D and 2D NMR, CD and mass spectrometry and it was identified as isoalantolactone. HeLa cancer cells were treated with isoalantolactone and cytotoxicity was exhibited in a dose-dependent manner. A low IC_{50} value of 8.15 ± 1.16 µM was achieved. This study showed that isoalantolactone is partly responsible for the observed *A. afra* cytotoxicity.

Due to the evidence of G2/M arrest, the anti-mitotic potential and the possible onset of mitotic catastrophe by *A. afra* and isoalantolactone was investigated. It was evident from various flow cytometric analysis of cyclin B1 and phospho-H3 and confocal microscopy that *A. afra* does possess anti-mitotic activity by causing hyperpolymerisation of tubulin and cells progress into the mitotic phase where M arrest is experienced.

The anti-inflammatory activity of sesquiterpene lactones is well documented; however, the anti-inflammatory activity of *A. afra* is not. Here, it is reported that the production of NO and COX-2 protein levels in RAW 264.7 cells decrease in the presence of *A. afra* and isoalantolactone after stimulation with LPS. The activated NF-κB subunit, p65 was also investigated. The results suggest that *A. afra* and isoalantolactone inhibit p65 activation as a decrease in the activated subunit was evident. Thus, the results indicate that exposure to *A. afra* and isoalantolactone induces an anti-inflammatory response.

In conclusion, this study shows, for the first time, the mechanism of induced apoptosis, the anti-mitotic and anti-inflammatory activity of *A. afra* and its isolated compound, isoalantolactone. It also proves that although extensive research may have been done on a particular plant, as with *A. afra*, more can be discovered leading to the identification of new compounds and integration of signalling pathways that can be exploited for the treatment of various diseases and ailments.

Keywords: *A. afra*, cytotoxicity, isoalantolactone, anti-mitotic and anti-inflammatory activities.

LIST OF ABBREVIATIONS:

1D	one dimensional
2D	two dimensional
^{1}H NMR	proton NMR
^{13}C NMR	carbon NMR
5 - LO	lipoxygenase
A	alanine
AA	arachidonic acid
ADP	adenosine diphosphate
AIDS	acquired immunodeficiency syndrome
AKT	also known as protein kinase B
ALC	African Laser Centre
ALT	alanine transaminase
AP	alkaline phosphatase
Apaf-1	Apoptosis proteinase activating factor-1
APC	anaphase-promoting complex
Asp	aspartate
AST	aspartate transaminase
ATM kinase	ataxia telangiectasia mutated kinase
ATP	adenosine triphosphate
ATR (for IR spectroscopy)	Attenuated Total Reflectance
ATR kinase	AMT- and Rad3-related kinase
bp	base pairs of DNA
BSA	bovine serum albumin
C	cysteine
cAMP	cyclic adenosine monophosphate
CAM	Complementary Alternative medicine
CARD	caspase recruitment domain
CD95	cluster of differentiation 95 (death receptor protein)
CD	Circular dichroism
$CDCl_3$	deuterated chloroform
Cdc	Cell division control protein

Cdk	Cyclin-dependent kinase
Cdk 1 (Cdc2)	Cyclin-dependent kinase 1 also known as cell division control protein 2
Chk	Checkpoint kinase
CKI	Cyclin-dependent kinase inhibitors
CNS	central nervous system
COPD	Chronic obstructive pulmonary disease
COSY	correlation spectroscopy
COX	cyclooxygenase
Cyt-*c*	chytochrome -*c*
cys	cysteine
D	aspartate
Da	dalton
DAPI	4'6-diaminidine-2'-phenylindole dihydrochloride
DCM	dichloromethane
DEDs	death effector domains
DEPT	distortionless enhancement by polarisation transfer
DFQ-COSY	Double quantum filtered COSY
DISC	death-inducing signalling complex
DMEM	Dulbecco's Modified Eagle's Medium
DMSO	dimethyl sulfoxide
DNA	deoxyribonucleic acid
DNA-PK	DNA protein kinase
DNMT	DNA methyl transferase
DPBS	phosphate buffered saline without Mg2+ and Ca2+
dUTP	deoxyuridine triphosphate
E	glutamate
E2F	Early gene 2 factor
EGFR	epidermal growth factor receptor
EGTA	ehtylene glycol tetraacetic acid
Em	emission
eNOS	endothelial NOS
ER	endoplasmic reticulum

ERK	extracellular signal-regulated kinase
Ex	excitation
FADD	Fas-associated death domain
FBS	foetal bovine serum
FITC	fluorescein isothiocyanate
FLAP	5-lipoxygenase activating protein
FLICE	FADD-like interleukin-1 beta-converting enzyme (known as caspase 8)
FLIP	FLICE-inhibitory protein
FT-IR	Fourier transform - infrared spectroscopy
FT-FIR	Fourier transformed - far infrared spectroscopy
G	glycine
G0-phase	quiescent phase
G1-phase	gap phase 1 of the cell cycle
G2-phase	gap phase 2 of the cell cyle
$GABA_A$	Gamma-aminobutyric acid A
GADD	growth arrest and DNA-damage inducible genes
GC	gas chromatography
GPx	glutathione peroxidase
GR	glutathione reductase
GTP	guanosine triphosphate
H	histidine
H2A	histone 2A
H2B	histone 2B
H3	histone 3
H4	histone 4
H+L	heavy and light chain of antibody
HATs	histone acetyltransferases
HDAC-1	histone deacetylase 1
his	histidine
HIV	human immunodeficiency virus
HMBC	heteronuclear multiple-bond correlation spectroscopy
HPETE	5-hydroperoxy-6,8,11,14-eicosatetraenoic acid

HSQC	heteronuclear single-quantum correlation spectroscopy
HT-1	Hereditory tyrosinaemia type 1
IARC	International Agency for Research on Cancer
IAP	inhibitors of apoptosis
IC_{50}	half maximum inhibitory concentration
IFN-γ	inteferon gamma
IκB	inhibitory protein of NF-κB
IKK	IκB kinase
INH	isonicotinic hydrazine
iNOS	inducible nitric oxide synthase
IgG	Immunoglobulin G
IL	interleukin
IR	Infrared
JC-1	5',6',6'-tetrachloro-1,1',3',3'-tetraethylbenzimidazolylcarbocyanine iodide
kb	kilo bases of DNA
kDa	kiloDalton
L	leucine
LDH	lactate dehydrogenase
LPS	lipopolysaccharide
LTs	leukotrienes
LTA_4	leukotriene A_4
LTB_4	leukotriene B_4
LTC_4	leukotriene C_4
Lys	lysine
M	mitosis
mAb	monoclonal antibody
MAPK	mitogen-activating protein kinase
MC	mitotic catastrophe
MCP-1	monocyte chemotactic protein-1
Me	methyl group
MeOH	methanol
MMP	mitochondrial membrane potential

MMP (adhesion molecule)	matrix metalloproteinase
MS	mass Spectrometry
MT	microtubules
MTT	3-(4,5-dimethylthiazol-2-yl)-2,5-diphenyltetrazolium bromide
m/z	mass-to-charge ratio
N	natural products
N_2O_2	nitrogen dioxide
$NaNO_2$	sodium nitrite
NB	botanical natural products
NCCD	Nomenclature Committee on Cell Death
NCEs	natural chemical entities
ND	molecules derived from natural products
NED	*N*-(1-naphtyl) ethylenediamine
NEMO	NF-κB essential modifier/modulator
NF-κB	Nuclear factor kappa B
NIK	NF-κB inducing kinase
NM	natural product mimic
NMMU	Nelson Mandela Metropolitan University
NMR	Nuclear Magnetic Resonance
nNOS	nuclear NOS
NO	nitric oxide
NOESY	nuclear Overhauser effect spectroscopy
NOS	nitric oxide synthase
NRF	National Research Fundation of South Africa
NSAIDs	non-steroidal anti-inflammatory drugs
$OONO^-$	peroxinitrite
PARP	poly (ADP-ribose) polymerase
PBS	phosphate buffered saline containing Mg^{2+} and Ca^{2+}
PGs	prostaglandins
PGE_2	prostaglandin E_2
PI3K	phosphatidylinositide 3-kinases
PI	propidium iodide

PIPES	Piperazine-1,4-bis(2-ethanesulfonic acid)
PLA_2	type II phospholipases A_2
PLK1	polo-like kinase 1
PMTs	photomultiplier tubes
PPAR-δ	peroxisome proliferato-activated receptor-delta
PS	phosphatidylserine
PSA	prostate-specific antigen
Q	glutamine
R	arginine
Rb	Retinoblastoma protein
Rf	Relative migration
RHD	Rel homology domain
RIF	rifampin
ROS	reactive oxygen species
RPMI	Roswell Park Memorial Institute
S-phase	synthesis of DNA during the cell cycle
S (compounds)	synthetic compound
S* (compounds)	synthetic compound with natural pharmacophore
SD	standard deviation
Ser	serine
SERCA pump	sarco/endoplasmic reticulum calcium ATPase pump
SL	sesquiterpene lactone
SOD	superoxide dismutase
STZ	streptozocin
TAMs	tumour-associated macrophages
TB	tuberculosis
tBid	truncated Bid
TdT	terminal deoxynucleotidyl transferase
TGF-β	Transforming growth factor beta
Thr	threonine
TLC	thin layer chromatography
TM	Traditional medicine
TNF	tumour necrosis factor

TNFR	tumour necrosis factor receptor
TP	tubulin polymerisation
TRAF6	TNFR-associated factor 6
TRAIL	TNF-related apoptosis-inducing ligand
TRAIL-R	TNF-related apoptosis-inducing ligand receptor
TRITC	Tetramethylrhodamine-5-(and 6)-isothiocyanate
TUNEL	TdT-mediated dUTP Nick End Labeling
Tx	thromboxanes
TxA_2	thromboxane A_2
Tyr	tyrosine
Ub	ubiquitin
UCT	University of Cape Town
UV	ultraviolet light
V	vaccine
V (amino acid)	valine
VEGF	vascular endothelial growth factor
v/v	volume/volume
W	tryptophan
WHO	World Health Organization

CHAPTER 1: Introduction to this study

Since the beginning of time, man has made use of nature for his needs. Man has been able to use and exploit natural resources for survival, comfort, pain alleviation and disease treatment (Patil *et al.*, 2011). Plants have been used as a source of therapeutic agents for thousands of years and are still being used today as crude drugs under the flag of traditional medicine. The study of phytomedicine has grown and isolation and identification of biologically active compounds is performed all over the world. In a recent review by Newman and Cragg (2012), it is indicated that more than half the approved clinical drugs in the U.S.A are of natural sources and thus, the importance of ethnomedicine is absolutely clear.

1.1. Traditional Medicine (TM):

The major traditional healing systems that have survived the impact of modern medicine are the Indian system, the Chinese system and the African system. The World Health Organization (WHO) describes traditional medicine as diverse health practices, approaches, knowledge and beliefs incorporating plant, animal and/or mineral based medicines. It includes spiritual therapies, manual techniques and exercises applied singularly or in combination to maintain well-being, as well as to treat, diagnose or prevent illness (www.who.int). The term "traditional" refers to the fact that the system evolved endogenously in a society and has been handed down from generation to generation. In contrast, "Western" medicine or biomedicine refers to the treatment of the physical body only and is based on the principles of science, technology, knowledge and clinical analysis. Traditional healers take a more holistic approach to treating an illness and consider both the physical and spiritual well-being of a patient, while "western" medicine considers only the material causation and treat the symptoms of the illness (Gurib-Fakim, 2006). In literature, the use of TM is often referred to as phytomedicine and forms part of a broad field of study classified as ethnomedicine (Richter, 2003).

The U.S. National Institutes of Health has grouped TM and complementary and alternate medicine (CAM) into 5 overlapping groups (Peltzer, 2009; http://nccam.nih.gov):

1. Biologically based practices: This practice uses the biological approach and includes the use of natural products such as vitamins and minerals, herbal remedies such as ginkgo biloba and unconventional diets to manage weight, etc.

2. Manipulative and body-based approaches: This practice includes massage, chiropractic and osteopathic medicine. It originated to relieve structural forces on the vertebrae and spinal nerve roots.
3. Mind-body medicine: This practice attempts to reassert the proper harmony between mind and body using spiritual, meditative and relaxation techniques.
4. Alternative medical systems: This practice is based on cultures that believe health depends on the balance and flow of vital energies through the body which is achieved by placing needles at critical points on the body, for example.
5. Energy medicine: An example of this practice is Reiki therapy, which aims to realign and strengthen healthful energies, which is achieved through the hands of a master healer.

The WHO has defined African Traditional Medicine as: "The sum total of all knowledge and practices, whether explicable or not, used in diagnosis, prevention and elimination of physical, mental, or societal imbalance, and relying exclusively on practical experience and observation handed down from generation to generation, whether verbally or in writing" (www.who.or.jp).

The WHO has recognized that 80% of the African population makes use of TM (Gurib-Fakim, 2006; Peltzer, 2009). In Asia and America, populations still use TM as a result of historical circumstances and cultural beliefs. In China, 40% of the population still use TM and in Ghana, Mali, Nigeria and Zambia, 60% of children are treated for high fever using TM (Peltzer, 2009). In 2002, it was recognized that in sub-Saharan Africa, the ratio of traditional healers to the rest of the population is 1:500, compared to the ratio of medical doctors to the rest of the population, which is 1:40 000 (Abdool Karim *et al.*, 2002). In developed countries CAM has become popular. The percentage of the population that has used CAM at least once is 48% in Australia, 70% in Canada, 42% in the USA, 38% in Belgium and 75% in France (www.who.int). In San Francisco and London, 75% of people living with HIV/AIDS use TM/CAM (Peltzer, 2009). The level of utilization of TM and CAM worldwide is indicated in Figure 1.1.

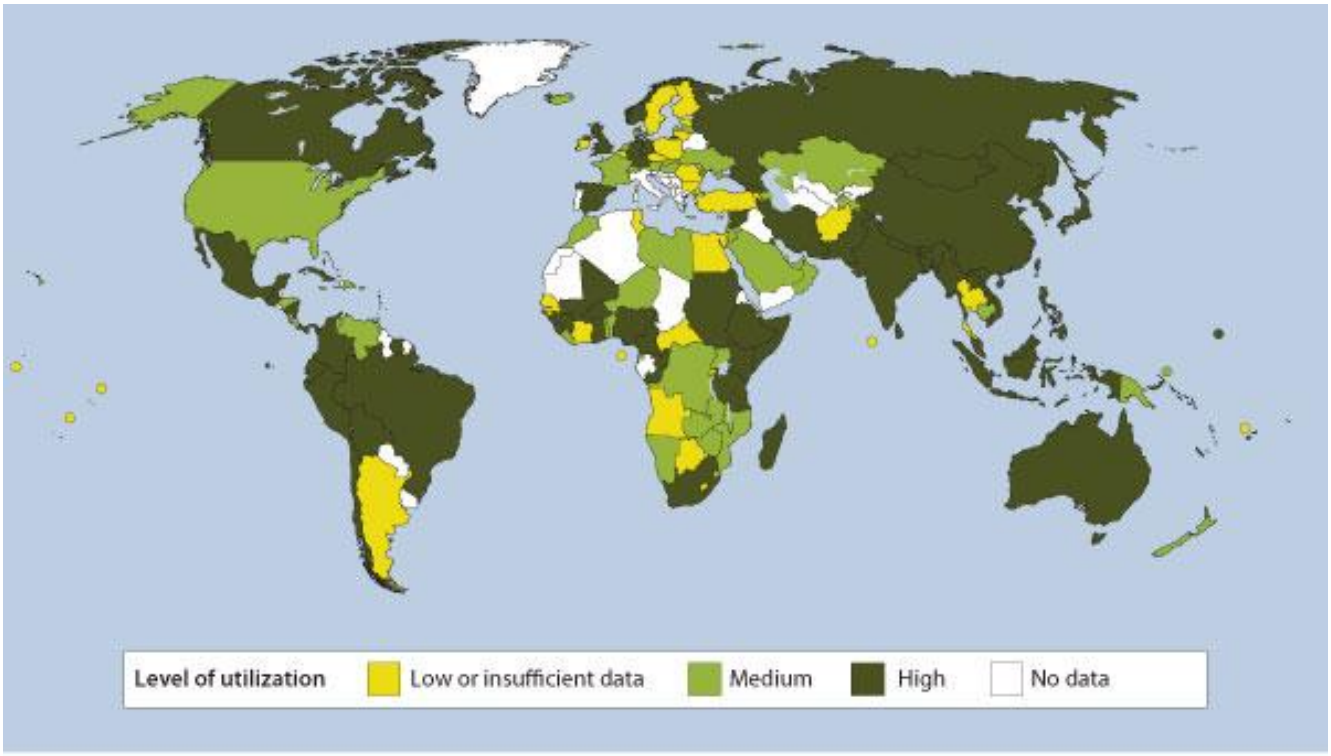

Figure 1.1: Map of the World indicating the prevalence of Traditional Medicine and Complementary and Alternative Medicine (www.who.int).

The broad use of TM/CAM can be attributed to two main factors, accessibility and affordability. Most healthcare practitioners are found in the cities and urban areas and thus difficult for the rural population to access. Herbal medicines are significantly cheaper than chemical drugs. In developed countries, the popularity of CAM is due to the adverse side effects of chemical drugs.

An overwhelming argument has been presented by Groundup that the fact that 80% of Africans make use of TM is false (http://groundup.org.za). Statistics South Africa conducted a General Household Survey in 2011 and the results of the Health-care provision and quality survey are indicated in Figure 1.2. This graph indicates 9 types of health-care facilities that are consulted first by households in South Africa. They are listed in the Figure. "Other", "Pharmacy" and "Traditional healer" numbers are not visible on the graph as the numbers are too low. The results of this survey show that only 0.1% of South Africans favoured traditional healers over "western" medicine as their first choice of health-care with the majority of our population, 70.7%, making use of public clinics and hospitals (the red and dark blue bar, respectively). A study conducted by Nxumalo and colleagues in 2011 also showed a significantly lower number of South Africans that consult traditional healers first, only 1.2%, compared to the reported value of 80% by WHO.

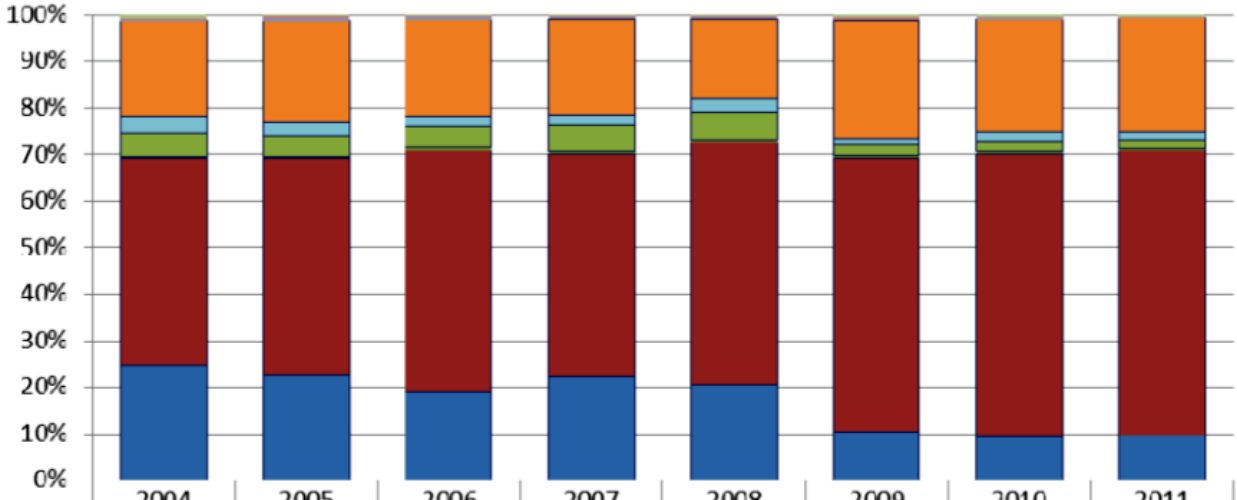

	2004	2005	2006	2007	2008	2009	2010	2011
Other	0,7	0,3	0,1	0,3	0,2	0,6	0,5	0,5
Pharmacy	0,4	0,4	0,4	0,3	0,4	0,4	0,3	0,2
Traditional healer	0,2	0,6	0,4	0,3	0,3	0,2	0,2	0,1
Private doctor	20,5	21,9	20,7	20,7	17,2	25,3	24,3	24,3
Private Clinic	3,5	2,7	2,3	2,1	2,7	1,4	1,7	1,7
Private Hospital	5,1	4,6	4,6	5,7	6,0	2,3	2,5	2,0
Other Public Institution	0,2	0,2	0,6	0,3	0,5	0,4	0,4	0,4
Public Clinic	44,4	46,8	52,0	48,0	52,0	59,0	60,8	61,2
Public Hospital	24,9	22,5	18,9	22,3	20,7	10,4	9,4	9,5

Figure 1.2: Summary of types of health-care facilities visited when survey members fall ill or get injured, 2004 – 2011 (Statistics South Africa).

1.2. Problems associated with Traditional Medicine in Africa:

The WHO has stated: "The quantity and quality of the safety and efficacy data on traditional medicine are far from sufficient to meet the criteria needed to support its use worldwide. The reasons for the lack of research data are due not only to health care policies, but also to a lack of adequate or accepted research methodology for evaluating traditional medicine. It should also be noted that there are published and unpublished data on research in traditional medicine in various countries, but further research in safety and efficacy should be promoted, and the quality of the research improved" (www.who.int).

In conjunction with the statement from WHO, information about the efficacy and safety of traditional medicine in Africa is seriously lacking. However, in South Africa, the government

approved a bill [Traditional Health Practitioners Act (No 35 of 2004)] to formalize the African traditional healing system. Thus, it is now more important than ever to address the lack of information to ensure that the traditional healers, who are respected members of their communities, can contribute to primary health care in a meaningful way without losing their identity. In all other countries where traditional medicine is recognized by their governments such as China and India, much more scientific research has been done to validate their methods.

1.3. Natural products are a major source of effective drugs:

Natural products and plants have played a very important role throughout the world in the treatment of various diseases and ailments (Chin *et al.*, 2006). Extensive reviews have been published with overwhelming evidence of the importance of natural products as a source of new, effective drugs. Newman and Cragg (2012) indicated that from January 1981 to December 2010, 1355 new chemical entities (NCEs) covering all diseases, countries and sources were recorded. Of these, 29% were of synthetic origin. A total of 21% (6% vaccines and 15% biological) were non-small molecule compounds. The rest of the NCEs were of natural origin, clearly establishing the importance of natural products as an important source of potential drugs. This is shown in Figure 1.3.

In addition to the information shown in Figure 1.3, the natural products field is still producing approximately 50% of all small molecule drugs from 2000 to 2010. This does not include the small molecule drugs inspired by natural products; this refers to only natural products (N), botanical natural products (NB) and molecules derived from natural products (ND).

Plants have been and still are an effective source of natural drugs. Marine organisms and microorganisms also contribute significantly as sources of natural small molecule drugs. The study of plants as a source of drugs has provided new and important leads against various pharmacological targets including cancer, HIV/AIDS, Alzheimer's, malaria, pain and infectious diseases (Balunas and Kinghorn, 2005). Isolation of active compounds from plants has become more popular over the years for the identification of potential new drugs and lead compounds. In the early 19th century, morphine was isolated from opium poppy and is still

used today. Other early drugs include cocaine, codeine, digitoxin and quinine (Newman *et al.*, 2000).

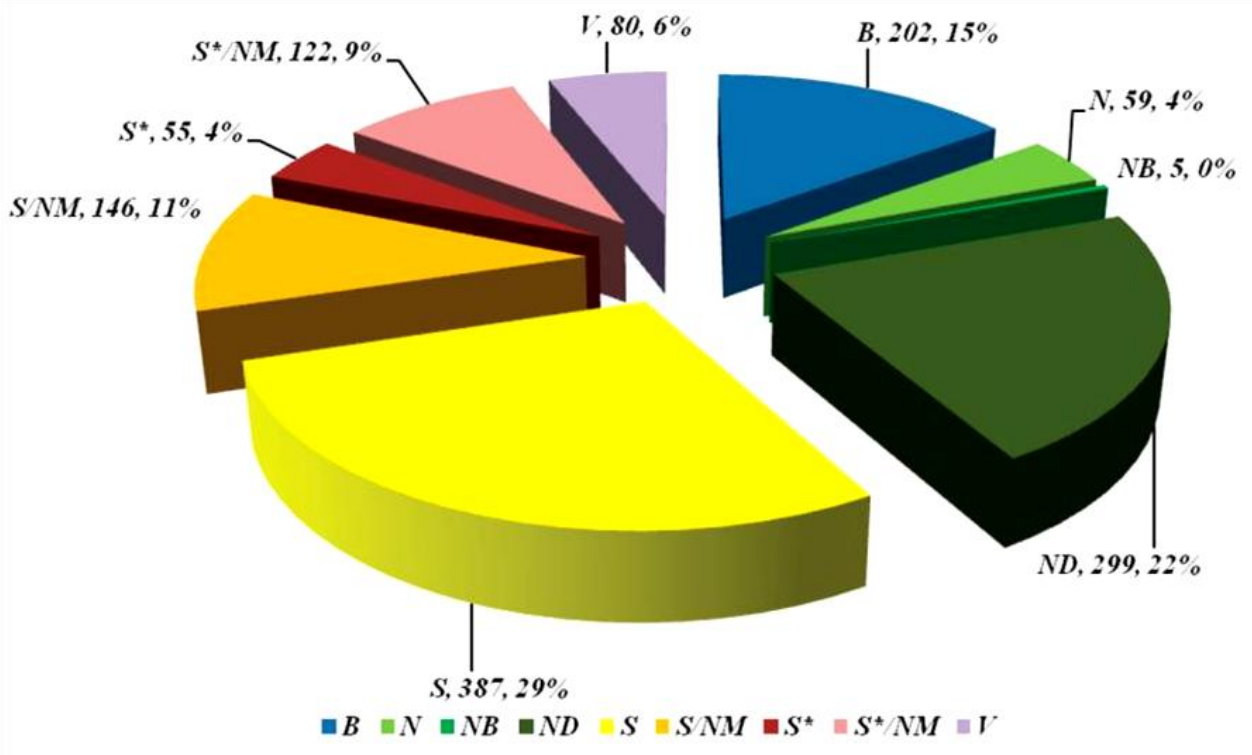

Figure 1.3: All new approved drugs from 1981 to 2010. B: Biologicals; N: Natural product; NB: Natural product Botanical; ND: Derived from a natural product and is usually a semisynthetic modification; S: totally synthetic, normally an improvement of an existing agent; S*: made by total synthesis but its pharmacophore is of natural origin; V: vaccine; NM: Natural product mimic. The first number corresponds to the actual number of drugs in that group. The second number refers to the percentage in that group (Newman and Cragg, 2012).

Different approaches are used for the study of plants as candidates for drug potentials. These are (Fabricant and Farnsworth, 2001):

- Random selection followed by chemical screening: This is defined as phytochemical screening of random plants and is mainly used in developing countries. Researchers screen for the presence of known active compounds however, results are difficult to assess. This method also requires significantly more financial resources.

- Random selection followed by one or more biologic assays: From 1986, plants have been screened using *in vitro* methods as well as *in vivo* models for the establishment of its biological activity. Thereafter, isolation of active compounds of positive plant hits is conducted.
- Follow-up of biologic reports: This is where interesting biological activity has been reported but the extract was not studied for its active compounds.
- Follow-up of ethnomedical (traditional medicine) uses of plants: Phytochemists use information based on the use of plants by traditional healers for the treatment of a particular disease or ailment. This has been the most successful approach.
- Use of databases.

Although it is clear how important natural products and plants are to the identification and development of NCEs, there are several disadvantages that do emerge when using plants as a source of potential new drugs. Plants as biological systems have inherent potential variability in their chemistry and thus their biological activity. The time of the year of plant collection plays an important role here due to the production of system compounds for the needs of the plant at a specific time. Taxonomic identification is also very important to prevent mix-ups of plants. Countries have also started to protect their natural material by prohibiting the collection of plants or have implicated regulations and restrictions to make it difficult for plant collection. It can take up to 2 years to gain permission to collect plant material. Although collection of plant material is simple, considerable planning and knowledge of the plant, its abundance in a specific area, etc. is required when basing a study of ethnobotanical claims of biological activity. In saying all this, the major disadvantage of plants as a source of new drugs is the time it takes from plant collection to the drugs' clinical approval. It has been estimated that this process take 10 to 20 years (Fabricant and Farnsworth, 2001). Development and improvement of methods currently employed is ongoing to allow for quick identification of lead compounds from natural sources and plants.

The advantages of natural products as starting points for new drugs are their structural diversity and multiple stereocentres that are challenging synthetically. Many of the structural features of metabolites of plants such as chiral centres, aromatic rings, complex ring systems, degrees of unsaturation and number and ratio of heteroatoms, have been shown to be highly relevant in drug discovery efforts. Thus, natural products are not only a great source of drugs but also serve as excellent lead compounds (Balunas and Kinghorn, 2005). It has also been

stated that natural products are thought to harbour less harmful side effects. The use of natural products has proven extremely successful over the last 30 years (Newman and Cragg, 2012).

1.3.1. New approved drugs from terrestrial plants:

From 1981 to 2010, a total of 1130 NCEs were screened for the treatment of various conditions of which more than 50% are of natural origin (Newman and Cragg, 2012). Table 1.1 lists a few examples of approved drugs isolated from plants and their specific use (Chin *et al.*, 2006).

Table 1.1. Five examples of approved drugs from 2000 – 2005 from terrestrial plants (Chin *et al.*, 2006).

Drug name	Plant	Usage
Apomorphine hydrochloride	*Papaver somniferum*	Parkinson's disease
Tiotropium bromide	*Atropa belladonna*	Treatment of bronchospasm associated with chronic obstructive pulmonary disease (COPD)
Nitisinone	*Callistemon citrinus*	Hereditary tyrosinaemia type 1 (HT-1)
Galantamine hydrobromide	*Galanthus nivalis*	Alzheimer's disease
Arteether	*Artemisia annua*	Treatment of malaria

Combrestatin A4 phosphate and a compound known as AVE-8062 are derivatives of combrestatin A4, a compound isolated from *Combretum caffrum*, a medicinal tree from South Africa. These compounds have reached clinical trials for the treatment of cancer. They are known to bind tubulin and disrupt tumour vasculature (Chin *et al.*, 2006).

1.4. South Africa and useful medicinal plants:

South Africa has a rich biodiversity and has approximately 30 000 species of higher plants, ±10% of the world total (Rybicki *et al.*, 2012). Although the occurrence of use of TM in South Africa is unclear due to the 2011 General Household survey by Statistics South Africa, the South African Health Ministry has estimated that 70% of South Africans seek advice from traditional healers at some point or another and thus considered for incorporation within its formal health care system.

Many plants, too many to list, are used for the treatment of a variety of diseases, infections, injuries and ailments by South African traditional healers. The demand for medicinal plants and their products (metabolites) is increasing according to UNCTAD COMTRADE, a database that contains worldwide statistics pertaining to the import and export of pharmaceutical plants since 1962. Bulk trade of medicinal plants generally takes place in informal street markets in South Africa and whole plants as well as semi-processed plant products are sold (Institute of Natural Resources).

In a study by Thring and Weitz in 2006, it was shown that the dominant plant families used and sold as traditional medicines in the Western Cape are Asteraceae, Lamiaceae, Alliaceae and the Solanaceae. In the survey it was revealed that all its participants reported the medicinal use of *Artemisia afra* for the treatment of various ailments (1.5.4). It is a widespread and abundant plant that grows well in most provinces of South Africa (Liu *et al.,* 2009).

1.5. *Artemisia afra:*

Artemisia afra is one of the oldest, most well known and widely used traditional medicinal plants in South Africa. Due to its popularity, Liu *et al.* (2009) suggested that *A. afra* may be the potential flagship for African medicinal plants. Its name is derived from the Greek goddess of hunting, Artemis and afra means Africa. It is commonly referred to as the African wormwood and its uses resemble those of the European wormwood, *A. absinthium.* (Scott *et al.,* 2004). The genus *Artemisia* consists of over 500 species and important drugs have been isolated from this genus. The most well known is artemisinin, an anti-malarial drug that is now in clinical trials for the treatment of cancer (Liu *et al.,* 2009; Ghantous *et al.,* 2010).

1.5.1. Morphology:

A. afra is a highly aromatic perennial shrub which grows up to 2 m tall with a leafy, hairy and ridged stem. Its leaves are finely divided and are dark green on its adaxial surface and light green on its abaxial surface. The aerial parts are pungent and bitter tasting. *A. afra* produces flowers from January to June which are yellow in colour (Van Wyk *et al.,* 1997). *A. afra* is

drought resistant and can grow easily in any soil just needing occasional watering and cutting back (Hutchings *et al.*, 1996).

Figure 1.4: **The leaves of *Artemisia afra.***

1.5.2. Taxonomy:

A. afra is classified as follows: Kingdom: Plantae, Division: Mannoliphyta, Class: Magnoliopsida, Sub-class: Asteridae, Order: Asterales, Family: Asteraceae, Genus: *Artemisia*, Species: *Artemisia afra.*

A. afra has many vernacular names. These include wilde als (Afrikaans), wild wormwood, African wormwood (English), umhlonyane (Xhosa), zengana (Southern sotho) (Scott *et al.*, 2004).

1.5.3. Distribution:

A. afra has a wide distribution across Africa and occurs in the mountain regions of Kenya, Tanzania, Uganda and even as far north as Ethiopia. It thrives in the southern African countries of Zimbabwe, Namibia and South Africa. The distribution of growth in South Africa is shown in Figure 1.5. *A. afra* grows in almost every province and is abundantly found in the Eastern Cape. It can grow at altitudes between 20 to 2440 m on damp slopes, along streamsides and forest margins (Liu *et al.*, 2009).

Figure 1.5: Map of distribution of *A. afra* in South Africa (Patil *et al.,* 2011).

1.5.4. Medicinal uses:

Since 2000, significant increases in the number of publications of *A. afra* have been noticed. It has been reported that an average of 18 publications of *A. afra* is being produced per year since 2005 (Patil *et al.*, 2011). *A. afra* is used to treat a variety of conditions. These include coughs, colds, headaches, chills, dyspepsia, loss of appetite, gastric derangements, colic, croup, whooping-cough, gout, asthma, malaria, diabetes, bladder and kidney disorders, influenza, convulsions, fever, heart inflammation, rheumatism and is also used as a purgative (Liu *et al.*, 2009).

The part of the plant that is mostly used is the leaves due to its odour and taste. The roots are also sometimes used. Many different preparations of the plant are employed depending on the condition or symptom to be treated. The most popular use is for respiratory and congestive symptoms and ailments. The leaves are dried and added to hot, boiling water. The vapours are then inhaled. Leaves can also be placed in the nostril for the same purpose as well as for the relief of headaches. An infusion of the leaves and roots are drunk for the treatment of diabetes in the Eastern Cape Province. A brewed tea (a quarter cup of leaves added to hot water, allowed to draw for 10 minutes and thereafter strained and sweetened with honey) is drunk for the oral relief of many of the mentioned symptoms. Infusions and decoctions of the plant are used as a lotion to bathe haemorrhoids and to treat earache. A poultice of the leaves is prepared and used to apply to areas to relieve pain and swelling as well as skin inflammation, e.g. to the abdomen for the relief of infantile colic. A tincture can be prepared

by wetting the leaves with brandy and then administered to treat abdominal pain (Liu *et al.,* 2009; Patil *et al.,* 2011). *A. afra* is commonly used in combination with other plants such as ginger, garlic, eucalyptus, thyme, rosemary, mint and chamomile (Suliman *et al.,* 2010; Patil *et al.,* 2011).

1.5.5. Chemical components of *A. afra*:

Many chemical compounds and metabolites have been isolated from *A. afra*. Liu *et al.* (2009) lists 132 volatile secondary metabolites that have been isolated from this plant, most of them being monoterpenes and sesquiterpenes. Non-volatile secondary metabolites that have been isolated include the sesquiterpene β-farnesene, sesquiterpene lactones (glaucolides and guaianolides), taurin, triterpenes, long chain alkanes, coumarins, organic acids glycosides and flavanoids.

Geographical variation has shown to play an important role in the components of volatile secondary metabolites of *A. afra.* In the Ethiopian oil, artemisyl acetate was found to be the major component, while 1,8-cineole was the main component of the Kenyan oil. In the Zimbabwean oil, α- and β-thujone made up 52% of the volatile oil while only α-thujone was found in the South African oil. The parts of the plant used and the methods with which they are extracted also cause chemical variation. Viljoen *et al.* (2006) also found differences in chemical components within and between populations of the plant.

1.5.6. Biological activity of *A. afra:*

Due to the presence of many terpenes, it is likely that *A. afra* has interesting biological activity. It has been shown to have effective activity against many microorganisms. The lipophilic extracts of *A. afra* showed to have the highest activity against chloroquine-sensitive and chloroquine-resistant *Plasmodium* species (Kraft *et al.,* 2003). The dichloromethane (DCM)/methanol (MeOH) (1:1) extract exhibits strong antiplasmodial activity (Clarkson *et al.,* 2004). Kraft *et al.* (2003) showed that the compounds responsible for antiplasmodial activity included flavonoids and sesquiterpene lactones. Antimicrobial activities of organic extracts of *A. afra* is also evident in literature. The oil of the plant also exhibits antimicrobial activity. Tests of antimicrobial activity have been conducted using the zone of inhibition method and results for the minimum inhibitory concentration of plant extract against a chosen

bacteria is lacking. A recent study showed that a DCM extract of *A. afra* inhibited the growth of *Mycobacterium tuberculosis* at a high IC_{50} of 290 µg/mL. Fractionation of the extract resulted in a significant decrease in the IC_{50} value and the active fraction showed to be comprised of sesquiterpene lactones (Ntutela *et al.,* 2009). *A. afra* is also known to exhibit anti-fungal activity (Patil *et al.*, 2011).

An ethanol extract of *A. afra* possesses spasmolytic properties showing that treatment of mice and guinea pigs with the extract reduced spontaneous rhythmic and agonist-induced contractions. It has been demonstrated that *A. afra* has cardiovascular effects. The aqueous extract has displayed a hypotensive effect *in vivo* (Guantai and Mensah, 1999). Pretreatment of myocardial injured male Wister rats with the aqueous extract for 30 days resulted in an elevation of serum marker enzymes lactate dehydrogenase (LDH), aspartate transaminase (AST), alanine transaminase (ALT) and alkaline phosphatase (AP). This was accompanied by restoration of normal levels of glutathione reductase (GR), glutathione peroxidase (GPx), superoxide dismutase (SOD) and glutathione in the heart after treatment with the aqueous plant extract (Sunmonu and Afolayan, 2010).

The aqueous extract of *A. afra* has recently been shown to possess antidiabetic activity. Diabetes induced rats (intravenous injection of STZ) were used to test the extract for 15 days at different concentrations. From this study it was concluded that *A. afra* may protect the liver and blood against impairment due to diabetes, but kidney functions may be compromised at high dosages of the plant extract (Sunmonu and Afolayan, 2013).

Artemisia species have also been implicated in CNS- acting and sedative activities. It has been shown to do so through $GABA_A$-benzodiazepine receptor binding. It has been determined that flavonoids are responsible for this activity (Stafford *et al.,* 2005). It has even been suggested that *A. afra* may have antidepressant activity (Nielsen *et al.,* 2004).

Many *Artemisia* species are used for anti-inflammatory ailments (Abad *et al.,* 2012). Although *A. afra* is not popularly used for inflammatory conditions, it has been shown to be used on swellings and for skin inflammation, heart inflammation and rheumatism (Liu *et al.*, 2009). In 2009, Ntutela accidently found the anti-inflammatory potential of *A. afra* when investigating the plants effect on tuberculosis. During the study, it was found that pulmonary inflammation was significantly reduced and the extract proved to be as efficient as the TB

drug, isonicotinic hydrazine/Rifampin (INH/RIF). Hong *et al.* (2004) showed that *A. capillaris* reduced LPS-mediated inflammatory responses in rat liver and human hepatocarcinoma cells.

1.5.7. Toxic and adverse effects of the use of *A. afra:*

The unfavourable effects of the use of *A. afra* are due to the high content of thujone in the oil of the plant. It has been shown that the volatile oil of *A. afra* has produced hemorrhagic nephritis, degenerative changes in the liver and pulmonary oedema in rabbits (Watt and Beyer-Brandjik, 1962). It has also been reported that excessive and prolonged ingestion of *A. afra* has resulted in vomiting, restlessness, vertigo, tremours, convulsions, and fatty degeneration of liver. The volatile oil also produces hallucinogenic effects, thus continued use of the oil is not recommended. The solubility of thujone is extremely low in water and thus it is unlikely that this component is present in the aqueous extract. In a study evaluating the acute and chronic toxicity induced by an aqueous extract of *A. afra*, it was shown that the plant was non-toxic to mice and rats when administered orally at doses up to 2 g and 1 g/kg, respectively. The 3 month chronic toxicity study revealed that *A. afra* did not appear to affect the bodyweight or the behaviour of the rats and caused no change in food uptake and utilization of food indicating an unaffected metabolism (Mukinda and Syce, 2007).

Cytotoxic evaluation of the plant has also been carried out using three different human cell lines, namely renal TK10, breast MCF7 and melanoma UACC62 cells. Total growth inhibition values obtained against these cell lines for a DCM:MeOH (1:1) were 26.62 µg/mL, 15.00 µg/mL and 9.73 µg/mL, respectively. It was indicated that *A. afra* possesses moderate cytotoxic activity (Fouche *et al.*, 2008). The crude ethanolic extract of *A. afra* has also shown cytotoxicity against Vero cells with an IC_{50} value of 113.2 ± 2.05 µg/mL (Mativandlela *et al.*, 2008). Jenett-Siems *et al.* (2002) found that sesquiterpene lactones present in the plant are partly responsible for cytotoxic effects. Although cytotoxicity is evident, the mode of cell death or growth inhibition has not yet been elucidated and reported by any research group.

CHAPTER 2: Research Rationale, Aims and Objectives

Significant increases in the number of publications on *A. afra* have been noticed since the year 2000. It has been reported that an average of 18 publications of *A. afra* is being produced per year since 2005. Figure 2.1 illustrates the dramatic increase in the number of hits on Scirus for *A. afra* (Patil *et al.*, 2011). Extensive literature is available for the potential of *A. afra* to be the "cure all" plant of South Africa. Chapter 1 clearly indicates the diverse use and biological activities of *A. afra*, thus establishing its importance as a medicinal plant. It has been proven that its traditional use is validated by biological assays *in vitro* and *in vivo.*

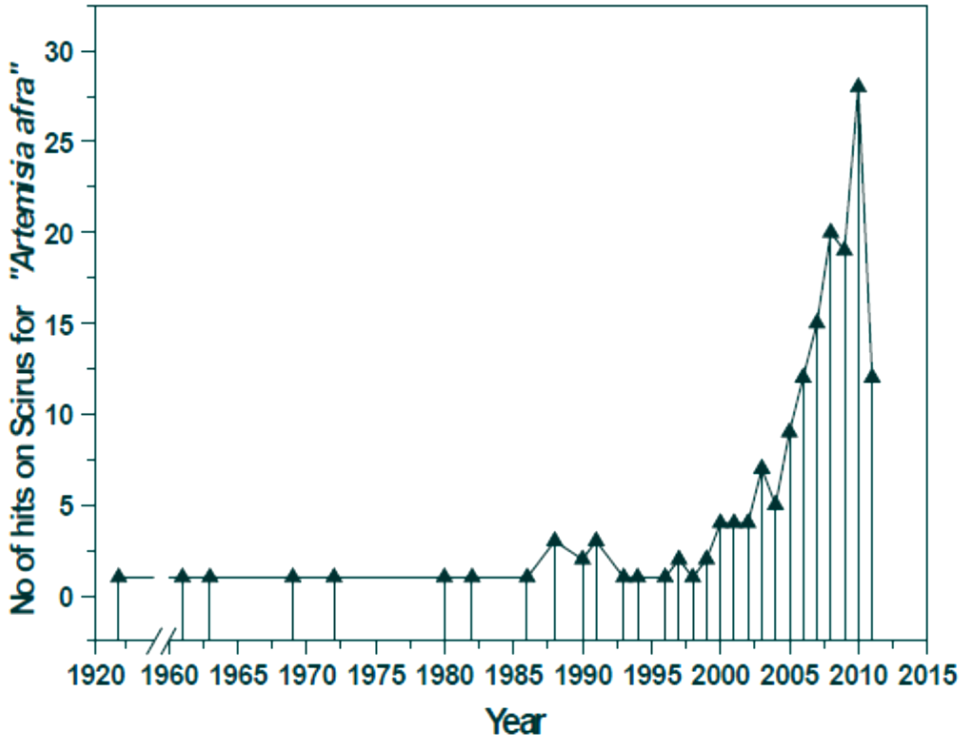

Figure 2.1. A graphical representation of the dramatic increase in the interest in *A. afra* (Patil *et al.*, 2011).

Extracts of *A. afra* has shown to be cytotoxic against breast, renal and melanoma cancer cell lines as well as the African green monkey kidney cell line, Vero (Liu *et al.*, 2009). However, the mode of cytotoxicity and its anticancer potential has not yet been reported. Thus, it was our main aim to determine the anticancer potential of *A. afra.*

Many compounds have been isolated from the plant, which is well documented in a review by Liu *et al.* (2009), sesquiterpene lactones being among these compounds. Approximately 15 sesquiterpene lactones have been isolated from *A. afra* (as discussed in Chapter 1 and Chapter 4). It is well known that sesquiterpene lactones possess cytotoxic and anti-inflammatory activity. Therefore, in addition to the lacking information with regards to the mode of cytotoxicity of *A. afra,* we aimed to identify the cytotoxic compounds responsible for induced cell death by the plant extract. In this way a direct comparison could be made of the cytotoxic effect of *A. afra* and the compound(s) responsible for the observations.

A. afra is used to treat inflammatory ailments as well as tuberculosis (TB). Inflammation is critical for the pathogenesis of TB (Kaufmann and Dorhoi, 2013) and although *A. afra* is used to treat TB, no reported evidence of anti-inflammatory activity of the plant exists. Thus, we also aimed to determine the anti-inflammatory activity of *A. afra.* A well established link between cancer and inflammation has been made (Lin and Karin, 2007) and although *A. afra* is not known to treat cancer, it is used for the treatment of inflammation. Medicinal plants have yielded drugs for treatment of diseases other than those that they are used for traditionally. The Madagasca Rosy Periwinkle, *Catharanthus roseus,* is used by the Madagascan people to treat diabetes and fever. Research of *C. roseus* led to the isolation of two alkaloids that are used to treat childhood leukaemia and Hodgkin's disease with a very high success rate (Gurib-Fakin, 2006). Many more examples exist and thus emphasize the importance of natural product research.

To meet the aims of the project, the objectives were to:

- Determine the cytotoxic effects of an ethanol and aqueous extract of *A. afra* against HeLa, U937, Chang liver and Vero cell lines.
- Characterise the possible cytotoxic mechanism(s) of action of *A. afra* extract(s).
- Isolate and identify the cytotoxic compound(s) partly or wholly responsible for the observed cytotoxic effects.
- Characterise the mode of induction of cell cycle arrest and hence, the mode of anti-mitotic effect of *A. afra* and the isolated compound.
- Compare the cytotoxic, antimitotic and anti-inflammatory activity of the crude plant extract and the isolated compound(s).
- Determine the anti-inflammatory activity of *A. afra* and the isolated compound(s).

The project has been divided into 5 experimental chapters, Chapters 3 – 7. In each experimental chapter, a literature survey or introduction is followed by the materials and methods used to meet the objectives of the chapter (described below). Results and discussion are presented in separate sections of the chapter.

Chapter 3 focuses on the determination of the cytotoxic effects and the characterization of the anticancer potential of *A. afra*. Chapter 4 focuses on the isolation of active cytotoxic compound(s) from the ethanol extract of *A. afra* and the identification of a compound using various spectroscopic techniques including IR, NMR and CD as well as MS. Chapter 5 focuses on the mechanism of action of cell death induced by the isolated compound. The same methods were used here as for Chapter 3 to compare the results of the crude plant extract and the cytotoxic compound. Chapter 6 focuses on the mechanism of cell cycle arrest induced by both the crude plant extract and the compound. In this way, the anti-mitotic effect on HeLa and U937 cells was determined. In Chapter 7, the anti-inflammatory effects of *A. afra* and the isolated compound was determined using RAW 264.7 murine macrophages by measuring nitric oxide production and the levels of COX-2 and active NFκB. The last chapter, Chapter 8, highlights the findings of this study and suggestions and recommendations are made for future work.

CHAPTER 3: *In vitro* anticancer activity of *Artemisia afra.*

3.1. Introduction:

Cancer is a heterogenous disease and is defined as a class of diseases in which a group of cells grow and divide uncontrollably and do not die. Cancer arises from multiple tissue types and displays great genetic diversity. Cancer is characterized by the onset of genetic mutations that will have growth advantages for the cell. These mutations as well as disruptions of the cells ability to survive are the two main contributing factors that ensure a state of excessive proliferation and ultimately lead to the development of cancer (Kasibhatla and Tseng, 2003).

Genetic mutations found in cancer normally affect two classes of genes; oncogenes and tumour suppressor genes. Oncogenes are mutant versions of protooncogenes and the products function in signal transduction pathways that promote cell proliferation. This genetic alteration is referred to as a gain-of-function mutation. The second class of genes are the tumour suppressor genes and they are referred to as the loss-of-function mutation. These mutations were first recognized to have a major role in cancer susceptibility. It is known that inactivation of both copies of a tumour suppressor gene is required for the loss of function. In normal cells, tumour suppressor genes encode for proteins that normally negatively regulate the cell cycle. Mutations of tumour suppressor genes play a major role in hereditary and spontaneous cancers (Collins *et al.*, 1997b).

Cancer cells are different to normal tissue cells in that they possess abilities to elude physiological processes that promote cell death, thus evading it. Genetic changes cause unregulated proliferation of cells and this allows for the preservation of the mutations (Simstein *et al.*, 2003). Cancer cells are able to evade apoptosis by altering components of the apoptotis machinery, can multiply without limit, are insensitive to anti-growth signals which enable them to continuously divide, sustain angiogenesis and are able to invade neighbouring tissues and metastasise (Hanahan and Weinburg, 2000).

3.1.1. Cancer statistics:

In 2010, the World Health Organization (WHO) declared that the leading cause of deaths globally is cancer, claiming the lives of 7.6 million people. According to the *IARC Globocan Report*, it was estimated that 12.7 million new cases of cancer had occurred in 2008. It has been estimated that by 2030 there could be 27 million incident cases of cancer globally; 17 million cancer deaths annually and 75 million persons alive with cancer within five years of diagnosis. In the same year in South Africa, 207 males per 100 000 deaths and 124 females per 100 000 deaths were because of cancer. According to the latest available statistics from the National Cancer Registry, one in four South Africans will be affected by cancer in his or her lifetime (www.cansa.org.za).

The primary objectives for the treatment of cancer are to provide equitable, appropriate and effective treatment as well as to care for the cancer patient. The type of care received is dependent on the type of cancer, the site of the cancer, the tumour size and the stage of the cancer. The most frequent treatments are:

- Surgery
- Cytotoxic chemotherapy
- Radiotherapy
- Hormonal Manipulation
- Biological therapy
- Combined treatment of two or more of the above.

In many cases, developing countries cannot afford these therapies and treatment facilities are not available for economic reasons in most African countries, thus traditional medicine is used as an integral component of public health care as well as for the treatment of cancer.

3.1.2. Cancer and plants:

Plants have been used as medicines for thousands of years and were normally used in their crude forms, including tinctures and teas and powders. The knowledge of what plants to use for specific ailments was passed down through oral history (Balunas and Kinghorn, 2005). Plants have been used as treatments for cancer. The problem here is that in many cases the term “cancer” is poorly defined and is often referred to as hard swellings like calluses, polyps

or tumours. This applies to visible conditions, but may correspond to a cancerous condition. Thus, research into the efficacy and the safety of plants used for treatment is promoted as plants have played an important role as a source of anti-cancer compounds. It has been reported that over 60% of the anti-cancer drugs that are in use today are derived from natural sources, including terrestrial plants, marine organisms and micro-organisms (Cragg and Newman, 2005). Agents derived from plants are in clinical use, in clinical development and in preclinical development.

Africa is one of the continents with the richest biodiversity in the world, however little effort has been devoted to development of chemotherapeutic agents from medicinal plants. It is estimated that only 15% of the world's plants have been screened for their therapeutic values (Louw *et al*., 2002; McGaw and Eloff, 2008). The World Health Organization (WHO) has recognized that 80% of the African population make use a traditional medicine (Gurib-Fakim, 2006) and therefore it is important to report on the efficacy and the safety of the use of medicinal plants.

3.1.3. Cell death and Apoptosis:

Cell death can be classified in one of four ways according to the Nomenclature Committee on Cell Death (NCCD) 2009.

1. Morphological appearance
2. Enzymological criteria
3. Functional aspects
4. Immunological characteristics

Several distinctive modes of cell death exist and are characterized by differences in morphology and biochemical changes between the modes of cell death. Modalities of cell death include apoptosis, necrosis, autophagy and cornification. Atypical cell death modalities include mitotic catastrophe, anoikis, excitotoxicity, Wallerian degeneration, paraptosis, pyroptosis, pyronecrosis and entosis (Kroemer *et al.*, 2009). Dying cells are in a process that is reversible until a "point of no return" is passed. Once this is passed, one can only define the cell as dead if the cell has lost the integrity of the plasma membrane, the cell has completely fragmented and its fragments are then engulfed by other cells. "Points of no return" to define a dying cell are considered to be massive activation of cysteine-dependent aspartate-directed

proteases (caspases), mitochondrial membrane permeabilisation, depolarisation of the mitochondrial membrane and exposure of phosphatidyl serine on the outer plasma membrane. These specific biochemical changes can be detected using various immunochemical methods including microscopy and flow cytometry (Kroemer *et al.*, 2009).

As discussed, cancer is described as a cells ability to continue proliferating without the ability to die. Kroemer *et al.* (2009) describes many ways that cells die, so the question arises: What makes apoptosis such a popular target to treat cancer?

Apoptosis was first defined by Kerr *et al.* (1972), where the term was proposed as a mechanism of controlled cell deletion and appeared to have a complementary but opposite role to mitosis for the regulation of cell populations. Kerr *et al.* (1972) showed that apoptosis occurs in two distinctive stages. The first stage is the formation of apoptotic bodies and the second stage is the engulfment of these bodies. Today, apoptosis is characterized by morphological changes such as membrane blebbing, cytoplasmic and chromatin condensation as well as apoptotic body formation. It is also characterized by biochemical changes including caspase activation, DNA fragmentation and phosphatidylserine (PS) translocation (Elmore, 2007). Caspases are responsible for the proteolytic cleavage of cellular proteins leading to the characteristic apoptotic features (Vermeulen *et al.*, 2005).

Apoptosis is initiated by extracellular or intracellular signals in which a complex machinery is activated to start a cascade of events ultimately leading to the degradation of nuclear DNA and dismantling of the cell. The event of apoptosis needs to be regulated as too little apoptosis may result in cancer, autoimmune or chronic inflammatory diseases; too much apoptosis may lead to stroke-induced neuronal damage and neurodegenerative disorders (Zangemeister-Wittke and Simon, 2001).

The process of apoptosis is controlled by a diverse range of cell signals. Extracellular signals include growth factors and cytokines and must either cross the plasma membrane or transduce to affect a response. These signals may trigger or repress apoptosis. A cell initiates intracellular apoptotic signalling in response to a stress, which may bring about cell suicide. The binding of nuclear receptors can trigger the release of intracellular apoptotic signals by a damaged cell. Before the actual process of cell death occurs, apoptotic signals must cause regulatory proteins to initiate the apoptosis pathway.

Two apoptotic pathways exist and are known as the extrinsic and intrinsic apoptotic pathways. These pathways are also referred to as the death receptor pathway and the mitochondrial pathway, respectively.

3.1.3.1. Extrinsic apoptotic pathway:

Death receptors present on the surface of the outer membrane of the cell are members of the tumour necrosis factor (TNF) receptor gene superfamily that consists of more than 20 proteins. Death receptors are recognized by their 80 amino acid cytoplasmic domains which are known as the "death domains" and this domain plays the important role of transmitting the death signal from the surface of the cell to the intracellular signalling pathways. A number of death receptor proteins have been identified (Fulda and Debatin, 2006). When an extracellular signal is received and transmitted, initiator caspases, caspase-2, -8, -9, -10, -11 and -12, will respond. Initiator caspases are closely coupled to pro-apoptotic signals. Activation of death receptors such as Fas and TNF receptor (TNFR) leads to the activation of caspase-8 and -10. Ligand binding induces receptor clustering and recruitment of the adaptor protein Fas-associated death domain (FADD) and the initiator caspases 8 or 10 as procaspases, forming a death-inducing signalling complex (DISC). Formation of the DISC brings procaspase molecules into close proximity of one another, facilitating their autocatalytic processing and release into the cytoplasm where they activate effector caspases 3, 6, and/or 7. These activated caspase molecules execute apoptosis by cleaving cellular proteins following specific Asp residues (Thornberry and Lazebnik, 1998; Vermeulen *et al.*, 2005; Zangemeister-Wittke and Simon, 2001). Death receptor signalling through CD95, TNF-related apoptosis-inducing ligand (TRAIL) receptors 1 and 2 (TRAIL-R1 and TRAIL-R2, respectively) also allow for the activation of caspases and the onset of apoptosis (Reed and Pellecchia, 2005; Fulda and Debatin, 2006).

Cancer cells have evolved a number of strategies to evade cell death via the extrinsic apoptotic pathway. It has been shown that surface expression of death receptors vary between different cell types and can be downregulated or even absent in resistant forms of tumours (Fulda and Debatin, 2006). Strong downregulation of CD95, deficient transport of TRAIL-R1 and -R2, mutations of the CD95 gene, expression of decoy receptors which competitively bind CD95 ligands, loss of expression of TRAIL-R1 and -R2 and impaired surface expression of death receptors have all been implicated in the resistance of cancer cells to apoptosis

(Friesen *et al.*, 1997; Pitti *et al.*, 1998; Roth *et al.*, 2001; van Noesel *et al.*, 2002; Debatin *et al.*, 2003; Jin *et al.*, 2004).

Cell signalling by the death receptors can also be negatively regulated by proteins that associate with the cytoplasmic domain of the death receptor protein, e.g. FLICE-inhibitory protein (FLIP). The recruitment of FLIP to the DISC instead of pro-caspase 8 or -10 can block the activation of effector caspases (Krueger *et al.*, 2001).

The CD95 receptor system has been implicated in chemotherapy as a target to induce cell death. Treatment with various anticancer agents including doxorubicin and cisplatin has triggered an increase in the expression of CD95L (Fulda and Debatin, 2006).

3.1.3.2. Intrinsic apoptotic pathway:

The intrinsic pathway is initiated from within the cell. This is usually in response to cellular signals resulting from DNA damage, a defective cell cycle, detachment from the extracellular matrix, hypoxia, loss of cell survival factors, or other types of severe cell stress. This pathway involves the release of pro-apoptotic proteins from the mitochondria which in turn activates caspases. This process ultimately triggers apoptosis. The intrinsic apoptotic pathway depends on the balance of activity between pro- and anti-apoptotic members of the Bcl-2 superfamily of proteins, which act to regulate the permeability of the mitochondrial membrane (Vermeulen *et al.*, 2003).

The anti-apoptotic proteins Bcl-2 and Bcl-xL reside in the outer mitochondrial membrane and inhibit cytochrome *c* (cyt-*c*) release. The proapoptotic Bcl-2 proteins Bad, Bid, Bax and Bim may reside in the cytosol but translocate to mitochondria following death signalling, where they promote the release of cyt-*c*. Bad translocates to mitochondria and forms a pro-apoptotic complex with Bcl-xL. This translocation is inhibited by survival factors that induce the phosphorylation of Bad, leading to its cytosolic sequestration. Cytosolic Bid is cleaved by caspase-8 following signalling through Fas, its active fragment truncated Bid (tBid) translocates to mitochondria. Bax and Bim translocate to mitochondria in response to death stimuli, including survival factor withdrawal. Activated following DNA damage, p53 induces the transcription of Bax, Noxa and PUMA (Adams and Cory, 1998; Vermeulen *et al.*, 2005). Upon release from mitochondria, cyt-*c* binds to Apaf-1 and forms an activation complex with

caspase -9, called the apoptosome. The primary function of the apoptosome seems to be multimerisation and allosteric regulation of the catalytic activity of caspase -9. Initiator caspase -9 is recruited into the apoptosome and activated from within the adaptor protein complex, which in turn activates the downstream effector caspases -3, -6, and/or -7, resulting in apoptosis (Zangemeister-Wittke and Simon, 2001).

Mutations in genes involved in the regulation of the mitochondrial proteins and are common in cancer cells and hence, cancer cells can evade apoptosis (Fulda and Debatin, 2006). Examples include the overexpression of anti-apoptotic Bcl-2 proteins as a result of chromosomal translocation of the *BCL-2* oncogene into the immunoglobulin heavy chain gene locus (Tsujimoto *et al.,* 1984). A decrease or the absence of activity of Apaf-1 has also been found in ovarian cancer, melanoma and leukaemia (Fulda and Debatin, 2006).

Strategies in targeting the intrinsic apoptotic pathway include the development of drugs regulating *BCL-2* gene expression, drugs attacking Bcl-2 mRNA and drugs attacking Bcl-2 proteins. Gossypol is a compound that has been isolated from cottonseeds that are traditionally used as a herbal medicine in China. It is a small molecule inhibitor that directly binds Bcl-2 proteins in a hydrophobic pocket of the protein (Kitada *et al.,* 2002; Pellecchia and Reed, 2004). Activating endogenous antagonists of Bcl-2 proteins has also been implicated in targeting the intrinsic pathway of apoptosis (Reed and Pellecchia, 2005).

Links between the extrinsic and the intrinsic apoptotic pathways exist at different levels and thus both pathways can be activated at the same time (Fulda and Debatin, 2006). The two apoptotic pathways are summarised in Figure 3.1.

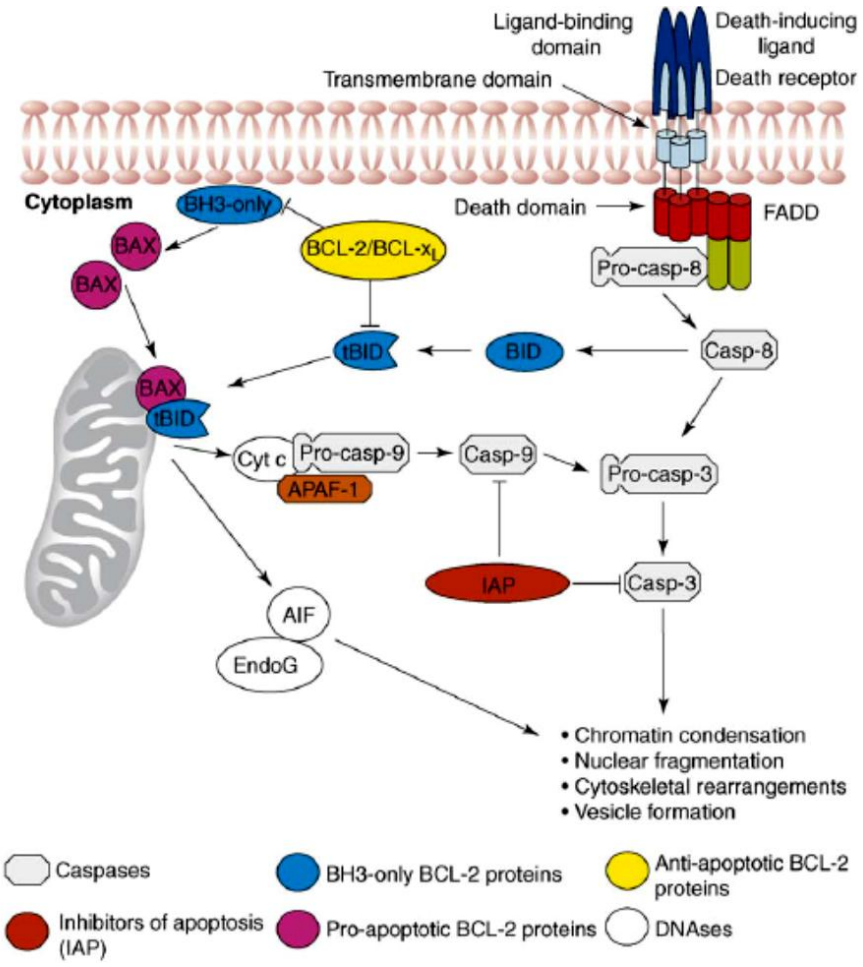

Figure 3.1: Molecular mechanisms of apoptosis showing the intrinsic and extrinsic pathways (Bremer *et al.*, 2006).

3.1.4. The cell cycle:

Cell division requires a precisely ordered sequence of biochemical events that assures every daughter cell a full complement of the biological molecules required for the functioning of the body. When the regulatory mechanisms of cell division become defective, the result can be catastrophic and cancer can arise (Collins *et al.*, 1997b). The cell cycle is the mechanism by which cells grow and divide. The progression of a cell through the cell cycle involves the complex interaction of a number of proteins in a systematic and co-ordinated fashion. Apoptosis is the controlled mechanism of cell death and also involves distinct processes, as discussed. Both the cell cycle and apoptosis play important roles in cellular homeostasis and the development and progression of cancer (Shah and Schartz, 2001).

The normal cell cycle is divided into 4 phases, the G1, S, G2 and M phase. The G0 phase is a phase where cells enter into when it has stopped cycling after division and can enter a state of quiescence. The differences in the phases of the cell cycle can be characterised by the differences in the DNA content or ploidy of the cell in a certain phase. The G1/G0 phase consists of diploid (2N), the G2/M phase consists of tetraploid (4N) and the S phase consists of intermediate DNA content.

At least two types of control mechanisms for the progression of the cell cycle are recognized. The first mechanism is the cascade of phosphorylation of proteins that allow the cell to pass from one phase into the next. The second mechanism is the set of checkpoints that monitor the completion of events of the cell cycle and prevent or delay progression to the next phase if necessary (Collins *et al.*, 1997b). This is regulated by proteins known as Cdks (also known as Cdc) and cyclins (Figure 3.2) and is discussed in more detail in Chapter 6.

Cancer occurs when cells experience uncontrolled cell division and growth when there is damage to the DNA of the cell or when mutations arise in the DNA of the cells. Cell division is regulated by extracellular growth factors, proteins that cause a resting cell to divide. Defects in the synthesis, the regulation or the recognition of growth factors can lead to cancer.

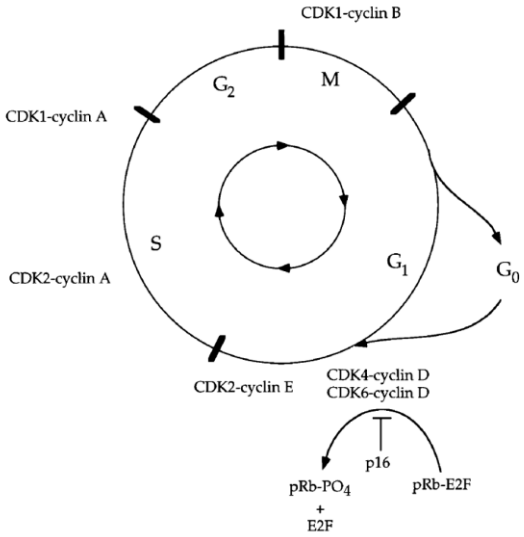

<u>Figure 3.2:</u> A schematic representation of the mammalian cell cycle, indicating the position of the checkpoints and the Cdk-cyclin complexes regulating the transition of the cell through every phase (Collins *et al.*, 1997b).

3.1.5: Aims:

Cytotoxity of *A. afra* has been previously reported as stated in Chapter 1 and 2, but no reported evidence of its mode of induced cell death exists. Cells can die in many different ways (3.1.3) and the modes of cell death vary greatly biochemically and morphologically. These changes can be exploited in the investigation of the mechanisms of cell death induced by a plant extract or compound(s). Due to the evident cytotoxicity induced by *A. afra* (Liu *et al*, 2009), it was hypothesized that *A. afra* induces apoptosis as the mechanism of cell death. Biochemical analysis was performed by investigating phosphatidylserine translocation, mitochondrial membrane permeabilization, caspase activation and DNA fragmentation. Cell cycle checkpoints appear to link the cell cycle and apoptosis and thus, analysis of the cell cycle was also performed after exposure to the plant extract. The data obtained in this chapter will clearly outline the induced mode of cell death experienced as a result of exposure to *A. afra.*

3.2. Materials:

Cervical (HeLa) cancer and human promonocytic leukaemia U937 cells as well as Chang Liver cells were purchased from Highveld Biological, South Africa. Cleaved caspase-3 (Asp175) and -8 (Asp391) antibodies as well as goat anti-rabbit IgG (H+L chain specific) and rabbit IgG isotype, both conjugated with Alexa 488 were purchased from Cell Signaling Technology, Inc. (Danvers, MA, USA). The Coulter® DNA Prep™ reagents kit and IsoFlow™ EPICS™ sheath fluid were purchased from Beckman Coulter (CA, USA). MEBSTAIN apoptosis kit direct and IntraPrep™ permeabilising reagent were purchased from Immunotech (Marseille, France). Annexin V-FITC kit was purchased from MACS Miltenyi Biotec (Auburn, USA). 3-(4,5-dimethyl-2-thiazolul)-2,5-diphenyl-2H-tetrazolium bromide (MTT) and 5,5',6,6'tetrachloro-1,1',3,3'-tetraethylbenzimidazol-carbocyanine iodide (JC-1) was purchased from Sigma (St. Louis, MO, USA). CellTiter-Blue® reagent was purchased from Promega (Madison, WI, USA).

3.3. Methods:

3.3.1. Aqueous and ethanol extraction preparation of *Artemisia afra* leaves:

Herbarium specimen voucher nember *A. afra* 15487 was deposited in the Nelson Mandela Metropolitan University Herbarium, Botany Department, South Campus. Fresh leaves were obtained, dried, weighed and ground using a blender. An aqueous extract and ethanol extract was prepared by submerging the ground leaves in deionized water and 80% ethanol, respectively. The submerged leaves were incubated in the dark at room temperature overnight. After incubation, the liquid was filtered through 11 µm Whatman filter paper. Thirty milliliter aliquots of the aqueous filtrate were placed in 50 mL tubes and left at -80°C overnight. The ethanol filtrate was concentrated by placing the filtrate in a round bottomed flask, securing it in a 45°C water bath and the ethanol was evaporated using nitrogen gas. The remaining ethanol was reconstituted in deionised water and frozen, overnight, at -80°C in 40 mL aliquots. The samples were then placed on the freeze dryer until the samples had a powder appearance. The aqueous and ethanol extracts were pooled separately. Extracts were stored in a dessicator at 4°C in the dark.

3.3.2. Cell line maintenance:

The cell lines that were selected for the study of the anti-cancer mechanism of *A. afra* were the cervical cancer cell line, HeLa and the human promonocytic leukemia cell line, U937. The continuous human Chang liver cell line and the normal African green monkey kidney cell line, known as Vero, were used as a control cell line. The two cancer cell lines were routinely maintained in 10 cm culture dishes and flasks, respectively, in Roswell Park Memorial Institute (RPMI) 1640 cell culture medium containing 25 mM Hepes, 2 mM glutamine and 10% foetal bovine serum (FBS) (ThermoScientific, Logan, Utah, USA) in a humidified 5% CO_2 incubator at 37 ºC. No antibiotics were added to the medium. Chang liver cells were maintained in the same way as HeLa cells. Vero cells were maintained in DMEM medium supplemented with 5% FBS.

3.3.3. Cytotoxicity of *A. afra* extracts:

3.3.3.1. Background:

Cytotoxicity is defined as the ability of an agent to produce a toxic effect on a cell. Cytotoxicity assays are used to test the ability of cells to continue proliferating in the presence of a test compound or substance over a specific time period. Cytotoxicity testing is a popular method used for the screening of pharmaceutical products and is also popular in the field of ethnopharmacology where plant extracts are screened.

The methods used in this study to determine cell viability were the MTT and CellTitre-Blue assays. The MTT assay is a quantitative colourimetric assay that makes use of 3-(4,5-dimethylthiazol-2-yl)-2,5-diphenyltetrazolium bromide (MTT) sodium salt. The tetrazolium salt is water soluble yielding a yellow colour when prepared in medium or buffers. Mitochondrial enzymes of living cells are able to reduce the tetrazolium dye to formazan, an insoluble purple product (Figure 3.3). The purple formazan product is not able to escape living cells due to the impermeability of cell mambranes and thus accumulates in the cell. Therefore, the amount of formazan product is directly proportional to the amount of healthy, living cells (Holst-Hansen and Brünner 1998; Sylvester, 2011, www.sigma.com). The insoluble formazan product is then dissolved in an organic solvent, popularly DMSO, and the colour product is quantified spectrophotometrically (540nm) as a function of the concentration of reduced tetrazolium dye. In this study, the MTT assay was used for the adherent cell lines HeLa, Chang liver and Vero cells. However, the MTT assay was modified as plant extracts with high antioxidant activity can interfere with the original assay described by Mossman where MTT is added directly to the test wells. The plant extract is first removed and replaced with fresh medium containing the required concentration of MTT.

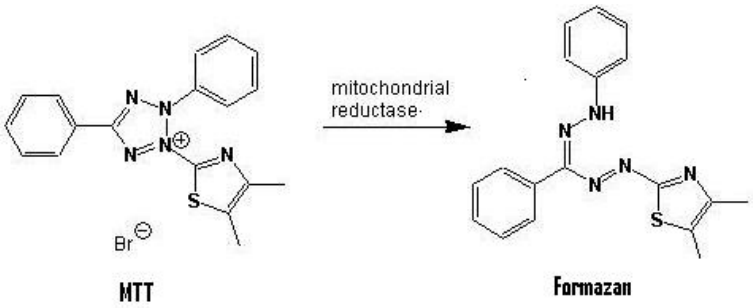

Figure 3.3: The reduction of soluble MTT to insoluble formazan by mitochondrial reductase (www.biotek.com) .

The viability of U937 cancer cells was determined using the CellTiter-Blue cell viability assay from Promega. This assay provides a homogeneous, fluorescent method for monitoring cell viability. It is based on the ability of living cells to convert the redox dye resazurin into a fluorescent end product resorufin as shown in Figure 3.4 (O'Brien *et al.*, 2000; Gonzalez and Tarloff, 2001). The homogeneous assay procedure involves adding the single reagent directly to cells.

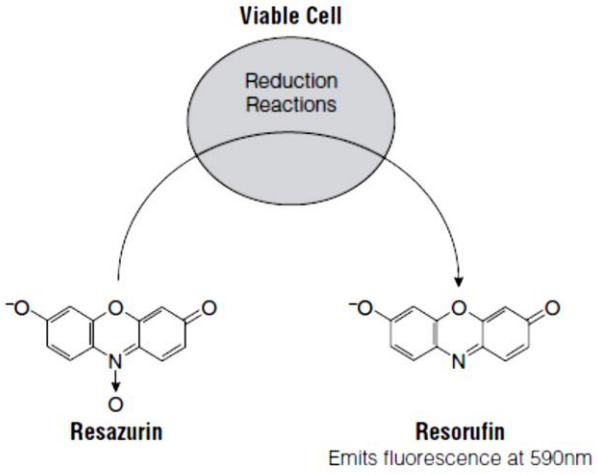

Figure 3.4: Conversion of resazurin to resorufin by metabolically active cells resulting in the generation of a fluorescent end product that can be measured at 590nm (www.promega.com).

3.3.3.2. Cytotoxic evaluation of an aqueous and ethanolic extract of A. afra *using MTT and CellTiter Blue cell viability assays:*

HeLa and U937 cells were seeded in 200 and 100 µL aliquots, respectively, at $3x10^4$ cells/mL in 96 well plates and HeLa cells were left overnight to attach. U937 cell were also incubated overnight at 37°C before treatment. For treatment of HeLa cells the medium was replaced with fresh medium containing varying concentrations (1.25 - 250 µg/mL) of aqueous and ethanolic extracts. One hundred microlitre aliquots of fresh medium containing double the appropriate extract concentration was added to the respective wells for treatment of U937 cells. Both cell lines were incubated at 37°C in a humidified 5% CO_2 incubator for 48 hours. The medium containing *A. afra* extract was removed prior to addition of MTT to HeLa cells. Melphalan (40 µM) was used as a positive control for all experiments. Treatments (*A. afra)* were removed and replaced with 200 µL of medium containing 0.5 mg/mL MTT. Cells were incubated for 3 hours. Thereafter, medium was removed and the blue formazan product was solubilized in DMSO. Chang liver cells and Vero cells were treated in the same way as

described for HeLa cells, however, confluent cells were tested whereas cancer cells were treated in log phase. Absorbance was read at 540 nm using a BioTek® PowerWave XS spectrophotometer (Winooski, VT, USA) for HeLa, Chang liver and Vero cells. Forty microlitres of CellTiter Blue was added directly to each well for the cytotoxicity determination against U937 cells and incubated for 3 hours at 37°C. Fluorescence was read at $544_{Ex}/590_{Em}$ using a Fluoroskan Ascent FL fluorometer (ThermoLabsystems, Finland) for U937 cells. Each treatment was performed in quadruplicate and the experiment was carried out 3 independent times. IC_{50} values of *A. afra* extracts were determined using GraphPad Prism Version 4.0 (GraphPad Software, San Diego, USA).

An IC_{50} was also determined for melphalan against HeLa cells in the same way as for *A. afra* extracts. The concentration range used was 1.5625 µM – 400 µM, based on previously reported IC_{50} data of melphalan on other cell lines (Kühne *et al.,* 2009).

3.3.4. Cell cycle analysis:

3.3.4.1. Background:

As described in section 3.1.4, cells need to progress through every phase of the cell cycle to assure a full copy of DNA for a new daughter cell. Checkpoints regulate the progression of cells through the cycle and will cause cell cycle arrest if DNA damage or DNA stress has occurred. Cell cycle arrest is defined as a high proportion of cells found in the same cycle event at a specific time. Cell cycle arrest will be maintained until DNA repair is complete (Nojima, 2004). Cell cycle analysis is performed to determine the state of DNA in response to treatment of the cell with a particular compound or extract. The distribution of DNA content is important as it will lead to the identification of targets or pathways to target for the treatment of cancer and tumours (Planchais *et al.,* 2000).

DNA distribution is analysed using propidium iodide (PI), a double stranded DNA-binding dye. Cells first need to be fixed and permeabilized in order to allow the entry of PI into the cell (Krishan, 1975).

3.3.4.2. DNA distribution and cell cycle analysis:

U937 cells were seeded at $1x10^5$ cells/mL in 10 mL aliquots in culture flasks and HeLa cells were seeded at $5x10^4$ cells/mL in 10 mL aliquots in 10 cm culture dishes and treated with 20 µg/mL and 30 µg/mL of ethanolic *A. afra* extract, respectively. Melphalan (40 µM) was used as a positive control. Cells were incubated for 12, 24 and 48 hours. After the appropriate incubation period, HeLa cells were trypsinized for 10 minutes, resuspended in phosphate buffered saline containing Ca^{2+} and Mg^{2+} (PBS) and transferred to polypropylene tubes. U937 cells did not require trypsinization. The Coulter® DNA Prep™ reagents kit was used for DNA cell cycle analysis, as per manufacturer's instructions. Briefly, 100 µL lysis reagent (<0.1% sodium azide, non-ionic detergents, saline and stabilizers) was added to each tube and incubated for 5 minutes at room temperature. Thereafter 500 µL propidium iodide (50 µg/mL) was added and tubes were incubated for 15 minutes at 37 °C. Flow cytometric analysis was performed directly after incubation. A Beckman Coulter Cytomics FC500 was used for all flow cytometry analysis (3.3.10). Each experiment was performed in triplicate and each experiment was repeated 3 times. Results were analysed using Multicycle version 4.0 software.

3.3.5. Phosphatidylserine translocation (PS):

3.3.5.1. Background:

Healthy, viable cells maintain an asymmetric distribution of phospholipids between the inner and the outer leaflet of the cell membrane. PS is an aminophospholipid that is primarily located on the inner leaflet of the cell membrane. Flippases are enzymes that maintain the asymmetry of the plasma lipid membrane and it is known that the translocation of phospholipids is Mg^{2+}/ATP-dependent (Connor *et al.,* 1994; van Engeland *et al.,* 1998).

Cell surface exposure of PS is important in catalysing coagulation by activated platelets and the elimination of senescent erythrocytes through the reticuloendothelial system (Chancerelle *et al.,* 1994). It was shown that an early feature of apoptosis is the loss of phospholipid asymmetry and this resulted in the exposure of PS on the outer surface of the cell membrane (Koopman *et al.,* 1994; Martin *et al.,* 1995). Fadok *et al.* (1992) and Fadok *et al.* (1993) showed that leukocytes expose PS on the outer surface during apoptosis and that PS functions

as a tag for the engulfment of this cell by surrounding macrophages, respectively. Thus, a marker of early apoptosis is the loss of phospholipid asymmetry and the resultant appearance of PS on the outer surface of the cell membrane (Koopman *et al.,* 1994). However, in necrosis, PS also becomes accessible due to the disruption of the cell lipid membrane (Martin *et al.,* 1995).

PS can be detected using Annexin V, a 35kDa Ca^{2+} dependent protein that has a high affinity for PS and not phosphatidylcholine, phosphatidylinositol, phosphatidic acid, sphingomyelin and phosphatidylethanolamine (Martin *et al.,* 1995). Koopman *et al.* (1994) described a method for the detection of PS using Annexin V with a conjugated fluorophore, flourescein isothioscyanate (FITC). FITC has excitation and emission wavelengths of approximately 495nm and 519nm, respectively (Figure 3.5).

PI is used in conjunction with Annexin V to discriminate between early apoptotic cells, necrotic cells and dead cells. PI is a membrane impermeable dye, but it can enter cells that have lost membrane integrity. Hence, PI will not enter apoptotic cells. Therefore, the Annexin V-FITC/PI apoptosis assay is a popular method to distinguish between four cell populations. These populations are unstained or viable cells (Annexin V-negative; PI-negative), early apoptotic cells (Annexin V-positive; PI-negative), late apoptotic cells (Annexin V-positive; PI-positive) and unviable, necrotic or permeabilized cells (Annexin V-negative; PI-positive) (Aubry *et al.,* 1999).

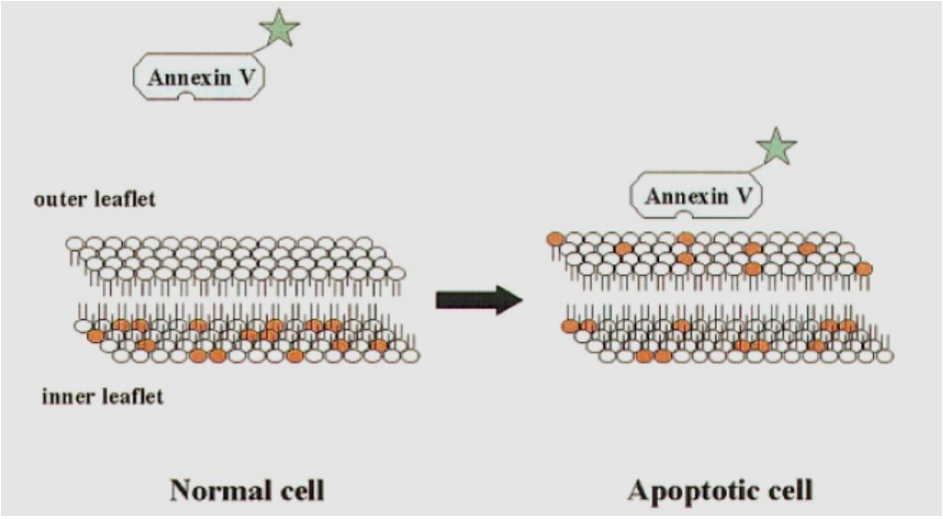

Figure 3.5: Loss of cell membrane asymmetry and the exposure of PS (red circles) on the outer surface of the lipid membrane during apoptosis. Annexin V binds with high affinity to PS and can be detected (van Engeland *et al.,* 1998).

3.3.5.2. Determination of PS translocation:

U937 cells were seeded at $1x10^5$ cells/mL in 10 mL aliquots in culture flasks and HeLa cells were seeded at $5x10^4$ cells/mL in 6 well culture plates, using 3 mL per well, and treated with 20 µg/mL and 30 µg/mL of ethanolic *A. afra* extract, respectively. Cells were incubated for 24 hours at 37°C. After treatment and incubation, HeLa cells were washed with ice-cold Dulbecco's Modified Eagle's Medium (DMEM). Accutase was used to detach the HeLa cells from the culture plate. Cells were incubated for 10 min with accutase and then resuspended in PBS. Cells were transferred to polypropylene tubes and centrifuged at 500 x g for 5 minutes at room temperature and washed with PBS to remove accutase. U937 cells did not require the detachment step. Cells were then stained according to Annexin V-FITC/PI Kit protocol (MACS Miltenyi Biotec). In brief, after centrifugation, the supernatant was discarded and cell pellets resuspended in ice-cold 1X binding buffer. Annexin V-FITC (1 µL; 25 µg/mL) and PI (5 µL; 250 µg/mL) were added to each tube. Compensation control tubes contained cells with Annexin V-FITC only, PI only and combination of Annexin V-FITC and PI. Tubes were gently mixed and incubated on ice for 15 min in the dark. Samples were read within 30 min on a Beckman Coulter Cytomics FC500 and recorded in FL1. Each experiment was performed in triplicate and each experiment was repeated 3 times.

3.3.6. Depolarisation of the mitochondrial membrane:

3.3.6.1. Background:

Permeabilisation of the mitochondrial membrane is a feature of apoptosis. Permeabilization of the mitochondrial membrane results in the release of pro-apoptotic proteins, particularly cyt-*c.* The release of these pro-apoptotic proteins allows for the formation of an apoptosome and the activation of caspases that orchestrate the process of apoptosis (Gogvadze *et al.*, 2009).

The mitochondria are responsible for energy production of the cell in the form of ATP. Energy is released during oxidation reactions of the mitochondrial respiratory chain and the energy is stored as an electrochemical gradient. This generates a transmembrane electrical potential across the mitochondrial membrane with a negative potential inside of 180 – 200 mV. Membrane permeable and membrane potential-sensitive compounds exploit this

property. Advantages associated with the successful use of these dyes are attributed to their non-destructive properties and lack of immediate toxicity (Reers *et al.,* 1991). Popular fluorescent probes that have been used are divided into two classes based on their response time, i.e. fast and slow dyes. It has been established that slow dyes have more applications and are thus used more frequently. These dyes include rhodamines and carbocyanines (Sims *et al.,* 1974; Johnson *et al.,* 1980).

Carbocyanines are lipophilic cationic dyes that are able to cross membranes (Sims *et al.,* 1974). These molecules redistribute between cellular compartments according to the membrane potential experienced. The only forces that determine the equilibrium of the dye distribution is the negative electric field inside and the chemical gradient (Reers *et al.,* 1991). JC-1, (5',6',6'-tetrachloro-1,1',3',3'-tetraethylbenzimidazolylcarbocyanine iodide) is a carbocaynine with a delocalized positive charge which allows for the electrophoretic uptake towards a negatively charged matrix. Thus, the dye exhibits potential-dependent accumulation in the mitochondria. It contains a highly symmetrical polymethine-linked fluorophore that consists of two heterocyclic structures. Both heterocyclic moieties contain chlorine molecules which are described as electron-drawing and accounts for the low pKa of the molecule (structure indicated in Figure 3.6). Its structure relates directly to its function as a membrane permeable dye.

JC-1 forms aggregates when present in high concentrations. JC-1 will enter the cell and accumulate in the mitochondria and form J-aggregates. During apoptosis, the mitochondrial membrane potential decreases and the mitochondria become permeable; JC-1 will not aggregate in the mitochondria, and will remain in its monomeric form. This is indicated by a fluorescence emission shift from 530nm to 590nm, i.e. from green to red (Reers *et al.,* 1991).

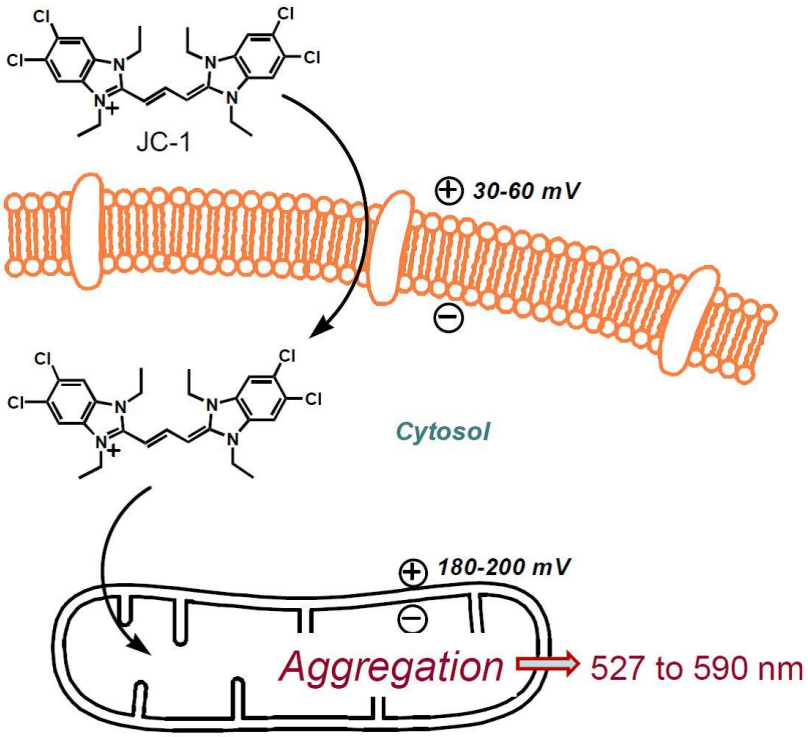

Figure 3.6: The mechanism of action and the structure of JC-1 (http://lcbim.epfl.ch/research).

3.3.6.2. Mitochondrial membrane potential (MMP) analysis:

U937 and HeLa cells were seeded and treated as described in section 3.3.5.2. Cells were incubated for 24 and 48 hours. HeLa cells were washed with Ca^{2+} and Mg^{2+} free PBS (DPBS), trypsinised for 10 min and resuspended in PBS. Cells were centrifuged at 500 x g for 5 minutes at room temperature and washed with PBS to remove trypsin. U937 cells did not require the trypsinisation step. Cells were then collected by centrifugation at 500 x g for five minutes at room temperature. Thereafter, JC-1 was added to each tube to a final concentration of 2 µg/mL. Cells were incubated for 10 minutes at room temperature in the dark. The cells were washed using 500 µL PBS and centrifuged at 500 xg for 5 minutes. The wash step was repeated three times before flow cytometric analysis. Data was recorded in FL1. Treatment was performed in triplicate and the determination of the effect of *A. afra* ethanolic extract on MMP was repeated three independent times at 24 hours. The assay was not repeated at 48 hours due to the increased number of apoptotic cells.

3.3.7. Caspase activation:

3.3.7.1. Background:

Caspases are a family of cysteine proteases that play an important role in apoptosis. Their role first became evident when a death-related gene of *Caenorhabditis elegans, ced-3,* was found to be essential for apoptosis and was also found to be homologous to the mammalian caspases (Wang and Lenardo, 2000). It has since been shown that caspases are the essential effector molecules that are responsible for many of the morphological and biochemical features of apoptosis.

Caspases are synthesized as proenzymes and exist as zymogens. These enzymes contain a prodomain (amino-terminal domain) and a protease domain, consisting of a small and large subunit. The prodomain needs to be cleaved in order for it to be active (Thornberry and Lazebnik, 1998, Thornberry, 1998). The prodomain and the protease domain are partitioned by an Asp residue and cleavage occurs at this specific Asp residue to activate the enzyme. Substitution of the Asp residue with another amino acid, including glutamate, results in a >100 fold decrease in catalytic efficiency (Sleath *et al.,* 1990). The active enzyme exists as a heterodimer. All caspases contain an active site pentapeptide with the general structure of QACXG, where X can be R, Q or G. This pentapeptide motif surrounds the catalytic centre containing the amino acids Cys and His (Cohen, 1997).

At least 14 members of the caspase family exist. They are distinguished by differences in

i) Their substrate specificity.
ii) The length of their prodomain.

Group I caspases favour hydrophobic amino acid residues with the optimal sequence WEHD (caspase -1, -4 and -5). Group II caspases prefer the sequence DEXD (caspase -2, -3 and -7) and Group III caspases prefer the substrate sequence of V/LEXD (caspase -6, -8, -9 and -10). Group I are known as the mediators of inflammation, Group II as the effectors of apoptosis and Group III as the activators of apoptosis (Thornberry, 1998).

The length of the prodomain of caspases varies between 2 – 25 kDa. Caspases with long prodomains are believed to be the upstream initiator caspases. By contrast, caspases with

short prodomains are said to be the executioner caspases (Figure 3.7). Caspase -8 and -10 contain two tandem repeats known as the "death effector domains" (DEDs) within their prodomains. This is important for their recruitment to the death-inducing signalling complex (DISC) via the interaction with FADD. Caspase -1, -2, -4 and -9 contain a "caspase recruitment domain" (CARD) and it mediates the interaction and the aggregation of Apaf-1 and pro-caspase 9 (Wang and Lenardo, 2000).

Initiator caspases can be activated by the extrinsic and/or the intrinsic pathways of apoptosis. Caspase -8 can directly induce apoptosis by the cleavage of executioner caspases or indirectly by cleaving Bid. Bid is a pro-apoptotic protein that provides a link between the extrinsic and intrinsic modes of apoptosis (Kantari and Walczak, 2011). Once cleaved, Bid is known as truncated Bid (tBid) and is capable of altering the permeabilising of the outer mitochondrial membrane. This allows for the release of other pro-apoptotic proteins, including cyt-*c* from the mitochondria. Bid can also be cleaved by caspase -3, if caspase -3 is in high concentrations (Luo *et al.,* 1998).

As mentioned, the executioner caspases are responsible for the morphological evidence of apoptosis. This evidence includes membrane blebbing, DNA fragmentation and cytoskeleton rearrangement (Elmore, 2007). Cleavage of several proteins results in the morphological changes and caspase -3 is responsible for the cleavage of a large number of these proteins. The proteins include PARP, DNA-dependent protein kinase, sterol regulatory binding proteins, Huntingtin protein and the retinoblastoma protein, Rb. A common feature of these substrates is the presence of the DXXD motif (Cohen, 1997).

Because of the central role that caspases play in the onset of apoptosis, the presence of active caspase -8 and -3 after treatment of cancer cells with an ethanolic extract of *A. afra* were investigated in this study.

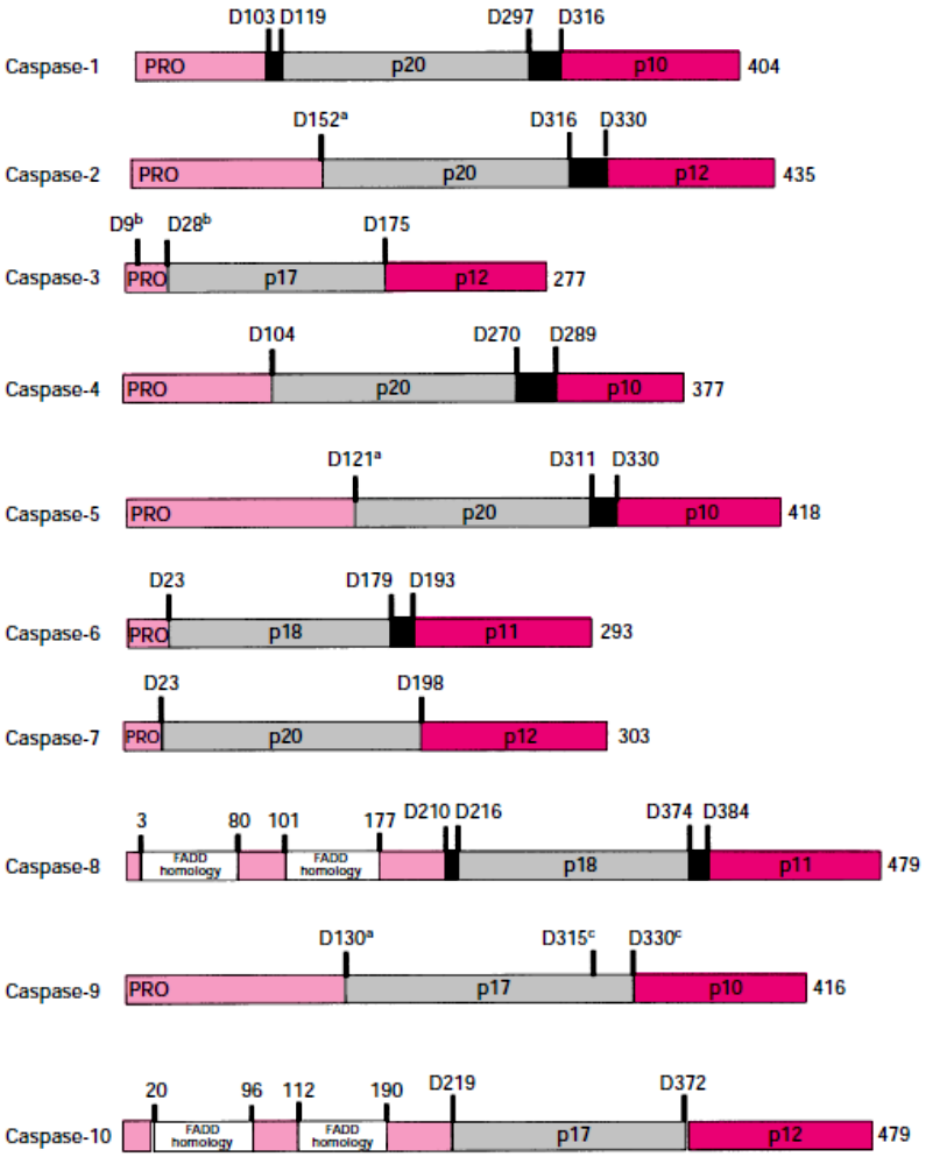

Figure 3.7: Proenzyme organization of caspases indicating the variable length of prodomains (Cohen, 2000).

3.3.7.2 Caspase -8 and -3 activation:

HeLa and U937 cells were seeded as described for PS translocation (3.3.5.2). HeLa and U937 cell lines were treated with 30 µg/mL and 20 µg/mL ethanolic extract of *A. afra*, respectively. Cells were also treated with 40 µM melphalan, the positive control. Treatments were performed in triplicate and each experiment was conducted three independent times. Cells were fixed and permeabilized using the IntraPrep kit as per manufacturer's instructions (Beckman Coulter). This kit allows for the immunological detection of intracellular antigens

by creating apertures in the cell membrane without affecting the morphology of the cell. Cleaved caspase -8 (Asp 391) and cleaved caspase -3 (Asp 175) monoclonal antibodies (Cell Signaling Technology) were used to determine the presence of activated caspase -8 and caspase -3 respectively. A rabbit IgG isotype control was used. Cells were first blocked using PBS containing 0.5% BSA and thereafter incubated with the antibodies separately (1:100 for caspase -8 and 1:50 for caspase -3) for 1 hour at 37°C. Cells were washed and incubated with the Alexa 488 conjugated secondary antibody (1:1000) for 30 minutes at 37°C in the dark. This step was not required for caspase -3 analysis as the antibody contains a conjugated Alexa 488 fluorophore. Cells were washed 3 times by resuspending cell pellets in PBS and centrifuging at 500 xg for 5 minutes. This is required to eliminate unbound antibodies. Cells were then analyzed using flow cytometry.

3.3.8. DNA fragmentation:

3.3.8.1. Background:

The controlled degradation of nuclear DNA is a biochemical feature of apoptosis and is evident after the activation of executioner caspases. Caspase -3 and -7 are responsible for the cleavage and activation of proteins that allow for the fragmentation of nuclear DNA. Degradation of DNA occurs in two steps. The first step is the cleavage of chromosomes into large fragments ranging from 50 kb to 300 kb. The second step is the fragmentation of these large chromosomal fragments. Ca^{2+} and Mg^{2+} dependent endonucleases cleave the chromatin at the linker DNA sites and this results in smaller DNA fragments of approximately 180 bp to 200 bp (Marini *et al*., 1996; Nagata, 2000).

The TUNEL (TdT-mediated dUTP Nick End Labeling) assay is a method that was developed to identify cells that are undergoing apoptosis. The assay allows for the labelling of the ends of DNA with the polymerase terminal deoxynucleotidyl transferase, TdT. This polymerase catalyses the addition of deoxynucleotide triphosphates to the 3'-OH ends of DNA in a template-independent manner (Figure 3.8). In this assay, deoxynucleotide triphosphates are labelled with a fluorophore and this allows for the detection of DNA fragments using standard immunofluorescent techniques.

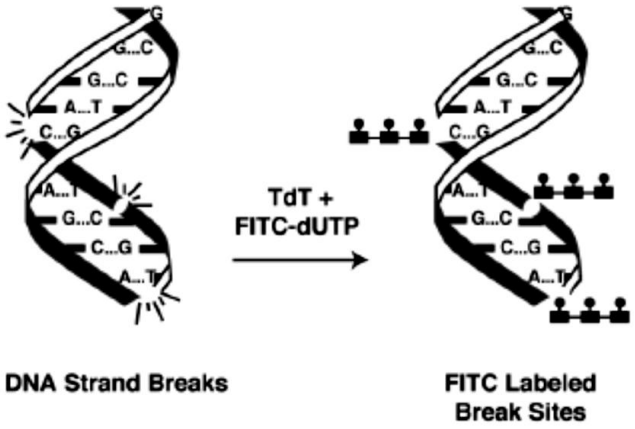

Figure 3.8: Schematic representation of the labelling of fragmented DNA with FITC-labelled deoxyuridine triphosphates to the 3'-OH ends of double- and single stranded DNA (www.bdbiosciences.com).

3.3.8.2. Detection of DNA fragmentation:

HeLa and U937 cells were seeded, treated, fixed and permeabilized as described in 3.3.6.1. The MEBSTAIN Apoptosis kit (Immunotech) was used as per manufacturer's instructions to determine the effect of ethanolic *A. afra* extract on the two cell lines. In brief, 50 µL TdT reaction reagent, made up of TdT buffer, FITC-dUTP and the TdT enzyme in a 18:1:1 (v/v/v) ratio, was added to each cell pellet. The cell pellet was then incubated in the dark for 1 hour at 37 °C. The mean fluorescence intensity (x-mean) was expressed as a percentage of the x-mean of untreated control cells.

3.3.9. Statistical analysis:

All treatments of both cell lines were conducted in triplicates. All experiments were carried out at three independent times. Histogram overlays are one representation of each experiment. Standard deviation (SD) of the mean of three independent experiments was calculated. For each assay, the Student two-tailed *t*-test was performed to determine significance. $p<0.05$ was considered significant, indicated by *, $p<0.005$ is indicated by **. For all flow cytometry assays, a minimum of 10 000 events were recorded for each sample.

3.3.10. Flow Cytometry:

All flow cytometric analysis was performed using a Beckman Coulter Cytomics FC500 equipped with CXP Analysis 2.1 software. Excitation using a uniphase Argon ion, 488 nm (20 mW output) laser or a coherent red solid state diode, 635 nm (25 mW output) laser (single laser system) or both (dual laser system) is possible. Ten thousand events were recorded per sample and detected by customized photomultiplier tubes (PMTs). Interchangeable optical filters are used to detect five different fluorescent colours in a specific channel (FLs). FL1 records green (525 nm), FL2 records orange (575 nm), FL3 records yellow (620 nm), FL4 records red (675 nm) and FL5 records long wavelength red/purple (755 nm) (www.beckmancoulter.com). FL1 was mostly used to detect green fluorescence.

3.4. Results:

The aim of this chapter was to determine the mechanism of cell death induced by *A. afra* extract using HeLa and U937 cancer cells. This was achieved by analysing biochemical features of apoptosis, namely phosphatidylserine translocation, mitochondrial depolarization, caspase activation, DNA fragmentation and cell cycle arrest.

3.4.1. Cytotoxicity and IC_{50} determination::

HeLa, U937, Vero and Chang liver cells were treated with various concentrations of aqueous and ethanol extracts to determine their cytotoxic abilities and thereafter IC_{50} values were determined for each cell line, where applicable. Figures 3.9 and 3.10 are dose-response curves resulting from treatment of the two cancer cell lines with ethanolic and aqeous *A. afra* extract, respectively. The ethanol extract of *A. afra* proved to be cytotoxic against both HeLa and U937 cells, with IC_{50} values of 31.88 ± 1.09 µg/mL and 18.21 ± 0.9 µg/mL, respectively. The aqueous extracts did not exhibit any cytotoxicity even at the maximum extract concentration of 250 µg/mL. Thus, this extract was not used for further investigations and Chang liver cells and Vero African monkey kidney cells were treated only with ethanolic *A. afra* extract (Figure 3.11). The ethanolic extract was not toxic against confluent Chang liver or Vero cells at concentrations of up to 250 µg/mL.

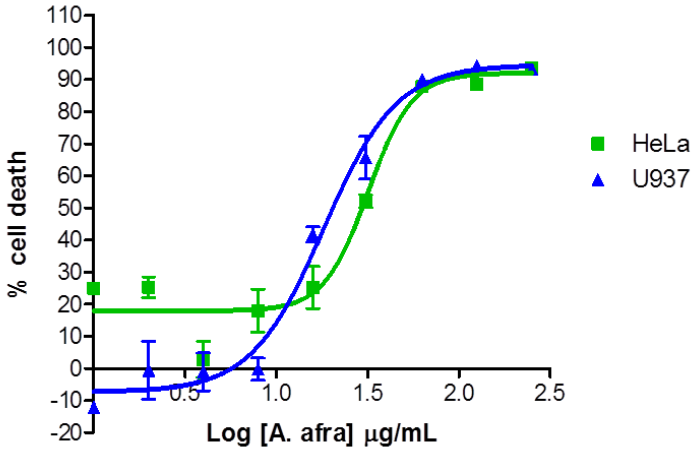

Figure 3.9: **Cytotoxic effect of *A. afra* ethanol extract on cancer cell lines after 48 hours of exposure. Cell viability was determined using the MTT assay for HeLa and CellTitre Blue assay for U937 cells. Error bars indicate SD of four replicate values of a single experiment.**

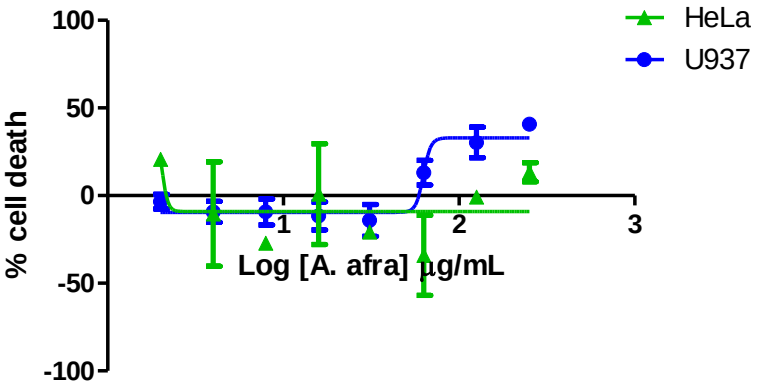

Figure 3.10: **Cytotoxic effect of *A. afra* aqueous extract on cancer cell lines after 48 hours of exposure. Cell viability was determined using the MTT assay for HeLa and CellTitre Blue assay for U937 cells. Error bars indicate SD of four replicate values of a single experiment.**

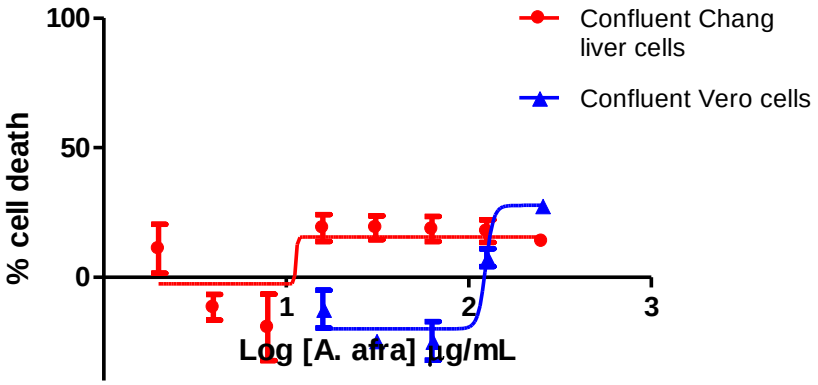

Figure 3.11: **Cytotoxic effect of *A. afra* ethanol extract against confluent Chang liver cells (red) and confluent Vero cells (blue) after 48 hours of exposure. Cell viability was determined using the MTT assay. Error bars indicate SD of four replicate values of a single experiment.**

From these results, only the ethanol extract was selected for further investigations. The concentration that was used for HeLa and U937 cells in all further experiments was fixed at 30 µg/mL and 20 µg/mL, respectively. The IC_{50} of melphalan against HeLa was determined as 42.36 µM (Appendix A, Figure A1). An IC_{50} of 45.2 µM against U937 cells (Kühne *et al.*, 2009). Thus, the concentration of melphalan used as a positive control for all subsequent assays was 40 µM in both cell lines.

3.4.2. Cell cycle analysis:

DNA cell cycle analysis was performed to determine arrest of cells in a certain phase of the cell cycle. HeLa and U937 cells were exposed to ethanolic *A. afra* extract at their respective concentrations of 30 and 20 µg/ml for 12, 24 and 48 hours. It was shown that both cell lines arrested in the G2/M phase of the cell cycle after 12 hours of exposure (Figure 3.12). This was still evident at 24 and 48 hours (Table 3.1).

Table 3.1: Summary of cell cycle analysis results obtained for HeLa and U937 cells at 12, 24 and 48 hours.

Treatment		HeLa cells				U937 cells			
		Sub G1	G1/G0	S	G2/M	Sub G1	G1/G0	S	G2/M
12 hours	Control	2.15 ± 0.07	31.87 ± 2.3	55.95 ± 2.85	12.18 ± 0.55	16.43± 0.35	59.91± 0.63	26.56± 1.04	13.51± 0.58
	Melphalan	1.43 ± 0.31 *	43.31 ± 0.51 **	56.69 ± 0.51	0 ± 0 **	21.23± 0.4 **	62.38± 1.06 *	32.0± 0.97 **	5.63± 0.19 **
	A. afra	1.87 ± 0.38	17.37 ± 2.36 *	27.38 ± 1.35 **	55.25 ± 2.47 **	31.97± 0.15**	55.37± 0.74 **	24.41± 0.70 **	21.93± 2.89 **
24 hours	Control	1.23 ± 0.11	30.05 ± 0.27	49.46 ± 0.93	20.48 ± 0.4	6.63 ± 7.45	55.84 ± 8.79	31.87 ± 13.08	12.29 ± 4.29
	Melphalan	7.32 ± 1.17**	40.06 ± 5.33 **	58.86 ± 5.3 **	1.05 ± 0.76 **	40.32 ± 9.36 **	61.18 ± 3.58	33.14 ± 9.11	8.44 ± 9.44
	A. afra	2.72 ± 0.25 *	13.02 ± 3.34 *	14.02 ± 0.87 **	72.96 ± 2.15 **	17.9 ± 0.85 **	53.38 ± 14.72	26.93 ± 10.04	20.37 ± 3.70
48 hours	Control	1.08 ± 0.2	37.99 ± 0.36	47.45 ± 0.19	14.55 ± 0.81	4.46 ± 4.67	55.35 ± 8.43	33.43 ± 11.25	13.02 ± 5.45
	Melphalan	40.15 ± 5.56 *	13.97 ± 0.02 *	52.89 ± 2.15 *	32.19 ± 4.42 **	64.22 ± 1.39 **	71.7 ± 1.98 *	9.25 ± 7.48 *	19.05 ± 5.50
	A. afra	4.13 ± 0.14 **	49.96 ± 5.03	26.68 ± 5.21 **	23.2 ± 0.21	21.77 ± 11.36 **	52.46 ± 3.31 **	34.67 ± 4.56 **	17.55 ± 5.36

Each experiment was performed 3 times for each time study. Each experiment was carried out in triplicate.
Values indicate mean % ± SD of all experimental data
* Significantly higher than control; $p<0.05$
** Significantly higher than control; $p<0.005$: Significance was determined using the two-tailed Student t-test.

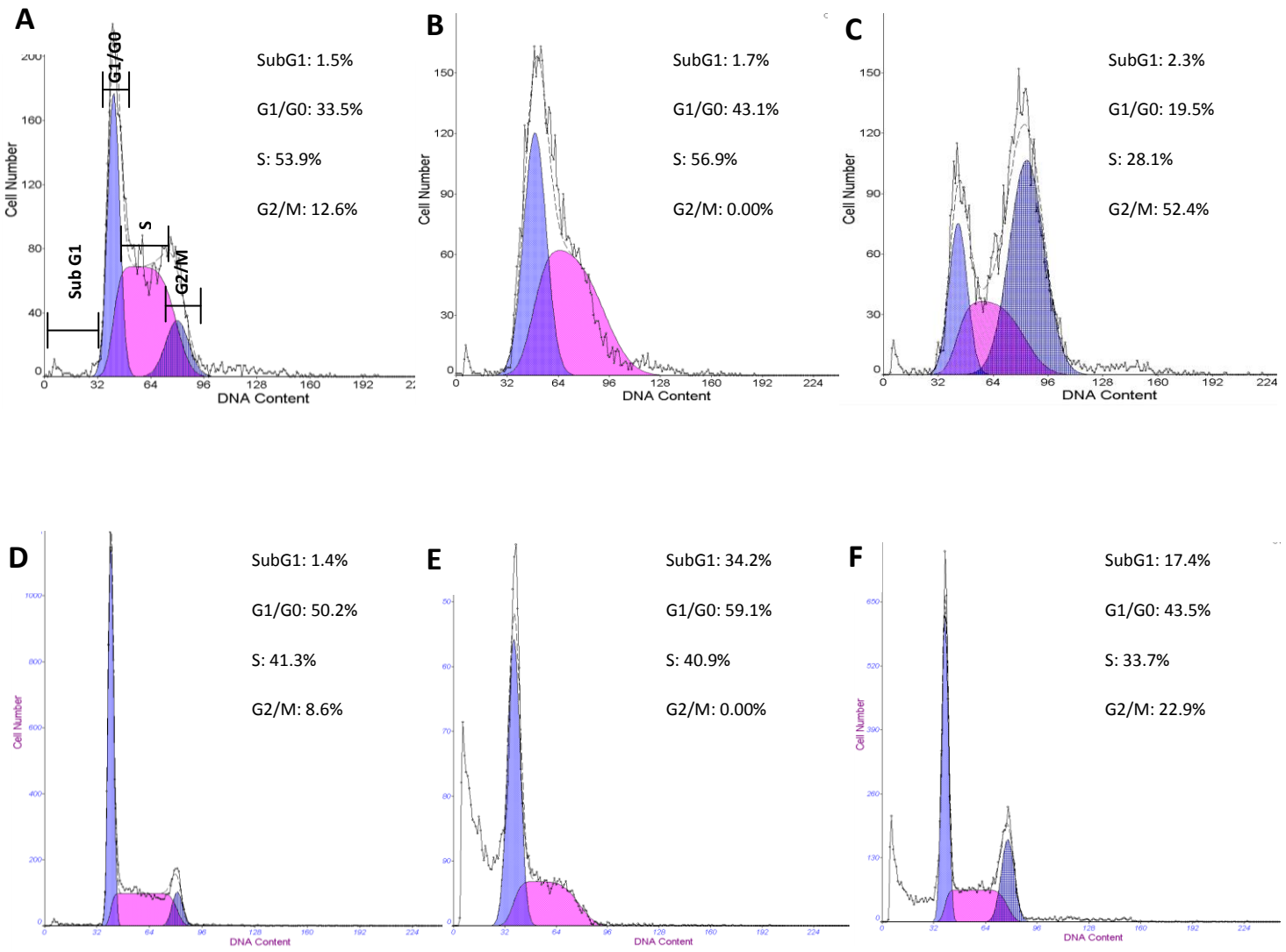

<u>Figure 3.12:</u> Histograms representing DNA cell cycle analysis after 12 hours of treatment in HeLa cells (A-C) and U937 cells (D-F). HeLa cells were treated with 40 µM melphalan (B) and 30 µg/mL *A. afra* (C). U937 cells were treated with 40 µM melphalan (E) and 20 µg/mL *A. afra* (F). Control cell populations are represented by histograms A and D for HeLa and U937 cells respectively. Cell cycle analysis was recorded on a Beckman Coulter Cytomics FC500 after PI staining of DNA and analysed using Multicycle version 4.0 software. Ten thousand events were recorded for each sample. (One representative for 3 individual experiments, each performed in triplicate).

An interesting observation upon viewing HeLa cells after 12 hours of exposure was the appearance of multinucleated cells. Phase contrast photographs were taken of untreated and *A. afra* treated cells indicating the presence of multinucleation (Figure 3.13).

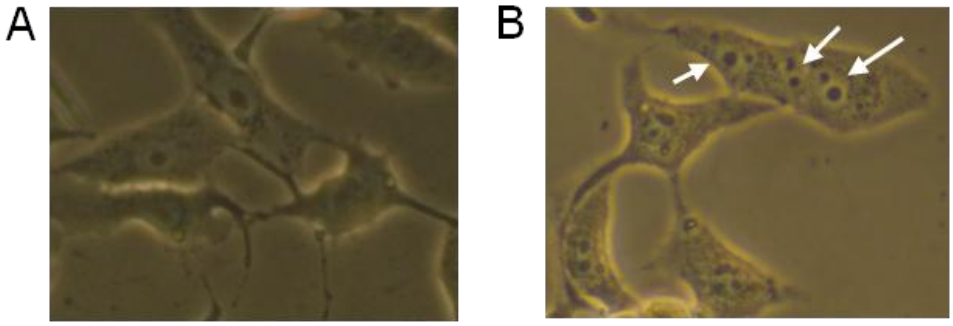

Figure 3.13: Phase contrast photographs of untreated HeLa cells (A) and cells treated with *A. afra* ethanol extract for 12 hours (B). White arrows indicate the appearance of multinucleated cells.

3.4.3. Phosphatidylserine translocation:

The effect of ethanolic *A. afra* extract on the integrity of the cell membrane of HeLa and U937 cells was determined. PS translocates to the outer surface of the cell membrane as an early feature of apoptosis. The presence of PS on the outer cell surface was determined using Annexin V-FITC assay. Both HeLa and U937 cells stained positive for Annexin V and negative for PI after 24 hours of treatment with the plant extract. Results recorded for this experiment is represented in Figure 3.14. A significant increase from 5.83 ± 1.33% to 37.53 ± 2.68% ($p<0.005$) of apoptotic cells was recorded in HeLa cells and an increase from 4.73 ± 0.38% to 15.23 ± 0.57% ($p<0.005$) was recorded in U937 cancer cells (Figure 3.15).

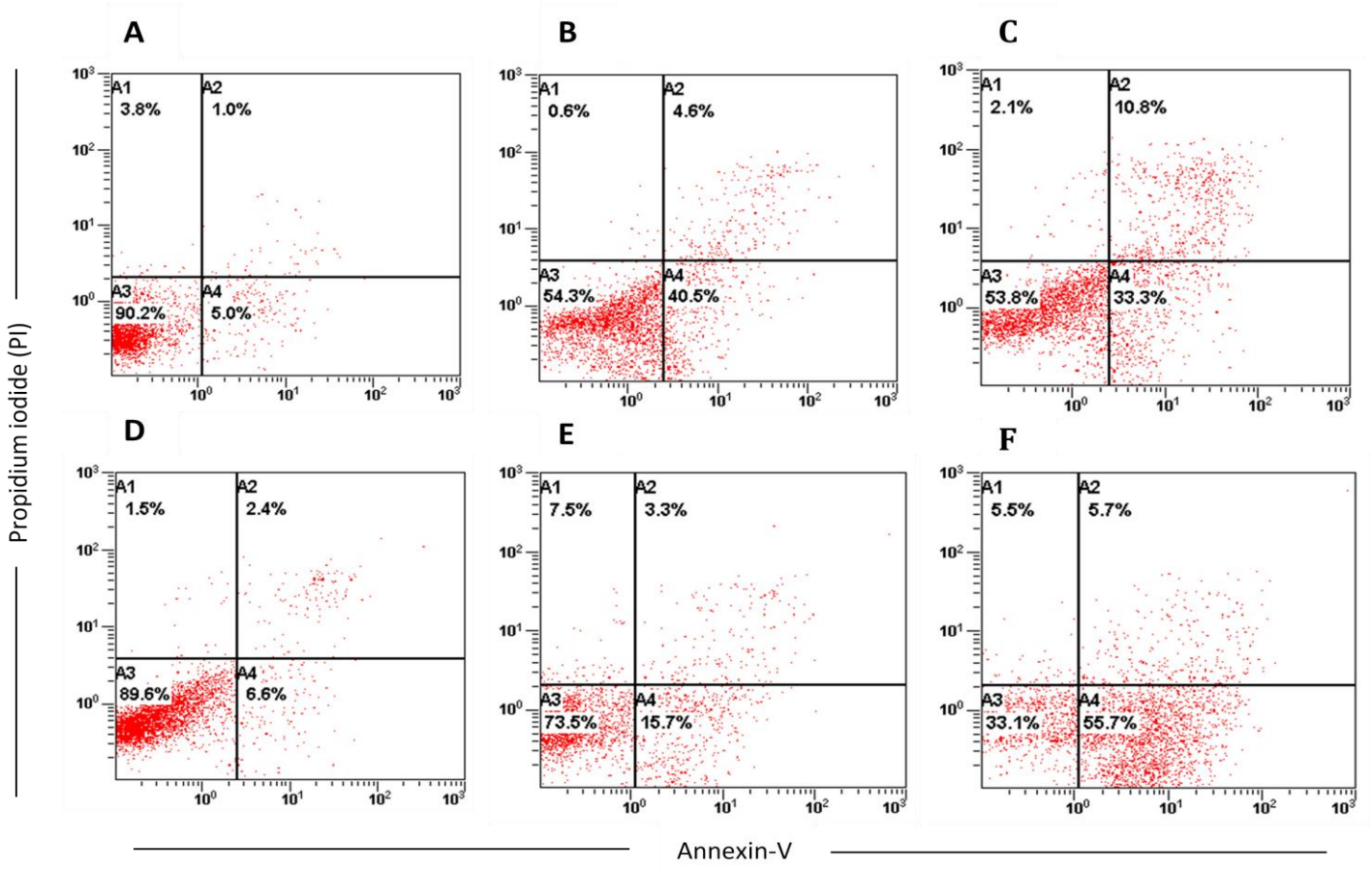

Figure 3.14: **Dot plots of Annexin V-FITC stained HeLa (A, B and C) and U937 cells (D, E and F) after 24 hrs exposure to medium only (A, D), 30 µg/mL and 20 µg/mL *A. afra* (B, E; respectively) and 40 µM melphalan (C, F). Four quadrants represent unstained/live cells (A3: Annexin V-negative; PI-negative), early apoptotic cells (A4: Annexin V-positive; PI-negative), late apoptotic cells (A2: Annexin V-positive; PI-positive) and necrotic cells (A1: Annexin V-negative; PI-positive). A minimum of 20 000 events were read (n=3). (One representative for 3 individual experiments, each performed in triplicate).**

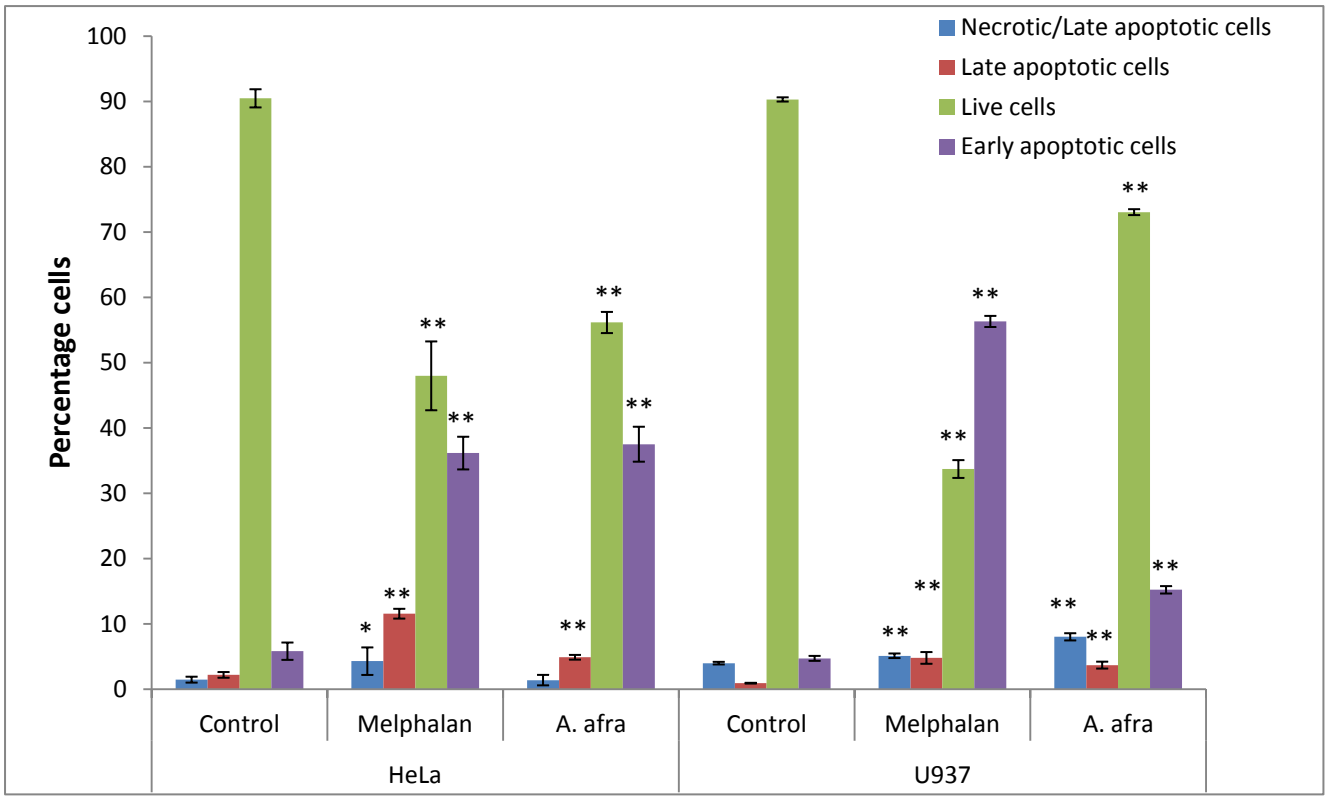

Figure 3.15: Analysis of HeLa and U937 cells using Annexin V-FITC and PI dual staining after 24 hours of exposure to treatments. Cells were treated with 40 µM melphalan, 20 µg/mL *A.afra* ethanolic extract (U937) or 30 µg/mL *A.afra* ethanolic extract (HeLa). Bar graph represents the average of three individual experiments each performed in triplicate. 20 000 events were recorded per sample. SD is represented as error bars. Significance was determined using the two-tailed Student t-test: *p<0.05; **p<0.005 compared to control.

3.4.4. Analysis of mitochondrial membrane potential:

Depolarisation of the mitochondrial membrane is an indication of the onset of the intrinsic mode of apoptosis and indicates the release of pro-apoptotic proteins from the mitochondria. JC-1 was used to determine the state of the mitochondrial membrane. An increase in green fluorescence intensity would indicate that JC-1 remained in its monomeric state in the cell cytosol and did not accumulate in the mitochondria and form J-aggregates (Smiley *et al.*, 1991; Reers *et al.*, 1991). Significant increase in green fluorescence intensity was evident after 24 and 48 hours of treatment with *A. afra* ethanol extract in both cell lines as indicated in Table 3.2. This indicates the involvement of the mitochondria in the onset of apoptosis.

Table 3.2: Summary of results obtained for analysis of mitochondrial membrane potential after treatment with melphalan (40 µM) and *A. afra* ethanol extract.

Treatment		Mean green fluorescence intensity[#] for HeLa cells	Mean green fluorescence intensity[#] for U937 cells
24 hours	control	19.03 ± 3.46	19.25 ± 3.46
	melphalan	41.93 ± 0.21**	85.75 ± 0.21**
	A. afra	70.40 ± 0.92**	69.45 ± 0.92**
48 hours	control	9.99 ± 2.81	24.93 ± 1.44
	melphalan	105.77 ± 9.62**	257.71 ± 16.40**
	A. afra	34.83 ± 0.97**	144.25 ± 4.29**

[#] Mean of green fluorescence intensity. Depolarization is accompanied by an increase in green and a decrease in red fluorescence. Values indicate mean log green fluorescence intensity ± SD of all experimental data

** Significantly higher than control; $p<0.005$: Significance was determined using the two-tailed Student t-test.

3.4.5. Caspase -8 and caspase -3 activation:

Activation of caspase -8 and -3 was determined using an immunochemistry technique. Antibodies against activated/cleaved caspase -8 and -3 were used for their detection. An increase in mean green fluorescence intensity is an indication of the increase in presence of activated caspase -8 or -3. This was evident for both caspase -8 and -3 (Figure 3.16 and Table 3.3).

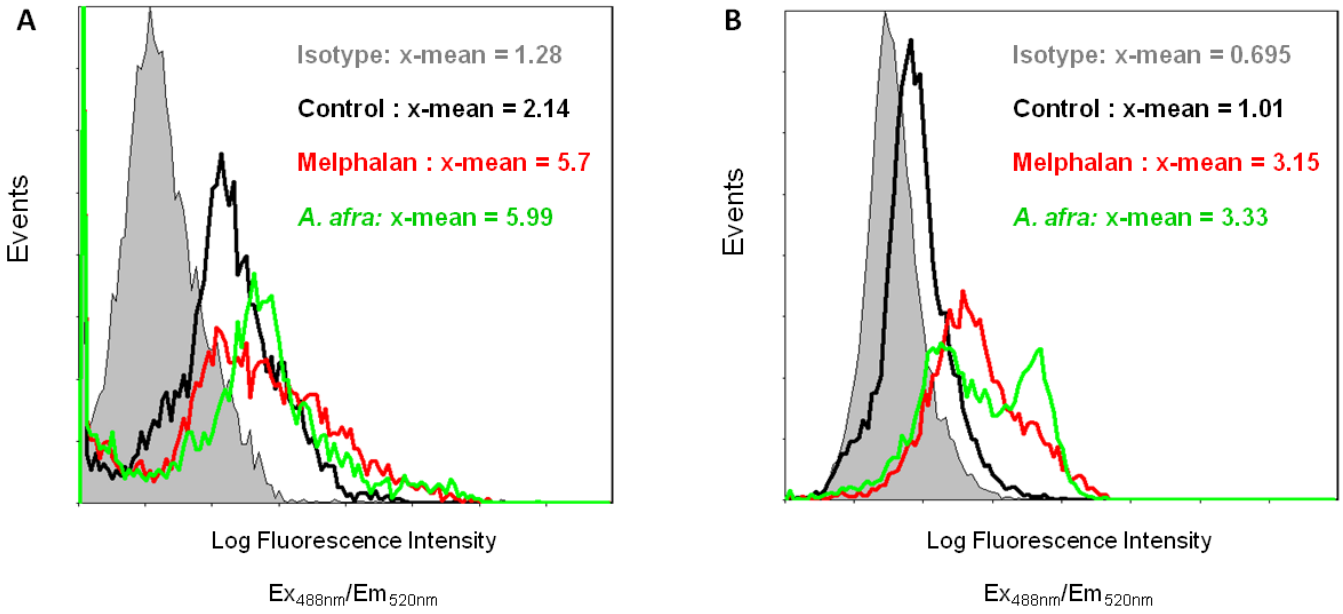

Figure 3.16: Histogram overlays representing activated caspase -8 (A) and caspase -3 (B) in HeLa cells after 24 hours (A) and 48 hours (B) of exposure to treatments. 10 000 events were recorded per sample. X-mean values indicate the mean of fluorescence intensity of cells staining positive for active caspase -8 and caspase -3. (One representative for 3 individual experiments, each performed in triplicate).

Table 3.3: Changes in cleaved caspase -8 and caspase -3 levels after treatment with melphalan (40 µM) and *A. afra* ethanol extract.

Treatment		Percentage of control (%)			
		U937		HeLa	
		Cleaved caspase -8	Cleaved caspase -3	Cleaved caspase -8	Cleaved caspase -3
12 hours	Control	0.00 ± 0.53	0.00 ± 1.80	0.00 ± 0.53	0.00 ± 0.75
	Melphalan	27.39 ± 0.83	0.00± 2.56	27.787 ± 1.34	0.00 ± 1.37
	A. afra	5.77 ± 2.04	15.89 ± 3.35	5.362 ± 1.59	15 ± 2.29
24 hours	Control	0.00 ± 0.57	0.00 ± 1.51	0.00 ± 0.48	0.00 ± 0.87
	Melphalan	27.44 ± 0.31	43.08 ± 0.74	57.469 ± 3.42**	61.801 ± 1.95**
	A. afra	129.41 ± 5.21**	66.9 ± 1.04**	89.279 ± 4.48**	53.375 ± 1.96**
48 hours	Control	0.00 ± 0.31	0.00 ± 0.59	0.00 ± 0.58	0.00 ± 0.58
	Melphalan	167.29 ± 0.87**	88.7 ± 2.23**	188.887 ± 3.94**	31.773 ± 3.93**
	A. afra	48.96 ± 0.87**	47.21 ± 1.39**	43.067 ± 2.32*	85.154 ± 4.89**

Each experiment was performed 3 times for each time study. Each experiment was carried out in triplicate. Values indicate mean % ± SD of all experimental data. Control treatment refers to an untreated cell population. * Significantly higher than control; $p<0.05$. ** Significantly higher than control; $p<0.005$: Significance was determined using the two-tailed Student t-test.

3.4.6. DNA fragmentation:

DNA fragmentation is characteristic of late apoptosis and was investigated in HeLa and U937 cancer cells (Figure 3.17). Significant increases in the amount of fragmented DNA were evident after 24 and 48 hours in both cell lines.

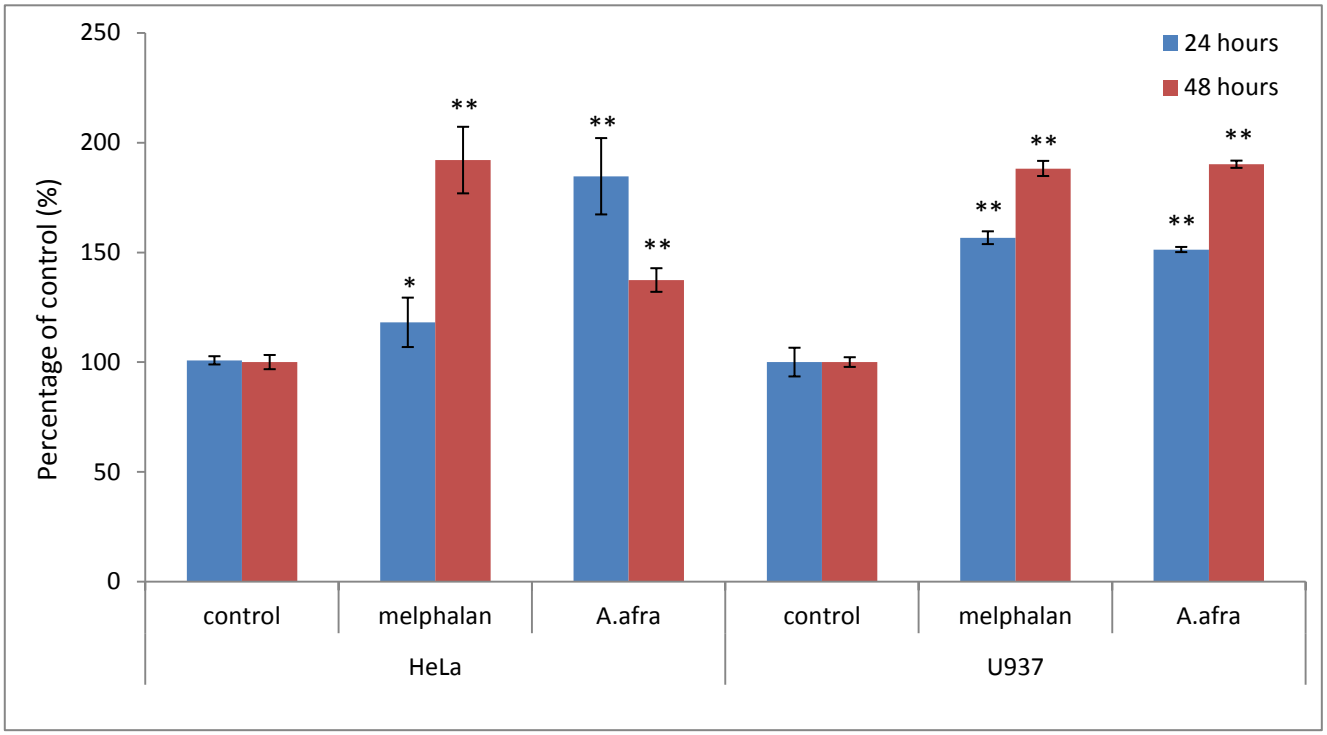

Figure 3.17: DNA fragmentation in HeLa and U937 cells after 24 and 48 hours of exposure to treatments. Cells were treated with 40 µM melphalan, 20 µg/mL *A.afra* ethanolic extract (U937) or 30 µg/mL *A.afra* ethanolic extract (HeLa). Bar graph represents the average of three individual experiments each performed in triplicate. Error bars indicate SD of the mean of the three independent experiments. 10 000 events were recorded per sample. Significance was determined using the two-tailed Student t-test: *p<0.05; **p<0.005 compared to control.

3.5. Discussion and Conclusion:

The aim of this chapter was to determine the mechanism of cell death induced by *A. afra* extract. Several modes of cell death can occur, but the most controlled mechanism of cell death is apoptosis. Apoptosis is characterized by distinct changes in morphology of cells created by biochemical changes of the cell. These included activation of caspases, mitochondrial membrane permeabilisation and exposure of PS on the outer surface of the plasma membrane.

Cytotoxicity of a DCM:MeOH (1:1 v/v) extract of *A. afra* against renal and breast cancer cells as well as melanoma cells has been previously reported (Fouche *et al.,* 2008). Mativandlela *et al.* (2008) showed that a crude ethanolic extract of *A. afra* was cytotoxic against Vero cells with an IC_{50} of 113.0 ± 2.05 µg/mL. Although cytotoxicity has been implicated, the mechanism of induced cytotoxicity and cell death has not been reported as yet. *A. afra* is used as a traditional herbal medicine for the treatment of various ailments particularly inflammation and respiratory conditions in South Africa (Liu *et al.,* 2009). Various studies have shown this plant extract to have antibacterial, antiviral and anti-inflammatory activities (Liu *et al.,* 2009). The plant is prepared in many different ways depending on its use. A tea is brewed using the leaves of the extract. It is left to draw for 10 minutes and thereafter it is strained and the infusion is sweetened with honey and drank for the relief of symptoms of respiratory discomfort (Roberts, 1990). A tincture is also made by wetting the leaves with brandy and is administered for the treatment of colic (Watt and Breyer-Brandwijk, 1962).

Aqueous and ethanol extracts of *A. afra* were prepared and tested on HeLa and U937 cancer cells for cytotoxic activity. Dose-response curves were plotted and analysed to determine an IC_{50} value for each plant extract. The aqueous extract did not show relevant cytotoxicity against HeLa and U937 cells as seen in Figure 3.10. Gertsch (2009) stated that extracts that are used at concentrations of 200 µg/mL and above are likely to display artificial results in *in vitro* assays, even though the data is reproducible. Gertsch (2009) also states that crude extracts should only be considered meaningful if an IC_{50} of less than 50 µg/mL is obtained against a cell line. The highest recorded % cell death upon treatment of HeLa and U937 cells with 250 µg/mL crude aqueous *A.afra* extract was 13.39 ± 5.41% and 33.57 ± 6.57%, respectively.

HeLa and U937 cells were exposed to crude ethanol *A. afra* extract concentrations as described for the aqueous extract. Figure 3.9 shows the results of the cytotoxicity assay. IC_{50} values of 31.88 ± 1.09 µg/mL and 18.21 ± 0.9 µg/mL were achieved for HeLa and U937 cells, respectively. These values are 3 to 5 times lower than the previously reported IC_{50} value of 113.0 ± 2.05 µg/mL where an ethanolic extract of *A. afra* was evaluated against Vero cells (Mativandlela *et al.*, 2008). These values are also consistent with the argument by Gertsch (2009) that IC_{50} values of >50 µg/mL are not physiologically meaningful. Due to the observed cytotoxicity of ethanolic *A. afra* extract, it was also tested against confluent Chang liver and Vero cells (Figure 3.11) as models for normal cells with a low proliferation rate. At the concentration range tested, the extract was not cytotoxic against these cell lines. IC_{50} values of >250 µg/mL would have resulted, which is considered physiologically meaningless. Chang and Vero cells were used at 100% confluency when *A. afra* ethanol extract was tested for cytotoxicity. HeLa and U937 cancer cells were used while in the log phase of growth, i.e. proliferating cells. Cells at confluence cease proliferating and undergo contact inhibition of growth and enter the G0 phase of quiescence (Coller *et al.*, 2006). Uncontrolled cell proliferation is a major feature of cancer cells and thus it is important to use proliferating cells to determine the cytotoxic mechanism of action of the plant extract and its anti-cancer potential.

Melphalan (L-phenylalanine mustard) was used as a positive control for all experiments carried out in this chapter. It is an alkylating cytotoxic drug that is used in high doses as part of a therapy regime for the treatment of multiple myeloma. Alkylating agents have the ability to add alkyl groups to electronegative groups under specific conditions within a cell. They are effective against tumour growth by the cross-linking of guanine bases of DNA (Green *et al.*, 1984). The IC_{50} of melphalan varies considerably amongst different cell lines and generally has a high IC_{50} value when considering pure compounds (Kühne *et al.*, 2009).

Cell cycle arrest enhances cytotoxicity of extracts and agents. The absence of significant toxicity on confluent Chang liver and Vero cells compared to the low IC_{50} values on proliferating cancer cell lines suggest that *A. afra* ethanolic extract may induce cell cycle arrest in actively proliferating cells. DNA cell cycle analysis was performed to determine the effect of the ethanol *A. afra* extract on the two cell lines. Cells were exposed to the extract for 12, 24 and 48 hours. After 12 hours of exposure, an arrest in the G2/M phase of the cell cycle was evident in both cell lines. Table 3.1 shows a summary of the results of cell cycle analysis.

HeLa cells showed a significant increase in tetraploid DNA from 12.18 ± 0.55% in the untreated cell population to 55.25 ± 2.47% in extract treated cells. U937 cells also showed an increase in 4N DNA content. A significant increase from 13.51 ± 0.58% in the untreated cell population to 21.93 ± 2.89% in extract treated cells was observed. Upon treatment of both cell lines with melphalan, an arrest in the S phase of the cell cycle was evident in Figure 3.12 B and 3.12 E.

The mechanism of cell cycle arrest in the G2/M phase cannot be determined using PI. In the G2 phase, repair to the DNA of the cell may occur before the cell enters the mitotic (M) phase. The G2/M checkpoint serves to prevent a cell that has DNA damage from entering mitosis. Cells entering the M phase with mutations will pass these mutations on to daughter cells. The phosphatases Cdc25B and Cdc25C are regulators of the progression of the cell cycle from the G2 phase through the M phase and play an integral role in the G2/M checkpoint. These proteins regulate the progression by its activity on Cdc2/cyclinA and Cdc2/cyclinB complexes (Busino *et al.,* 2004). DNA damage causes G2/M arrest by inhibition of the activation of Cdc2 (Hwang and Muschell, 1998). Active Cdc2 complexed to cyclin B1 is required for the progression from the G2 phase to the M phase of the cell cycle. Cdc25C dephosphorylates the active site of Cdc2, which increases its activity. When DNA damage occurs, Chk1 is activated and deactivates Cdc25C. This results in the phosphorylation and inactivity of Cdc2/cyclinB complex and the cell arrests in the G2/M phase. G2/M arrest can also be associated with problems in the formation of the mitotic spindle resulting in mitotic catastrophe. G2/M arrest is an early event as it is apparent after 12 hours of exposure to *A. afra.* Other apoptotic markers investigated were evident later, thus G2/M arrest may be the primary event occurring upon treatment with *A. afra* and apoptosis results in response to mitotic catastrophe (Vakifahmetoglu *et al.,* 2008). Studies have suggested that the arrest in the G2/M phase of the cell cycle may be secondary to the effects on microtubules, which will induce mitotic arrest (DiPaola, 2002). The event of mitotic catastrophe was investigated (Chapter 6).

After determination of the cytotoxic ability of the ethanol extract of *A. afra* and that cell cycle arrest in the G2/M phase aids in cytotoxicity, it was important to determine the mode of cell death induced by the plant extract. This was achieved using the Annexin V-FITC/PI apoptosis assay. This assay exploits the fact that during apoptosis, PS is translocated to the outer surface of the cell membrane and can hence be detected by Annexin V-FITC, a protein

that has a high affinity for PS. PI is used to indicate necrotic cells (van Engeland *et al.*, 1998). In this study, HeLa and U937 cells were exposed to ethanol *A. afra* extract for 24 hours. Although PS translocation is an early event in apoptosis, 24 hours was thought to be the ideal time required to detect this phenomenon as concentrations used to treat the cells were set at their respective IC_{50} values which was determined over a 48 hour incubation. Significant increases in the percentage of cells stained positive for Annexin V and negative for PI was shown here, indicating the onset of apoptosis with exposure of ethanolic *A. afra* extract to HeLa and U937 cells (Figure 3.14). Little increase in PI positive cells was observed in this study, confirming that cell death is not due to necrosis.

Apoptosis can be initiated by extracellular or intracellular signals and thus the extrinsic or intrinsic mode of apoptosis is activated, respectively. However, a link between the two pathways exists and overwhelming evidence has indicated that more often than not, both pathways are induced upon *in vitro* treatment with crude plant extracts. The intrinsic pathway of apoptosis is also referred to as the mitochondrial pathway due to the orchestration of apoptosis conducted by the mitochondria. This pathway involves the release of pro-apoptotic proteins from the mitochondria in response to cellular signals resulting from cell stress such as DNA damage etc. (Vermeulen *et al.*, 2003). The pro-apoptotic proteins promote the release of cyt -*c* from the mitochondrion, which then binds to Apaf-1 and forms a complex with caspase -9. This complex of proteins is referred to as the apoptosome (Zangemeister-Wittke and Simon, 2001). Upon mitochondrial depolarisation, cyt –*c* is released. This can be detected using the carbocyanine dye, JC-1, as described in section 3.3.6.1.

The involvement of the mitochondria in the onset of apoptosis was determined in both HeLa and U937 cells. It was shown that the mitochondria do experience depolarisation of its membranes as there were significant increases in the mean green fluorescence intensity in both cell lines (Table 3.2). Complete MMP results in the liberation of lethal enzymes or activators of lethal enzymes including cyt-*c*, Bax and Bad (pro-apoptototic proteins). Analysis of the presence of pro-apoptotic mitochondrial proteins can be performed, however, the depolarisation of the mitochondria is generally considered as a point of no return in the onset of intrinsic apoptosis.

A major biochemical feature of apoptosis is the activation of caspases. Caspases play a central role in the morphological changes associated with apoptosis. Caspase -8 is an initiator

caspase that is characterised by its long prodomain that consists of two domains with marked identity with the N-terminal death effector domain (DED) of FADD/MORT1 indicated by "FADD homology" in Figure 3,7 (Cohen, 1997). CD95 and TNF receptor (TNFR) are members of the TNF/nerve growth factor receptor families and activation of these receptors results in the induction of the extrinsic pathway of apoptosis. These receptors contain death domains on their C-terminal end that is present on the cytosolic region of the cell. FADD/MORT1 (Fas-associating protein with death domain) and TRADD (TNFR-1-associated death domain protein) bind to CD95 and TNFR-1, respectively. This is known as the formation of the death inducing signalling complex (DISC) (Fulda and Debatin, 2006). FADD/MORT1 and TRADD both contain DED's at its N-terminal end that triggers apoptosis. It does so by the protein-protein interactions between the FADD homologous regions of caspase -8 and the DED's of FADD. This allows for the conformational change in the DED of FADD and so facilitates the autocatalytic activation of caspase -8 (Cohen, 1997). Therefore, activated caspase -8 was used as a marker for the induction of the extrinsic mode of apoptosis in this study. An increase in activated caspase -8 was investigated after 12, 24 and 48 hours of exposure with ethanol *A. afra* extract to the two cell lines. Table 3.3 indicates a summary of these results. The histogram overlays show an increase in the log fluorescence intensity (Ex_{488nm}/Em_{520nm}) indicated by a shift to the right of the plot area. Changes in mean green fluorescence between cell populations treated with melphalan and ethanol *A. afra* extract independently were expressed as percentage of control (control refers to an untreated cell population). Significant increases in cleaved caspase -8 in HeLa and U937 cells were evident after 24 hours of treatment with the extract. Greater levels of active caspase -8 were evident at 24 hours as compared to 48 hours as shown in Table 3.3. This indicates that caspase -8 is activated early. A significant increase was not noticed after 12 hours of exposure to the extract. HeLa and U937 cells showed to respond slower to melphalan treatment than to *A. afra* treatment.

Caspase -3 is a key executioner of apoptosis as this protein is either partially or totally responsible for the cleavage of many key proteins such as PARP, DNA protein kinases and retinoblastoma protein (Cohen, 1997). It is activated by initiator caspases. In the same way as described for caspase -8, changes in mean green fluorescence intensity was expressed as a percentage of the untreated control cell population. Significant increases in percentage of control were evident after 24 hours but greater increases were noticed after 48 hours of

treatment (Table 3.3). This was expected as caspase -3 activities are directly linked to DNA fragmentation and the last stages of apoptosis (Thornberry, 1998).

The last aspect of apoptosis that was investigated was the degradation of cellular DNA. DNA fragmentation occurs as a result of activated DNA cleavage enzymes (Collins *et al.*, 1997a). Figure 4.16 shows a significant increase in DNA fragmentation after 24 and 48 hours after the treatment of HeLa and U937 cells with *A. afra* extract. This was expected due to the increase in the levels of activated caspase -3. A two-fold increase in the amount of fragmented DNA was seen after 24 hours of treatment to HeLa cells and after 48 hours of treatment to U937 cells.

In conclusion, the results obtained from the investigation of how *A. afra* exerts cytotoxic effects on cancer cells were demonstrated in this chapter. It was shown for the first time that caspase-dependent apoptosis is induced in a mitochondrial-dependent manner after arrest in the G2/M phase of the cell cycle on both HeLa and U937 cancer cells. It was also clearly shown that the aqueous extract of *A. afra* did not exhibit cytotoxic abilities and the ethanol extract was not toxic against confluent Chang liver and Vero cells. As indicated, the studies were conducted using a crude plant extract and therefore, it is not possible to rule out the possibility that different primary cell death mechanisms were activated due to the multicomponent nature of crude extracts. Thus, it is important to determine the cytotoxic compounds/metabolites that are responsible for the observations demonstrated here.

CHAPTER 4: Isolation and Identification of a cytotoxic compound from an ethanol extract of *Artemisia afra.*

4.1. Introduction:

A crude plant extract contains a very complex mixture of different primary and secondary metabolites. The chemical nature of the constituents can vary greatly within an extract (Wolfender *et al.,* 1998). To identify a compound or class of compounds that is responsible for a biological activity, an efficient and sensitive characterization and identification method is essential. Before structural elucidation and identification of an active plant compound is possible, isolation of the biological active compound(s) is required. Bioassay-guided fractionation is employed on a routine basis in many laboratories for this task.

Plants have been used as medicines for thousands of years and were originally known as crude drugs. These crude drugs take the form of teas, tinctures, powders, etc. Over the years, the isolation of active compounds within a crude extract has become popular, not only for the isolation and identification of bioactive compound(s), but also for these compounds to act as lead compounds for synthetic drugs (Pan *et al.,* 2013). Examples of isolated drugs from medicinal plants are morphine, cocaine, codeine, digitoxin and quinine (Balunas and Kinghorn, 2005). Drug discovery from plants involves a number of steps. The process normally begins with a botanist or an ethnopharmocologist who collects and identifies plants according to their use, traditionally. Natural product chemists then prepare extracts using a solvent system relevant to the study. Plant extracts are then subjected to various screening methods. Thereafter, isolation and identification of the active constituent(s) are performed via bioassay-guided fractionation. Physiologically relevant targets of the active compounds are then identified using molecular biology techniques (Balunas and Kinghorn, 2005). The typical method for drug/lead compound discovery from natural sources is shown in Figure 4.1. This schematic illustrates the lengthy process for drug candidates to be identified.

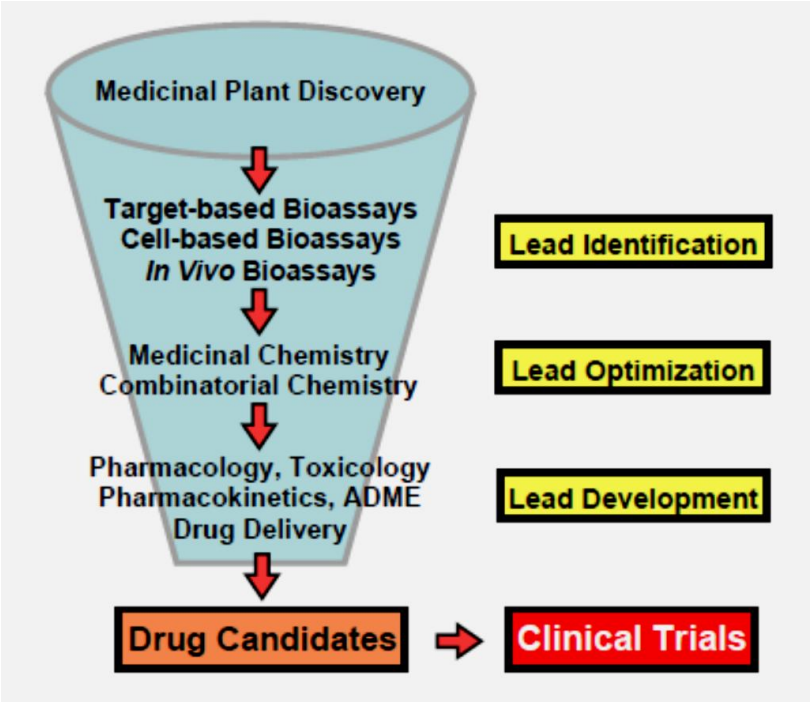

Figure 4.1: Schematic diagram illustrating the methods used for typical plant drug discovery and development (Balunas and Kinghorn, 2005).

4.1.1. Anti-cancer compounds from terrestrial plants:

Drug discovery from medicinal plants has played a pivotal role in the discovery of new anti-cancer drugs. The search for new anti-cancer drugs from plant origin started in the 1950s. The first plant-derived anti-cancer drugs to advance to clinical use were the vinca-alkaloids that were isolated from *Catharanthus roseus*, the Madagascar periwinkle (Cragg and Newman, 2005). Plant-derived compounds that are in clinical use for anti-cancer treatment are divided into 4 major groups (Pan *et al.*, 2013).

1. Vinca alkaloids
2. Epipodophyllotoxin lignans
3. Taxane diterpenoids
4. Camptothecin quinoline alkaloid derivatives.

A relatively large number of natural plant products are currently in development for the treatment of cancer. From 1981 to 2010, Newman (2012) reported that 128 new chemical entities (NCEs) were being examined for anti-cancer potential and in clinical development. Ninety nine (99) of the total number of NCEs are small molecule drugs. 79.8 % of 99 NCEs

are biologic, natural product mimics or synthetic but based on a natural compound, leaving only 20.2 % as purely synthetic. An example of a South African plant where a family of compounds has been isolated is *Combretum caffrum* Kuntze (Combretaceae). The compounds are known as the combretastatins. These compounds are stilbenes and act as anti-angiogenic agents and cause vascular shutdown in tumours, resulting in tumour necrosis. Combretastatins also acts as a tubulin-disrupting agent as it binds to the colchicine site of tubulin and leads to the failure of microtubule formation (Cragg and Newman, 2005; Pan *et al.*, 2013).

4.1.2. Compounds of cytotoxic interest from *Artemisia afra*:

The Asteraceae family of plants have received a lot of attention due to its phytochemical profile. Phytochemical investigations of this family, to which *A. afra* belongs, have led to the identification of structurally diverse and biologically active sesquiterpenoids, secondary metabolites that are most prevalent in the Asteraceae family (Ma *et al.*, 2013; Chadwick *et al.*, 2013). Sesquiterpene lactones (SLs) have been isolated from many plants belonging to the Asteraceae family and from the *Artemisia* genus (Lee and Geissman, 1970; Lee *et al.*, 1971; Nagaki, 1984; Bhakuni *et al.*, 2001). Sesquiterpenoids can account for a significant portion of the total dry mass of a plant, 3% being recorded in *Helenium amarum* (Raf) (Chadwick *et al.*, 2013). SLs are typically found in laticifers, highly specialized cells that produce latex and/or rubber as secondary metabolites (Hagel *et al.*, 2008). The contents of laticifers are of particular importance. Toxins and valuable bioproducts have been isolated from laticifers such as cardiac glycosides from *Antiaris spp*, opiates from opium poppy (*Papaver somniferum*) and rubber produced by *Hevea brasiliensis* and *Ficus elastic* is formed in laticifers. It is speculated that these secondary metabolites are harboured in these specialized cells to protect the plant from their cytotoxic effects. It has also been demonstrated that latex serves as an important defendant of certain plants against herbivores (Hagel *et al.*, 2008). SLs and phenolics have been implicated in the chemical defence of the chicory plant by secreting latex as a barrier to herbivory and insect feeding (Rees and Harborne, 1985; Harmatha and Nawrot, 1984). It has been shown that the highest concentration of SLs is present in the actively growing regions of the plant (Rees and Harborne, 1985). Fischer *et al.* (1990) indicated that SLs stimulate germination of witchweed and also showed that two eudesmanolides stimulated growth faster than a germacranolide.

4.1.3. Groups of sesquiterpene lactones:

SLs are 15 carbon compounds consisting of 3 isoprene units and a *cis*- or *trans*- fused lactone group (cyclic ester). SLs are classified into groups according to their carbocyclic skeletons (Krueger *et al.,* 2012). Some of which are:

1. Germacranolides
2. Eudesmanolides
3. Guaianolides
4. Pseudoguaianolides

Common structural features of the above mentioned compounds are shown in the figure below.

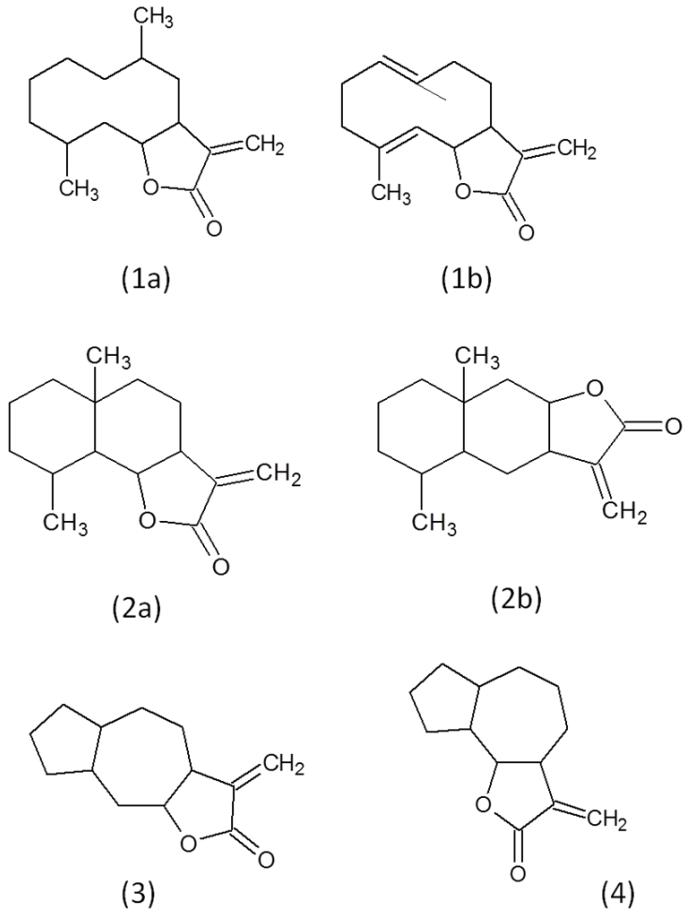

Figure 4.2: Carbocyclic skeletons of germacranolides (1a-1b), eudesmanolides (2a-2b), guaianolides (3) and pseudoguaianolides (4).

4.1.4. Aim:

Most work carried out on *A. afra* focuses on volatile secondary metabolites. Liu *et al.* (2009) states that a major problem with the traditional methods of preparing the plant for use is that many of the volatile components are lost. Volatile secondary metabolites identified are monoterpenoids and sesquiterpenes. Non-volatile secondary metabolites include sesquiterpene lactones, triterpenes, long chain alkanes, coumarins, organic acids, glycosides and flavonoids (van Wyk, 2008; Liu *et al.*, 2009). A few reports on other types of secondary metabolites exist.

A. afra is rich in terpenes and is therefore likely to possess many biological activities (Liu *et al.*, 2009). Two classes of sesquiterpene lactones have been isolated from *A. afra.* These are the glaucolides and the guaianolides (Jakupovic *et al.*, 1988; Kraft *et al.*, 2003).

SLs possess cytotoxic activity and it has been shown that these compounds inhibit proliferation of different cell types (Lee *et al.*, 1971; Bhakuni *et al.*, 2001). Spies *et al.* (2013) reported the *in vitro* cytotoxic properties of an ethanol extract of *A. afra,* exhibiting anti-cancer activity by inducing apoptosis in a caspase- and mitochondrial-dependent manner. It was hypothesized that the SLs present in this plant contribute to the observed cytotoxic activity. Thus, the aim of this study was to isolate and identify cytotoxic compound(s) of *A. afra*. Bioassay-guided fractionation of only the ethanol extract was performed as the aqueous extract did not show any relevant cytotoxic activity.

4.2. Materials

Silica Gel 60 (0.063 – 0.200 mm) and solvents (hexane, ethyl acetate and methanol) used for column chromatography were purchased from Merck (Germany). Deuterated chloroform, $CDCl_3$ (S5536220), used for NMR experiments, IR and CD spectroscopy were purchased from Merck Millipore (Germany). Deuterated acetone-D6 used for crude extract ^1H NMR was also purchased from Merck Millipore (Germany). Analytical grade dichloromethane used for GC/ EI MS was purchased from Merck (Germany). Materials used for cytotoxicity assays were as described in Chapter 3, section 3.2.

4.3. Methods:

Fractionation, isolation, structural elucidation and identification of the cytotoxic compound(s) were carried out as indicated in the purification scheme below. Each methodology is discussed in detail in the relevant section.

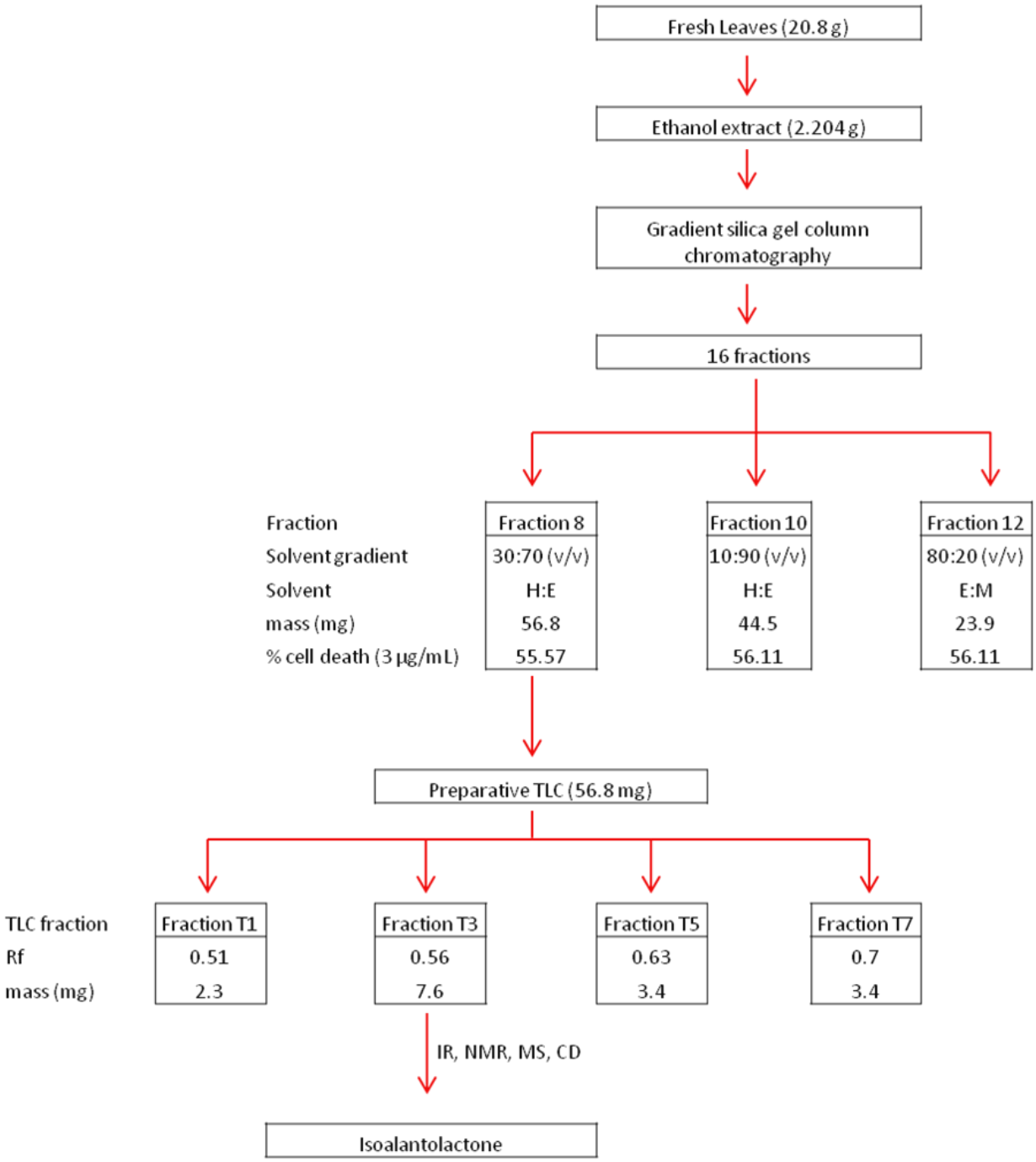

<u>Figure 4.3:</u> Purification scheme of the step-by-step method used to isolate and identify the cytotoxic compound(s) of *Artemisia afra,* highlighting the fractions of interest. Abbreviations: H, hexane; E, ethyl acetate; M, methanol).

4.3.1. Bioassay-guided fractionation of *A. afra* ethanol extract:

4.3.1.1. Background:

Discovery of potential drugs from medicinal plants has always been a lengthy and laborious task. For this reason, many pharmaceutical companies have scaled down or eliminated their natural product research. However, positive steps have been taken by institutional departments by developing centres for natural product research and thus, natural product research has regained momentum (Pan *et al.,* 2013). Because the process of isolation and identification of bioactive compounds in plants is so time-consuming, efforts in the development of faster and better methodologies for plant collection, bioassay screening, compound isolation and compound development is ongoing (Balunas and Kinghorn, 2005).

Bioassay-guided fractionation refers to a technique for assigning the observed activity of a complex mixture to individual constituents/compounds in the mixture (Weller, 2012). This technique was used to isolate the active compound(s) responsible for the cytotoxic activity of an ethanol extract of *A. afra.*

4.3.1.2. Fractionation of A. afra *extract using column chromatography:*

Column chromatography was conducted using the gradient solvent systems shown in Table 4.1 and Table 4.2 using 2.204 g of plant extract. A column was prepared in a burette using approximately 25 mL of silica (0.063 mm – 0.200 mm, Merck 7754) and forming a slurry in hexane before packing. The plant extract was adsorbed to silica by dissolving it in 100% methanol. The methanol was removed using a Büchi rotary evaporator. The adsorbed extract was added to the prepared column. This resulted in an extract band width of 5 mm. The extract was fractionated by using gradient hexane: ethyl acetate and ethyl acetate: methanol solvent systems (Table 4.1 and Table 4.2). Ten millilitre fractions were collected in pre-weighed pill vials and solvent was evaporated under nitrogen gas. Each pill vial was weighed after solvent removal and respective masses were recorded.

Table 4.1: First solvent system used for fractionation.

Fraction	Hexane (mL)	Ethyl acetate (mL)	mass (mg)
1	10	0	0.2
2	9	1	0
3	8	2	0.1
4	7	3	0.1
5	6	4	0.1
6	5	5	0.3
7	4	6	5.3
8	3	7	9.6
9	2	8	4.1
10	1	9	3.7
11	0	10	5.1

Table 4.2: Second solvent system used for fractionation.

Fraction	Ethyl acetate (mL)	Methanol (mL)	mass (mg)
12	8	2	16.4
13	6	4	12.1
14	4	6	26.6
15	2	8	46.7
16	0	10	151.5
17	0	10	62.7

Each fraction was dissolved in hexane or ethyl acetate and was spotted onto an 8 x 10 cm silica coated aluminium TLC plate and air dried. Chromatogram tanks were equilibrated for 20 minutes using a 1:1 v/v hexane: ethyl acetate as the mobile phase. TLC plates were developed until the solvent front was approximately 0.5 cm from the top of the plate. After development, TLC plates were air dried at room temperature and visualized at 254 nm. Photographs of all TLC plates were taken in normal and under UV light.

4.3.1.3. Determination of the cytotoxic fraction(s) using the MTT cytotoxicity assay:

The resulting fractions from column chromatography were subjected to a cell-based screening procedure for the identification of cytotoxic fractions. The MTT cytotoxicity assay was carried out against cervical cancer cells, HeLa cells. The MTT assay was performed in the same way as described in Chapter 3. Briefly, HeLa cells were seeded in 200 µL aliquots

at a density of 3 x 10^4 cells/mL and left overnight to attach. Cells were treated with 3 different concentrations of fractions 7 – 16 in triplicate. The concentrations used were 3, 30 and 100 µg/mL. Cells were exposed to the fractions for 48 hours. Thereafter, wells were aspirated and MTT (0.5 mg/mL) was added to each well and cells were incubated for 3 hours. The blue formazan product was solubilised by adding DMSO to each well and absorbance was read at 540 nm using BioTek® PowerWave XS spectrophotometer (Winooski, VT, USA).

4.3.1.4. Preparative isolation of the cytotoxic compound of A. afra *crude extract:*

Preparative TLC was conducted to further purify the active fraction. The active fraction was dissolved in *n*-hexane and was applied to a 20 x 20 cm silica coated aluminium TLC plate. A large chromatogram tank was equilibrated for 30 minutes using hexane: ethyl acetate (1:1 v/v). Plates were developed for ± 1 hour until the solvent front was approximately 1 cm from the top of the plate. The plates were air dried and separated bands were identified by UV light at 254 nm and removed from the plate and placed in pill vials. The silica containing each fraction was submerged in dichloromethane for the removal of the compound from the silica. Each of these fractions was filtered into a clean, dry, pre-weighed pill vial and the solvent was removed using a Büchi rotary evaporator.

4.3.2. Structural elucidation and identification of the active compound:

4.3.2.1. Infrared (IR) spectroscopy:

4.3.2.1.1. Background:

Bonds within molecules are continually vibrating and moving. Bonds can vibrate or move by stretch motions (either symmetrical or asymmetrical) or bend motions (angle between the bonds change). In order to identify different types of bonds that exist in a molecule, it requires exposure to frequency in the infrared region of the electromagnetic spectrum.

The absorption wavenumber for a stretching vibration can be defined by Hooke's Law shown in the equation below (Coates, 2000):

$$\bar{\nu} = \frac{1}{2\pi c}\left[k\left(\frac{m_1 + m_2}{m_1 \cdot m_2}\right)\right]^{1/2}$$

This relates the absorption wavenumber for a stretching vibration to both the force constant between two atoms (k) and the mass of the two atoms (m_1 and m_2). This law explains that lighter atoms and stronger bonds lead to higher frequencies. Only vibrations producing a change in the dipole moment of a bond are detected as absorption and intensity of absorption depends on this change and the numbers of bonds present (McMurray, 2008).

An infrared spectrum of a molecule is formed because of the absorption of electromagnetic radiation at frequencies that correlate to the vibration of chemical bonds from within the molecule (Coates, 2000). IR spectroscopy is popularly used for the determination of functional groups in a molecule, as most functional groups have characteristic IR absorption bands (McMurray, 2008). IR spectroscopy was used in this study for the identification of the γ-lactone group and the two exocyclic methylene groups present in this sesquiterpene lactone.

4.3.2.1.2. Determination of functional groups present in the isolated compound using IR spectroscopy:

The compound already dissolved in $CDCl_3$ for NMR experiments was used to record the IR spectrum on a Perkin Spectrum 400 FT-IR/FT-FIR spectrometer with an Attenuated Total Reflectance (ATR) sampling accessory.

4.3.2.2. Nuclear Magnetic Resonance (NMR) spectroscopy:

4.3.2.2.1. Background:

NMR spectroscopy is a non-destructive technique that is capable of complete structural and conformational analysis of complex molecules. High resolution NMR spectroscopy was developed to determine molecular structure. NMR refers to the absorption and release of radio frequency energy by nuclei in a magnetic field (Smith and Blandford, 1995).

NMR spectroscopy is used to determine a molecule's carbon-hydrogen framework. Magnetic nuclei (^1H and ^{13}C) spin randomly in the absence of a magnetic field. In the presence of an

external magnetic field (B_o), the nuclei become oriented in a specific way, i.e. either parallel or anti-parallel to the magnetic field. Nuclei are then irradiated with electromagnetic radiation of a particular frequency and the magnetic nuclei are said to be in resonance with the applied radiation (McMurry, 2008).

In bulk matter, nuclei are surrounded by electronic clouds, i.e. electrons, which are also effected by an applied magnetic field. The electronic clouds exert a small but significant deshielding or shielding effect due to magnetic anisotropy. Because each nucleus has different electronic environments, each nucleus is deshielded or shielded to a slightly different extent. Thus a distinct NMR signal for each ^{1}H and ^{13}C nucleus is detected (Smith and Blandford, 1995; McMurry, 2008).

One-dimensional (1D) NMR spectroscopy refers to the individual resonance frequencies for a particular nucleus, either ^{1}H or ^{13}C. Distortionless Enhancement by Polarisation Transfer (DEPT) ^{13}C experiments is a popular method for determining the multiplicity of coupled spins between ^{13}C and ^{1}H nuclei. It is used to differentiate between C, CH, CH_2 and CH_3 groups. As a molecule becomes more complex, it is advantageous to perform two-dimensional (2D) NMR spectroscopy, which will provide information regarding the interactions and the arrangements between the different atoms of the molecule. 2D NMR spectroscopy techniques used in this study were homonuclear and heteronuclear through-bond correlation and through-space correlation methods. These were correlation spectroscopy (COSY), heteronuclear single-quantum correlation spectroscopy (HSQC), heteronuclear multiple-bond correlation spectroscopy (HMBC) and nuclear Overhauser effect spectroscopy (NOESY). The relevant information gained from each 2D NMR technique is listed below (Silverston, 2005):

- COSY: gives rise to cross peaks (signals) for all protons that have spin-spin coupling, i.e. cross peaks correlate coupled protons through bonds. Double quantum filtered (DFQ) COSY is a phase sensitive COSY technique and decreases the intensity of diagonal signals. This gives a cleaner spectrum by preventing diagonal signals from obscuring cross signals.
- HSQC: detects proton-carbon coupling which are separated by one bond.
- HMBC: gives rise to cross peaks with proton-carbon coupling over longer ranges of 2 to 4 bonds.

- NOESY: cross peaks connect resonances from nuclei that are spatially close and not those that are coupled through bonds.

4.3.2.2.2. Method of structural elucidation of the isolated compound using NMR spectroscopy:

^{1}H NMR was performed on the crude ethanol extract of *A. afra* and at various steps in the isolation of the compound to determine the purity of the compound. To determine the structure of the compound, 1D and 2D NMR experiments were conducted. All spectra were obtained in $CDCl_3$. ^{1}H and ^{13}C NMR spectra were recorded at 600.03 and 150.89 MHz, respectively, using residual solvent signals as internal references.

NMR spectra were processed using MestReNova Version 6.2 0-7238 and Bruker Topspin Version 2.1. software. Structures shown in Figure 4.21 and 4.22 were done with ACD Chemsketch Freeware Version 12.01. Structure optimisation (Figure 4.25) was done using iSpartan from Wavefunction, Inc.

4.3.2.3. Circular Dichroism (CD) Spectroscopy:

4.3.2.3.1. Background:

CD spectroscopy is an analytical technique that is used in conjunction with other spectroscopic techniques to determine the absolute configuration of chiral centres in a molecule. It is based on the interaction between circularly polarized light and the chiral chromophoric sites on a molecule. It is measured over a range of wavelengths, usually in the visible and ultraviolet range of the electromagnetic spectrum. CD spectroscopy measures the difference in absorbance of right- and left-circulatory polarised light by a molecule (Kelly and Price, 2000; Kelly *et al*, 2005). This yields a difference in absorption coefficients $\Delta\varepsilon = \varepsilon_{left} - \varepsilon_{right}$ (Wilson and Walker, 2010).

CD can be applied to any chromophore containing optically active molecule which will give rise to a Cotton effect. This effect is associated with a chromophore that is in the vicinity of a chiral centre. Peaks and troughs in the spectrum where the chromophores absorb are considered to be anomalous and called a Cotton effect. The carbonyl group in the lactone ring

is the major chomophore giving rise to a Cotton Effect. There are a number of empirical rules that are used to interpret Cotton effects of saturated and unsaturated carbonyl groups as well as a sector rule for lactones (Crabbé, 1971), none of which describe the Cotton Effect observed for sesquiterpene lactones adequately. Stöcklin *et al.* (1970) determined that the α-methylene-γ-lactone lactone moieties that are *cis*-fused on carbon atoms 7 and 8 will display a negative Cotton effect.

4.3.2.3.2. Determination of absolute structure and configuration of the isolated compound:

The isolated compound was analysed using CD spectroscopy. The CD spectrum of the compound was recorded in methanol on an Applied Photophysics Chirascan Plus spectrometer at 293 K with a pathlength of 10 mm at the Central Analytical Facility (CAF) at the University of Stellenbosch.

4.3.2.4. Mass Spectrometry (MS):

4.3.2.4.1. Background:

EI-MS is an analytical technique that enables the determination of the mass and certain structural aspects of a compound by ionizing it to generate radical cations and measuring their mass-to-charge ratio (*m/z*). Ions are separated according to their *m/z*. MS was used for confirmation of the chemical formula and mass of the compound.

4.3.2.4.2. Molecular mass determination:

EI-MS was performed at InnoVenton/DCTS using GC/EI-MS. The compound was dissolved in dichloromethane (DCM) before injection.

4.4. Results:

4.4.1. Bioassay-guided fractionation of an ethanol extract of *A. afra*:

4.4.1.1. Fractionation of A. afra *crude extract:*

Fractionation was performed to separate compounds based on their polarities (Table 4.1.and 4.2). Fractions were collected in pre-weighed pill vials and solvent was evaporated. Pill vials were weighed after solvent evaporation and the mass of each fraction was recorded. TLC in a 1:1 hexane: ethyl acetate solvent system was done for all fractions (Figure 4.4).

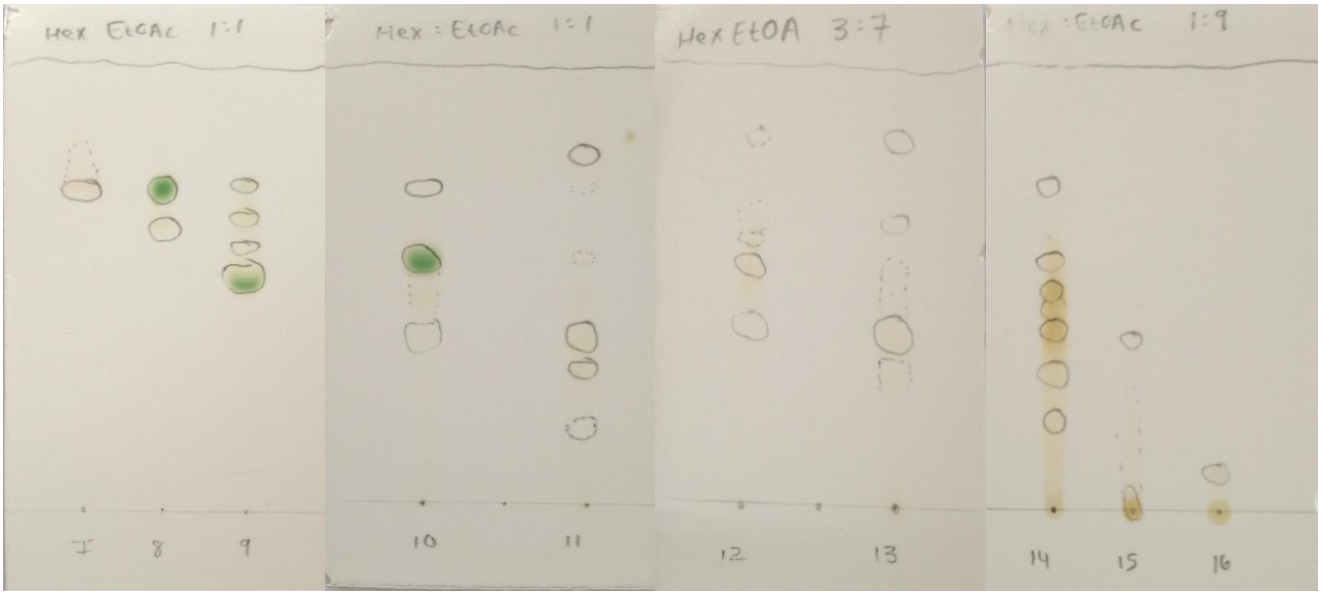

Figure 4.4: TLC plates of fractions obtained from the gradient fractionation of ethanol *A. afra* extract. Numbers 7 – 16 correlate to the fractions described in Table 4.1. and 4.2.

4.4.1.2. Determination of cytotoxic fractions using the MTT cytotoxicity assay and ^{1}H NMR spectroscopy of test fractions:

Fractions 7-16 were tested for cytotoxicity using HeLa cancer cells. HeLa cancer cells were used. Figure 4.5 shows this result. Fractions 8 – 14 all exhibited cytotoxic activity at 30 µg/mL and 100 µg/mL.

At the lowest concentration used, 3 µg/mL, fractions 8, 10 and 12 showed the most promising results. ^{1}H NMR spectroscopy of the most active fractions (fractions 8, 10 and 12) was done. Results are shown in Figure 4.7.

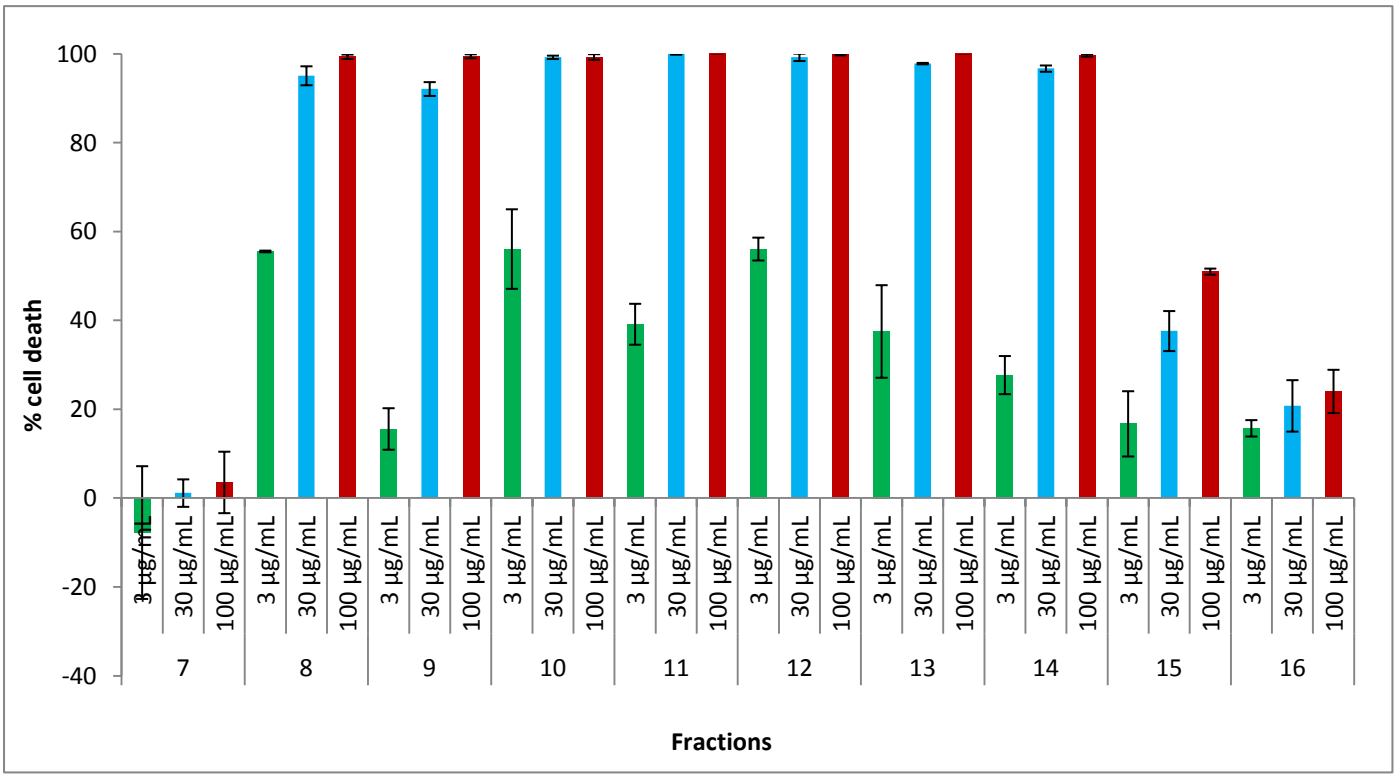

Figure 4.5: Percentage cell death of HeLa cells induced upon treatment with collected fractions. Error bars indicate SD values of triplicate readings.

There was insufficient material in fractions 1-6 to perform NMR spectroscopy and the MTT assay. As seen in Figure 4.5, fractions 8, 10 and 12 had the most promising cytotoxic effects at a concentration of 3 µg/mL, thus the ^{1}H NMR spectra were compared (Figure 4.7). An NMR spectrum of the crude ethanol extract was also obtained (Figure 4.6). It clearly shows the presence of signals with chemical shift values that are characteristic of sesquiterpene lactones indicated by red arrows in Figure 4.6. This is also clear in the spectrum of fraction 8, indicated by the blocked section on Figure 4.7. Due to the results of the MTT assay and the ^{1}H NMR spectra, fraction 8 was chosen to be further purified and characterized.

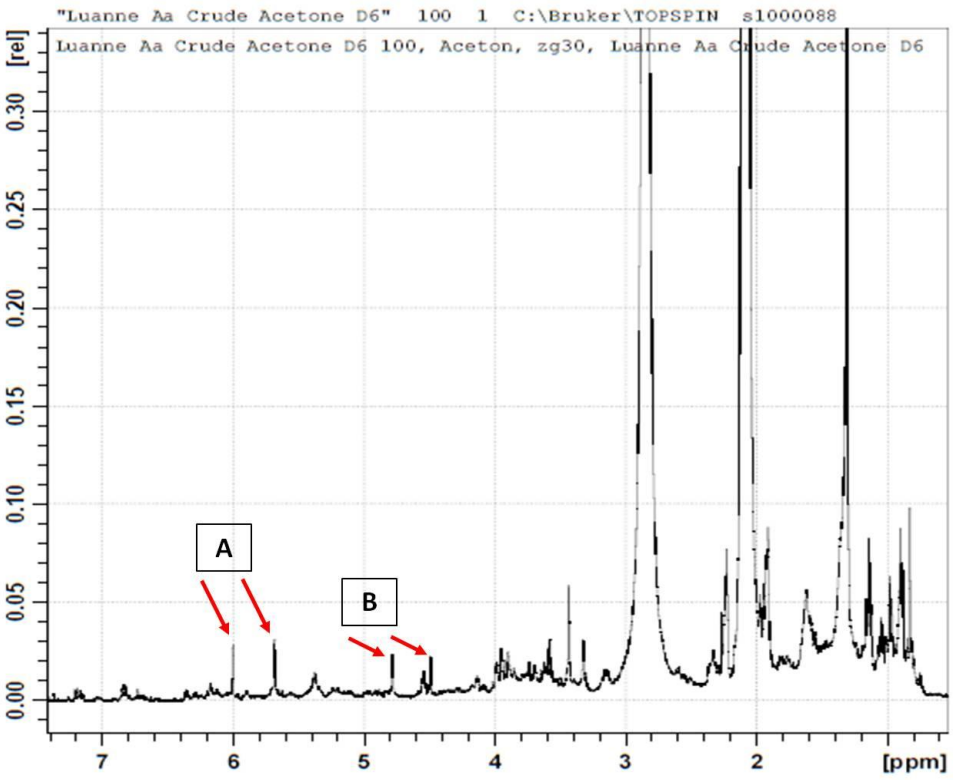

Figure 4.6: **^{1}H NMR spectrum for crude ethanol *A. afra* extract (600 MHz, deuterated acetone). Red arrows at A indicate characteristic exocyclic methylene groups belonging to lactone ring. Red arrows at B indicate an exocyclic methylene group at another position in the structure.**

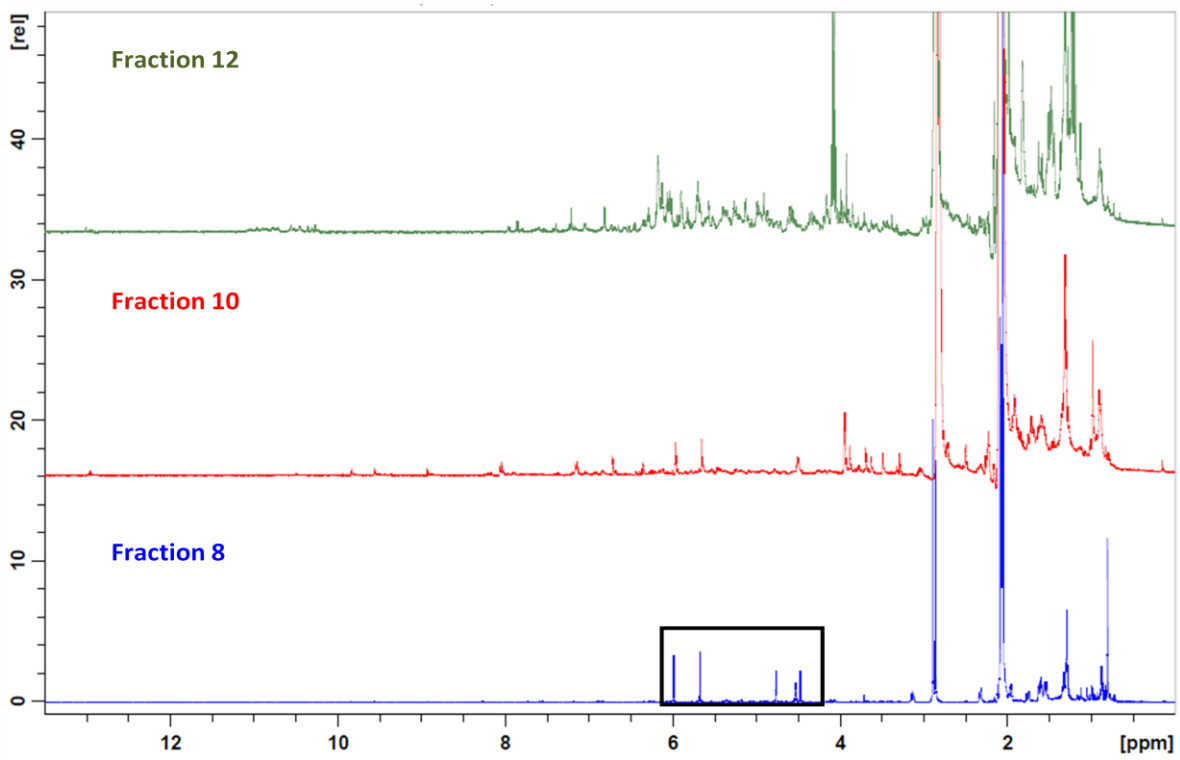

Figure 4.7: **^{1}H NMR spectra for fractions 8, 10 and 12 (600 MHz, deuterated acetone). The characteristic signals of exocyclic methylene groups belonging to sesquiterpene lactones are highlighted by the black box.**

4.4.1.3. Preparative fractionation of cytotoxic compounds from ethanol A. afra *extract*:

Two preparative TLC separations were done to further purify only the cytotoxic fraction 8. The same mobile phase of hexane: ethyl acetate (1:1 v/v) was used. Figure 4.8 shows the purification of the cytotoxic fraction using this method. Four clear bands were visible with different masses and Rf as indicated.

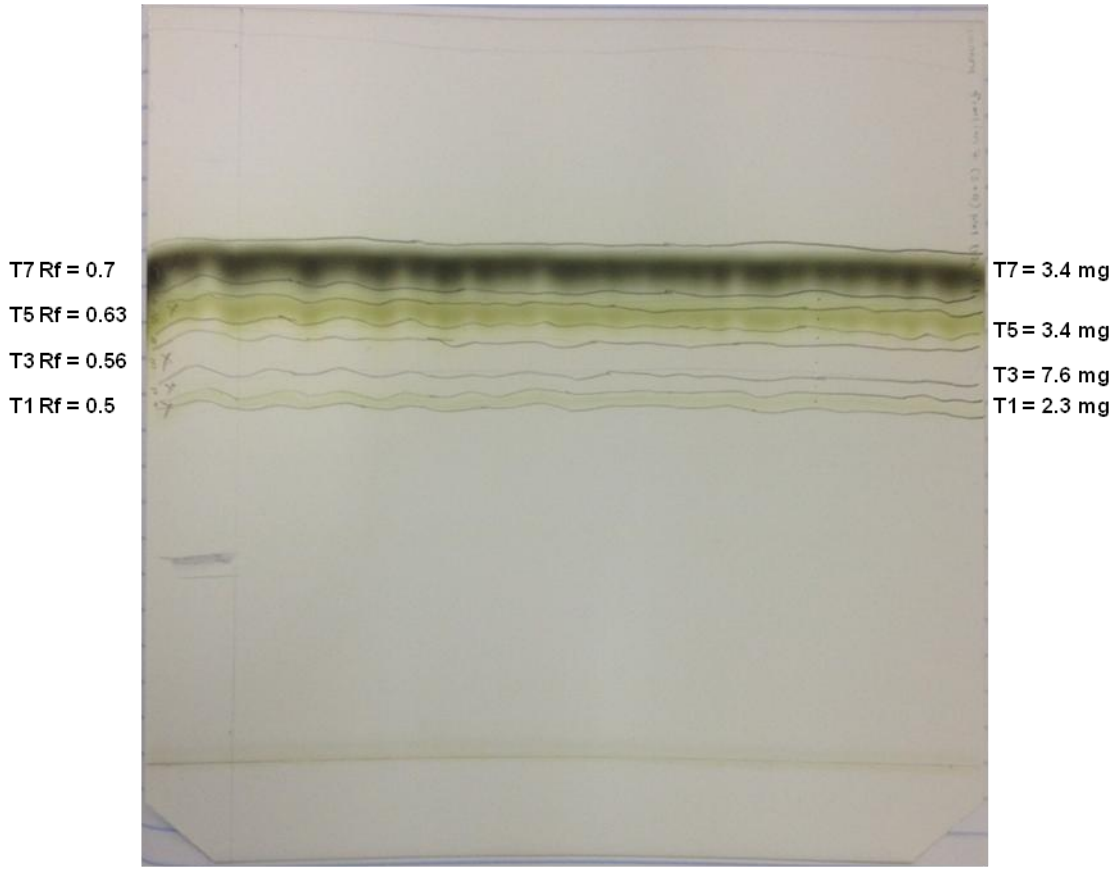

<u>Figure 4.8:</u> Preparative TLC for the separation and isolation of cytotoxic compound(s) using hexane: ethyl acetate (1:1 v/v) solvent system. Bands of interest were identified using UV light at 254 nm and are labelled and masses indicated.

4.4.2. Structural elucidation and identification of the active compound:

4.4.2.1. IR spectroscopy:

The presence of particular functional groups was determined using IR spectroscopy. The characteristic strong absorption of a γ-lactone ring appear at 1758.71 cm^{-1}(C=O stretching vibrations) and at 1263.14 cm^{-1} (C-O stretching vibrations). The strong absorptions at 905.15 cm^{-1} and 891.11 cm^{-1} are characteristic of the C-H vibrations of the exocyclic methylene (vinylidene) groups (Silverstein *et al.*, 2005) as indicated in Figure 4.9.

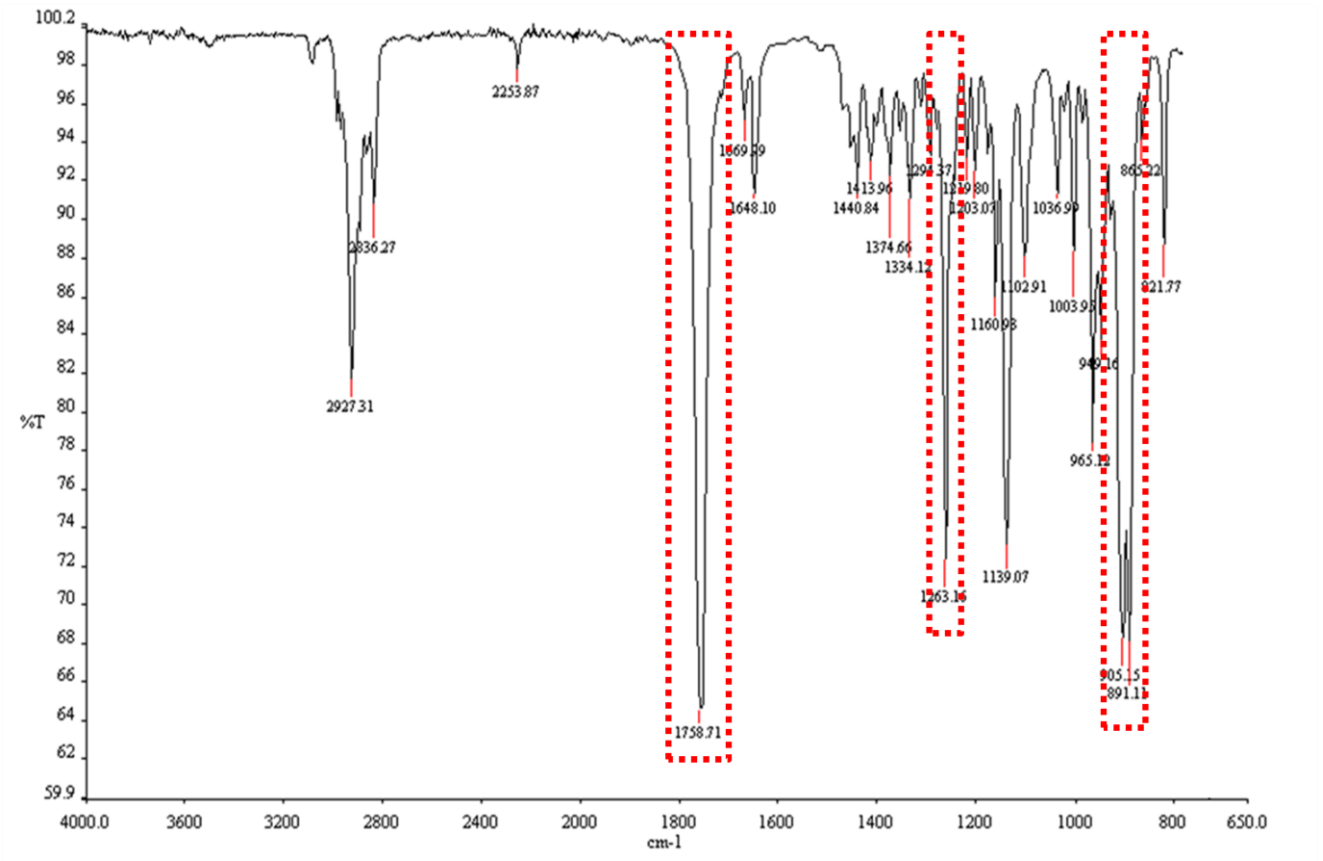

Figure 4.9: Identification of functional groups of the isolated compound using IR spectroscopy. Characteristic strong absorptions are indicated by red boxes.

4.4.2.2. NMR spectroscopy:

a) ^{1}H NMR spectroscopy:

^{1}H NMR spectroscopy was used regularly to check the purity of the compound before bioassays were done. Figure 4.10 shows the ^{1}H NMR spectrum of the final purified molecule indicating the assignment of protons and integration values.

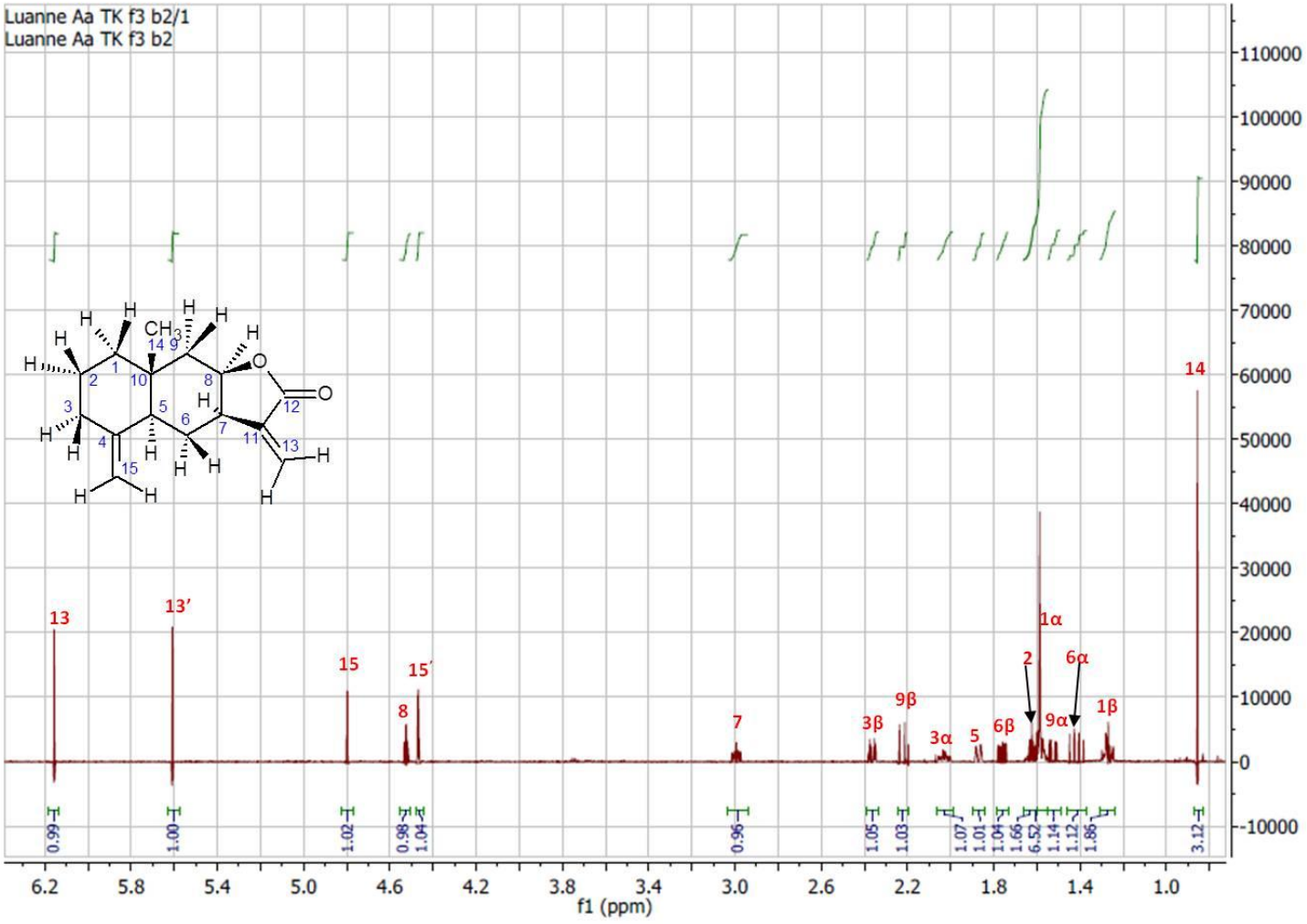

Figure 4.10: ^{1}H NMR spectrum of the isolated compound (600 MHz,$CDCl_3$). Protons are assigned to signals and are indicated in red and integration values below signals indicate the relative numbers of hydrogen nuclei represented by each signal.

Table 4.3 indicates the chemical shift values as well as the multiplicity of the protons. The chemical shift values were used to compare the data gained here to spectral data of other

sesquiterpene lactones isolated from *Artemisia* species. Reported structures (Jakupovic *et al.*, 1988) were used to predict possible ^{1}H NMR spectral outcomes and these data were compared to the ^{1}H NMR spectrum of the isolated compound from *A. afra*. Chemical shift values of the isolated compound were also compared to reported ^{1}H NMR spectral data of sesquiterpene lactones isolated from other plant species.

Table 4.3: ^{1}H NMR spectral data of the isolated cytotoxic compound (600.03 MHz, $CDCl_3$, δ values).

H	δ value (ppm)	multiplicity
1β	1.26	*m*
1α	1.54 - 1.65	*m*
2α		
2β		
3α	2.03	*m*
3β	2.36	*dt*
5	1.87	*dd*
6α	1.76	*m*
6β	1.42	*m*
7	2.97	*m*
8	4.5	*td*
9α	1.53	*ddd*
9β	2.23	*dd*
13'	5.58	*d*
13	6.13	*d*
14	0.83	*s*
15'	4.45	*q*
15	4.77	*q*

b) ^{13}C NMR spectroscopy:

^{13}C NMR spectroscopy indicated the presence of 15 carbon atoms, confirming the presence of a sesquiterpenoid. The ^{13}C spectrum is shown in Figure 4.11. Due to problems encountered with software for processing DEPT experiments, a ^{1}H coupled ^{13}C experiment was done to determine the multiplicity of C atoms and the number of H atoms coupled to each C. Figure 4.12 shows the result of this experiment. Table 4.4 indicates the chemical shift values (δ value) for each C atom that correlates to the ^{13}C spectrum. Carbon nuclei were assigned using HSQC and HMBC spectroscopy (section 4.4.2.2 c and 4.4.2.2 f, respectively).

Table 4.4: **^{13}C NMR spectral data of the isolated compound (150.89 MHz, $CDCl_3$, δ values).**

C	δ value (ppm)	Multiplicity in ^{1}H coupled spectrum
1	42.22	t: CH_2
2	22.71	t: CH_2
3	36.83	t: CH_2
4	148.97	s: C
5	46.25	d: CH
6	27.5	t: CH_2
7	40.57	d: CH
8	76.82	d: CH
9	41.4	t: CH_2
10	34.31	s: C
11	142.22	s: C
12	170.63	s: C
13	120.05	t: CH_2
14	17.68	q: CH_3
15	106.63	t: CH_2

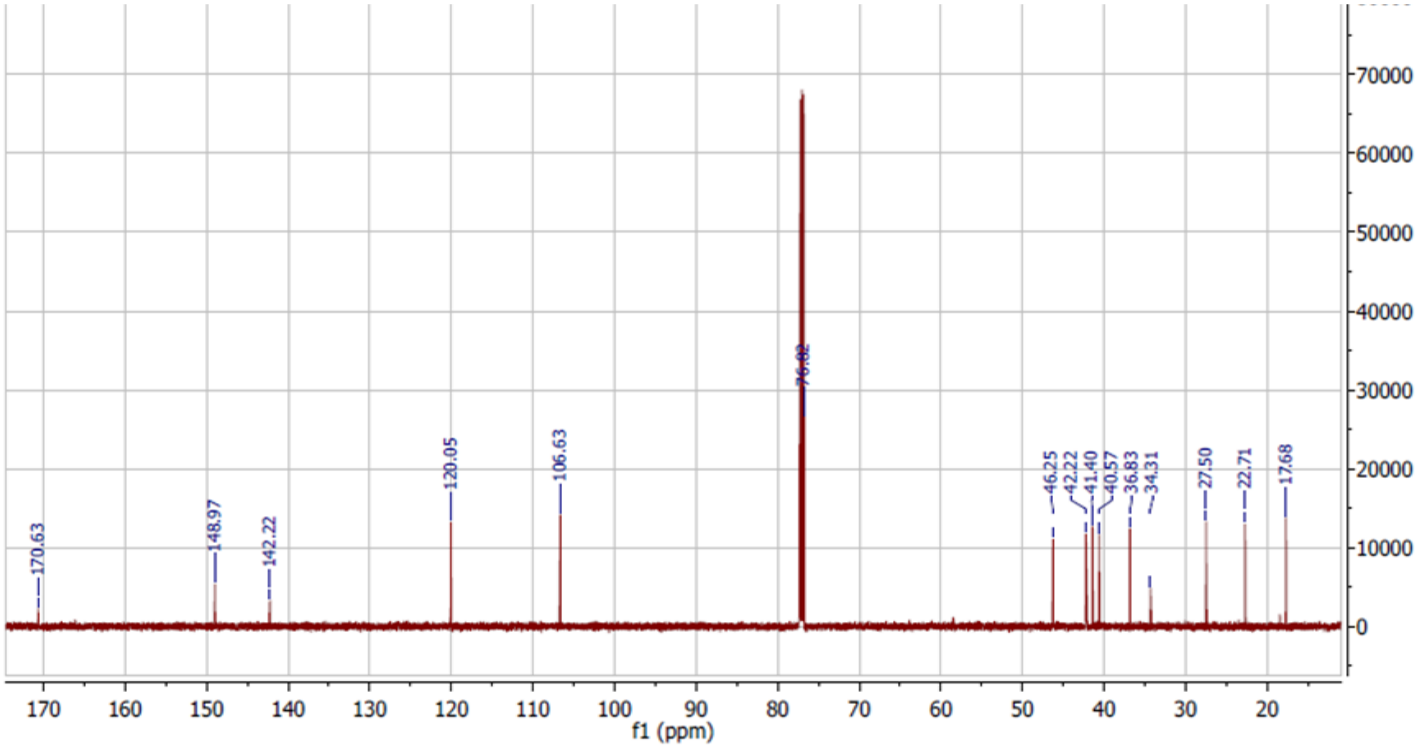

Figure 4.11: **^{13}C NMR spectrum of the isolated compound indicating the presence of 15 carbon atoms.**

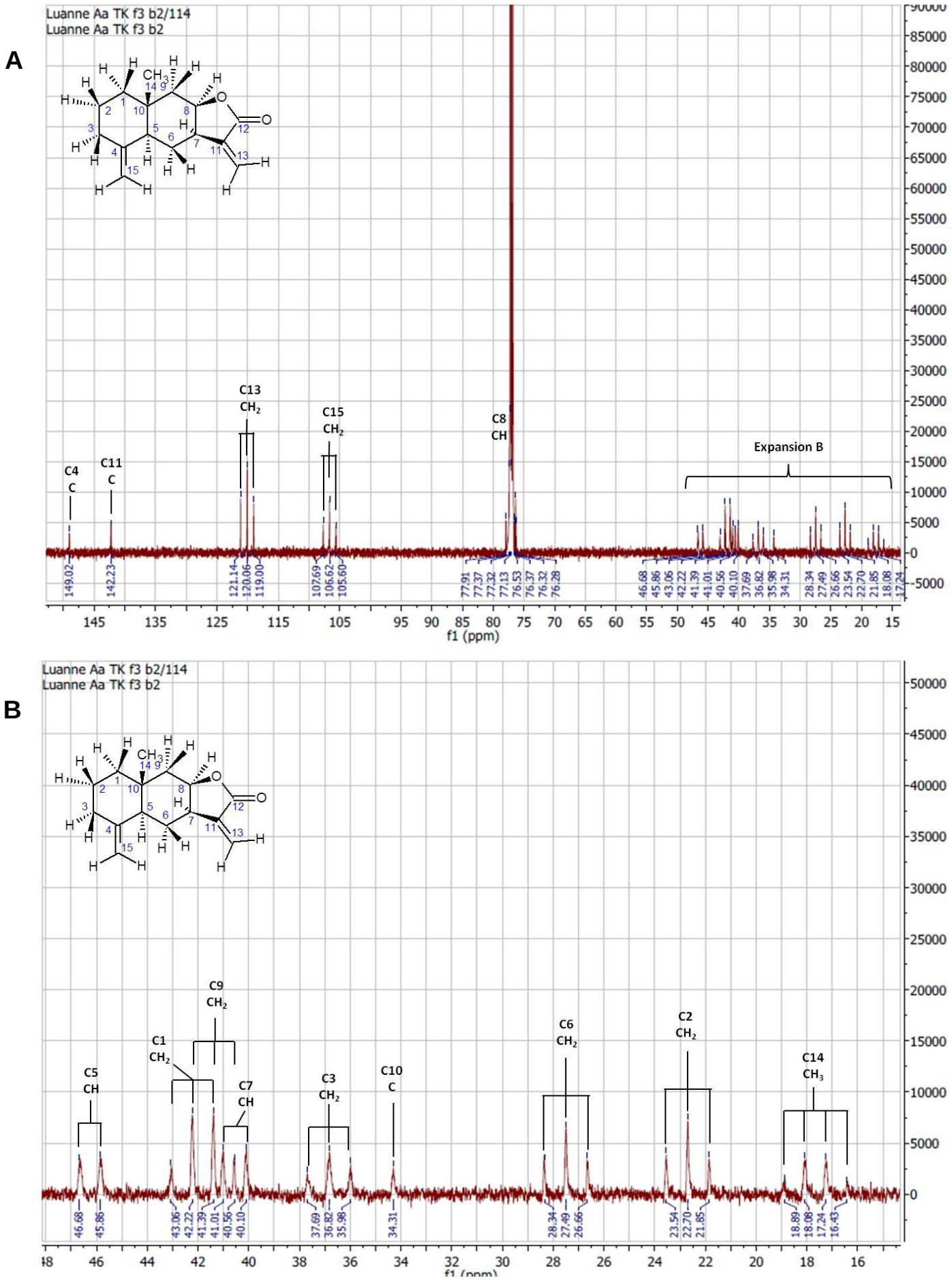

Figure 4.12: Determination of multiplicity of C and number of H atoms using ^{1}H coupled ^{13}C experiment. A) 15 – 150 ppm; B) 15 – 48 ppm.

c) HSQC spectroscopy:

HSQC correlation spectroscopy indicates proton-carbon coupling and will show the correlation of carbons and protons in the molecule. A 2D heteronuclear chemical shift correlation map between directly-bonded ^{1}H and ^{13}C heteronuclei is shown in Figure 4.13. The x-axis represents the ^{1}H NMR spectrum and the y-axis represents the ^{13}C spectrum. The resulting signals provide information of direct proton-carbon coupling. Expansion of the HSQC spectrum was done to unambiguously assign carbon nuclei to hydrogen nuclei. Figure 4.14 A and B show these spectra.

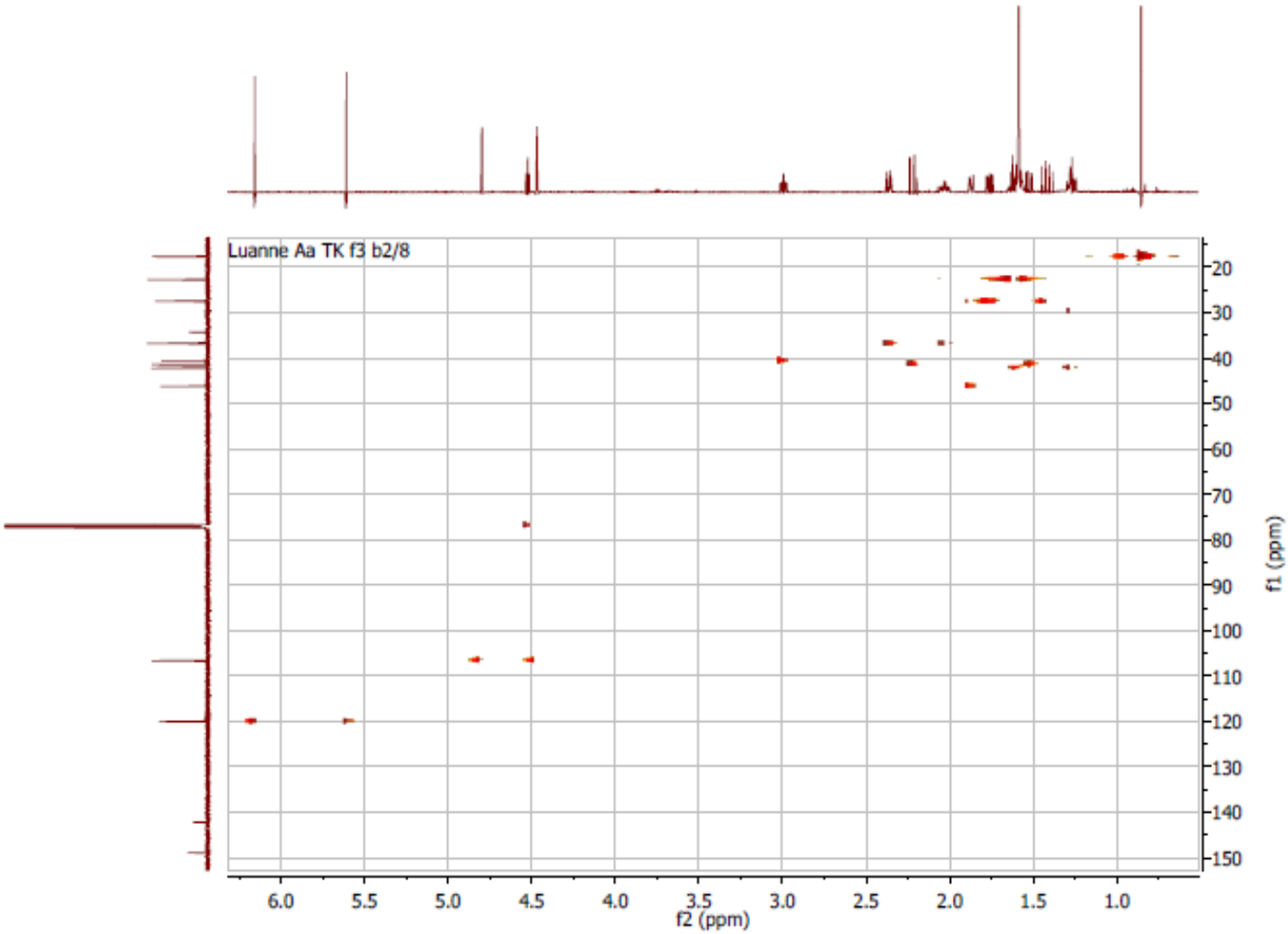

Figure 4.13: HSQC spectrum.

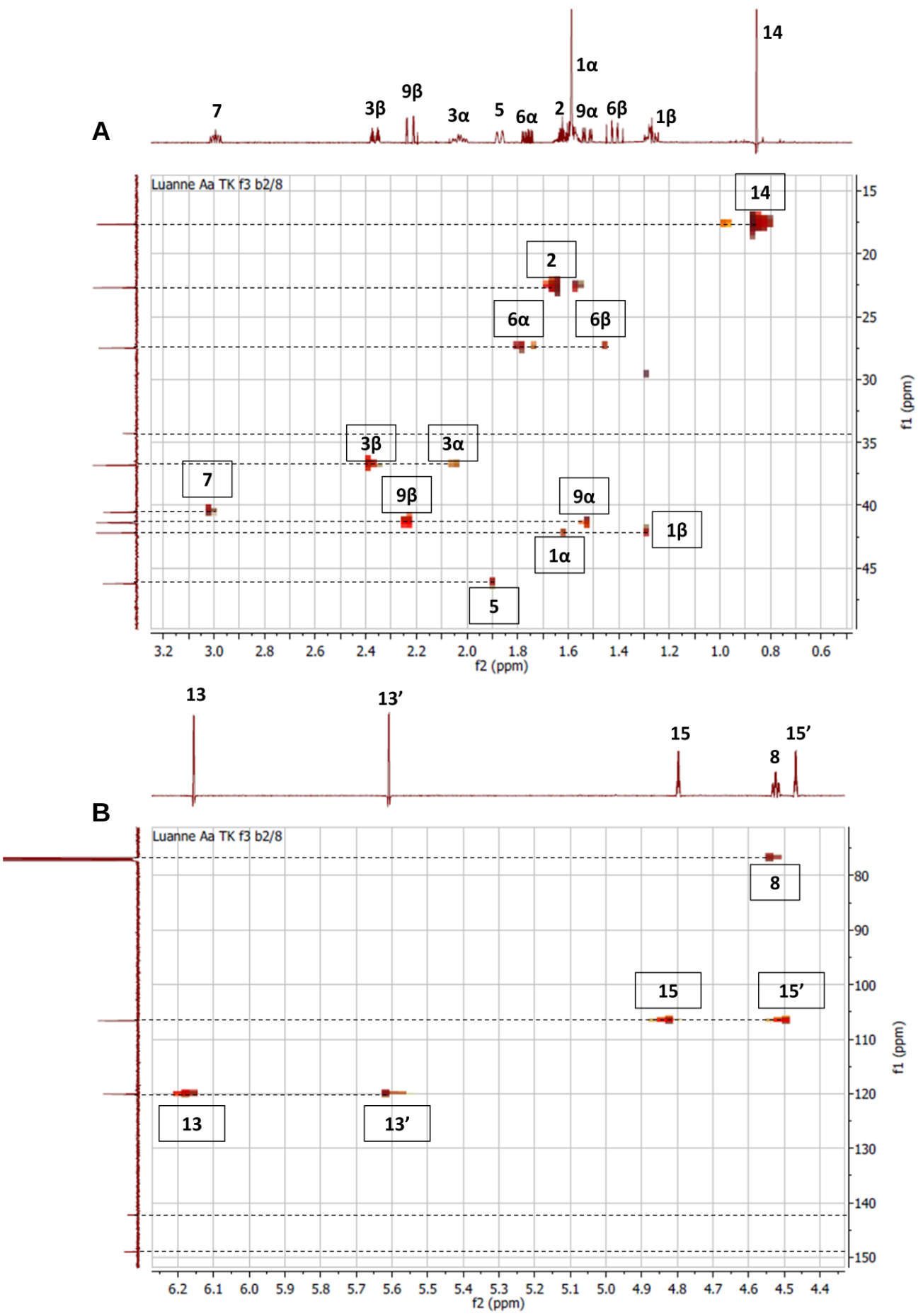

Figure 4.14: **HSQC expansion spectra showing assignment of C atoms on y-axis. A) 0.6 ppm to 3.2 ppm (x-axis) and B) 4.35 ppm to 6.25 ppm (x-axis).**

d) DQF-COSY:

A DQF-COSY was performed to correlate coupled of protons, i.e. cross signals that correlate coupled protons. Figure 4.15 shows the resultant COSY spectrum indicating cross signals for all protons that have spin-spin coupling. Three correlating proton signals are assigned here. Proton signals close to the diagonal were expanded as indicated in Figure 4.16. Assignments of coupled protons were done for all signals. Allylic coupling of exocyclic methylene groups are shown in Figure 4.17.

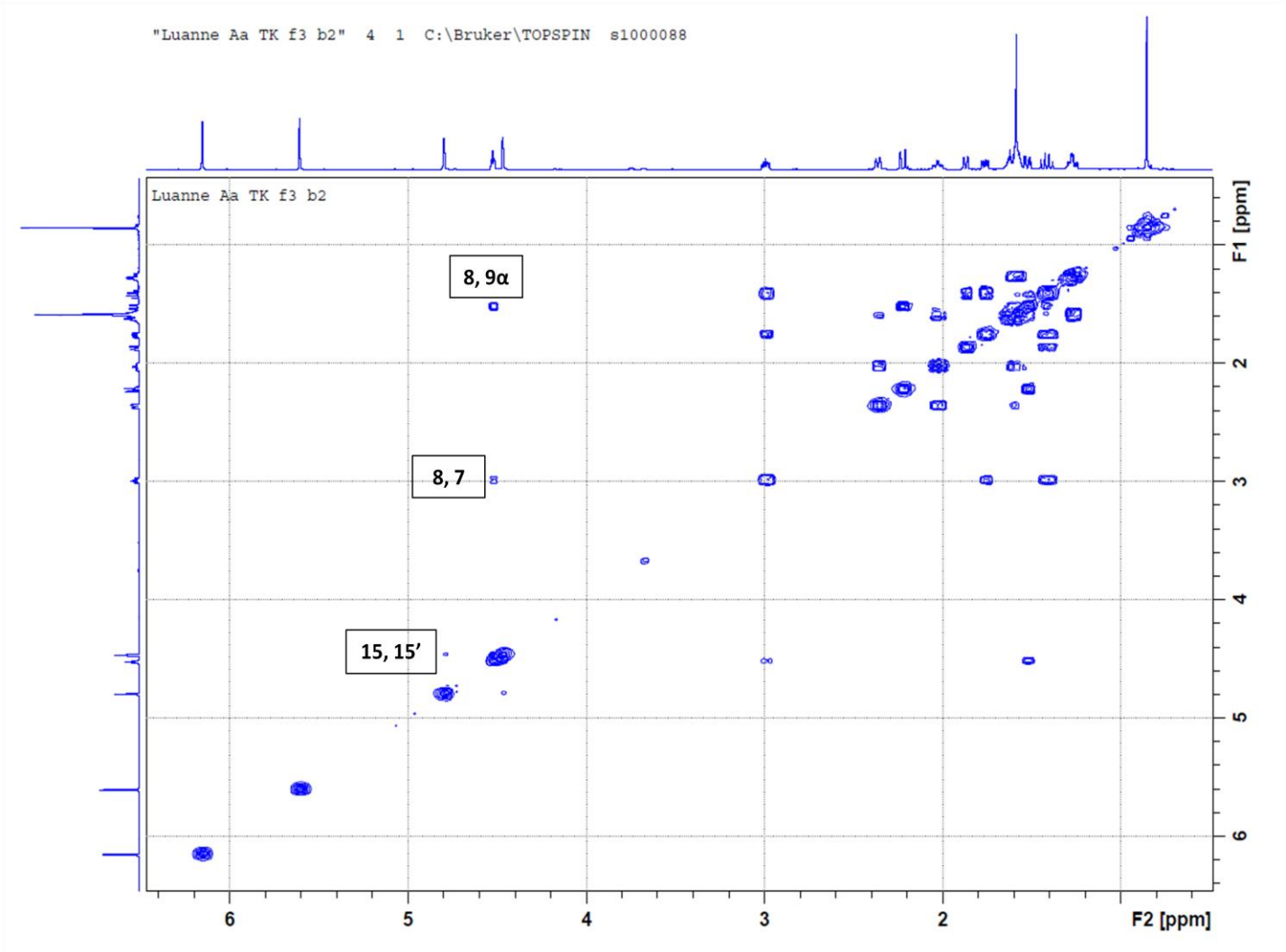

Figure 4.15: ^{1}H-^{1}H COSY spectrum indicating coupled protons highlighted in boxes. The number indicated first refers to the nucleus on the x-axis.

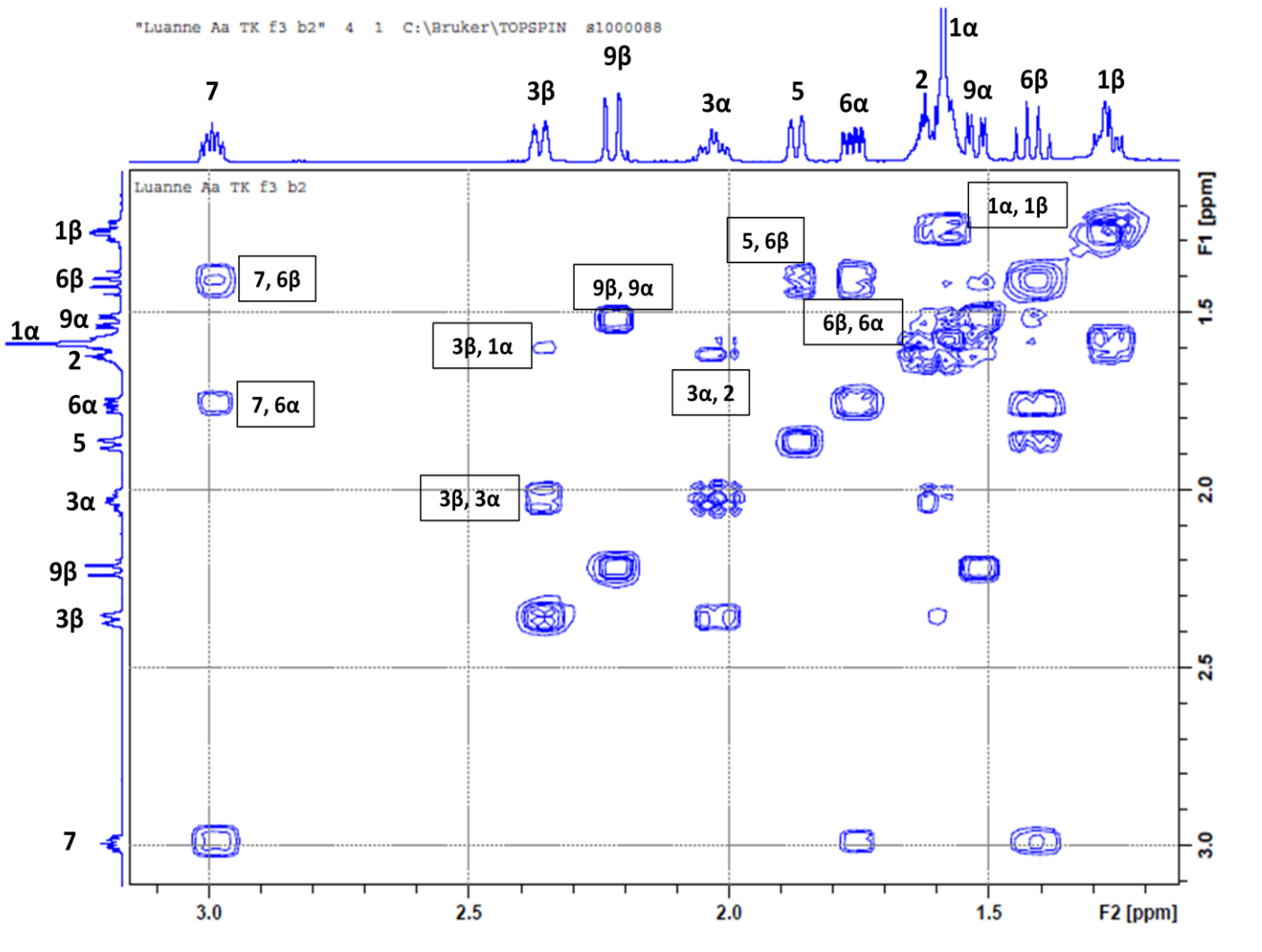

Figure 4.16: ^{1}H-^{1}H COSY expansion from 1.0 ppm to 3.6 ppm on both x- and y-axis. Proton correlation is assigned as indicated in the spectrum. The number indicated first refers to the nucleus on the x-axis.

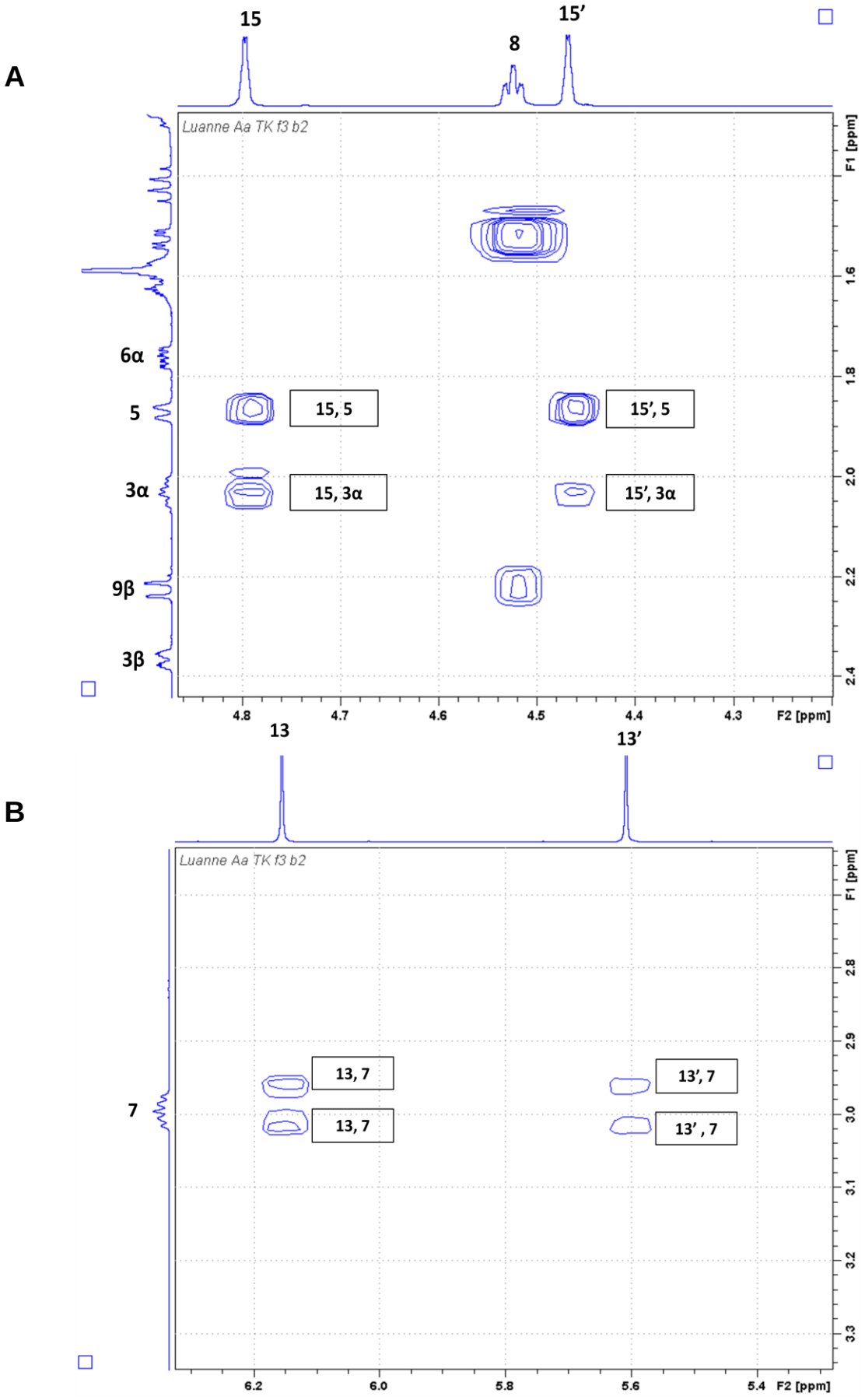

Figure 4.17: **^{1}H-^{1}H COSY expansion showing allylic coupling at the exocyclic methylene groups at C15 (A) and C13 (B). The number indicated first refers to the nucleus on the x-axis.**

e) NOESY:

NOESY was performed to detect correlations of protons through space [less than 5 Å in distance (Silverston, 2005)]. The resulting spectrum is shown in Figure 4.18 and correlations were assigned as indicated in Figure 4.19 A and B.

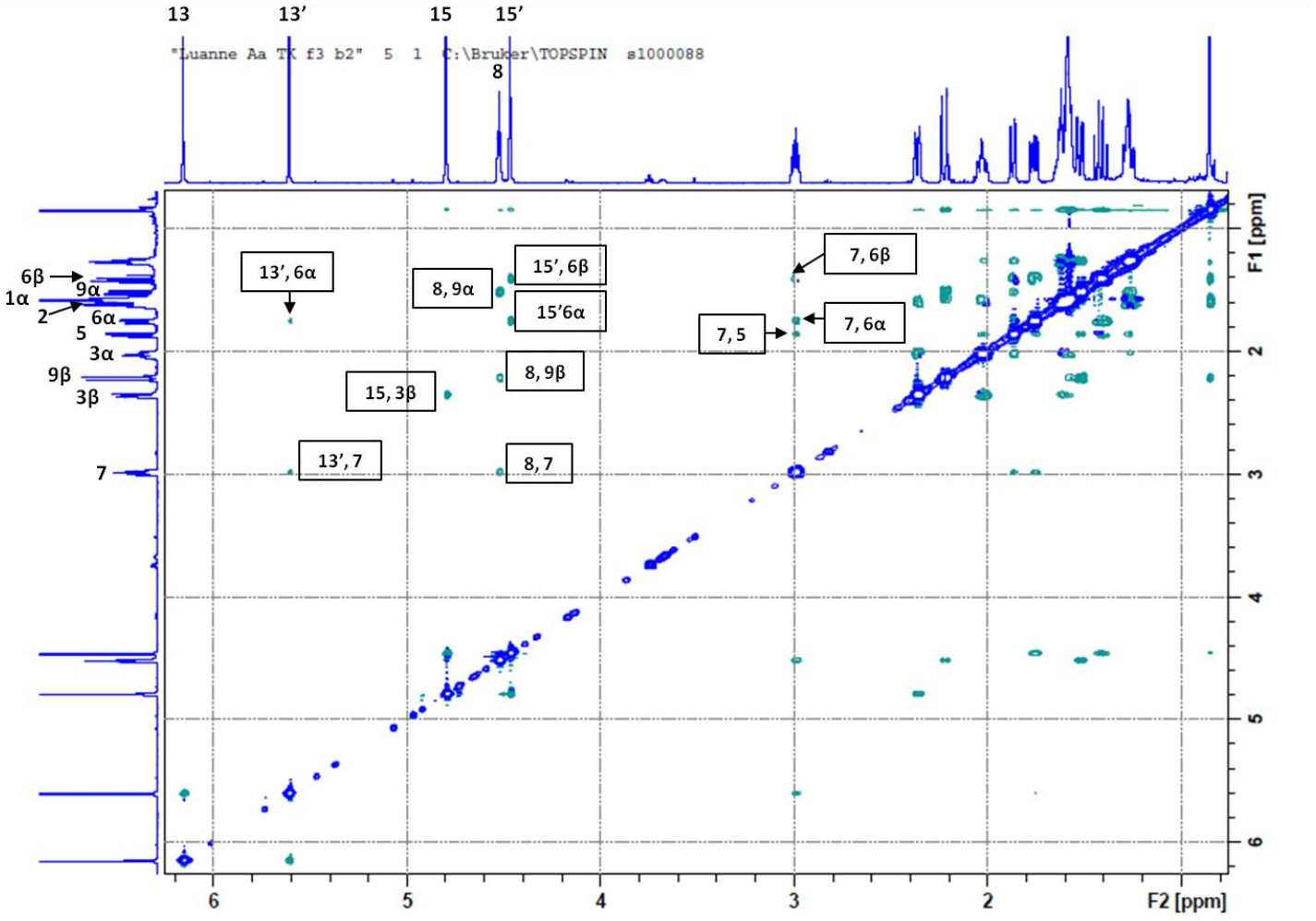

<u>Figure 4.18:</u> NOESY spectrum indicating correlations of protons through space highlighted in boxes. The number indicated first refers to the nucleus on the x-axis.

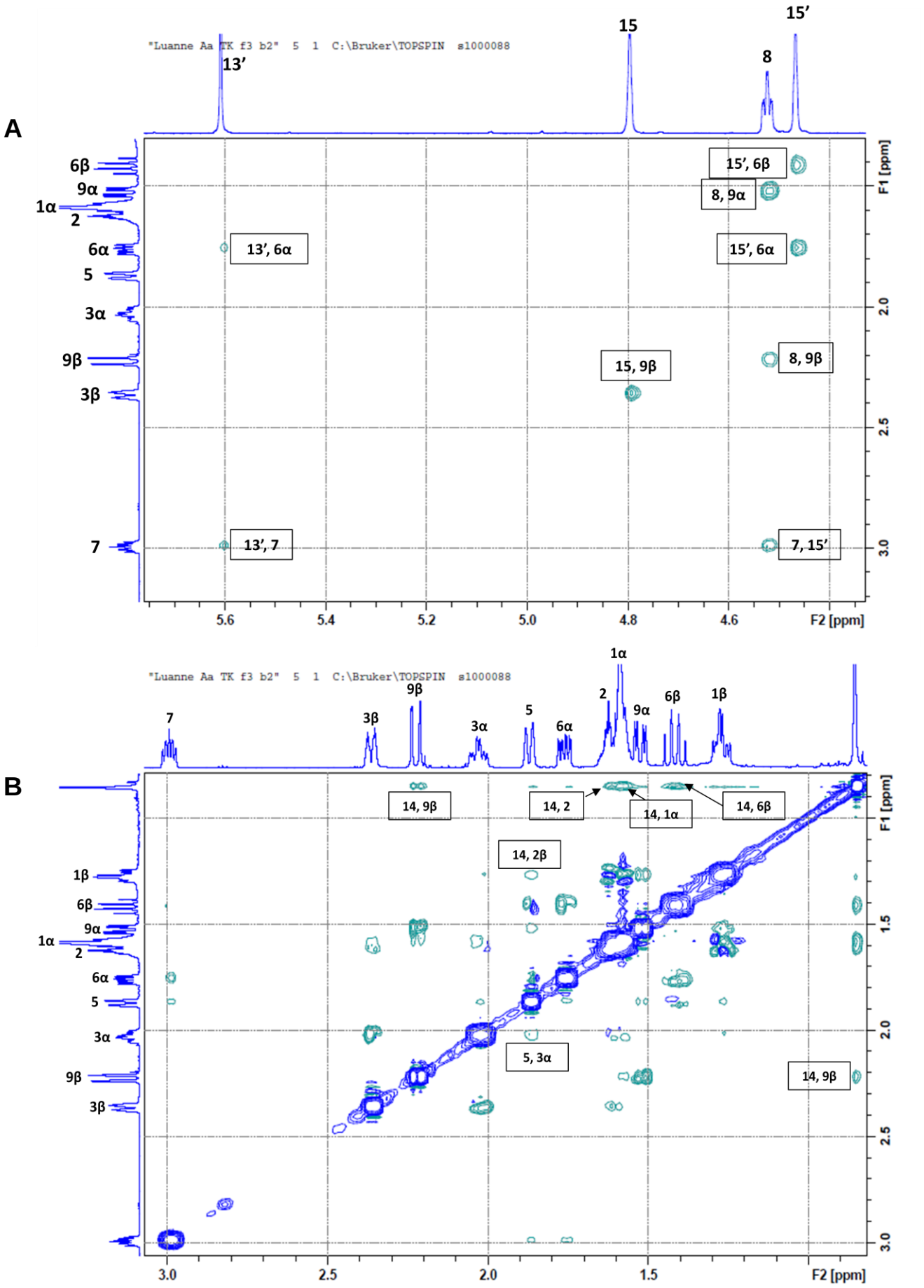

Figure 4.19: **NOESY expansion spectra indicating correlations of protons through space highlighted in boxes. A) 1.3 ppm to 3.2 ppm (x-axis) and 4.375 ppm to 5.625 ppm (y-axis). B) 0.8 ppm to 3.1 ppm (x- and y-axis).**

f) HMBC spectroscopy:

HMBC correlation spectroscopy indicates proton-carbon signals of protons and carbons that are coupled over a long range, 2 to 4 bonds apart (Figure 4.20). HMBC was used to assign C4, C10, C11 and C12 (Figure 4.21) to ^{13}C signals as indicated in Table 4.4.

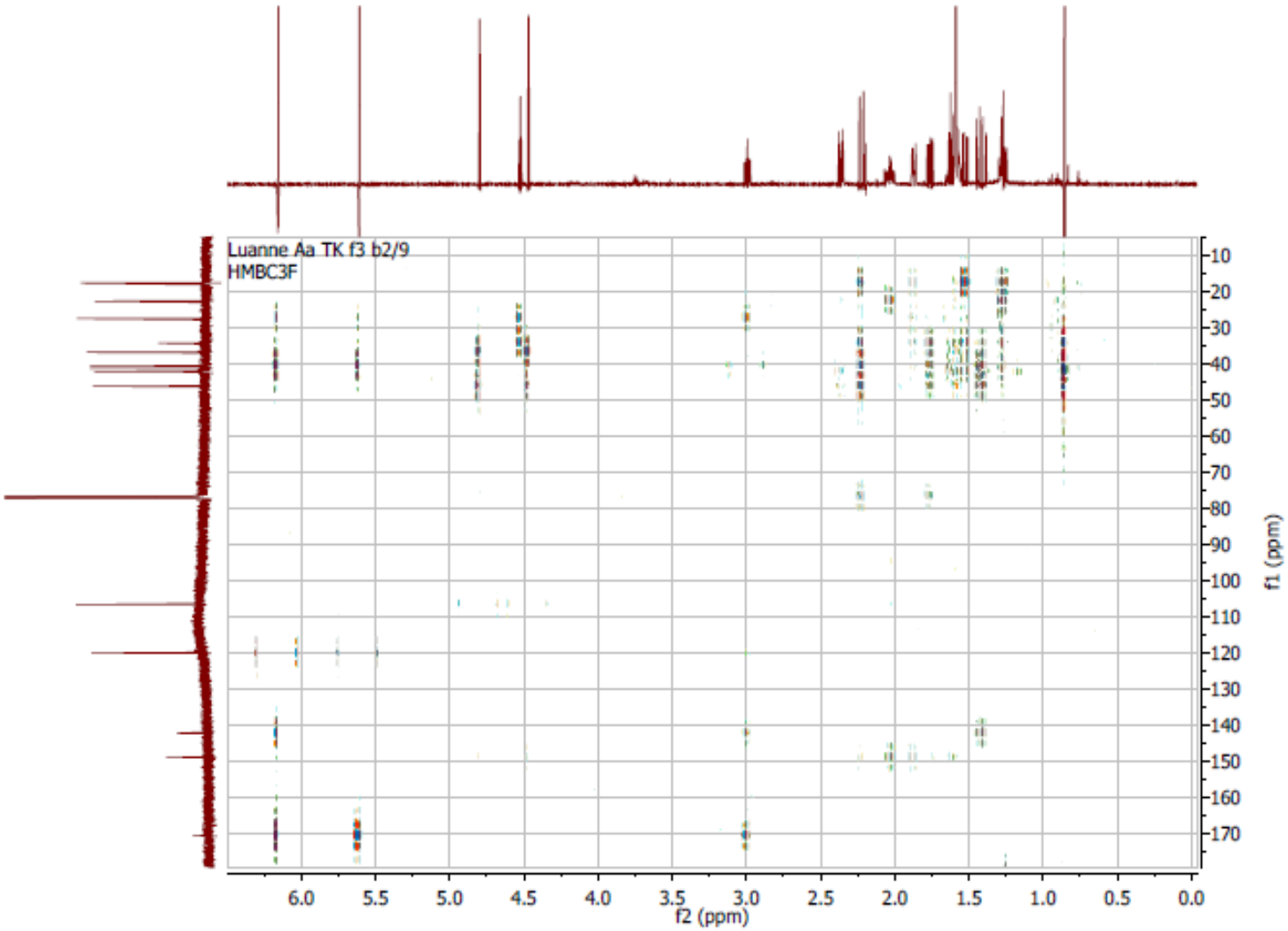

Figure 4.20: HMBC spectrum.

From all the NMR spectroscopy data, the structure shown in Figure 4.22 was elucidated. The correlations of H atoms through space are indicated in Figure 4.23. The structure was identified as the eudesmanolide, isoalantolactone.

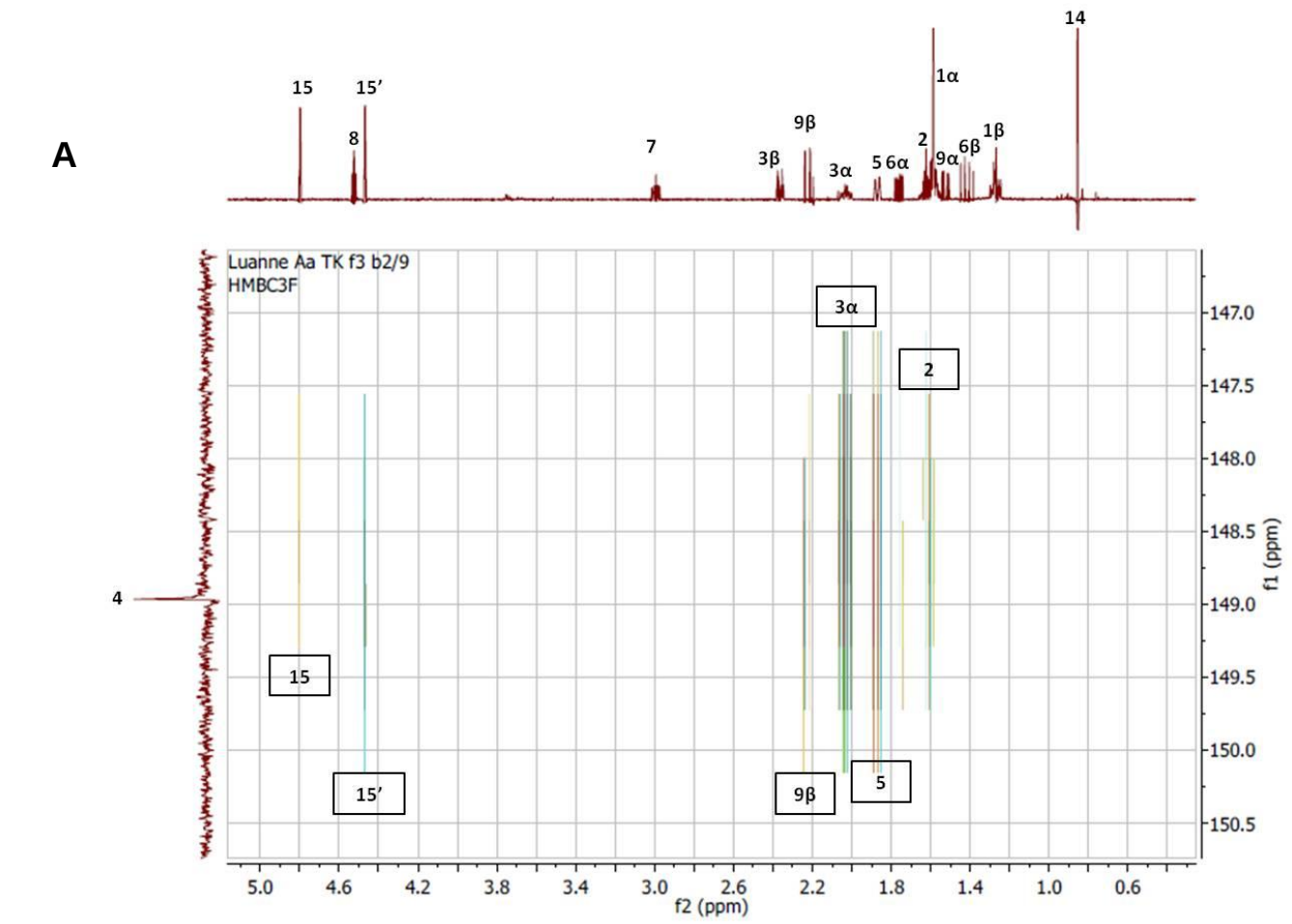
A
15
15’
8
7
3β
9β
3α
5
6α
2
9α
6β
1β
1α
14
Luanne Aa TK f3 b2/9
HMBC3F
3α
2
15
15’
9β
5
4
f1 (ppm)
f2 (ppm)

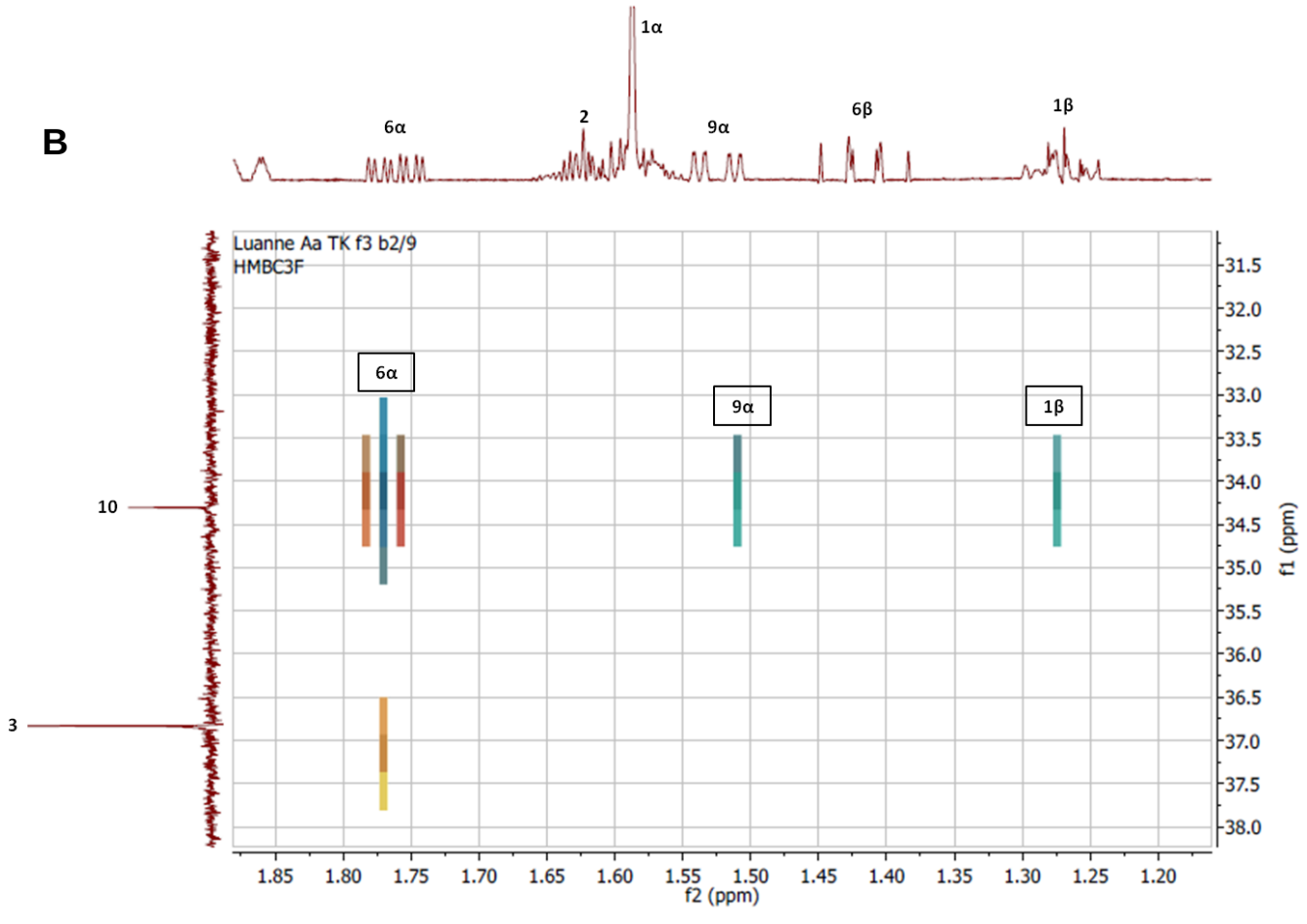
B
1α
6α
2
9α
6β
1β
Luanne Aa TK f3 b2/9
HMBC3F
6α
9α
1β
10
3
f1 (ppm)
f2 (ppm)

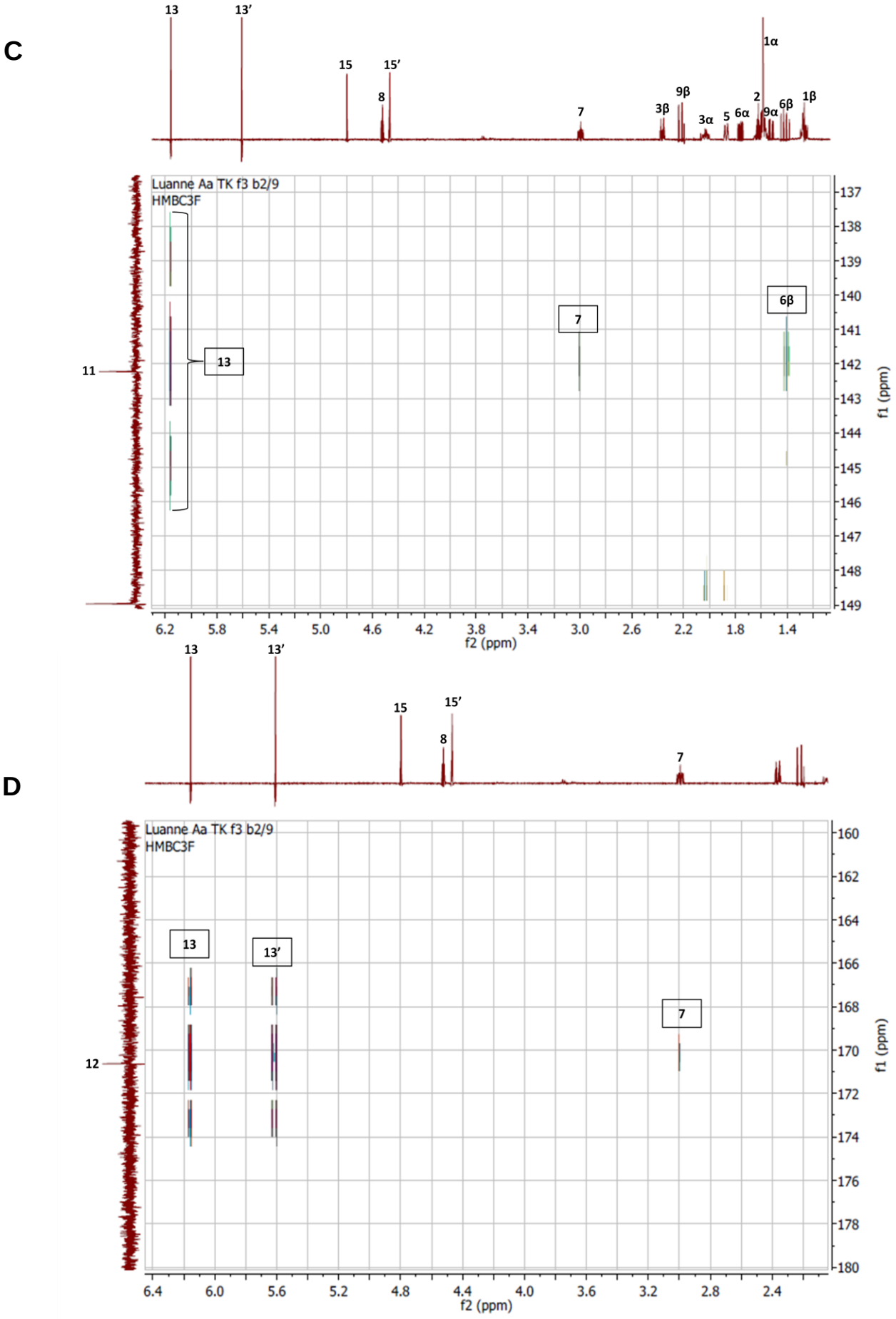

Figure 4.21: **HMBC correlations used for the assignment of A) C4, B) C10, C) C11 and D) C12.**

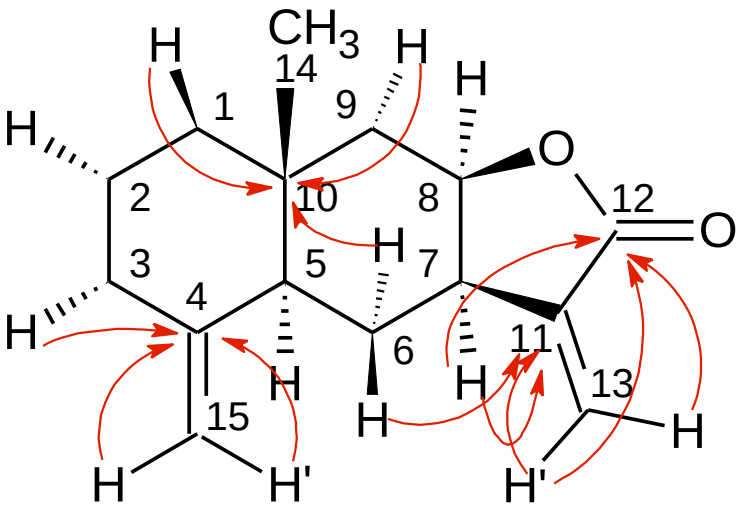

Figure 4.22: **The structure of isoalantolactone isolated from *A. afra*. HMBC correlations indicated by red arrows from ^{1}H to ^{13}C were used to identify the ^{13}C signals of C4, C10, C11 and C12.**

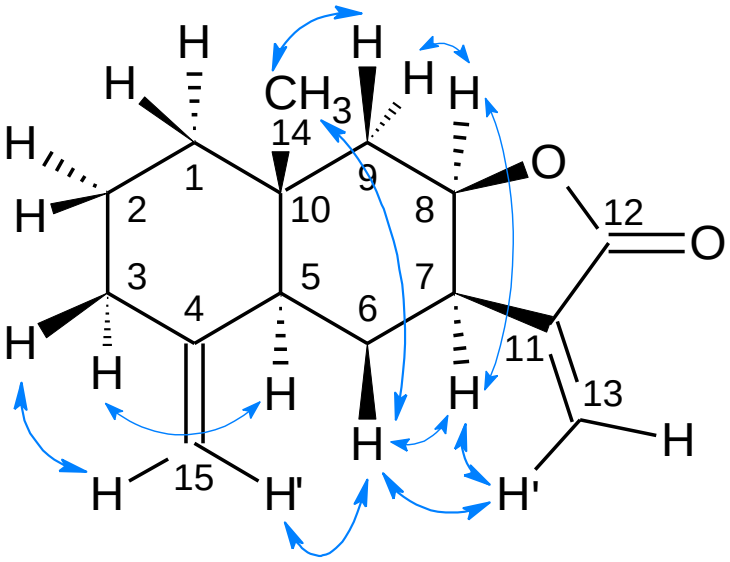

Figure 4.23: **Some of the major NOESY correlations of the compound indicated by blue arrows that were used to confirm the structure of the compound.**

4.4.2.3. CD spectroscopy:

HMBC data for C7 and C8 signals were ambiguous, thus CD spectroscopy was used to determine the absolute configuration and position of the lactone group. The CD spectrum shown in Figure 4.24 clearly indicates a negative Cotton effect at 257 nm and hence, the presence of a *cis*-fused lactone ring attached to carbon atoms 7 and 8.

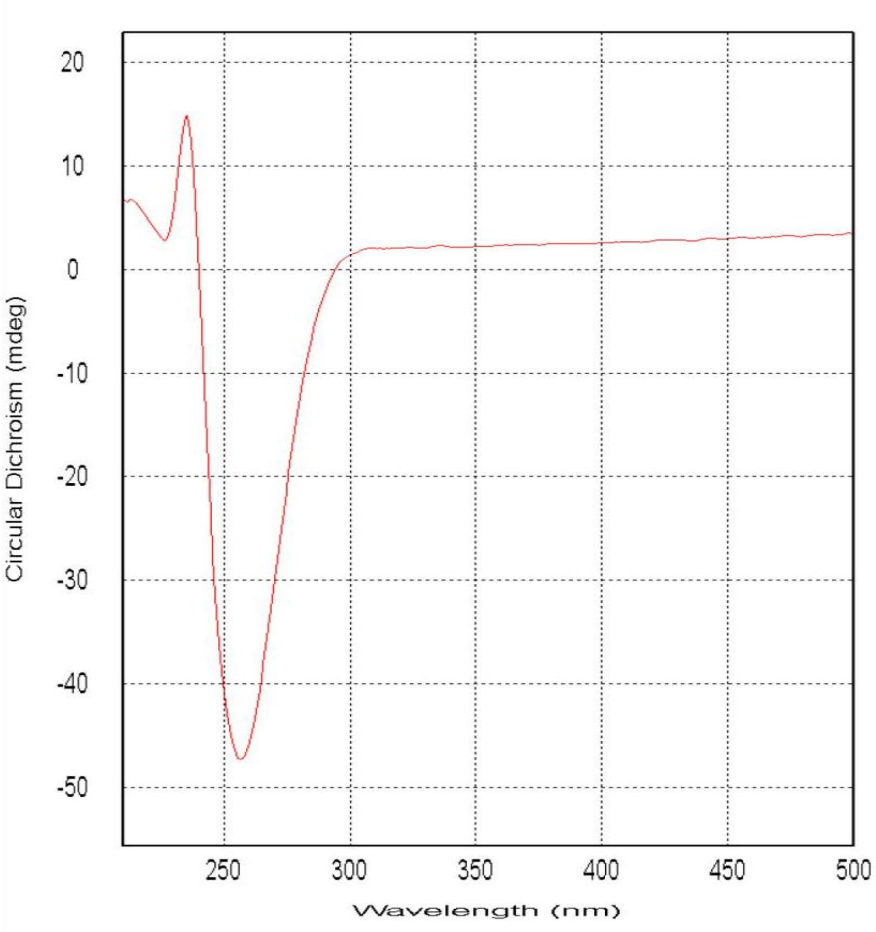

Figure 4.24: CD spectrum of isoalantolactone.

4.4.2.4. Mass Spectrometry:

The molecular mass of isoalantolactone was determined using GC/MS. Figure 4.25 shows the resulting spectrum and the GC. insert confirms the purity of the compound. A molecular mass of 232.15 g/mol was obtained.

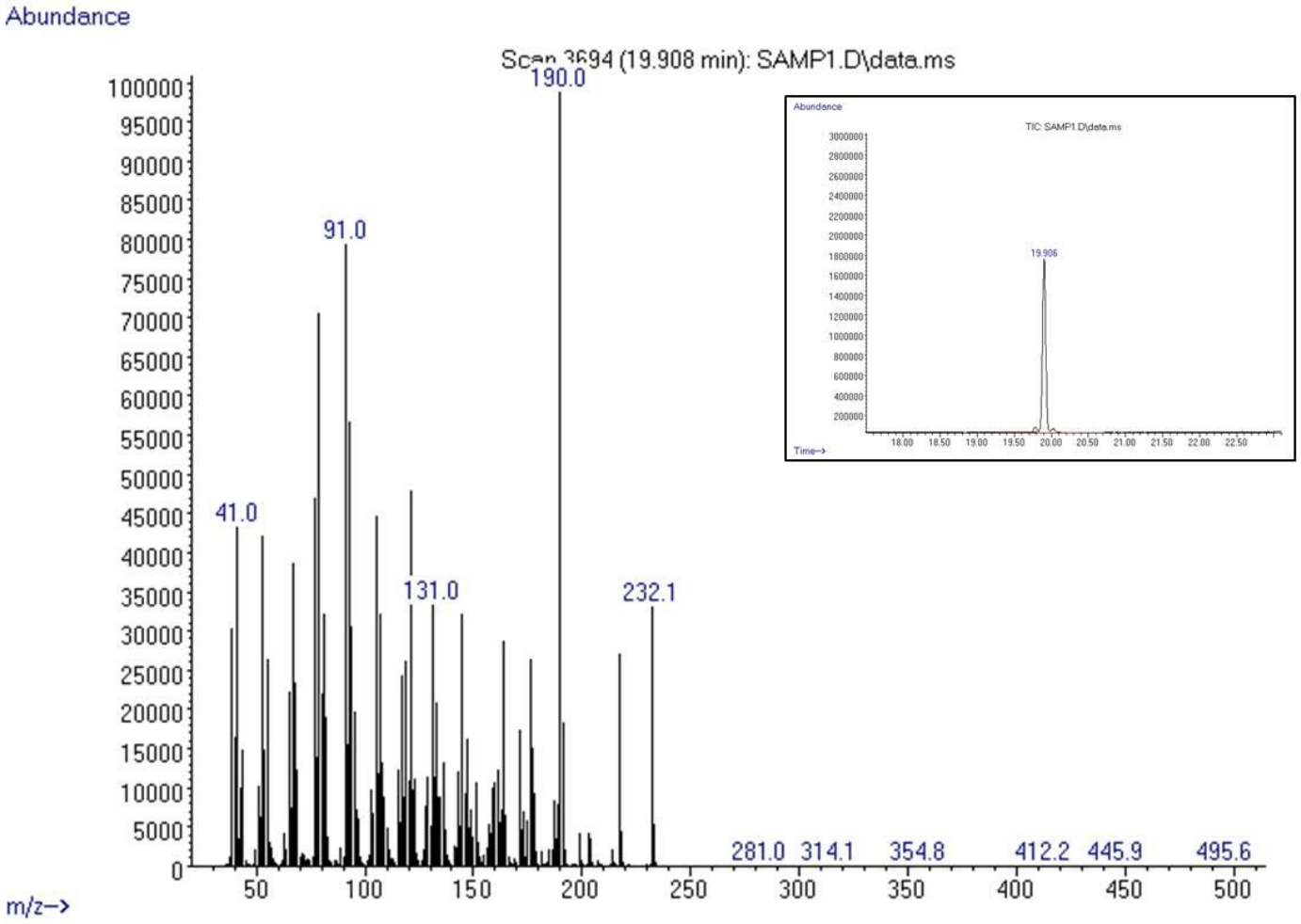

<u>Figure 4.25:</u> Mass spectrum of isoalantolactone indicating the molecular mass of 232.15 g/mol. Insert: GC chromatogram of the sample showing one clear peak.

Using the data of all structural elucidation methods, the 3D structure was elucidated, indicated in Figure 4.26.

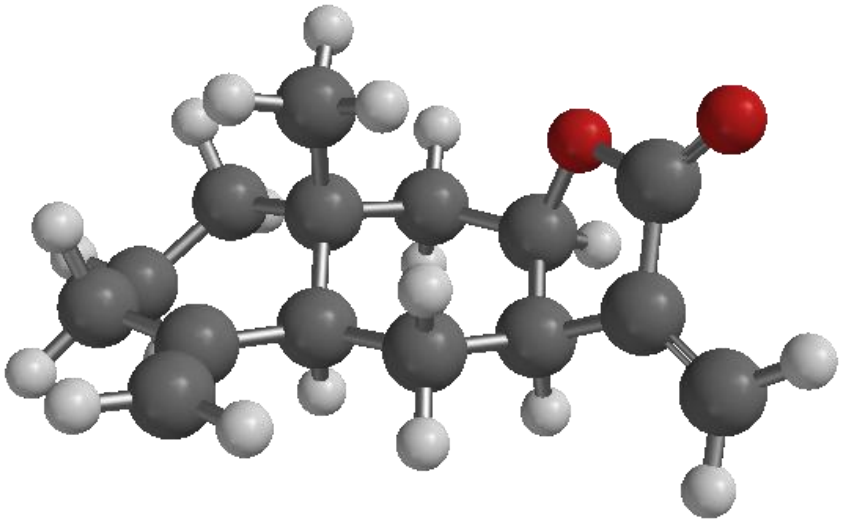

Figure 4.26: The 3D structure of isoalantolactone optimised using iSpartan software

4.5. Discussion and conclusion:

Bioassay-guided fractionation was used to isolate and identify cytotoxic compound(s) present in an ethanol extract of *A. afra*. Separation of compound(s) was performed using gravity column chromatography and TLC. Spectrophotometric techniques were employed for the identification of the compound(s).

Figure 4.4 shows the screening result of the fractions collected after column chromatography. From this figure it is evident that not only fraction 8 is cytotoxic. It is clear that fraction 9, 10, 11 and 12 are also potent in terms of cytotoxicity at a low concentration of 3 µg/mL. However, only fraction 8 was chosen for further purification as it was the most cytotoxic fraction and possessed a low IC_{50} value of 1.89 ± 0.11 µg/mL against HeLa cells. The other fractions have been retained and further work can be carried out in the way described in this chapter in order to characterize those cytotoxic fractions.

From the results obtained from the test fractionation of crude plant extract, preparative fractionation was performed using the same conditions. Column chromatography of 2.204 g

of the dried extract was performed using a 1cm diameter gravity column collecting 10ml fractions using a hexane/ethylacetate stepwise gradient. 56.8 mg of the cytotoxic fraction 8 was further purified by preparative TLC using 50% hexane/ethylacetate as eluent (Band T3, Figure 4.8. This yielded a total of 14.8 mg of pure compound. Although yield was low, 2.577 %, enough material was isolated from the initial 2.204 g of ethanolic plant extract to conduct structural elucidation experiments and to perform biological activity assays.

Identification of the isoalantolactone was done using IR, 1D and 2D NMR, CD spectroscopy and GC/EI-MS. IR spectroscopy indicated the presence of a γ-lactone ring due to the presence of the strong signal at 1758.71 and 1263.14 cm^{-1}. Strong absorptions at 905.15 and 891.11 cm^{-1} were also clear, indicating the presence of exocyclic methylene (vinylidene) groups. ^{13}C NMR spectrum indicated the presence of 15 carbon atoms suggesting the presence of a sesquiterpene lactone. Detailed NMR spectral analysis revealed the presence of 20 hydrogen atoms and from this information it was deduced that 6 double bond equivalents are present in the structure of the compound. From this information, the formula $C_{15}H_{20}O_2$ was deduced. All ^{1}H and ^{13}C NMR data were assigned by COSY, HSQC, HMBC and NOESY spectra.

A pair of doublets at δ_H 5.58 and 6.13 ($J_{H\text{-}13'}$ = 1.16 Hz and $J_{H\text{-}13}$ = 1.26 Hz, respectively) corresponded to the presence of the C-13 exocyclic methylene group of the lactone ring. A pair of quartets at δ_H 4.45 and 4.79 corresponds to the exocyclic methylene group of C-15 coupled to C-4. The two proton quartet signals of C-15 ($J_{H\text{-}15'} = J_{H\text{-}15}$ = 1.63 Hz), show allylic coupling with the doublet of doublets of C-5 at δ_H 1.87 (J_{H5} = 12.6 Hz) and C-3α at δ_H 2.03. The single proton triplet of doublets at δ_H 4.5 (*td*, J_{H8} = 1.8 Hz), C-8, is shifted downfield due to the presence of the oxygen group of the lactone ring. The three proton singlet signal at δ_H 0.835 corresponds to the CH_3 group of C-14. This is indicated by the COSY spectrum (Figure 4.13). A multiplet single proton signal at δ_H 2.97 of C-7 is downfield due to the presence of the lactone ring and is coupled to C-11 and C-8 at δ_H 4.5. The proton NMR data presented here is congruent with those published by Bohlmann *et al.* (1978) of isoalantolactone, (3a*R*,4a*S*,8a*R*,9a*R*)-decahydro-8a-methyl-3,5-dimethylidenenaphtho[2,3-b]furan-2(3H)-one), (Rf = 0.56).

The negative Cotton effect at 257 nm as shown in Figure 4.24 confirmed the absolute configurations at C-7 and C-8 as 7*R* and 8*R*, which is congruent with a *cis*-fused lactone ring attached to carbon atoms 7 and 8 (Stöcklin *et.al.*, 1970) as well as previously reported X-ray

data (Cantrell *et al.,* 2010). The GC/EI-MS data exhibited a molecular ion peak at *m/z* 232.15, which is consistent with a molecular formula of $C_{15}H_{20}O_2$.

The data presented here was compared to other spectral data of sesquiterpene lactones (SLs) in literature. It was concluded that the carbon skeleton of this molecule is an eudesmanolide and was further identified as isoalantolactone (Miller and Nash, 1974; Bohlmann *et al.,* 1978; Tan *et al.,* 1998). Isoalantolactone was originally obtained from the roots of *Inula helenium* (Bohlmann *et al.,* 1978), a plant belonging to the Compositae family. Isoalantolactone possesses multiple biological activities including antimicrobial, antifungal, antihelminthic and antiproliferative (Pal *et al.,* 2010).

SLs have been isolated from a number of plants belonging to the Asteraceae family and a large number of SLs have been isolated from the *Artemisia* genus (Geissman, 1970; Irwin and Geissman, 1973; Nagaki, 1984; Jakupovic *et al.,* 1986; Jakupovic *et al.,* 1991; Marco *et al.,* 1993; Sy and Brown, 2001; Iranshashi *et al.,* 2007). SLs are known to be the active constituents of many plants that are used for medicinal purposes and are known to be cytotoxic against various cell lines (Zhang *et al.,* 2005; Scotti *et al.,* 2007; Ghantous *et al.,* 2010). The biological activities of sesquiterpene lactones are mediated chemically by the α, β-unsaturated carbonyl structures such as the α-methylene-γ-lactone group. QSAR studies have indicated that the biological activities, including cytotoxicity, are mediated chemically by moieties such as the α-methylene-γ-lactone group present in Isoalantolactone (Scotti *et al.,* 2007). Glaucolides and guaianolides have been isolated and identified from *A. afra* (Jakupovic *et al.,* 1988), as mentioned previously and thus, we present proof that isoalantolactone can be added to the list of SLs of *A. afra* and it is hypothesized that isoalantolactone is partly responsible for the cytotoxic activity of *A. afra* (Spies *et al.,* 2013).

CHAPTER 5: *In vitro* mechanism of action of cell death induced by a sesquiterpene lactone, isoalantolactone, isolated from *Artemisia afra.*

5.1. Introduction:

The search for new and effective cancer drugs will never end. Natural products have been important and useful in anticancer drug development, particularly those derived from terrestrial microorganisms and higher plants. It has been shown that 47% of 155 anticancer drugs approved up to 2006 were either natural products or directly derived from a natural product lead compound by semi-synthesis (Pan *et al.,* 2013). Plants have been an important source of such compounds and many anti-cancer agents have been derived from plant compounds (Chin *et al.,* 2006). Plant-derived compounds include vinblastine, vincristine, camptothecin derivatives, topotecan, irinotecan, etoposide and paclitaxel. Not only are these compounds implicated in treatment, but a large number of derivatives based on these compounds are also used or are in clinical trials as anti-cancer drugs. In recent years, it has been shown that sesquiterpene lactones (SLs) are no exception and have too made clinical trials for the treatment of cancer (Pan *et al.,* 2013; Ghantous *et al.,* 2010).

SLs are a stable class of terpenoids and have been isolated from a number of plant families, but the greatest number of SLs has been isolated from the Asteraceae (Compositae) family with over 300 reported different structures (Ghantous *et al.,* 2010; Chaturvedi, 2011). They are colourless and bitter. SLs are 15-carbon compounds, including a lactone group, and can be categorized according to their carbocyclic skeleton. These categories include the germacranolides (one ten-membered ring), eudesmanolides and eremophilanolides (6/6 bicyclic compounds), and guaianolides and pseudoguaianolides (Figure 4.2). Many members of these groups also have open ring structures (Ghantous *et al.,* 2010).

5.1.1. Cytotoxic activity and anti-cancer studies on sesquiterpene lactones:

The biological activities of SLs are affected by three major chemical properties (Ghantous *et al.,* 2010). These include:

1. Alkylating center reactivity: Typical alkyating centers of SLs are the α-methylene-γ-lactone moiety, the α-methylene-δ-lactone moiety, conjugated cyclopentenone and conjugated side chain ester (Kupchan *et al.,* 1971; Lee *et al.,* 1971; Hall *et al.,* 1978). It has been shown that SLs need to contain one of these alkylating centres to mediate cytotoxicity. It has also been shown that SLs with two alkylating centers, known as bifunctional SLs, are more cytotoxic (Bruno *et al.,* 2005).
2. Side chain and lipophilicity: Higher lipophilicity of a SL can facilitate its entry into a cell and thus, increase its cytotoxicity *in vitro*. However, steric hindrance can alter the compounds' cytotoxic ability (Hall *et al.,* 1979).
3. Molecular geometry and electronic features: Conformational flexibility and stereochemistry of SLs play very important roles on the cytotoxicity of these compounds (Beekman *et al.,* 1997).

Various studies have shown that SLs have anti-cancer activity and are able to induce apoptosis in cancer cells. SLs have been reported to be involved in inhibition of cell proliferation, disruption of the cell cycle and promotion of cell differentiation. SLs also have sensitization activity, anti-metastasis and anti-inflammatory activity (Zhang *et al.,* 2005).

SLs have reached clinical trials and their effective treatment is through alleviation of tumour load and inhibition of cancer stem cells. As of 2010, the SLs in clinical trials are artemisinin from *Artemisia annua* L, thapsigargin from *Thapsia* and parthenolide from *Tanacetum parthenum* and/or many of their derivatives. The mechanisms of action include the inhibition of the sarco/endoplasmic reticulum calcium ATPase (SERCA) pump, generation of iron-dependent free radicals, inhibition of angiogenesis and metastasis, regulation of NF-κ*B* and p53 signalling pathways and the modulation of the epigenetic code.

Thapsigargin and its derivatives diffuse through the cell membrane and fit into the SERCA pump through lipophilic interactions. It inhibits the SERCA pump from transporting Ca^{2+} from the cytosol to the ER and this results in ER stress which leads to cell stress and death. A major drawback is that these compounds are also toxic to normal cells; hence they are used as

prodrugs. These prodrugs have been developed for the treatment of prostate cancer by conjugating a peptide unique to prostate-specific antigen enzyme and thus can successfully target prostate cancer cells (Christensen *et al.,* 2009).

Artemisinin is an antimalarial drug that has a endoperoxide bridge that is cleaved when it binds to Fe(II). Upon doing so, it produces toxic free radicals that destroy tumour cells. Cancer cells have high Fe(II) concentrations and they also express elevated levels of transferrin receptors compared to normal cells and thus cancer cells are more susceptible to stress caused by this SL. Artemisinin also inhibits NF-κB activity (Ghantous *et al.,* 2010).

SLs modulate many inflammatory processes by inhibiting NF-κB (Rüngeler *et al.,* 1999). Deregulation of NF-κB is implicated in human cancers (Shen and Tergaonkar, 2009) and thus there exists a link between cancer and inflammation. Parthenolide and artemisinin are both NF-κB inhibitors. Parthenolide inhibits this transcription factor by directly modifying the p65 subunit of NF-κB by alkylation at residue Cys38. Various studies have also shown that parthenolide is able to select for cancer cells as NF-κB signalling is elevated in cancer cells but not in normal cells. It also activates p53 and causes an increase in ROS (Ghantous *et al.,* 2010; Guzman *et al.,* 2005). Because of the simultaneous inactivation of p53 and hyperactivation NF-κB in human cancer cells, these compounds are known as "double-edged swords" (Dey *et al.,* 2008). Figure 5.1 illustrates the different mechanisms of action of the three SLs that are in clinical trials and their derivatives.

5.1.2. Reported biological and cytotoxic activity of isoalantolactone (isohelenin):

Isoalantolactone is known to be the major sesquiterpene lactone found in the roots of the *Inula racemosa,* an Indian medicinal plant used in India, China and Europe for the treatment of abdominal pain, acute enteritis and bacillary dysentery. The roots are used as an expectorant and a tonic for the above mentioned ailments (Jabeen *et al.,* 2007). Pal *et al.* (2010) reported evidence to show that an *n*-hexane fraction of *I. racemosa* (IC_{50} = 16.70 µg/mL) induces apoptosis in HL-60 cancer cells in a dose-dependent manner, indicated by phopshatidylserine translocation.

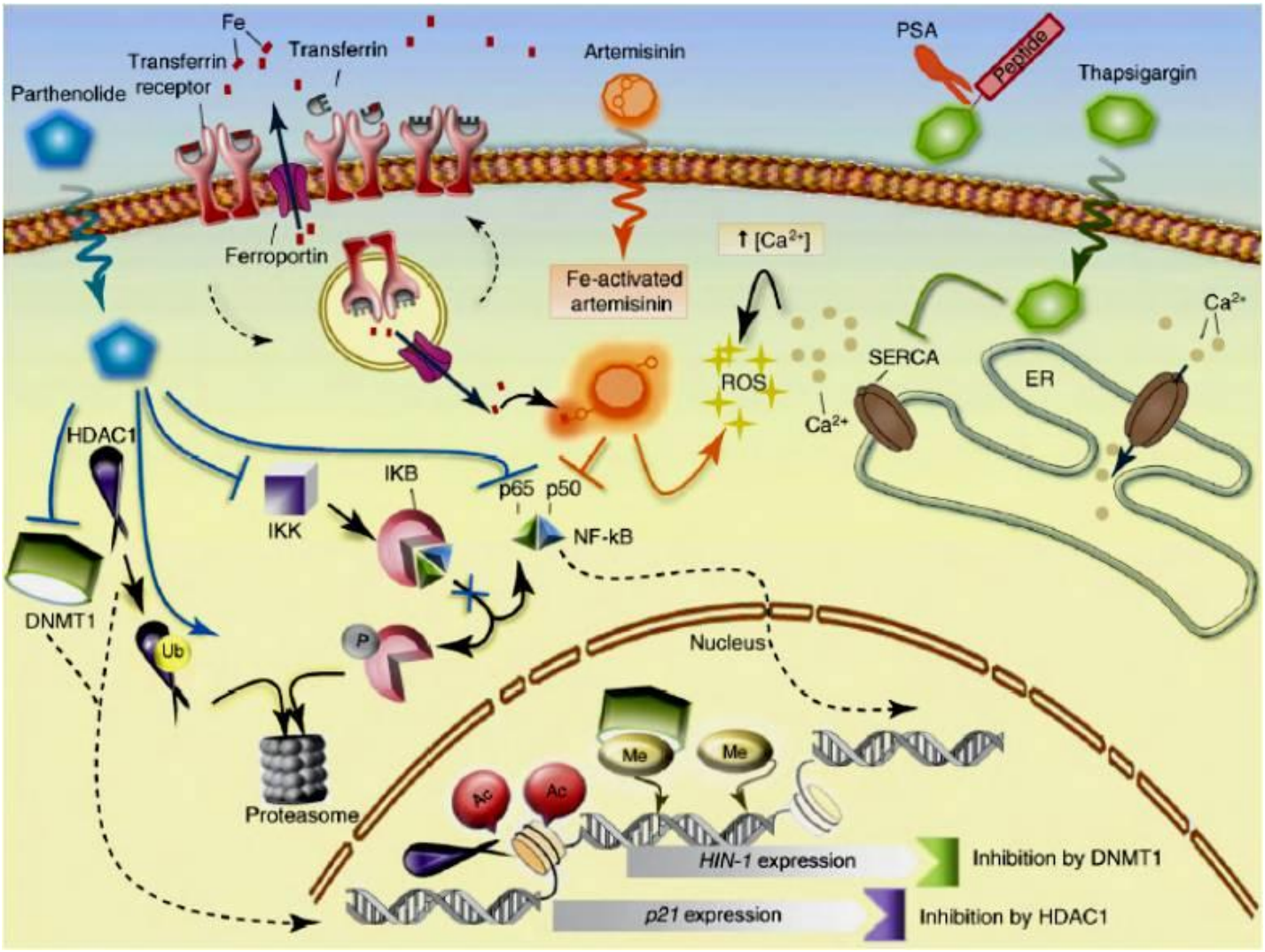

Figure 5.1: Parthenolide, artemisinin and thapsigargin target specific pathways in tumour and cancer stem cells as described in text. Abbreviations: Ac, acyl group; DNMT, DNA methyl transferase; ER, sarcoplasmic/endoplasmic reticulum; HDAC1, histone deacetylase 1; IKK, IκB kinase; PSA, prostate-specific antigen; Me, methyl group; NF-κB, nuclear factor-κB; ROS, reactive oxygen species; SERCA, ER calcium ATPase; Ub, ubiquitin. Dashed and solid lines indicate translocation and activation, respectively (Ghantous *et al.*, 2010).

Upon further investigation into the mechanism of cell death caused by this *I. racemosa* fraction, it was found that apoptosis was induced in a mitochondrial dependent manner, by translocation of Bax which leads to the release of cyt-*c* from the mitochondria due to the loss in the mitochondrial membrane potential. It was shown that apoptosis resulted in PARP cleavage and DNA fragmentation after 6 hours of exposure to the plant fraction. Upregulation of caspase -3 was evident as well as an increase in the levels of TNF-R1 expression.

Generation of reactive oxygen species (ROS) was also evident. From the study presented by Pal *et al.* (2010), it is tempting to suggest that sesquiterpene lactones, isoalantolactone in particular, present in *A. afra* are responsible for the cytotoxicity observed as it is known that the Asteraceae (Compositae) family is rich in sesquiterpene lactones, which do possess cytotoxic abilities (Lee *et al.*, 1971).

Liu *et al.* (2001) showed that isoalantolactone exhibits antibacterial activity against *B. subtilis, E. coli, P. fluorecense, S. lentus* and *S. aureus*, as well as antifungal activity against *G. graminis* var. *tritici, R. cerealis* and *P. capsici.* More recently, a study by Khan *et al.* (2012) showed that commercially available isoalantolactone has anti-cancer activity (IC_{50} = 40 μM). Ma *et al.* (2013) also presented data that isoalantolactone is cytotoxic against human non-small-cell lung cancer (A549), hepatocellular carcinoma (HepG2) and human fibrosarcoma (HT1080) cancer cells, with IC_{50} values of 0.38 μg/mL (1.64 μM), 1.77 μg/mL (7.65 μM) and 0.795 μg/mL (3.43 μM), respectively.

Khan *et al.* (2012) revealed that apoptosis was induced in pancreatic carcinoma cells (PANC-1) as well as S phase arrest of the cell cycle. A decrease in mitochondrial membrane potential was observed indicating the involvement of the mitochondria in the induction of apoptosis. The effect of isoalantolactone on mitochondrial regulatory proteins was also investigated and this revealed an increased expression of p38 MAPK and Bax, a decrease in the expression of Bcl-2 and the release of cyt-*c* from the mitochondria. Activation of caspase 3 was also observed. Interestingly, this study also revealed that induction of apoptosis by isoalantolactone was ROS-dependent and the cytotoxicity of isoalantolactone may be specific to cancer cells due to normal cells having lower levels of endogenous ROS (Khan *et al.*, 2012). This evidence almost confirms that isoalantolactone is wholly/partly responsible for the cytotoxicity of the *n*-hexane fraction of *I. racemosa* shown by Pal *et al.* (2010).

Overwhelming evidence has shown that many SLs exhibit cytotoxic activity. It has also been shown that an *n*-hexane fraction of *I. racemosa* roots, a plant rich in SLs, induces apoptosis in a mitochondrial- and caspase-dependent manner (Pal *et al.*, 2010). It is known that the major secondary metabolites of this plant are sesquiterpene lactones. Alantolactone and isoalantolactone have been reported to be the major SLs isolated from *I. helenium* (Bohlmann *et al.*, 1978) and the mechanism of action for the induction of apoptosis by commercially available isoalantolactone has been suggested (Khan *et al.*, 2012; Rasul *et al.*, 2013).

5.1.3. Aims:

Isoalantolactone has not been isolated from *A. afra,* but the mode of cell death of HeLa and U937 cancer cells caused by an ethanol extract of *A. afra* has recently been described (Spies *et al.*, 2013). Thus, the objective of this chapter was to characterize the mechanism of cytotoxic action that isolated isoalantolactone from this *A. afra* extract facilitates on HeLa cancer cells and to determine if the isolated compound is responsible for the onset of this particular mechanism of cytotoxic activity exhibited by crude ethanol *A. afra* extract.

5.2. Materials:

Cervical (HeLa) cancer and Vero cell lines were purchased from Highveld Biological, South Africa. Cleaved caspase-3 (Asp175) and caspase 8 (Asp391) antibodies were purchased from Cell Signaling Technology, Inc. (Danvers, MA, USA). The Coulter® DNA Prep™ reagents kit, goat anti-rabbit IgG (H+L chain specific) and rabbit IgG isotype, both labelled with fluorescein (FITC) conjugate and IsoFlow™ EPICS™ sheath fluid, were purchased from Beckman Coulter (CA, USA). IntraPrep™ permeabilising reagent was purchased from Immunotech (Marseille, France). Annexin V-FITC/PI kit was purchased from MACS Miltenyi Biotec (Auburn, USA). 3-(4,5-dimethyl-2-thiazolul)-2,5-diphenyl-2H-tetrazolium bromide (MTT), 5,5',6,6'tetrachloro-1,1',3,3'-tetraethylbenzimidazol-carbocyanine iodide (JC-1) and melphalan were purchased from Sigma (St. Louis, MO, USA). CellTiter-Blue® reagent was purchased from Promega (Madison, WI, USA). RPMI 1640 cell culture medium containing 25 mM Hepes and 2 mM glutamine, Dulbecco's Modified Eagle Medium (DMEM) containing 4 mM L-glutamine, 4500 mg/L glucose and sodium pyruvate as well as foetal bovine serum was purchased from ThermoScientific (Logan, Utah, USA). Apo-Direct DNA fragmentation kit was purchased from BD Pharmingen (USA).

5.3. Methods:

This study aimed to determine whether isoalantolactone isolated from ethanolic *A. afra* extract exhibited the same mode of cell death induced by the crude plant extract. Hence, the same methods were used as described in Chapter 3. Comparisons were made between the effects of the crude plant extract and the isolated compound to conclude its responsibility for the observed cytotoxicity.

5.3.1. Cell line maintenance:

HeLa cells were the only cancer cell line used here. Cytotoxicity of isoalantolactone was also tested against Vero kidney cells as a normal cell control. HeLa cells were maintained in 10 cm culture dishes, using RPMI 1640 medium supplememnted with 10% FBS in a humidified 5% CO_2 incubator at 37°C. Vero cells were maintained in DMEM medium supplemented with 5 % FBS. No antibiotics were added to the culture media.

5.3.2. Cytotoxic evaluation of isoalantolactone:

Cytotoxicity of isoalantolactone against HeLa and Vero cells was evaluated using the MTT assay. HeLa cells were seeded in 96 well plates in 200 µL aliquots at 3 x 10^4 cells/mL and left overnight in the incubator to attach. Vero cells were used at 100% confluency. The medium was replaced with fresh medium containing varying concentrations of isoalantolactone. Cells were treated with isoalantolactone at a concentration range from 0 to 30 µg/mL. Melphalan (40 µM) was used as the positive control. Cells were exposed to the compound for 48 hours at 37°C. The medium was then removed prior to the addition of MTT. Two hundred microlitre aliquots of medium containing 0.5 mg/mL MTT was added to each well and incubated for 3 hours. Thereafter, the medium was removed and the blue formazan product was solubilized in DMSO. Absorbance was read at 540nm using a BioTek® PowerWave XS spectrophotometer (Winooski, VT, USA). Dose-response curves were plotted and analyzed for the determination of an IC_{50} value for the compound using GraphPad Prism Version 4.0. Each treatment was performed in triplicate (n=3) and standard deviation (SD) was expressed as error bars. After the determination of the IC_{50} value, the oncentration used for further experimental procedure was set at 2 µg/mL, which is the equivalent of 8.62 µM.

5.3.3. DNA distribution and cell cycle analysis:

HeLa cells were seeded at 5 x 10^4 cells/mL in 10 mL aliquots in a 10 cm culture dish and incubated overnight to allow for attachment. Cells were then treated with 8.62 µM isoalantolactone and incubated for a further 12 hours. Melphalan (40 µM) was used as a positive control. Cell cycle analysis was performed using the Coulter® DNA Prep™ reagents kit as per manufacturer's instructions. PI is the DNA binding dye that is used in this kit. It is widely used to determine DNA distribution of the cells. After incubation, cells were trypsinised and transferred to polypropylene tubes. Cells were lysed and stained using the Coulter® DNA Prep™ reagents kit as described in section 3.3.4.2. Cells were analysed immediately using flow cytometry and data was recorded in FL1. This experiment was conducted in triplicate and each experiment was repeated 3 times.

5.3.4. Phosphatidylserine translocation:

Dual staining using PI and Annexin V-FITC of HeLa cells was performed to determine the mode of cytotoxicity induced by isoalantolactone. As described in 3.3.5.1, PI is used in conjunction with Annexin V to discriminate between early apoptotic cells, necrotic cells and dead cells. HeLa cells were seeded at 5 x 10^4 cells/mL in 6 well culture dishes and 3 mL per well was used. Cells were left overnight to attach and thereafter treated with 8.62 µM isoalantolactone and ethanol *A. afra* extract (30 µg/mL), separately. Cells were exposed to treatment for 24 hours before analysis. Before cells were stained with Annexin V-FITC, HeLa cells were transferred to polypropylene tubes. This was done using accutase to detach the cells from the culture plate as described in 3.3.5.2. Cells were then harvested by centrifuging at 500 xg for 5 minutes. PS translocation was then measured using Annexin V-FITC/PI kit according to the manufacturer's guidelines and is described in Chapter 3, 3.3.5.2. Flow cytometric analysis of samples was performed and data was recorded using channel FL1.

5.3.5. Mitochondrial membrane potential (MMP) analysis:

HeLa cells were seeded at 5 x 10^4 cells/mL in 6 well culture plates. Cells were treated with isoalantolactone and incubated for 24 hours. Melphalan was used as a positive control (40 µM). Cells were transferred to polypropylene tubes for flow cytometric analysis. This was

done by trypsinising and harvesting the cells by centrifugation as described for PS translocation analysis. Cells were washed using DPBS before the addition of JC-1. This was performed by adding 1 mL of DPBS to the cell pellet, gently resuspending the pellet and thereafter, centrifuging again at 500 xg for 5 minutes. This was done to remove all traces of medium from the cells. JC-1, constituted in DPBS (final concentration of 2 µg/mL) was added to each tube and cells were incubated for 10 minutes at room temperature in the dark. Cells were then thoroughly washed with DPBS to remove any excess JC-1. Washing was repeated four times to ensure the removal of excess JC-1 as excess JC-1 will result in false results and misinterpretation of the experiment. Analysis of the effect of isoalantolactone on the mitochondrial membrane potential of HeLa cells was performed using flow cytometry and data was recorded in FL1.

5.3.6. Caspase -8 and -3 activation:

Levels of cleaved caspase -8 and -3 were detected using immunochemistry. HeLa cells were seeded and treated as described in 3.3.7.2 and incubated for 12 and 24 hours for caspase -8 and caspase -3 detection, respectively. Briefly, cells were trypsinised, transferred to polypropylene tubes and harvested by centrifugation (500 xg for 5 minutes). Cells were fixed and permeabilised using the IntraPrep kit (Beckman Coulter), as per manufacturer's recommendations. Cells were then blocked using 0.5% BSA and thereafter incubated with cleaved caspase 8 (Asp391) and cleaved caspase 3 (Asp175) monoclonal antibodies, separately, for 1 hour. Detection of changes in the levels of cleaved/activated caspase -8 and -3, compared to an untreated cell population, was done using flow cytometry. Changes in levels of activated caspases were detected as an increase or decrease in log green fluorescence intensity (FL1).

5.3.7. DNA fragmentation:

HeLa cells were seeded, treated, fixed and permeabilised as described for cleaved caspase analysis. Cells were treated for 24 hours. The Apo-Direct DNA Fragmentation kit (BD Pharmingen, USA) was used as per manufacturer's instructions. In brief, cells were resuspended in 1 mL wash buffer and centrifuged at 500 xg for 5 minutes. Cell pellets were washed three times. DNA labelling solution was prepared using reaction buffer, TdT enzyme (1×10^5 U/mg), FITC dUTP and distilled water. The DNA solution was prepared as per

manufacturer's instructions. Cells were incubated in 50 µL DNA labelling solution for 60 minutes at 37°C and thereafter washed with 1 mL rinse buffer and centrifuged as described. This rinse step was repeated twice. Cells were then analysed using flow cytometry and data was recorded in FL1.

5.3.8. Statistical analysis:

Each treatment was performed in triplicate (n=3) and each experiment was conducted three independent times, unless stated otherwise. SD represents standard deviation of the mean of all experimental data. Statistical significance was determined using the two-tailed student's t-test and $p<0.05$ was considered significant. For flow cytometry, a minimum of 10 000 events were recorded (3.3.10) in FL1 for each sample.

5.4. Results:

5.4.1. Cytotoxicity of isoalantolactone:

A dose-dependent cytotoxicity assay yielded an IC_{50} value of 1.89 ± 0.11 µg/mL after 48 hours of treatment of HeLa cells with isoalantolactone (Figure 5.2 A). When considering the molecular mass of this compound, this IC_{50} value can be converted to a Molar value of 8.15 ± 1.16 µM. The concentration was thus set at 2 µg/mL (8.62 µM) for all further experiments. Cytotoxicity was also evaluated using confluent Vero cells, a normal cell line. An estimated IC_{50} value of ~ 260 µM resulted (Figure 5.2 B).

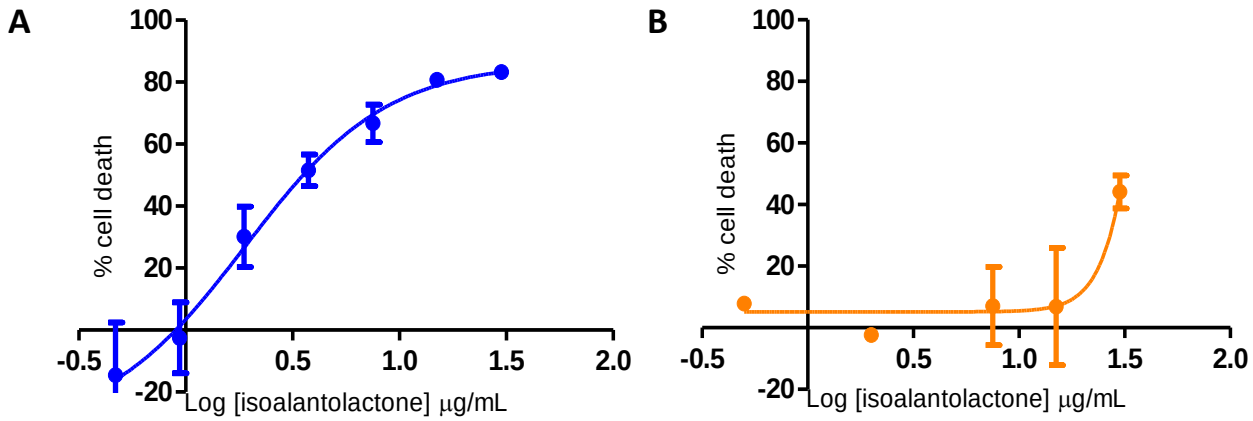

Figure 5.2: Cytotoxic effect of isoalantolactone against proliferating HeLa cells (A) and confluent Vero cells (B) after 48 hours of exposure. Cell viability was determined using the MTT assay. Error bars indicate SD of 3 replicate values.

5.4.2. Cell cycle analysis:

Cell cycle progression is tightly regulated and controlled by various checkpoints in normal cells. When the regulatory mechanisms of cell division become defective, the result can be catastrophic and cancer can arise (Schafer, 1998). DNA cell cycle analysis was performed on HeLa cells after 12 hours of exposure to isoalantolactone to determine whether cell cycle arrest is induced. After exposure, a significant increase from 16.3 ± 0.98% to 26.6 ± 1.21% of cellular DNA in the G2/M phase was evident. Table 5.1 indicates this result.

Table 5.1: The average percentage (%) cells present in the various indicated stages of the cell cycle after 12 hours of treatment in HeLa cells.

Treatment	sub G1	G0/G1	S	G2/M
Untreated control	1.33 ± 0.55%	50.23 ± 3.25%	20.1 ± 2.49%	16.3 ± 0.98%
isoalantolactone (8.62 µM)	8.03 ± 1.1% *	43.03 ± 2.7% *	13.25 ± 3.42%*	26.6 ± 1.21% *

Each experiment was performed 3 times for each time study. Each experiment was carried out in triplicate. Results are expressed as mean % ± SD of all experimental data.
* Significantly different from control; $p<0.05$

5.4.3. Phosphatidylserine translocation:

Phosphatidylserine translocation is an indicator of apoptosis and is an early feature of this cell death mechanism. Figure 5.3 show a significant increase in cells undergoing apoptosis was evident after 24 hours of treatment with isoalantolactone. A summary of the results is indicated in Figure 5.4.

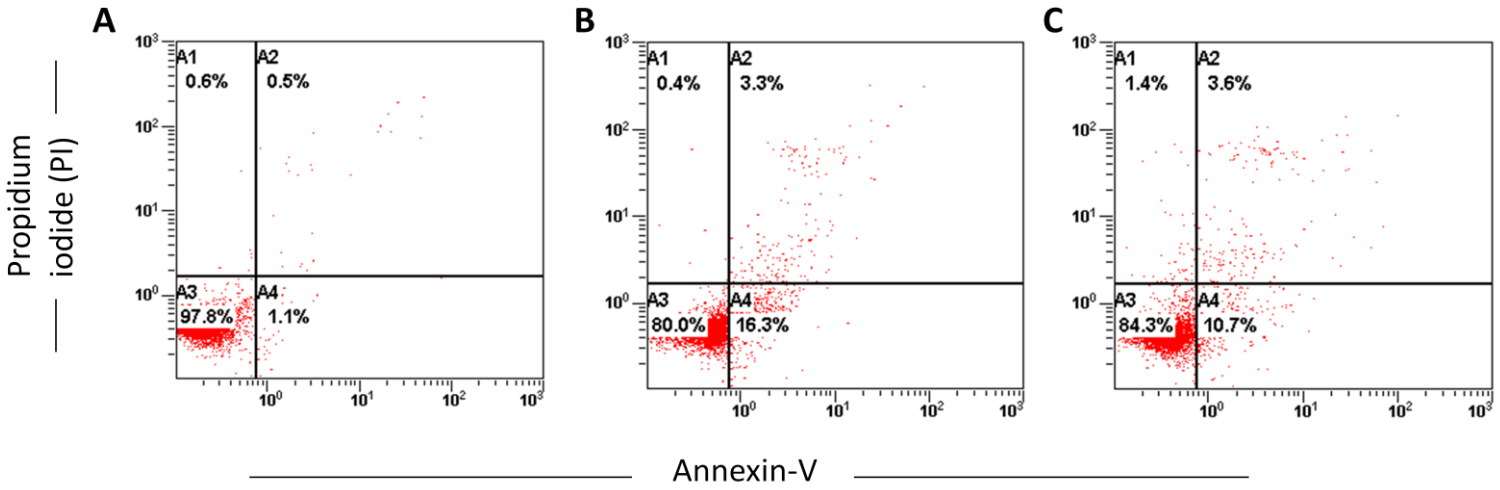

Figure 5.3: Dot plots of Annexin V-FITC stained HeLa cells (A, B and C). A; control population, B; cells treated with 30 µg/mL *A. afra,* C; cells treated with 8.62 µM isoalantolactone. Four quadrants represent unstained/live cells (A3: Annexin V-negative; PI-negative), early apoptotic cells (A4: Annexin V-positive; PI-negative), late apoptotic cells (A2: Annexin V-positive; PI-positive) and necrotic cells (A1: Annexin V-negative; PI-positive). A minimum of 20 000 events were read for each treated cell population (One representative of two individual experiments carried out in triplicate).

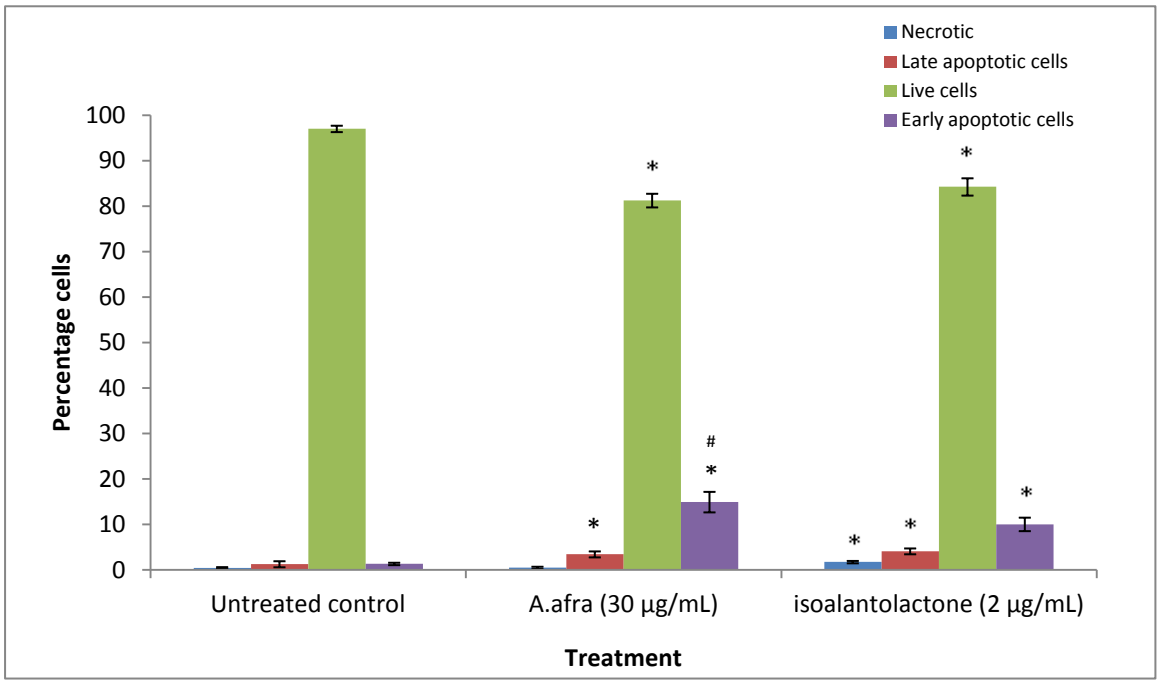

Figure 5.4: Analysis of HeLa cells using Annexin V-FITC and PI dual staining after 24 hours of exposure to treatments. Cells were treated with 30 µg/mL *A.afra* ethanolic extract and 8.62 µM isoalantolactone. Bar graph represents the average of two experiments each performed in triplicate. 20 000 events were recorded per sample. SD is represented as error bars. Significance was determined using the two-tailed Student t-test: *p<0.05 compared to untreated control, #p<0.05 compared to isoalantolactone.

5.4.4. Mitochondrial membrane potential (MMP) analysis:

Two possible pathways leading to cell death via apoptosis is known, the intrinsic pathway and the extrinsic pathway and a complex mix of the two. The intrinsic mode of apoptotic cell death involves the release of pro-apoptotic proteins from the mitochondria which, in turn, activates caspase proteins which ultimately leads to controlled cell death (Vermeulen *et al.*, 2003). The release of these proteins from the mitochondria is accompanied by a decrease in mitochondrial membrane potential and this can be measured by using the cationic dye JC-1. Table 5.2 shows the data resulting from this experiment. It is clearly evident that there is a significant increase in green fluorescence after 12 hours of treatment of HeLa cells with isoalantolactone.

Table 5.2: Mitochondrial membrane depolarization of HeLa cells after 24 hours of treatment.

Treatment	Mean log green fluorescence intensity
Untreated	1.39 ± 0.13
isoalantolactone (8.62 µM)	9.78 ± 0.56 **
melphalan (µM)	22.90 ± 1.36 **

Each experiment was performed 3 times for each time study. Each experiment was carried out in triplicate. Results are expressed as mean log green fluorescence intensity ± SD of all experimental data.
** Significantly higher than control; $p<0.005$: Significance was determined using the two-tailed Student t-test.

5.4.5. Cleaved caspase -8 and -3 analysis:

As described, apoptosis is a highly organized mechanism of cell death. The central executioner of apoptosis is the proteolytic system involving caspases (Fulda and Debatin, 2006). Caspase -8 is an upstream caspase and is known to be the major initiator caspase of the extrinsic pathway. It forms part of the death inducing signaling complex (DISC) once a death signal has been received by the cell. Caspase -3 is known to be the main executioner of apoptosis and does so by facilitating DNA fragmentation (Thornberry and Lazebnik, 1998). Figure 5.5 A and B show histogram overlays representing changes in levels of activated caspase -8 and -3, respectively. Significant increases in levels of cleaved caspase -8 and caspase -3 are indicated in Table 5.3.

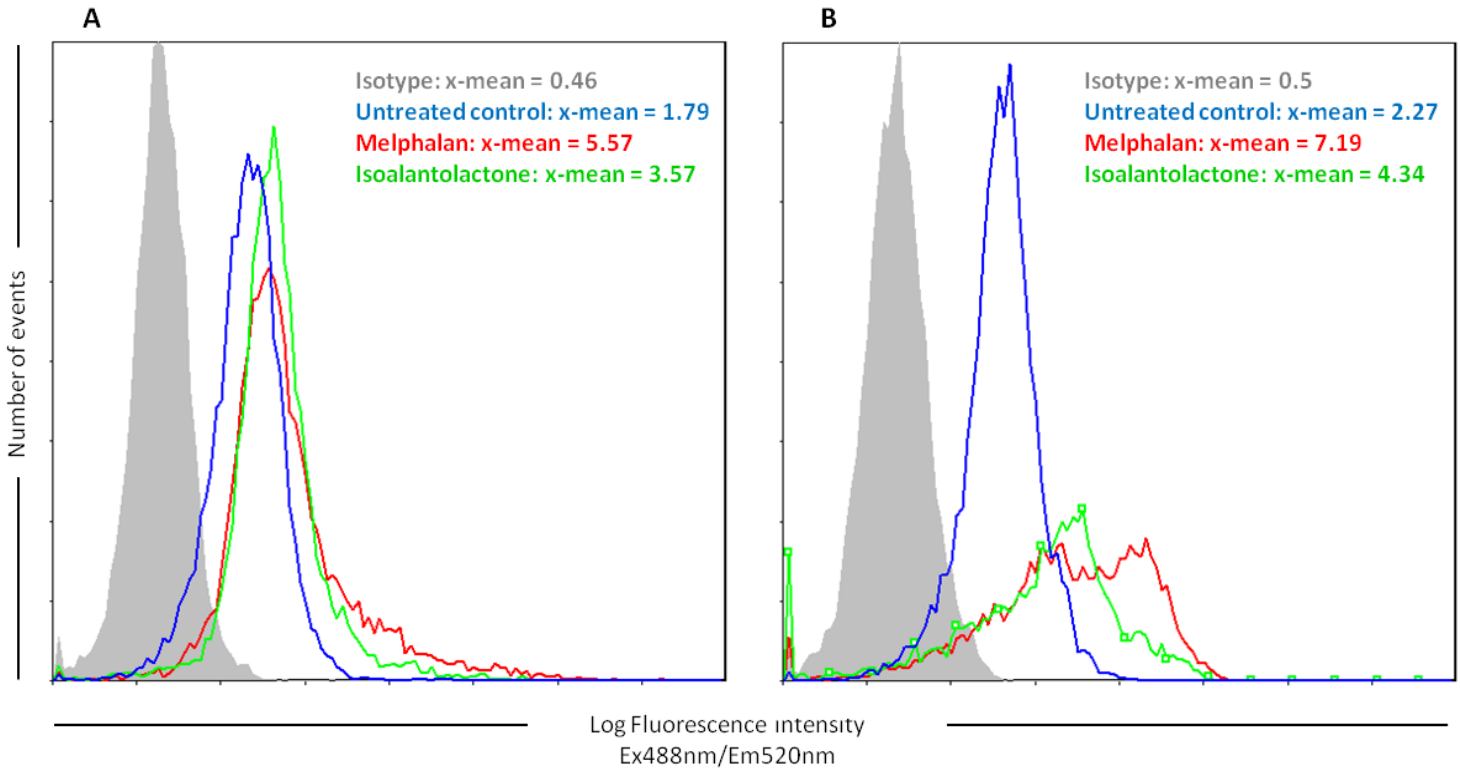

Figure 5.5: Histogram overlays representing activated caspase -8 (A) and activated caspase -3 (B) in HeLa cells after 24 hours of exposure to treatments. 10 000 events were recorded. X-mean values indicate the mean fluorescence intensity of cells staining positive for active caspase -8 and -3 (One representation of an experiment carried out in triplicate for cleaved caspase -8 and -3, respectively).

Table 5.3: Changes in levels of cleaved caspase -8 and caspase -3 levels after treatment with melphalan and isoalantolactone after 24 hours of exposure.

Treatment	Percentage of untreated control (%)	
	Cleaved caspase -8	Cleaved caspase -3
Untreated control	0.00 ± 1.69	0.00 ± 0. 47
Melphalan (40 µM)	156.06 ± 1.27**	103.14 ± 2.42**
Isoalantolactone (8.62 µM)	74.65 ± 0.80**	255.38 ± 2.58**

Each experiment was carried out in triplicate. Values indicate mean % ± SD of all experimental data.
** Significantly higher than control; $p<0.005$: Significance was determined using the two-tailed Student t-test.

5.4.6. DNA fragmentation:

DNA fragmentation is a late indicator of apoptosis. It is measured using the TUNEL method whereby FITC-labeled dUTP DNA fragments were detected using flow cytometry. Figure 5.6 shows a significant fold increase in the occurrence of fragmented DNA after 24 hours of treatment of cells with the compound.

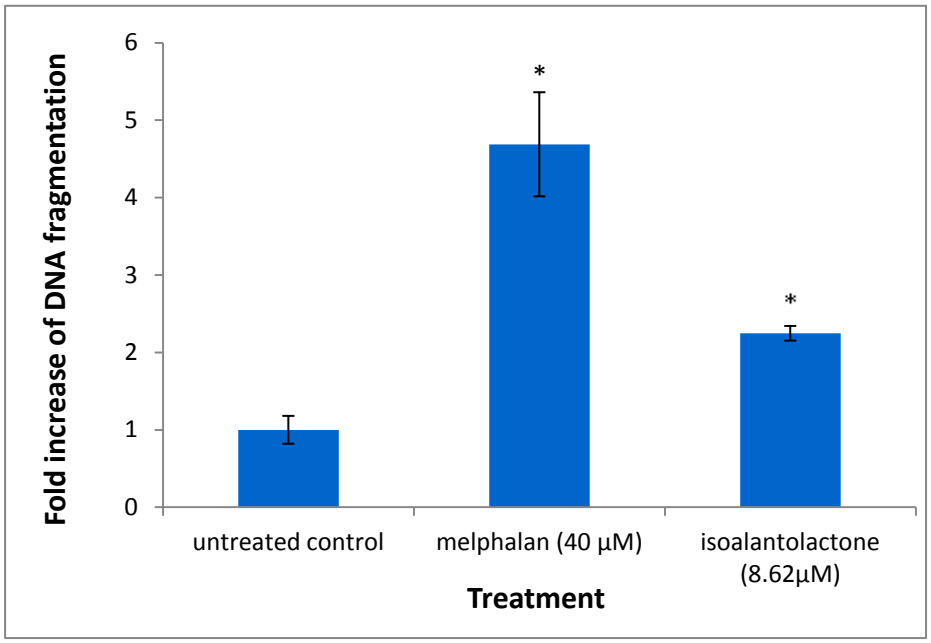

Figure 5.6: DNA fragmentation in HeLa cells after 24 hours of exposure to treatments. Bar graph represents the average of two individual experiments each performed in triplicate. 10 000 events were recorded per sample. Error bars indicate SD of all experimental data. Significance was determined using the two-tailed Student t-test: *p<0.05 compared to control.

5.4. Discussion and conclusion:

This chapter aimed to determine the mode of cytotoxicity of isoalantolactone against HeLa cells. It also aimed to establish a correlation between the reported mechanism of apoptosis induced by an ethanol extract of *A. afra* (Chapter 3; Spies *et al.*, 2013) and the mode of cell death induced by isoalantolactone. There has been no report of cytotoxic evaluation of isoalantolactone against HeLa cells.

In this study, the effects of the treatment of HeLa cells on DNA distribution (cell cycle analysis), phopshatidylserine translocation, mitochondrial membrane potential, analysis of levels of cleaved (active) caspase -8 and -3 as well as DNA fragmentation determination was performed. These are the same assays that were conducted to determine the mechanism of apoptosis induced by the ethanol extract of *A. afra*. Hence, data for both *A. afra* and isoalantolactone can be directly compared. A complete comparison of the results obtained for the exposure of cells to an ethanol extract of *A. afra* and to isoalantolactone isolated from this crude extract will be discussed in Chapter 8. Dose-response analysis of isoalantolactone against HeLa cells showed an IC_{50} value of 1.89 ± 0.11 µg/mL (8.15 ± 1.16 µM when considering its molecular weight). When considering sesquiterpene lactones of similar structure such as isocostunolide and costunolide, this IC_{50} value is considered meaningful. Khan *et al.* (2012) reported an IC_{50} value for isoalantolactone of 40, 43 and 48 µM against PANC-1 (pancreas/duct cancer), BxPC3 (pancreatic cancer) and HPAC (pancreatic adenocarcinoma epithelial) cells, respectively. In a study using prostate cancer cells, isoalantolactone induced cell death at IC_{50} values of 27.84, 33.84 and 29.84 µM for LNCap (androgen-responsive prostate cancer), PC-3 and DU-145 (androgen-insensitive prostate cancer) cells. A review article by Gertsch (2009) implies that this value is too high for a pure compound to have clinical significance. In our study, we show isoalantolactone isolated from *A. afra* to have an IC_{50} value of 8.15 µM, which is considered more meaningful. However, dose-response assays were conducted for a 24 hour exposure time for the above mentioned studies where the IC_{50} determined here was after 48 hours of exposure. IC_{50} value obtained here is in line with the data presented by Ma *et al.* (2013) where HepG2 cells were treated with isoalantolactone and an IC_{50} value of 7.65 µM was achieved using the CCK-8 method and exposing the cells to isoalantolactone for 72 hours.

A dose-response assay was also carried out using the Vero cell line. This cell line is derived from the kidney of adult *Cercopithecus aethiops,* the African green monkey. It is a normal cell line and is often used as a control cell line to investigate the effect of compounds on normal, non-continuous and/or non-cancerous cells. Our investigation shows that isoalantolactone is cytotoxic against Vero cells at the 2 highest concentrations tested, ± 65 and 130µM. The resulting IC_{50} is estimated at ~ 260 µM, which is a very high concentration of a pure compound to be used and is thus considered irrelevant (Gertsch, 2009). Vero cells were confluent when used to test cytotoxic activity of the compound whereas HeLa cells were proliferating. Cells at confluence cease proliferating and undergo contact inhibition of

growth and enter the G0 phase of quiescence (Coller *et al.,* 2006). Uncontrolled cell proliferation is a major feature of cancer cells and thus it is important for the development of new anti-cancer therapies. Evidence of thapsigargin, a SL in clinical trials, being toxic to normal cells has been shown. This major drawback was overcome using it as a prodrug by the conjugation of a PSA enzyme for the treatment of prostate cancer (Christensen *et al.,* 2009; Ghantous *et al.,* 2010).

DNA cell cycle analysis was performed in order to determine in which phase of the cell cycle the cells arrest in. Table 5.1 shows a significant increase in the amount of DNA in the G2/M phase of the cell cycle. This is consistent with the findings of Rasul *et al.* (2013), where prostate cancer cells were treated with isoalantolactone. However, cell cycle analysis of pancreatic cancer cells showed an arrest in the S phase of the cell cycle after 24 hours of treatment (Khan *et al.,* 2012).

Cell cycle analysis showed a G2/M arrest of HeLa cells when treated with the compound. This is consistent with the observation of G2/M arrest upon treatment with the crude plant extract. In the same way as with *A. afra* treatment, it is not possible to determine whether the delay is observed in the G2 phase or the M phase of the cell cycle. Further investigation is needed to determine whether cells progress from the G2 phase into the M phase and arrest as a consequence of aberrant mitosis. Cells can also arrest in the G2 phase. This can be done by evaluating the proteins involved in the progression from G2 to M phase, i.e. Cdc2, cyclin B1 and Cdc25. Mitotic catastrophe is a form of cell death that occurs during or shortly after dysregulated or failed mitosis. Cell cycle arrest in the G2/M phase is often a suggestion that mitotic catastrophe could be the form of cell death occurring and can lead to either an apoptotic cellular morphology or a necrotic one. Mitotic catastrophe is accompanied by additional morphological changes including micronucleation and/or multinucleation (Kroemer *et al.,* 2009). Micronucleation is defined as the formation of micro nuclei within one cell and multinucleation is the appearance of two or more nuclei in one single cell. An investigation into the probability that mitotic catastrophe leads to the apoptotic cell death mode experienced by HeLa cells treated with isoalantolactone and *A. afra* was investigated and is discussed in Chapter 6.

Phosphatidylserine translocation is a biochemical feature of apoptosis and is often used as a marker of apoptosis. During apoptosis, this phospholipid is translocated to the outside of the

membrane and can be detected by Annexin V labelled with a fluororescent probe, in this case FITC. Dual staining was performed with Annexin V-FITC and PI to distinguish between apoptotic and necrotic cells. Dot plots of Figure 5.3 indicate a significant increase in the percentage of cells in the A4 quadrant of the dot plots (Figure 5.3 C). This quadrant correlates with cells undergoing early apoptosis and is said to be Annexin V positive and PI negative. An increase in late apoptotic cells is also evident. This too is consistent with previous reports of apoptosis induction by isoalantolactone (Khan *et al.,* 2012; Rasul *et al.,* 2013) and also with reported evidence that ethanolic *A. afra* induces apoptosis (Chapter 3; Spies *et al.,* 2013). However, lower percentage of apoptotic cells is evident here when considering published data. Khan *et al.* (2012) and Rasul *et al.* (2013) used 20 μM and 40 μM isoalantolactone, at least double the μM concentration used in this study. This can explain the difference in the percentage of cells undergoing early and late apoptosis. A greater cell population stained positive for PI and negative for Annexin V is also evident in the result published for PS translocation by Rasul *et al.,* (2013). This is an indication of necrotic cell death. This result was not evident when treating HeLa cells with 8.62 μM isoalantolactone for 24 hours.

In the intrinsic pathway, apoptosis is initiated within the cell. It is usually in response to cellular signals resulting from DNA damage, a defective cell cycle, detachment from the extracellular matrix, hypoxia and severe cell stress (Vermeulen *et al.,* 2003). This pathway involves the release of pro-apoptotic proteins from the mitochondria which, in turn, results in the activation of caspases, which ultimately leads to apoptosis. The execution of the intrinsic pathway of apoptosis is dependent on the balance of activity between pro- and anti-apoptotic proteins in the cell (Saelens *et al.,* 2004). Upon release of pro-apoptotic proteins, the mitochondrial membrane will experience depolarization (Vermeulen *et al.,* 2003). As mentioned, JC-1 dye was used to determine the state of the mitochondrial membrane after treatment of cancer cells with isoalantolactone. A significant increase in the mean green fluorescence intensity was observed (Table 5.2), suggesting depolarization of the mitochondrial membrane. Previous studies have also indicated a decrease in mitochondrial membrane potential(Khan *et al.,* 2012; Rasul *et al.,* 2013). In conjunction with this evident MMP decrease, apoptotic regulatory proteins associated with the mitochondria have also been investigated. It has been shown that treatment of pancreatic cancer cells with isoalantolactone, 20 μM, results in increased expression of Bax, a decreased expression of

Bcl-2 accompanied by the release of cyt-*c*, which in turn activates caspase -3 (Khan *et al*, 2012).

Caspase -8, the major initiator caspase, is activated when the death inducing signalling complex (DISC) is formed in response to external stimuli and is first activated through a death signal, suggesting a cellular response to an external signal for cell death. Thus, caspase -8 is used as a marker for the extrinsic mode of apoptosis. Caspase -3, the major executioner caspase, is in turn activated by initiator caspases (Thornberry, 1998; Kantari and Walczak, 2011). Immunochemistry was used to determine levels of activated/cleaved caspases in this study. Figure 5.3 shows that both caspase -8 and -3 are activated upon treatment with isoalantolactone, thus it is deduced that both the intrinsic and extrinsic pathways of apoptosis is induced by this compound due to the decrease in MMP and the activation of caspase -8, respectively. The cleavage of caspase -8 in response to isoalantolactone exposure has as of yet not been reported.

DNA fragmentation is one of the later steps in apoptosis. It is a process which results from the activation of endonucleases (by caspase -3) during the onset of apoptosis. These nucleases degrade the higher order of chromatin structure into small ~300 kb fragments of DNA and then degrade these fragments further. The Apo-Direct assay labels these DNA fragments with FITC labeled dUTPs catalyzed by the TdT enzyme. This way, flow cytometric analysis will enable the observation of DNA fragmentation. The histogram overlay of Figure 5 indicates the increase in green fluorescence intensity (FL1) as a result of DNA fragmentation.

More studies can be done on the mode of action of apoptosis induced by isoalantolactone. As discussed in 5.1.2, three SLs and their derivatives have reached clinical trials and their precise mechanism of action has been elucidated. The results achieved here provide clues as to where to look further to precisely predict its mode of apoptosis induction. We report that isoalantolactone from *A. afra* induces apoptosis in HeLa cells by the indication of phosphatidylserine translocation, after G2/M arrest of the cell cycle. It was also evident that apoptosis was mediated by caspases, as both cleaved caspase -8 and caspase -3 levels increased significantly after 24 hours of exposure to the compound. The results also suggest the involvement of the mitochondria due to the depolarization of the mitochondrial membrane after exposure to isoalantolactone. From this information, we can conclude that isoalantolactone present in *A. afra* contributes to the observed cytotoxicity induced by an

ethanol extract of this plant. However, investigations into the biochemical reasons for G2/M arrest, depolarization of the mitochondria and caspase activation can be performed. Examples of studies include cell cycle checkpoint analysis, cyt-*c* release and other pro-apoptotic proteins release from the mitochondria as well as ROS production to analyse cellular stress.

The Asteraceae plant family is rich in SLs and many plants belonging to this family are used traditionally for the treatment of inflammatory ailments. A link between inflammation and cancer has been well documented and is discussed in Chapter 7. Parthenolide and artemisinin both inhibit the NF-κB p65 and p50 subunits, respectively and cause deregulation of the NF-κB signalling pathway. Parthenolide also activates p53 and increases the production of ROS. Because of the simultaneous inactivation of p53 and hyperactivation NF-κB in human cancer cells, this compound is known as a "double-edged sword" (Dey *et al.*, 2008). An interesting continuation of this investigation of induced apoptosis by isoalantolactone can also include the effect of the compound on NF-κB signalling, the difference in p53 levels and ROS production, using monoclonal antibodies and uniform staining using 2,7-dichlorofluorescein diacetate, respectively. Detection of significant changes between treated (with isoalantolactone and parthenolide as a positive control) and untreated cancer cells can be done using flow cytometry.

CHAPTER 6: Analysis of G2/M arrest and the possible onset of mitotic catastrophe as a special mode of apoptosis.

6.1. Introduction:

Cells proliferate by the mitotic cell cycle. This cycle allows for DNA synthesis during the S-phase and separation of the sibling chromosomes during mitosis, the M-phase. The two phases are separated by the Gap phases called G1 and G2. Thus, the ordered series of events is as follows: M → G1 → S → G2 → M. Cell division (cytokinesis) occurs immediately after mitosis. G1 phase cells contain two copies of their genome, i.e. 2N or diploid whereas cells in the G2 or M phases contain double the number of genetic material, 4N or tetraploid. Cells that contain more than tetraploid DNA are said to be polyploid (Ullah *et al.,* 2009).

Cell cycle checkpoints allow the progression of a cell through the cell cycle or allow arrest in response to DNA or cellular damage. Components of the checkpoints include sensors, mediators, transducers and effectors. These molecules all work cooperatively in each phase of the cell cycle (Buchner and Britten, 2008). Checkpoints allow for DNA repair and replication to take place with little introduction of mutations and occur late in the G1 and G2 phases, which prevent the entry of the cell into the synthesis phase and the mitotic phase, respectively, if repair is not possible (DiPaola, 2002). The checkpoint control system is regulated by a family of protein kinases known as the cyclin-dependent kinases (Cdks, also known as Cdc's) and has been considered to be at the center of the cell cycle (Fisher, 1997; Pestell *et al.,* 1999; DiPaola, 2002). However, association of cdk with its respective cyclin is essential for the activity of the enzyme.

Cdks are a family of well conserved serine/threonine kinases sharing between 40 to 75 % identity among them. Monomeric Cdks have almost no kinase activity (Lees, 1995). Cdks act at specific points in the cycle by responding to cellular signals, thus protein kinases and protein phosphorylation are central to the functioning of the cell cycle (Schafer, 1998). They require the binding of a regulatory subunit known as the cyclin to activate the kinase activity. The regulation of Cdks directs the cell through the cell cycle by forming complexes with their respective cyclin molecules. Cyclins heterodimerize with their specific Cdk to form holoenzymes (Lees, 1995; Pestell *et al.,* 1999). Each complex performs a particular role (DiPaolo, 2002). Cdk expression is relatively low during the G1 phase of the cell cycle and it

rises progressively as cells advance through the cell cycle. Levels peak during mitosis and then rapidly fall due to Cdk decay (Sherr and Roberts, 2004).

Cyclins have a unique pattern of expression (Figure 6.1) and timing of their expression is key in determining at which phase of the cell cycle their associate Cdk is active. Consequently, cyclin abundance is the rate limiting factor for progression of the cell through the cell cycle (Lees, 1995). Cyclin abundance is regulated by transcriptional regulation and by protein turnover. Cyclins of the G1 phase are unstable and only have a half-life of 20 minutes. Rapid degradation of cyclins occurs through the ubiquitination pathway (Pestell *et al.*, 1999; Lees, 1995).

Cdk/cyclin complexes are regulated by counteracting mechanisms. These include the association of cyclin-dependent kinase inhibitors (CKIs), activation by phosphorylation of Thr160/161 of the T-loop of the Cdk and the inhibitory phosphorylation on Thr14 and Tyr15 (Kristjánsdóttir and Rudolph, 2004).

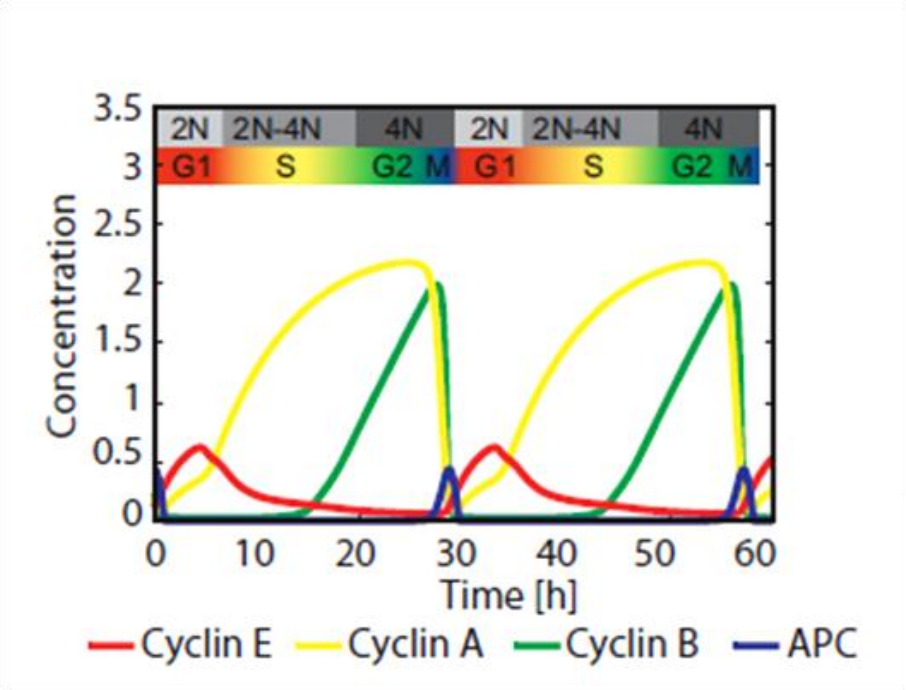

Figure 6.1. Cell cycle model indicating the levels of cyclin E, cyclin A and cyclin B as well as phosphorylated anaphase-promoting complex (APC). The cell cycle phase and DNA content is indicated above (Toettcher *et al.*, 2008).

Regulation of the transition of the cell from one phase of the cell cycle to the next is controlled by Cdks at two specific points in the cell cycle known as the G1/S checkpoint and the G2/M checkpoint.

6.1.1. G1/S checkpoint:

The G1 checkpoint is the first defense in response to DNA damage or cellular stress. It prevents cells from entering the S phase by inhibiting the process of DNA replication. The unphosphorylated retinoblastoma protein (pRb), inhibits the transcription of genes required for DNA synthesis when it binds to the transcription factor E2F. E2F, a gene regulatory protein is required for entry into the S phase. E2F is controlled by pRb.

The Cdks involved during the G1 phase are regulated by cyclin D and cyclin E (Sherr and Roberts, 2004). Cyclin D forms complexes with both Cdk 4 and 6, cyclin E forms a complex with Cdk 2. Cyclin D1/Cdk 4 and cyclin D1/Cdk 6 serve to inactivate the pRb and the related proteins p130 and p107 by phosphorylation and this inactivation allows the cells to progress through the restriction point and into the S phase of the cell cycle. Cyclin/Cdk inhibitor proteins (CKIs) inhibit the ability of the cyclin/cdk complexes of G1 to phosphorylate pRb. CKIs are divided into two broad categories. The first is the Ink4 proteins that specifically inhibit Cdk4 and Cdk 6. The second group is the Cip/KIP family of proteins, p21, p27 and p57. All CKIs promote G1 arrest if overexpressed (Pestell *et al.*, 1999).

The cyclin/Cdk complexes of the G1 phase phosphorylate pRb and reduces its affinity for E2F and this allows for the activation of genes required for progression to the S phase. If DNA damage is experienced, p53 stimulates the transcription of CKIs and subsequent inhibition of cyclin/Cdk complexes and a decrease in pRb phosphorylation. Arrest in the G1 phase occurs (DiPaolo, 2002). A multitude of different stimuli exert checkpoint control including TGF-β, DNA damage, replicative senescence and growth factor withdrawal (Lees, 1995; Schafer, 1998; Sherr and Roberts, 2004).

6.1.2. G2/M checkpoint:

The G2/M checkpoint serves to prevent the cell from entering the M phase with genomic DNA damage. The cyclin involved at these phases is cyclin B1 and to a lesser extent cyclin

A. Both bind Cdk 1 (Cdc 2) to allow for the progression of the cell from G2 to mitosis. However, cyclin A is not sufficient to trigger the transition from G2 to M (Pagliuca *et al.*, 2011).

The G2 checkpoint is a key guardian of the cancer cell genome. A cancer cell containing DNA damage that has progressed through the G1 and S phase may come to a halt at the G2 checkpoint and thus it has been said that the G2 checkpoint is an attractive target for anticancer therapy. G2 abrogation prevents cancer cells from repairing DNA damage and thus forces the cell into the M phase and cell death is experienced by mitotic catastrophe and apoptosis (Bucher and Britten, 2008). Figure 6.2 gives a clear summary of the involvement of various Chk, Cdc and cyclin molecules in cell cycle arrest.

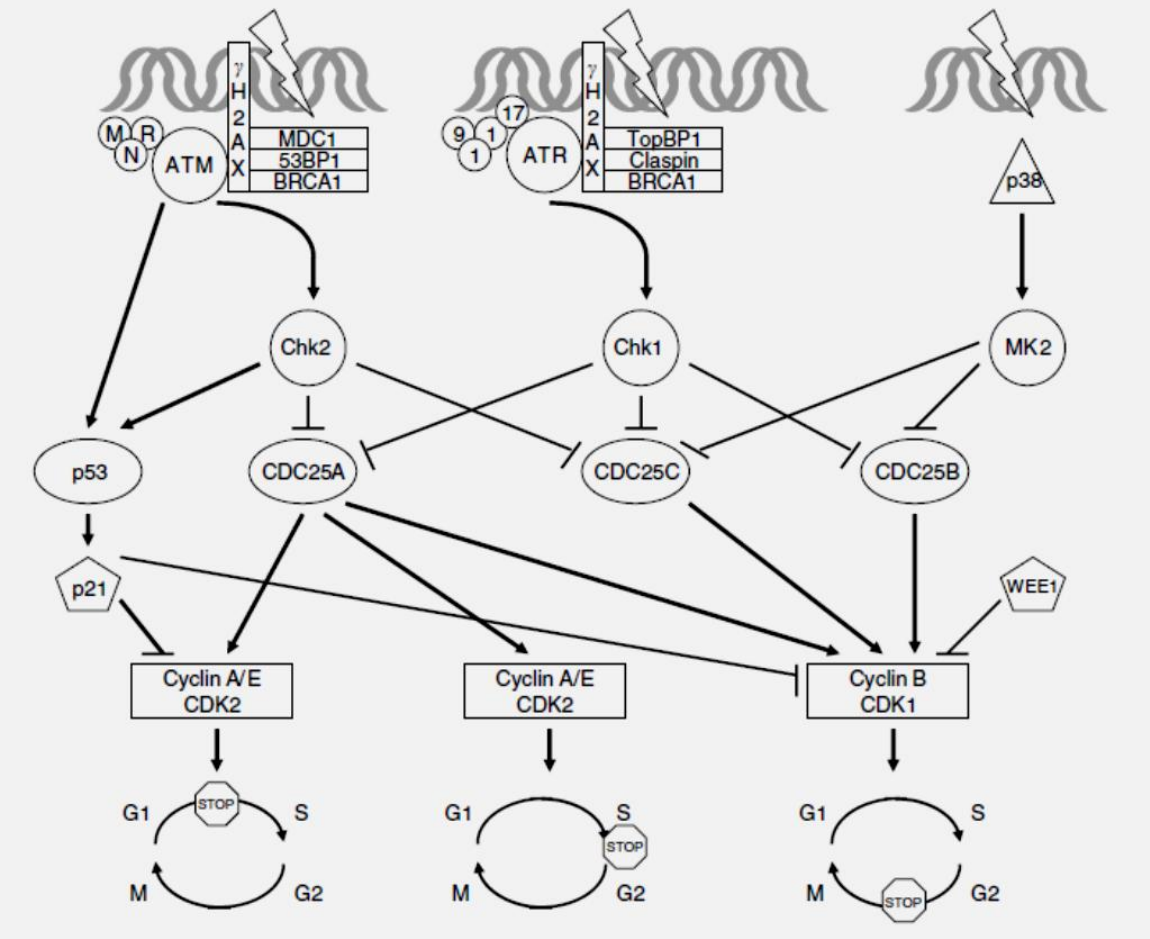

Figure 6.2. Cell cycle checkpoints showing the roles of the checkpoint transducer (ATM and ATR) and the activation of several downstream molecules. These include the checkpoint kinases (Chk1 and Chk2) which inactivate the Cdc25 phosphatases leading to cell cycle arrest (Bucher and Britten, 2008).

6.1.3. Mitotic catastrophe (MC):

Much controversy has surrounded the definition of mitotic catastrophe. A clear definition of the phenomenon has still not surfaced and the term "mitotic catastrophe" as a form of cell death is used with caution. In broad terms, MC is defined as a form of cell death that results from premature or inappropriate entry of cells into mitosis (Vakifahmetoglu *et al.*, 2008). The NCCD defines it as a cell death mode occurring either during or shortly after a failed mitosis. It can be characterized by the appearance of micronucleation and/or multinucleation and leads to either an apoptotic or necrotic cellular morphology upon cell death (Kroemer *et al.*, 2009).

It has been argued that MC is fundamentally different to apoptosis because it has been shown that overexpression of anti-apoptotic proteins can enhance the frequency of MC. It has also been shown using caspase inhibitors that death of giant, multinucleated cells does not fail, implying that MC is not caspase dependent and thus not related to apoptosis (Nabha *et al.*, 2002; Castedo *et al.*, 2004). However, it is known that apoptosis can occur independent of caspase activation (Castedo *et al.*, 2004).

It is also proposed that MC is a type of cell death that occurs during mitosis as a result of DNA damage or disruption of microtubule formation. It is suggested that a combination of G2/M checkpoint arrest and deficiencies in the spindle assembly checkpoint of anaphase and DNA damage leads to mitotic catastrophe. DNA damage or cellular stress and induction of microtubule-hyperpolymerising agents such as taxanes or microtubule-depolymerising agents such as vinca alkaloids and colchicine can lead to mitotic catastrophe (Castedo *et al.*, 2004; Singh *et al.*, 2010).

It is also suggested that MC is a special mode of apoptosis, where most of the features of apoptosis is evident coupled with G2/M arrest and evidence of micro- and/or multinucleation. It may also result in necrosis where an accumulation of micronuclei does not allow for nuclear fragmentation and death of the cell is characterized by necrosis. MC may also be a cell survival mechanism of tumours (Vakifahmetoglu *et al.*, 2008). The different concepts of MC are summarised in Figure 6.3.

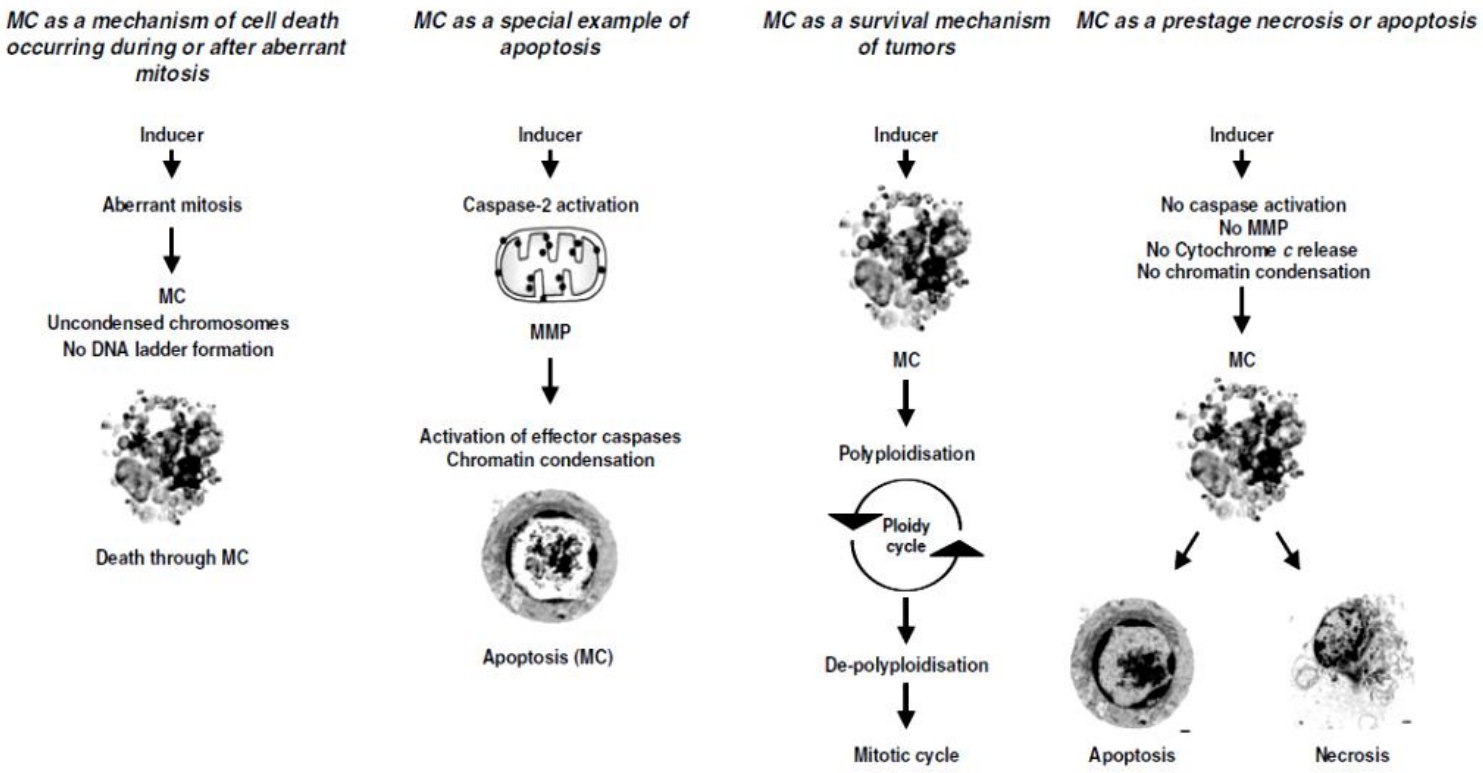

Figure 6.3. A summary of the concepts of MC (Vakifahmetoglu *et al.*, 2008).

MC can be induced in several ways. These are checkpoint deficiencies, anti-microtubular drugs, DNA damage and it could occur as a consequence of prolonged growth arrest (Roninson *et al.*, 2001).

6.1.4. Aim:

Upon observation of HeLa cells treated with 30 µg/mL *A. afra* ethanol extract for 24 hours, the appearance of multinucleated cells was evident (Figure 3.13). DNA cell cycle analysis was performed to determine the effect of the plant extract on the cell cycle and from this, G2/M arrest was evident (Chapter 3). Due to the evidence of multinucleated cells and G2/M arrest, it was hypothesized that mitotic catastrophe is induced by *A. afra* ethanol extracts and results in apoptosis.

6.2. Materials:

Cervical (HeLa) cancer and human promonocytic leukaemia U937 cells were purchased from Highveld Biological, South Africa. Cyclin B1 (V152) mouse mAb (Alexa Fluor 488 conjugate), phospho-cdc2 (Tyr15) rabbit mAb, phospho-cdc25C (Ser198) antibody, phospho-histone 3 (Ser10) rabbit mAb, α-tubulin rabbit mAb (Alexa Fluor 488 conjugate), anti-rabbit IgG F(ab')2 fragment (Alexa fluor 488 conjugate) and the rabbit and mouse IgG isotype controls (Alexa Fluor 488 conjugate) were all purchased from Cell Signaling Technology, Inc. (Danvers, MA, USA). Prolong Gold anti-fade reagent was also purchased from Cell Signaling Technologies. Paclitaxel, colchicine, DAPI, phalloidin-tetramethylrhodamine B isothiocyanate and paraformaldehyde were purchased from Sigma-Aldrich (St. Louise, MO, USA). Tubulin polymerization assay kit (BK006P) was purchased from Cytoskeleton (Denver, CO, USA). DPBS was purchased from Lonza (USA).

6.3. Methods:

6.3.1. IC_{50} determination of paclitaxel and colchicine:

6.3.1.1. Background:

It has been shown that mitotic catastrophe can be induced by microtubule-hyperpolymerising agents such as taxanes or microtubule-depolymerising agents such as vinca alkaloids and colchicine (Castedo *et al.,* 2004). Paclitaxel and colchicine are molecules that are used in the treatment of various cancers. Both are described as antimitotic agents causing arrest of cells in the G2/M phase. Although both are antimitotic agents, their modes of action are different.

Paclitaxel is a chemotherapeutic agent that is derived from the bark of the Western Yew tree, *Taxus brevifolia* (Wani *et al.,* 1971). Liebermann *et al.* (1993) demonstrated that paclitaxel is cytotoxic against various cell lines, including HeLa cells and IC_{50} values as low as 2.5 nM were obtained. Paclitaxel is a mitotic inhibitor and does so by causing hyperpolymerisation of microtubules. Paclitaxel binds to the N-terminal 31 amino acids of β-tubulin and induces the bundling of microtubules. Hence, paclitaxel promotes the polymerisation of tubulin. Colchicine binds to the tubulin dimers and causes dissembly of microtubules (Parness and Horwitz, 1981; Rowinsky and Donehower, 1995; Rao *et al.,* 1995). Paclitaxel and colchicine

were selected as control molecules for the investigation of the anti-mitotic potential of *A. afra* ethanol extract and isoalantolactone.

6.3.1.2. MTT cytotoxicity assay for the determination of IC_{50} values of paclitaxel and colchicine:

HeLa cells were seeded in 200 µL aliquots at $3x10^4$ cells/mL in 96 well plates and were left overnight to attach at 37 °C before treatment. The medium was replaced with fresh medium containing varying concentrations of paclitaxel (1.56 – 50nM) and colchicine (4.69 – 150nM). Cells were incubated at 37°C in a humidified 5% CO_2 incubator for 48 hours. The medium containing treatments were removed prior to addition of MTT (0.5 mg/mL). Absorbance was read at 540 nm using a BioTek® PowerWave XS spectrophotometer (Winooski, VT, USA).

6.3.2. Cyclin B1 (V152), phospho-Cdc2 (Tyr15) and phospho-Cdc25C (Ser198) analysis:

6.3.2.1. Background:

The interaction and association of Cdc2 (Cdk 1) and cyclin B1 forms an active heterodimer known as the "mitosis-promoting factor" (Pestell *et al.*, 1999). The progression of the cell from the G2 phase to the M phase is driven by active Cdc2/cyclin B1 complex. The activity of the complex must be sustained from prophase through metaphase. The activity of the complex rapidly drops in anaphase due to destruction of the complex (Castedo *et al.*, 2004).

The association of the proteins is regulated by transcription factors, endogenous Cdk inhibitors, modifications of the proteins by kinases and phosphatases present in the cytoplasm as well as subcellular distribution and regulated degradation of cyclin B1 (Castedo *et al.*, 2004). Wee1/Mik1/Myt1-related protein kinases phosphorylate Cdc2 at the active site at threonine 14 and tyrosine 15 (Thr 14, Tyr 15) residues to render the enzyme inactive. Dephosphorylation of Cdc2 at this site is mediated by active Cdc25Cand increases Cdc2 activity (DiPaola, 2002). Therefore, a crucial event in the progression of cells through the G2/M checkpoint is the activation of Cdc25C.
Cdc25C is a regulator of G2/M together with Cdc25B (Kristjánsdóttir and Rudolph, 2004). Cdc25C is constitutively phosphorylated at Ser216 throughout interphase of a cell.

Phosphorylation of Ser216 by checkpoint kinases 1 and 2 (Chk 1 and Chk 2) takes place at the G2/M checkpoint in response to DNA damage. When Cdc25C is phosphorylated at Ser216, it binds to members of the 14-3-3 protein family and this results in the sequestering of Cdc25C in the cytoplasm. The implication is that the cell will not progress through the G2 phase to M phase (Castedo *et al.*, 2004).

DNA damage activates the DNA-PK/ATM/ATR kinases, which in turn initiates two parallel cascades that inactivate the Cdc2-cyclin B complex. The first cascade rapidly inhibits progression from G2 into mitosis (Figure 6.4). The slower second parallel cascade involves phosphorylation of p53 and allows for its dissociation from MDM2 and MDM4, which activates DNA binding and transcriptional regulatory activity, respectively. The activation of p53 allows for the transcription and translation of 14-3-3s, which binds to the phosphorylated Cdc2/cyclin B1 kinase and exports it from the nucleus; GADD45, which binds to and dissociates the Cdc2/cyclin B kinase; and $p21^{Cip1}$, an inhibitor of a subset of the cyclin-dependent kinases including Cdc2. The inactivation of the Cdc2/cyclin B complex arrests the cell in the G2 phase (Harrison and Haber, 2006; Schafer, 1998, Scherr and Roberts, 2004).

During prophase, polo-like kinase 1 (PLK1) phosphorylates Cdc25C at Ser198. This allows for Cdc25C to translocate from the cytoplasm to the nucleus where it can interact with Cdc2/cyclin B1 and allow for the progression of the cell through mitosis (Toyoshima-Morimoto *et al.*, 2002).

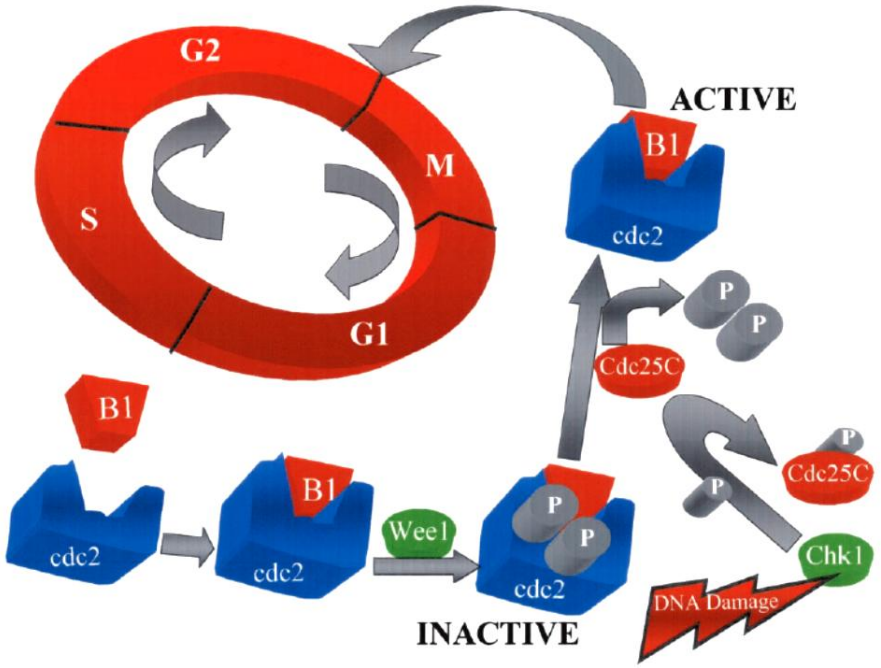

Figure 6.4. The late G2 checkpoint controlling the cell cycle progression from the G2 phase to the M phase (DiPaola, 2002).

6.3.2.2. Determination of change in levels of Cyclin B1 (V152), phospho-Cdc2 (Tyr15) and phospho-Cdc25C (Ser198):

U937 cells were seeded at $1x10^5$ cells/mL in culture flasks and HeLa cells were seeded at $5x10^4$ cells/mL in 6 well culture plates, using 3 mL per well, and treated with 20 µg/mL and 30 µg/mL of ethanolic *A. afra* extract, respectively. Cells were also treated with 8.62 µM isoalantolactone isolated from *A. afra*. Paclitaxel (8 nM) was used as a positive control for this series of experiments. HeLa and U937 cells were incubated at 37 °C for 12 and 24 hours. Hereafter U937 and HeLa cells were treated in the same way. Cells were fixed and permeabilised using the IntraPrep kit (Beckman Coulter). Cells were washed three times by resuspension in PBS containing 0.5% BSA (blocking buffer) and centrifugation at 500 xg for 5 minutes. Cells were blocked using PBS containing 0.5% BSA and thereafter incubated with the antibodies diluted in blocking buffer, separately. Cyclin B1 (V152), phospho-Cdc2 (Tyr15) and phospho-Cdc25C (Ser198) antibodies were used at 1:50, 1:25 and 1:25 dilutions respectively and incubated for 1 hour at 37°C. After incubation, cells were centrifuged at 500 xg for 5 minutes and thereafter washed as previously described. The wash step was repeated three times to eliminate unbound antibodies. Cells were then incubated with the conjugated secondary antibody (1:1000), anti-rabbit IgG F(ab') 2 fragment (Alexa fluor 488 conjugate),

for 30 minutes at 37°C in the dark and thereafter, washed again. Since the cyclin B1 antibody contained a conjugated fluorophore, incubation with the secondary antibody was not required. Mouse and rabbit IgG isotype controls were also prepared for analysis. Cell samples were analyzed within 30 minutes using the Beckman Coulter Cytomics FC500.

6.3.3. Phospho-H3 (Ser10) analysis:

6.3.3.1. Background:

DNA is highly organized into chromatin in which the basic unit is the nucleosome consisting of DNA tightly wound around 8 core histone (H) proteins. The core histone proteins are H2A, H2B, H3 and H4 and form an octamer. Each octamer exhibits a tripartite structure by the tetramer $(H3 – H4)_2$ which is centrally located and flanked by two H2A – H2B dimers. The common structural motif that they share is the histone fold and the N-terminal (Prigent and Dimitrov, 2003).

The N-terminal tails of the histone molecules are outside the relatively compact chromatin unit. This makes them readily available for post-translational modifications. Post-translational modifications of the histone tails include acetylation, phosphorylation, methylation, ADP-ribosylation and ubiquitination (Figure 6.5). Post-translational modifications are necessary for access to DNA for binding of transcription factors to regulate gene expression and for replication (Prigent and Dimitrov, 2003; Nowak and Corces, 2004; Wolffe and Hayes, 1999).

The N-terminal tails of H3 have the highest density of modifications among the histone proteins (Jeong *et al.,* 2010). Phosphorylation of H3 has been linked to chromosomal condensation during mitosis (Wei *et al.,* 1998; Wei *et al.,* 1999) and is also implicated in the transcriptional activation of genes in various organisms (Nowak and Corces, 2004). Phosphorylation of H3 at Ser10 is known as the “phos” switch and is the hallmark of mitosis. This modification is catalyzed by Aurora B kinase (Aur-B). Phosphorylation begins in the G2 phase and by metaphase, it has spread to entire chromosomes (Jeong *et al.,* 2010).

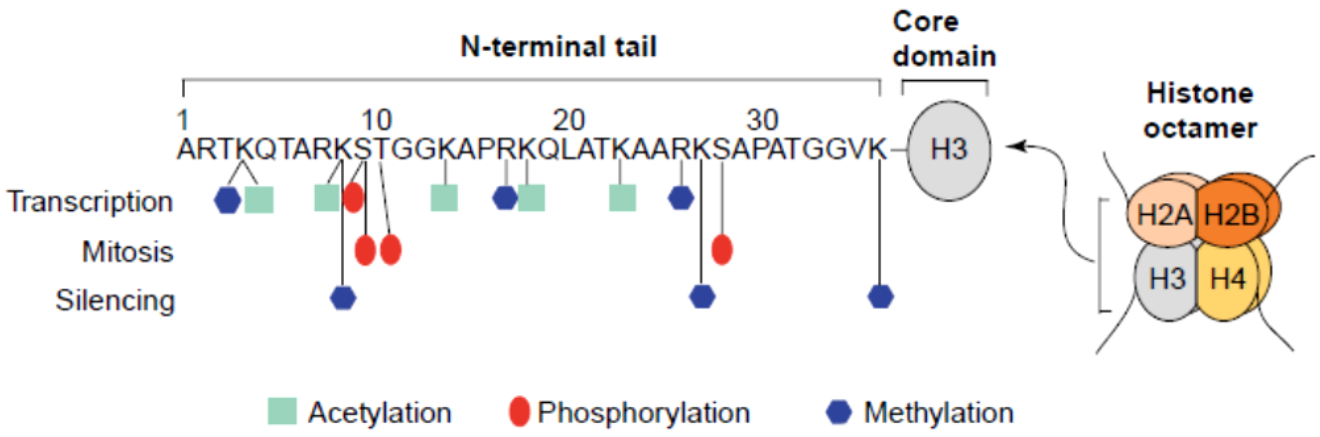

Figure 6.5. Modifications of H3 N-terminal tail. Acetylation, phosphorylation and methylation are indicated as well as the cellular process (indicated on the left) affected by the respective modification (Nowak and Corces, 2004).

In response to DNA damage, various kinases including ATM, ATR, Chk1 and Chk 2 (See Figure 6.2) are activated to halt cell cycle progression at a particular phase. Inhibition of Chk 1 has been implicated in the onset of mitotic catastrophe and it is reported that a potential biomarker of Chk 1 inhibition is phospho-H3 at Ser10 (Bucher and Britten, 2008). Matthews (2006) showed that a novel and specific inhibitor of both Chk 1 and Chk 2 abrogated the G2 checkpoint by the activation of Cdk1 (Cdc2) and an increase in phospho – H3 (Ser10) levels. Thus, cells progressing from G2 to M will experience an increase in phospho - H3 at Ser10.

6.3.3.2. Detection of change in levels of phospho-H3 (Ser10):

HeLa cells were seeded and treated as described in 6.3.2.2. Cells were treated for 12 and 24 hours. The same method of antibody staining was performed for the detection of phospho-H3 (Ser 10) as described in 6.3.2.2. Briefly, cells were fixed and permeabilised using the IntraPrep Kit and thereafter blocked using 0.5% BSA. Cells were then incubated for 1 hour with 1:250 phospho-H3 (Ser10) and then incubated for 30 minutes with anti-rabbit IgG F(ab')2 fragment (Alexa fluor 488 conjugate) at 37°C after three wash steps. Rabbit IgG isotype control was also prepared. Cells were analysed using flow cytometry and data was recorded in FL1.

6.3.4. Tubulin polymerisation:

6.3.4.1. Background:

Tubulin is a heterodimer consisting of two 55 kDa subunits, namely α- and β- tubulin. Tubulin polymerises to form microtubules (MTs) and initially forms proto-filaments. Generally, MTs consist of 13 proto-filaments and are 25 nm in diameter. Each µm of MT length is composed of 1650 heterodimers. MTs determine cell shape and play important roles in many cellular processes such as cell division, signal transduction, cell mobility and cellular transport (www.cytoskeleton.com).

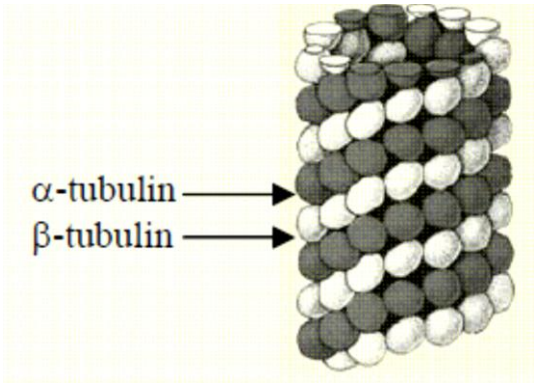

Figure 6.6. A schematic representation of a microtubule (www.cytoskeleton.com).

MTs are highly ordered fibres that have an intrinsic polarity and consist of two distinct ends, the fast growing "plus" end and the slow growing "minus" end. In most cells, MTs are organized into a single array with their plus end located near the nucleus and their minus end near the plasma membrane (Waterman-Storer and Salmon, 1997).

Tubulin dimers polymerise and depolymerise constantly and thus, MTs undergo rapid assembly and disassembly. The first stage of polymerisation is the nucleation phase. During nucleation, α – and β – tubulins join end-to-end to form protofilaments with altering α – and β – tubulin subunits (See Figure 6.6). This is a slow process and requires Mg^{2+} and GTP. The second phase of tubulin polymerisation is the elongation phase and is a rapid process. During elongation and the formation of heterodimers and MTs, the binding of GTP to both α – and β – tubulin subunits is required (Nelson and Cox, 2000).

During mitosis, the MT network is dismantled and a bipolar, spindle shaped array is formed that attaches to the chromosomes and moves them to opposite poles of the cell and MT dynamics increase up to 100 – fold at mitosis (Jordan and Wilson, 1998). Because of the important role of MTs for cell division, they have become an attractive target for cancer therapy. As mentioned in 6.3.1.1, anti-mitotic agents disrupt cell division by either causing inhibition of MT formation by tubulin binding, or by causing hyperpolymerisation and stabilising MTs. Paclitaxel has the ability to diffuse through the microtubule lattice and bind to the β – tubulin subunit resulting in an increase in microtubule polymerisation (Gallagher, 2007).

The effect of *A. afra* ethanol extract and isoalantolactone on tubulin polymerisation was investigated using purified porcine tubulin in the form of microtubules. Paclitaxel and colchicine were used as control molecules.

6.3.4.2. Detection of the effect of the rate of tubulin polymerisation in the presence of A.afra *and isoalantolactone:*

A. afra ethanol extract and isolalntolactone were used to determine their effect on tubulin polymerisation. This was performed using the Tubulin Polymerization Assay Kit from Cytoskeleton (USA). The assay is carried out in a sterile 96 well plate. The plate was pre-warmed to 37°C for 30 minutes. The kit is equipped with two buffers, the general tubulin buffer containing 80 mM PIPES, 2.0 mM $MgCl_2$, 0.5 mM EGTA (pH 6.9) and the tubulin glycerol buffer containing 60 % glycerol in general tubulin buffer (pH 6.9). It also contains GTP stock (100 mM) and lyophilised tubulin protein (10 mg). Tubulin polymerisation (TP) buffer was prepared using 750 µL general tubulin buffer, 250 µL tubulin glycerol buffer and 10 µL GTP stock. Thus tubulin polymerisation buffer comprised of 80 mM PIPES, 2.0 mM $MgCl_2$, 0.5 mM EGTA, 15 % glycerol and 1 mM GTP. Tubulin was reconstituted in ice cold general tubulin buffer supplemented with 1 mM GTP. The reaction was set up as follows:

Ten times concentrations of *A. afra* and isoalantolactone were prepared in general tubulin buffer and 10 µL were added to wells and incubated at 37°C for 2 minutes. Paclitaxel (final concentration 10 µM) was used as a positive control as recommended by the manufacturer and the general tubulin buffer was used for control wells (no compound added). Tubulin was diluted using TP buffer to give a final concentration of 3 mg/mL. One hundred micolitres of

tubulin (3 mg/mL working solution) was then added to each reaction well and immediately placed in the plate reader (BioTek® PowerWave XS spectrophotometer). Tubulin polymerization was monitored at 37°C at 340 nm for 1 hour. This assay was performed once in duplicate.

6.3.5. Evidence of antimitotic potential of an ethanol extract of *A. afra* and isoalantolactone using confocal microscopy:

HeLa cells were treated with *A. afra*, isoalantolactone and paclitaxel at their respective IC_{50} values. Cells were stained with DAPI, phalloidin-rhodamine B conjugate and α – tubulin-Alexa 488 conjugate. Confocal microscopy was performed to view the nuclei, actin filaments and tubulin, respectively.

Three LabTek 177399 four chamber slides were coated with 1 mL poly-L-lysine (0.01%) prior to cell seeding to aid in attachment of cells. Poly-L-lysine was removed and 1 mL aliquots of HeLa cells (at 1.2 x 10^4 cells/mL) were seeded per chamber and left overnight at 37°C to attach. Cells were treated with paclitaxel (10 nM), *A.afra* (30 μg/mL) and isoalantolactone (8.62 μM) for 12, 24 and 36 hours. An untreated control was also prepared per time interval. After each incubation time, cells were fixed using 3% paraformaldehyde (in DPBS) and incubated at room temperature for 15 minutes. Cells were then rinsed using DPBS three times for 5 minutes per rinse. Cells were permeabilised by adding 100% ice cold methanol to each chamber and placed at -20°C for 10 minutes. Thereafter, cells were rinsed as previously described. One percent BSA in DPBS supplemented with 0.3% Triton X-100 was used to block the cells. Cells were blocked for 1 hour using 500 μL aliquots. After the blocking step, α-tubulin was stained using 1:100 α-tubulin mAb. Cells were left in the presence of the antibody overnight at 4°C. Cells were then rinsed as previously described. Counterstaining using DAPI (0.1 μg/mL) and phalloidin-TRITC (20 μM) in DPBS was then done for the staining of nuclei and actin, respectively. Cells were incubated for 30 minutes at room temperature in the dark with counterstain. Cells were rinsed as previously described. After staining, samples were covered with Prolong Gold anti-fade reagent and a glass coverslip. Samples were cured overnight at room temperature and thereafter placed at 4°C until use.

Confocal microscopy was carried out at the Confocal and Light Microscope Imaging Facility at the University of Cape Town under the supervision of Professor Dirk Lang and Mrs Susan Cooper. The facility is equipped with a Zeiss Axiovert LSM 510 META confocal microscope. A Zeiss AxioCam is installed for fluorescence imaging. Post-acquisition processing was performed using ZEN 2009 Light Edition software.

6.3.6. Statistical analysis:

All treatments of both cell lines were conducted in triplicates. All experiments were carried out at two independent times. Histogram overlays are one representation of each experiment. Standard deviation (SD) was calculated for each experiment independently. For each assay, the Student two-tailed *t*-test was performed to determine significance. $p<0.05$ was considered significant, indicated by *, $p<0.005$ is indicated by **. For all flow cytometry assays, a minimum of 10 000 events were recorded for each sample.

6.4. Results:

6.4.1. IC_{50} determination of paclitaxel and colchicine:

Dose response assays were carried out to determine the IC_{50} values of paclitaxel and colchicine, molecules used as controls that induce G2/M arrest in HeLa cells (Liebmann *et al.,* 1993; Beckers *et al.,* 2002), but different influences on mitotic spindle formation.

Figure 6.7 shows the results of the dose-response assay. IC_{50} values of 9.78 nM and 7.72 nM were obtained for colchicine and paclitaxel, respectively.

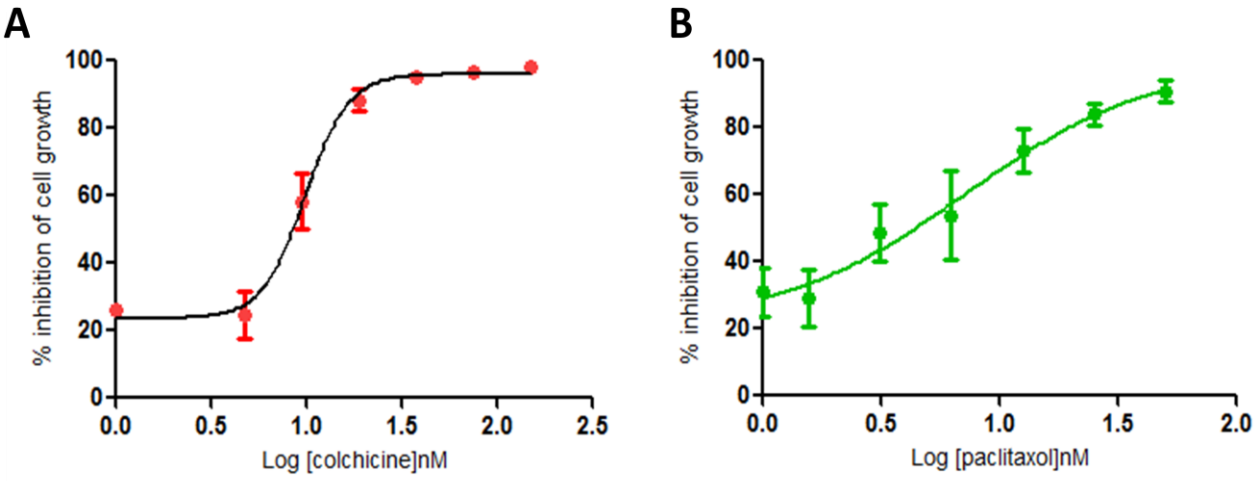

Figure 6.7: Cytotoxic effects of A) colchicine and B) paclitaxel against HeLa cells after 48 hours of exposure. Cell viability was determined using the MTT assay. Error bars indicate SD of four replicate values.

6.4.2. Cyclin B1 (V152), phospho-Cdc2 (Tyr15) and phospho-Cdc25C (Ser198) analysis:

Flow cytometric analysis of cyclin B1 (V152), phospho-Cdc2 (Tyr15) and phospho-Cdc25C (Ser198) was performed in order to detect changes in levels of these proteins after G2/M arrest, which is evident after 12 hours of treatment with *A. afra* ethanol extract and isoalantolactone.

Figure 6.8 shows the results of cyclin B1 (V152) analysis after 12 (Figure 6.8 A and C) and 24 hours (Figure 6.8 B and D). At 12 hours, in HeLa cells, a shift in the histogram is evident from right to left, indicating a decrease in the mean green fluorescence intensity (FL1). This decrease suggests that there is a decrease in the level of this protein. At 12 hours, in U937 cells, no significant change in fluorescence intensity was seen.

At 24 hours in both cell lines, a significant increase in fluorescence intensity was evident, except for isoalantolactone treated U937 cells, where no significant change was seen.

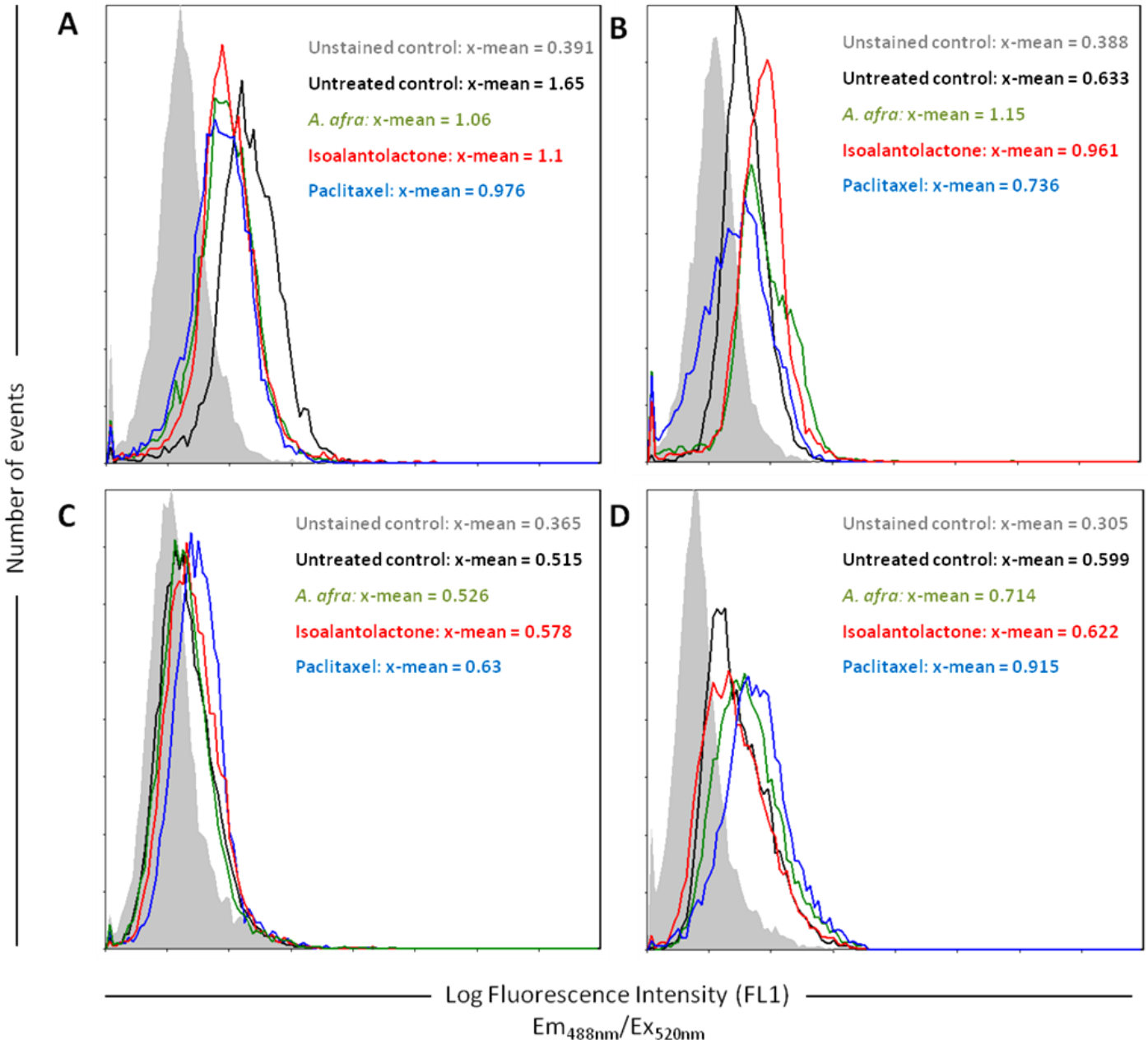

<u>Figure 6.8:</u> Histogram overlays representing cyclin B1 (V152) levels in HeLa (A and B) and U937 cells (C and D) after treatment with *A. afra* (green), isoalantolactone (red) and paclitaxel (blue) after 12 (A and C) and 24 (B and D) hours. Insert: The mean fluorescence intensity corresponding to a specific treatment. 10 000 events were recorded per sample. (One representative for 2 individual experiments each performed in triplicate).

Significant differences were evident from 12 hours of exposure to treatments to 24 hours when analyzing the change in levels of cyclin B1 (V152). This is shown in Figure 6.9.

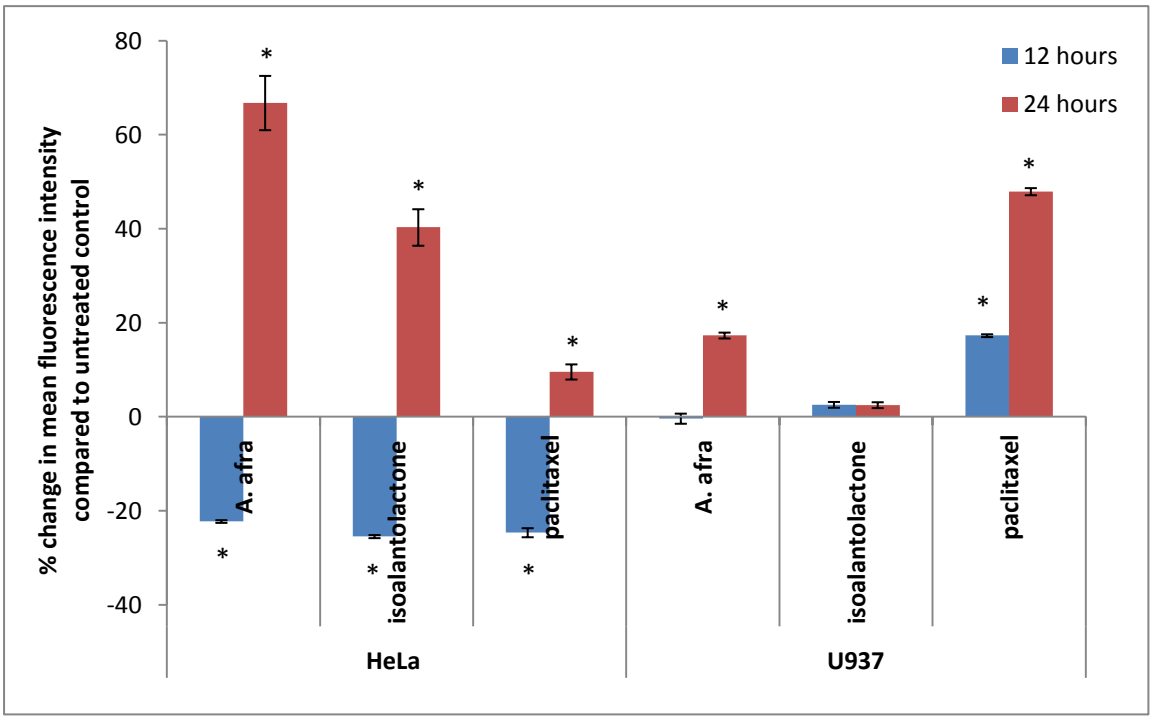

Figure 6.9: Changes in levels of cyclin B1 after exposure to *A. afra,* isoalantolactone or paclitaxel for 12 (blue) and 24 hours (red). Error bars indicate SD of the mean change in fluorescence intensity. Significance compared to an untreated control was determined using Student *t*-test: *p<0.05.

Analysis of levels of phospho-Cdc2 (Tyr15) was done in both HeLa and U937 cells. A representation of the results is shown in Figure 6.10. No significant changes were apparent after 12 hours of exposure to *A. afra,* isoalantolactone or paclitaxel in HeLa cells as clearly indicated by no shift in histograms, i.e. fluorescence intensity. Slight increases were evident after exposure of U937 cells to paclitaxel and *A. afra*, which was not expected.

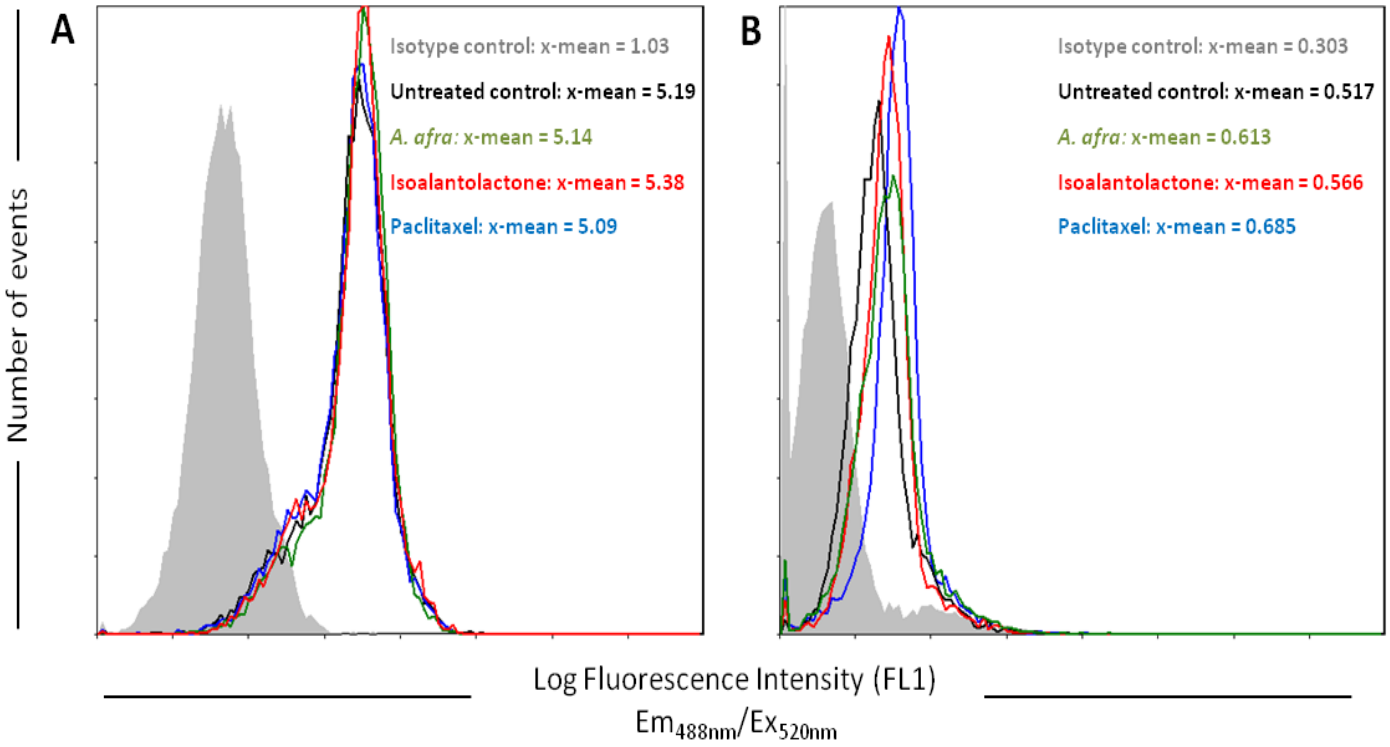

Figure 6.10: Analysis of phospho-Cdc2 (Tyr15) after treatment with *A. afra* (green), isoalantolactone (red), and paclitaxel (blue) for 12 hours in HeLa (A) and U937 (B) cells. Insert: The mean fluorescence intensity corresponding to a specific treatment. Histogram overlay is one representative for 2 individual experiments each performed in triplicate.

In the same way as for cyclin B1 and Cdc2, activated Cdc25C was investigated using a monoclonal antibody against phosphorylated Cdc25C at Ser198 (Figure 6.11). No significant increase in the levels of phospho-Cdc25C (Ser198) was apparent as no shift to the right of the histogram, i.e. an increase in the mean green fluorescence intensity (FL1), was evident in response to exposure to *A. afra*, isoalantolactone or paclitaxel in both cell lines.

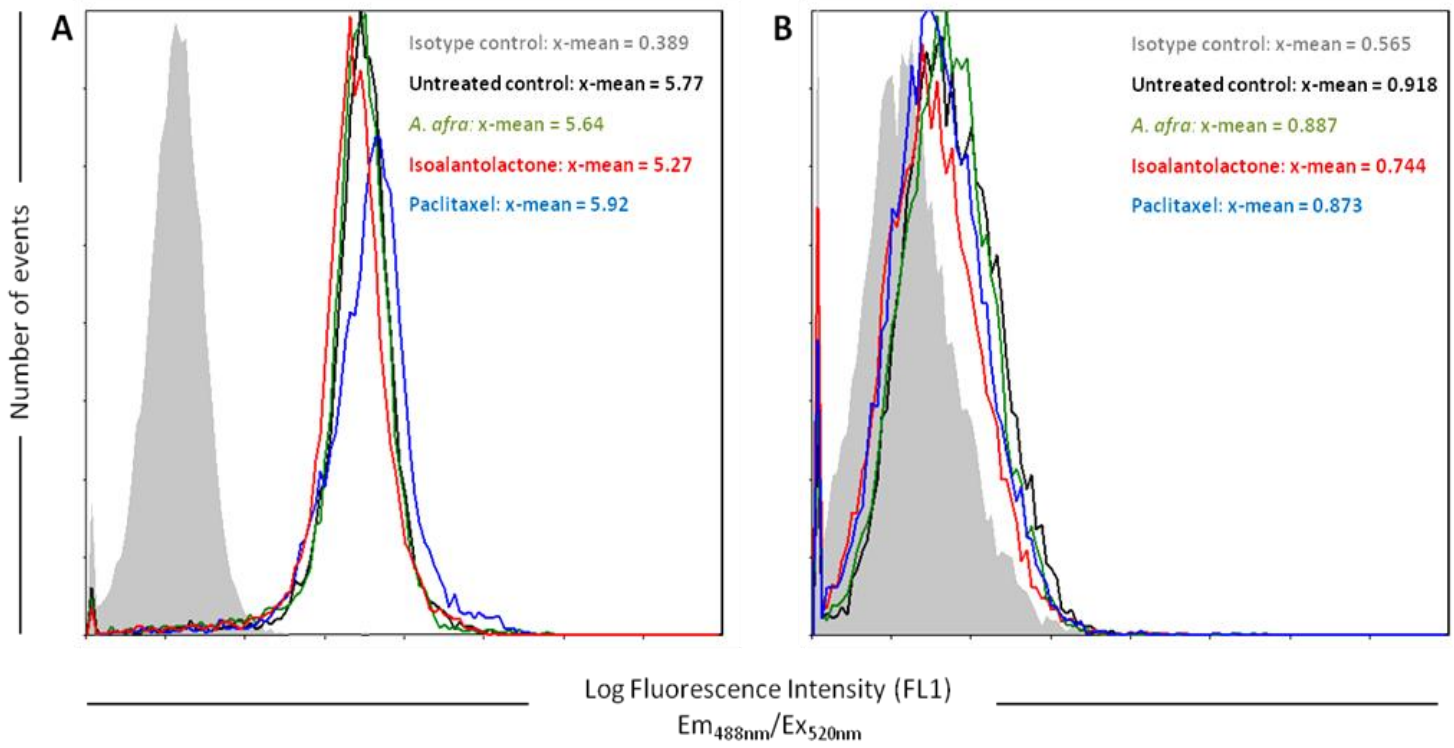

<u>Figure 6.11:</u> Analysis of phospho-Cdc25C (Ser198) after treatment with *A. afra* (green), isoalantolactone (red), and paclitaxel (blue) for 12 hours in HeLa (A) and U937 (B) cells. Insert: The mean fluorescence intensity corresponding to a specific treatment. Histogram overlay is one representative for 2 individual experiments each performed in triplicate.

Figure 6.12 shows a summary of the results obtained for cyclin B1, phospho-Cdc2 and phospho-Cdc25C after 12 hours of exposure to *A. afra*, isoalantolactone or paclitaxel. Changes in mean green fluorescence intensity were expressed as a percentage change of the untreated control.

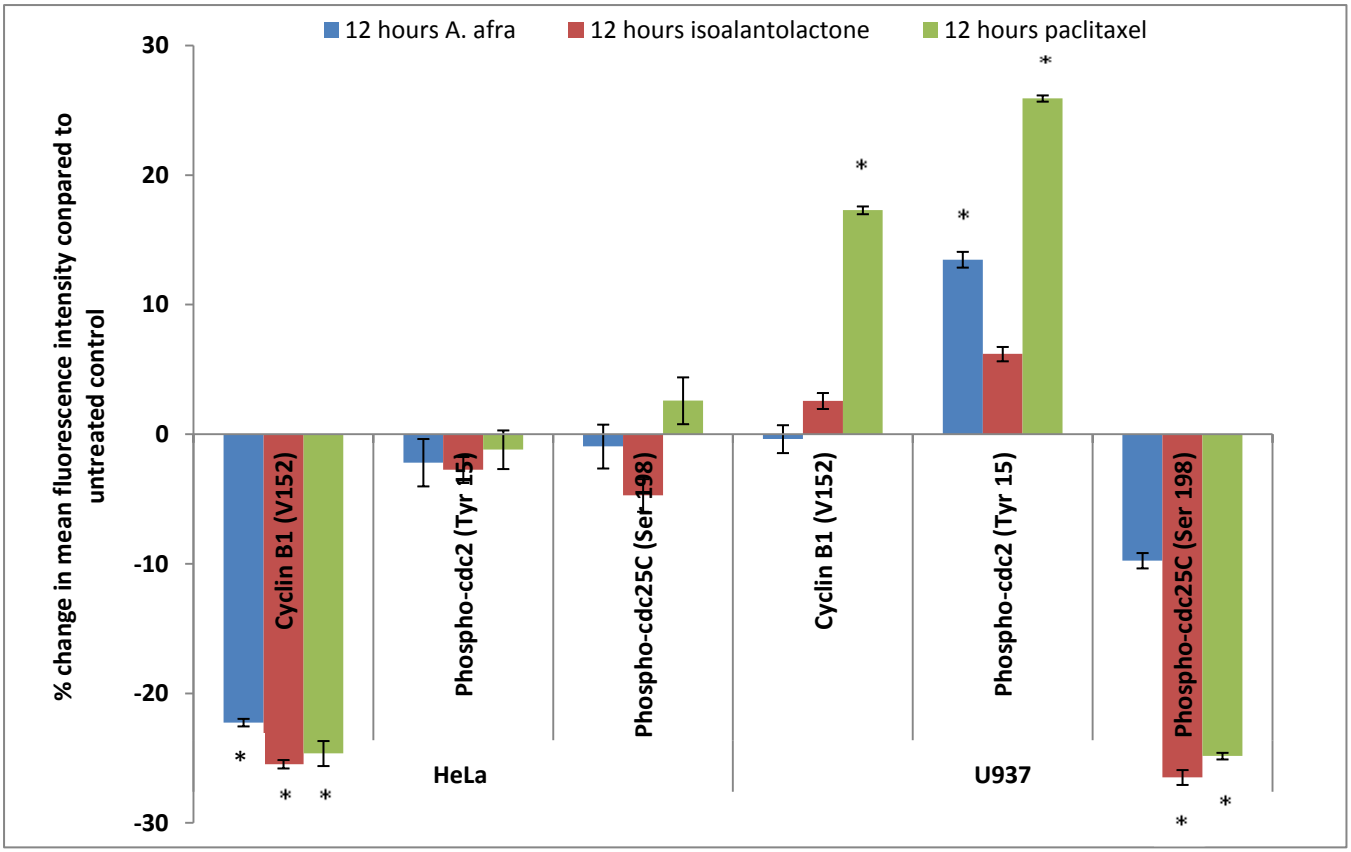

Figure 6.12: Changes in levels of three G2/M checkpoint proteins, cyclin B1, phospho-Cdc2 and phospho-Cdc25C after exposure to *A. afra*, isoalantolactone or paclitaxel for 12 hours. Error bars indicate SD of the mean change in fluorescence intensity. Significance compared to an untreated control was determined using Student *t*-test: *p<0.05.

6.4.3. Phospho-H3 (Ser10) analysis:

Histone 3 protein is phosphorylated at Ser10 and Ser28 during prophase and metaphase, respectively. Phosphorylation of H3 at Ser10 is an early indication of cells progressing through G2 and entering mitosis. An increase in levels of phospho-H3 at Ser10 will correlate to progression into the M phase. Changes in levels of phospho-H3 (Ser10) were detected using immunochemistry and flow cytometry. Overlay plots in Figure 6.13 A and B are representatives of the treatment of HeLa cells with *A. afra* and isoalantolactone, respectively. Cells were treated for 14 hours (blue), 18 hours (green) and 24 hours (red). An increase in the percentage of cells in region A correlates with an increase in the levels of the phosphorylated state of H3 at Ser 10.

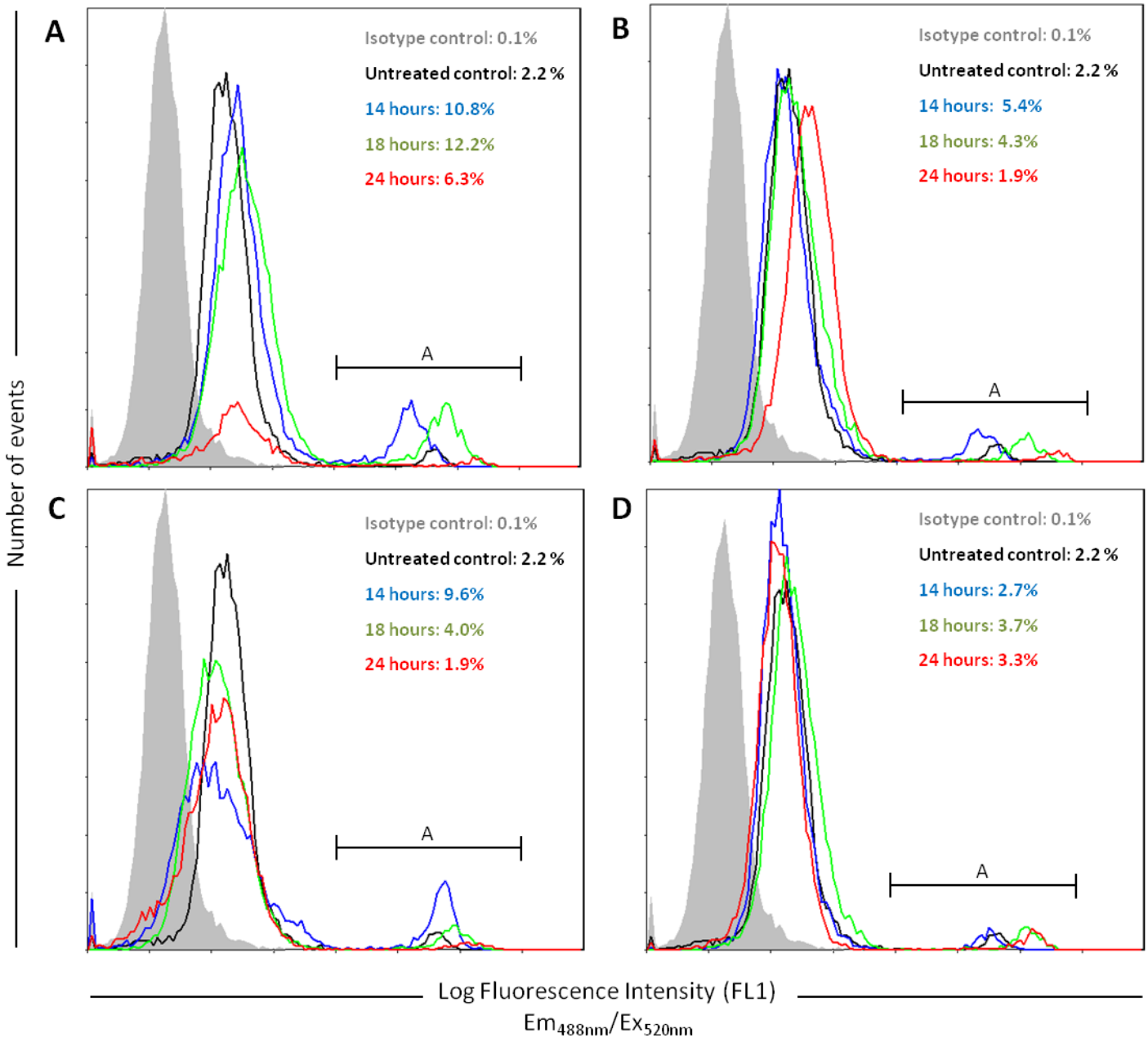

<u>Figure 6.13:</u> Histogram overlays representing phosphorylated H3 (Ser10) of HeLa cells after treatment with A) *Artemisia afra*, B) isoalantolactone, C) paclitaxel and D) colchicine at three different time intervals; 14 hours (blue), 18 hours (green) and 24 hours (red). Insert: Percentage cells stained positive for activated H3 in region A. 10 000 events were recorded per sample. (One representative for duplicate experiments, each performed in triplicate).

Significant changes in the number of cells stained positive for phospho-H3 in HeLa cells after various treatments and time intervals is indicated in Table 6.1. Data is represented as fold increase of HeLa cells positive for activated H3 as a function of an untreated control population.

Table 6.1: Fold increase in percentage of HeLa cells positive for phospho-H3 (Ser10).

Treatment	12 hours	18 hours	24 hours
Untreated control	1.00 ± 0.03	1.00 ± 0.17	1.00 ± 0.09
***A. afra* (30 µg/mL)**	3.56 ± 0.43**	3.01 ± 0.22**	1.87 ± 0.08*
isoalantolactone (8.62 µM)	1.44 ± 0.08*	2.03 ± 0.04*	1.49 ± 0.03*
Paclitaxel (10 nM)	2.78 ± 0.17**	1.41 ± 0.09	1.06 ± 0.06
Colchicine (10 nM)	1.04 ± 0.06	1.20 ± 0.10	1.40 ± 0.09*

Each experiment was carried out in triplicate.

* Significantly higher than control; $p<0.05$

** Significantly higher than control; $p<0.005$: Significance was determined using the two-tailed Student t-test.

6.4.4. Tubulin polymerisation:

The effect of the crude plant extract and the isolated cytotoxic compound on polymerisation of purified porcine tubulin was investigated. Figure 6.14 shows the result of the reaction assay performed. From this figure it is evident that both *A. afra* and isoalantolactone increase the rate of polymerisation. V_{max} was calculated (slope of the curves in Figure 6.14) and is indicated in Table 6.2.

Table 6.2: The effects of different treatments on the rate (V_{max}) of tubulin polymerization.

Treatment	V_{max} (ΔmAbs/min*)
Untreated control	17.0
Paclitaxel	25.0
Colchicine	0.0
A. afra	33.6
isoalantolactone	36.9

* ΔmAbs/min = (ΔAbs/min x 1000)

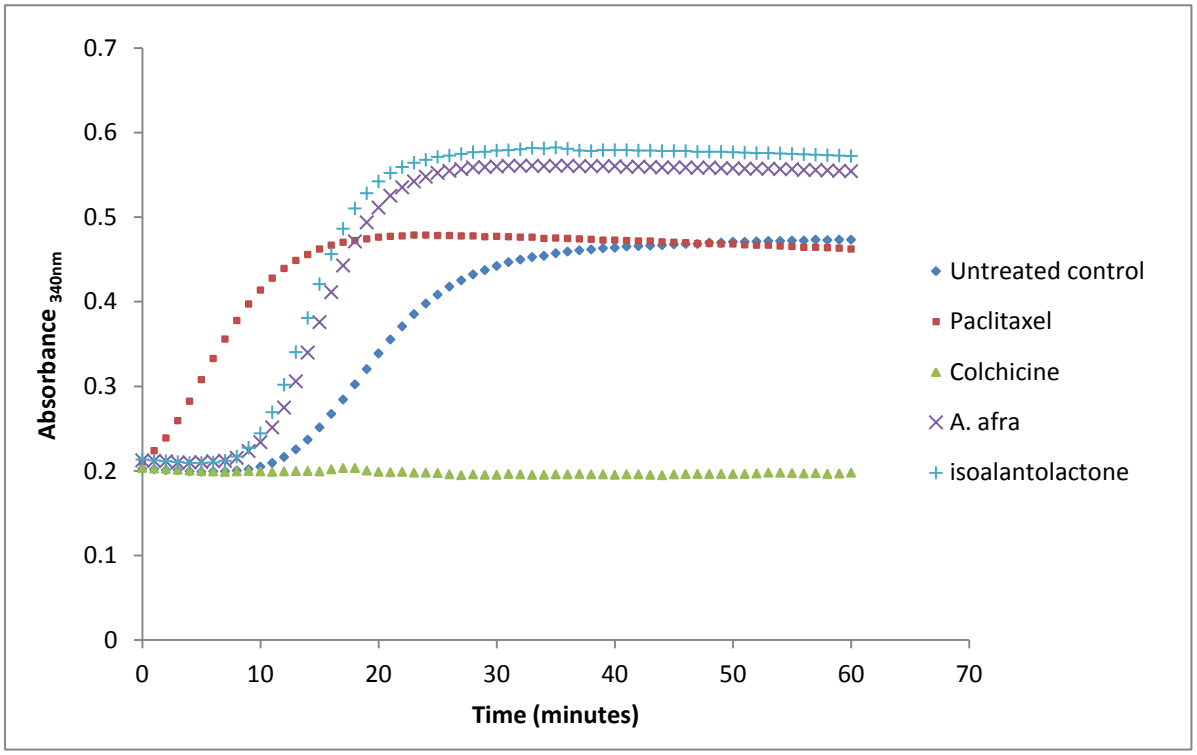

Figure 6.14: The effects of *A. afra* (x) and isoalantolactone (+) on tubulin polymerization. The effects of *A. afra* and isoalantolactone were compared to paclitaxel and colchicine.

6.4.5. Morphological evidence of anti-mitotic potential of *A. afra* and isoalantolactone using confocal microscopy:

Confocal microscopy was performed to observe morphological differences in HeLa cells after exposure to paclitaxel (8 nM), *A. afra* (30 µg/mL) and isoalantolactone (8.62 µM) at three different time intervals, namely 12, 24 and 36 hours. Figure 6.14 shows a wide field view of cells and Figure 6.15 shows individual cells in response to treatments.

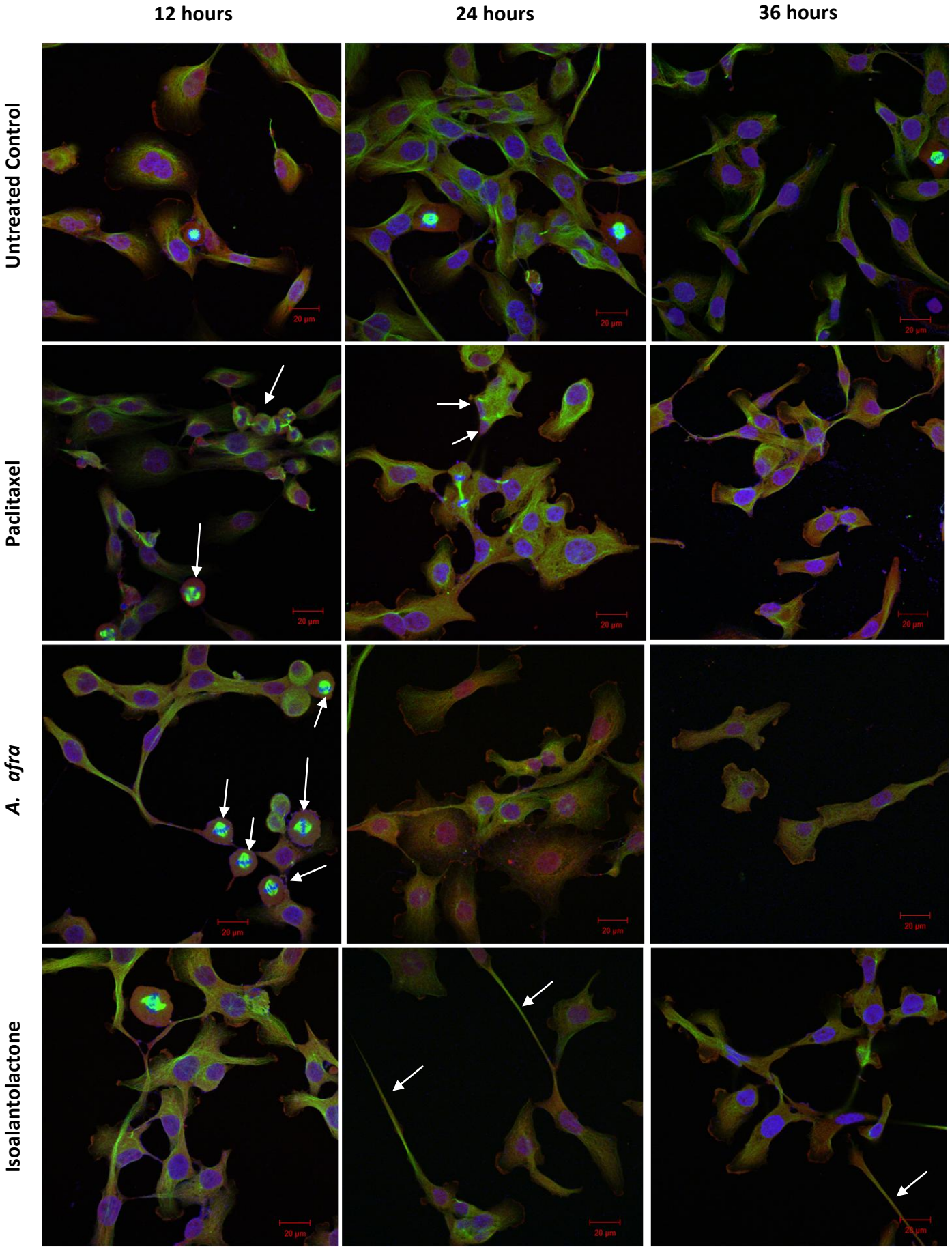

Figure 6.15: **Fluorescence images (63x oil immersion magnification) indicating morphological differences of HeLa cells in the presence of various treatments. White arrows highlight distinct differences in morphology compared to the untreated cells. Scale bar: 20 µm.**

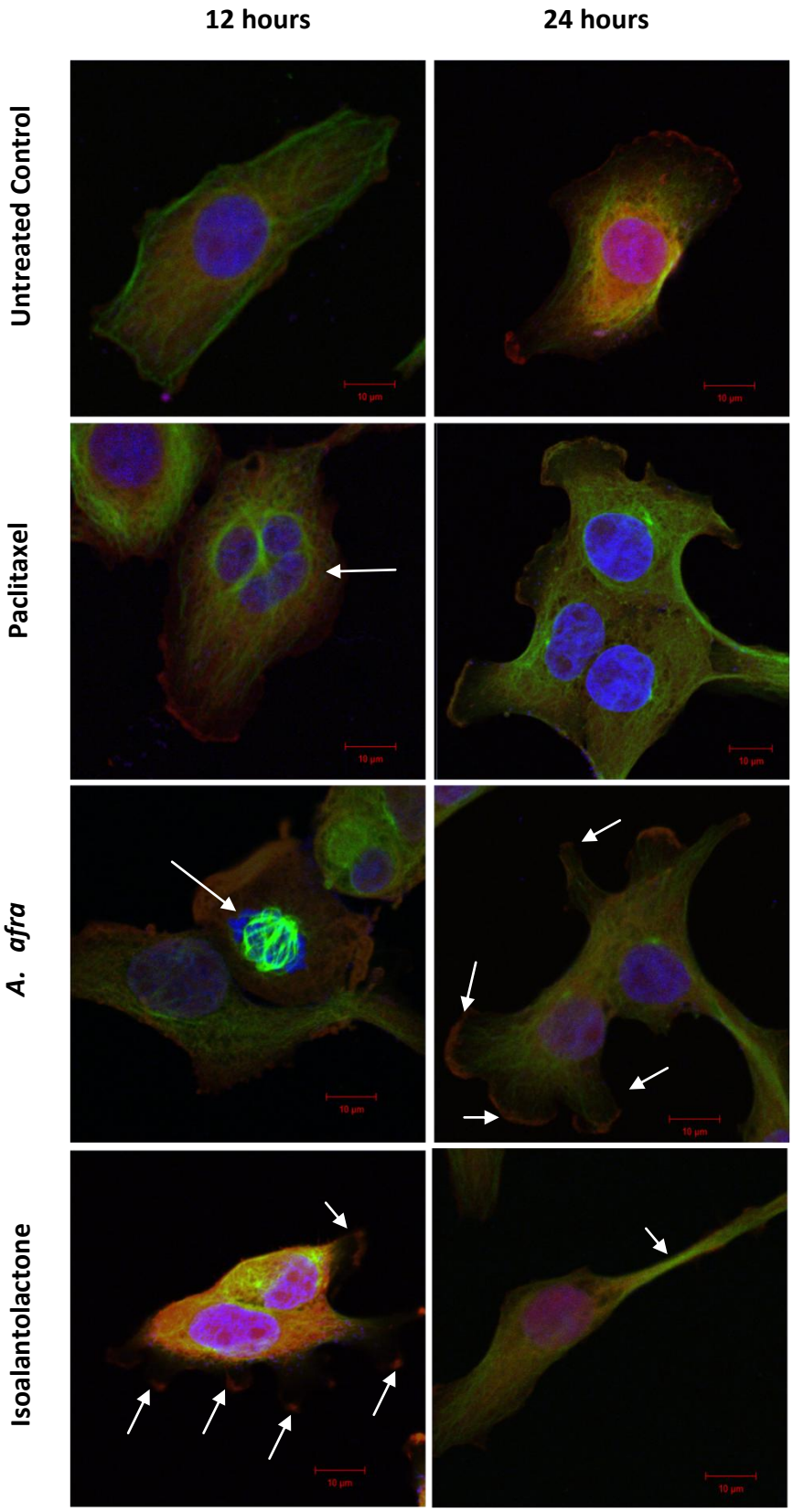

Figure 6.16: **Fluorescence images (63x oil immersion magnification) indicating morphological differences of HeLa cells in the presence of various treatments as indicated (blue, nuclei; green, tubulin; red, actin). White arrows highlight distinct differences in morphology compared to the untreated cells. Scale bar: 10 µm.**

6.5. Discussion and conclusion:

This study was aimed at determining the mode of cell cycle arrest and the onset of mitotic catastrophe resulting in cell death by apoptosis by investigating the enzymes involved in checkpoint regulation at the G2/M progression. These were cyclin B1, Cdc2 and Cdc25C. The state of H3, the histone protein that has been linked to the progression of the cell from the G2 to M phase, was also investigated. This led to an investigation on the effect of *A. afra* and isoalantolactone on the rate of tubulin polymerization using purified porcine brain tubulin. To confirm findings in this study, the morphological changes of HeLa cells treated with *A. afra* and isoalantolactone were investigated using confocal microscopy.

Protein levels of cyclin B1 after treatment with *A. afra* and isoalantolactone were detected using cyclin B1 (V152) monoclonal antibody and flow cytometry. Figure 6.1 shows that during the G2 phase of the cell cycle, the concentration of cyclin B1 increases and peaks in the M phase. Thereafter, the concentration drops drastically as the protein is degraded and is no longer useful until the next G2/M transition (Toettcher *et al.*, 2008). After 12 hours of treatment, a significant decrease in the unbound form of cyclin B1, cyclin B1 (V152), was evident in HeLa cells. This result suggests that after 12 hours of treatment with the extract or the purified compound, cyclin B1 (V152) binds to Cdc2 and can therefore no longer be detected by the antibody. After 24 hours of treatment, an increase in cyclin B1 (V152) was evident. This leads to the assumption of upregulation of cyclin B1; hence the accumulation of this protein as the cell reaches mitosis. The same result was evident for the positive control, paclitaxel. From this evidence, one can rightly assume that the increased cyclin B1 (V152) protein levels provide more substrate to which Cdc2 can bind to form the cyclin B1/Cdc2 complex which then becomes activated after the dephosphorylation of Cdc2 at Thr14 and Tyr15 by Cdc25C.

Detection of levels of cyclin B1 (V152) was also done in U937 cells after treatment for 12 and 24 hours with *A. afra* and isoalantolactone. An increase in protein levels was evident at both 12 and 24 hours. Again, this suggests the upregulation of cyclin B1 (V152) to facilitate progression from G2 to M phase.

The monoclonal antibody phospho-Cdc2 (Tyr15) detects the presence of phosphorylated Cdc2, thus, the inactive enzyme. Phosphorylation of Thr14 and Tyr15 by Wee1/Mik1/Myt1-

related protein kinases renders the complex inactive until Cdc2 is dephosphorylated at these sites (DiPaola, 2002). A decrease was expected after treatment as this would suggest that Cdc2 is dephosphorylated at the Tyr15 site and is rendered active. However, no significant differences in phosphorylated Cdc2 (Tyr15) between the various treatments at 12 hours was evident.

In response to DNA damage, Cdc25C is phosphorylated at Ser216 by Chk 1. This in turn inhibits Cdc25C from dephosphorylating Cdc2 at Thr14 and Tyr15, hence the cyclin B1/Cdc2 complex is inactive and progression from G2 to M is not permitted.During prophase, Cdc25C is phosphorylated at Ser198 by PLK 1 and is translocated to the nucleus where it interacts with Cdc2 and forms the active cyclin B1/Cdc2 complex known as the mitosis-promoting factor (Pestell *et al.,* 1999; DiPaola, 2002). The levels of phospho-Cdc25C (Ser198), the active form of the enzyme, were also investigated. Here, an increase of the active kinase was expected if cells were progressing into the M phase. However, no significant changes in protein levels were evident in both cell lines. Another phosphatase, Cdc25B is also known to dephosphorylate Cdc2 as indicated in Figure 6.2 (Kristjánsdóttir and Rudolph, 2004; Bucher and Britten, 2008). So, although no changes are evident in levels of Cdc25C (Ser198), active Cdc25B may be at work here.

The results of phospho-Cdc2 (Tyr15) and Cdc25C (Ser198) detection are inconclusive. One cannot determine, absolutely, that cells are progressing into the M phase. Because a decrease in these protein levels is not evident, we know that the cells are in the G2 phase of the cell cycle, but upregulation of cyclin B1 suggests passage of cells into the M phase.

At first glance, the results from the investigation of these three proteins would suggest arrest in the G2 phase; however, this is not congruent with the evidence of multinucleation of cells treated with *A. afra*. Thus, for more conclusive results, detection of phospho-H3 (Ser10) levels was done. Phosphorylation of H3 at Ser10 is known as the "phos" switch and is the hallmark of mitosis (Jeong *et al.,* 2010). Histogram overlay plots of Figure 6.13 A and B indicates an increase in levels of phospho-H3 (Ser10) when compared to an untreated control population. This was also true for the positive control, paclitaxel and colchicine after 14 hours of treatment. The greatest increase in phospho-H3 (Ser10) in *A. afra* and isoalantolactone treated cells appears to be after 12 hours of exposure to either plant extract or compound. This result may also indicate that Cdc2 was already active at 12 hours of

treatment. A higher level of phospho-H3 (Ser10) is still evident after 18 hours but drops after 24 hours. This suggests that cells progress into M phase early and thereafter arrest occurs as a consequence of aberrant mitosis. The results of phospho-H3 analysis suggest that Cdc2 may have already been dephosphorylated at the time of measurement which was unable to be detected.

Tubulin is a heterodimeric molecule that polymerises to form microtubules. Microtubules determine the shape of the cell and play important roles in many cellular functions, including cell division. During mitosis, the microtubules become dismantled and form spindles which allow for the separation of chromosomes and the formation of daughter cells (Nelson and Cox, 2005). Anti-mitotic agents can either disrupt tubulin polymerisation completely which results in the inhibition of microtubes or they can cause hyperpolymerisation and stabilisation of the microtubules. Paclitaxel is an anti-mitotic drug that disrupts spindle formation by interacting with the β-subunits of tubulin (Gallager, 2007). When cancer cells are treated with paclitaxel, G2/M arrest is evident and the formation of multinucleated cells is common. In our study, evidence of G2/M arrest as well as multinucleation after treatment with *A. afra* led to the investigation of anti-mitotic potential and possible onset of mitotic catastrophe. This was done by determining the effect of the plant extract on tubulin polymerisation and the formation of microtubules and mitotic spindles using a porcine tubulin polymerisation assay kit and confocal microscopy, respectively. Because isoalantolactone showed to have similar effects on HeLa cells when compared to *A. afra* treatment, an investigation of isoalantolactone treatment was also performed.

Figure 6.14 shows the effect of the plant extract and the compound on the rate of tubulin polymerisation. From this figure, it is evident that in response to both *A. afra* and isoalantolactone, the rate of tubulin polymerisation increases from 17 mAbs/min to 33.6 and 36.9 mAbs/min, respectively. A small decrease in the time of the nucleation phase is also evident. Upon treatment of tubulin with paclitaxel, the nucleation phase is abolished and an increased rate of polymerisation is evident as expected. Colchicine is also an anti-mitotic agent; however, it acts by inhibition of microtubule formation. This is evident in Figure 6.14 as no polymerisation is seen in the presence of this compound.

Morphological changes are typical of cells progressing through the cell cycle, entering mitosis and undergoing mitotic catastrophe and apoptosis (Cho *et al.*, 1998; King and

Cidlowshi, 2004; Kroemer *et al.*, 2009). During mitosis, the rounding of cells is a typical feature to accommodate microtubule formation and segregation of nuclear matter (Théry and Bornens, 2008). Microtubule formation and chromatin condensation is also evident during mitosis to allow for the formation of new daughter cells. Due to the significant increase in 4N DNA after exposure to *A. afra* and isoalantolactone (Chapter 3 and Chapter 5, respectively), as well as evidence of increased levels of cyclin B1 and phospho-H 3 (Ser10), the progression of cells into the M phase and the anti-mitotic potential of both *A. afra* and isoalantolactone was investigated using confocal microscopy. Paclitaxel was used as a positive control.

Cells were treated with either *A. afra,* isoalantolactone or paclitaxel for 12, 24 and 36 hours. In order to visualize architectural changes of HeLa cells, α-tubulin was detected using an Alexa 488 conjugated antibody, nuclei was stained with DAPI and actin was detected using phalloidin-rhodamine B. After 12 hours of exposure to *A. afra*, rounding of cells and a large increase in the number of mitotic cells is evident by the spindle structures of tubulin in the nucleus preparing to separate chromosomes that have been formed. This is indicated in Figure 6.15 and Figure 6.16 by white arrows. This was also evident after treatment with paclitaxel. Multinucleation, a typical feature after paclitaxel exposure, was clearly evident (Figure 6.16). Multinucleation was also evident in *A. afra* treated cells; however, it was not nearly as abundant as paclitaxel treated cells. In response to isoalantolactone treatment, rounding of cells was not as prominent as with the crude extract, and membrane blebbing, a typical morphological feature of apoptosis was noticed as early as 12 hours (Figure 6.15, white arrows).

After 24 hours of exposure to various treatments, apoptotic features dominated. Membrane blebbing is clearly visible, nuclear condensation is evident as well as tubulin dismantling (by a decrease in tubulin intensity). When comparing cell appearance to the untreated cell population, clear morphological and architectural differences are apparent (Figure 6.15 and 6.16). Cells treated with isoalantolactone showed the formation of long filamentous cellular structures, which was more dominant in comparison to *A. afra* and paclitaxel treated cells. After 36 hours, a decrease in cell numbers was seen in response to treatments, as expected.

In summary, the results presented here indicated that *A. afra* ethanol extract and isoalantolactone cause M phase arrest where disruption of the cell cycle occurs and apoptosis commences. Thus it can be concluded that both the crude extract as well as the purified

compound have anti-mitotic potential, hence causing aberrant mitosis and inducing mitotic catastrophe which results in apoptosis.

CHAPTER 7: Anti-inflammatory activity of *A. afra* and Isoalantolactone.

7.1. Introduction:

Inflammation is defined as the cellular reaction of innate immunity and is described as the cellular response to tissue injury that may be caused by physical or chemical stimuli as well as microorganism invasion. Innate immunity is the first line of defence against infections and injuries (Abbas and Lichtman, 2005). The primary process of inflammation includes the release of molecules known as the mediators of inflammation or proinflammatory agents. Inflammatory mediators are soluble, diffusible molecules that exert their actions at the site of injury. Endogenous mediators include lipid derived autocoids, large and small peptides such as cytokines and bradykinin, respectively, as well as amines such as histamine. The initial response and release of these molecules results in the symptoms of inflammation such as pain, fever, vasodilation and vasoconstriction, chemotaxis, leukocyte adhesion and tissue damage (Guzik *et al.,* 2003; Haworth and Buckley, 2007). Acute inflammation is the initial response to pathogens or injury but it may become systematic (chronic). Chronic inflammation is characterized by an accumulation of immune cells at the site of inflammation and an excess of proinflammatory mediators (Koch *et al.,* 2001; Spite and Serhan, 2010).

Lipid derived mediators are the eicosanoids, namely prostaglandins, thromboxanes and leukotrienes. These molecules are derived from arachidonic acid (AA), which is mobilized from the phospholipids of the cell membrane through the action of phospholipases, particularly type II phospholipases A_2 (PLA_2) and C. AA is then metabolized by either cyclooxygenases (COX) to produce prostaglandins (PGs) and thromboxanes (Tx) or by lipoxygenases to produce leukotrienes (LTs) (Dinarello, 2000; Rocca and FitzGerald, 2002; Haworth and Buckley, 2007). Eicosanoids are produced on demand rather than released from cellular stores. They carry out their action on parent and neighbouring cells and have a very short half-life. The biosynthesis of PGs and TXA_2 is shown in Figure 7.1. Their production is dependent on the activity of cyclooxygenases (COXs). These are bifunctional enzymes that contain both COX and peroxidase activity (Ricciotti and FitzGerald, 2011).

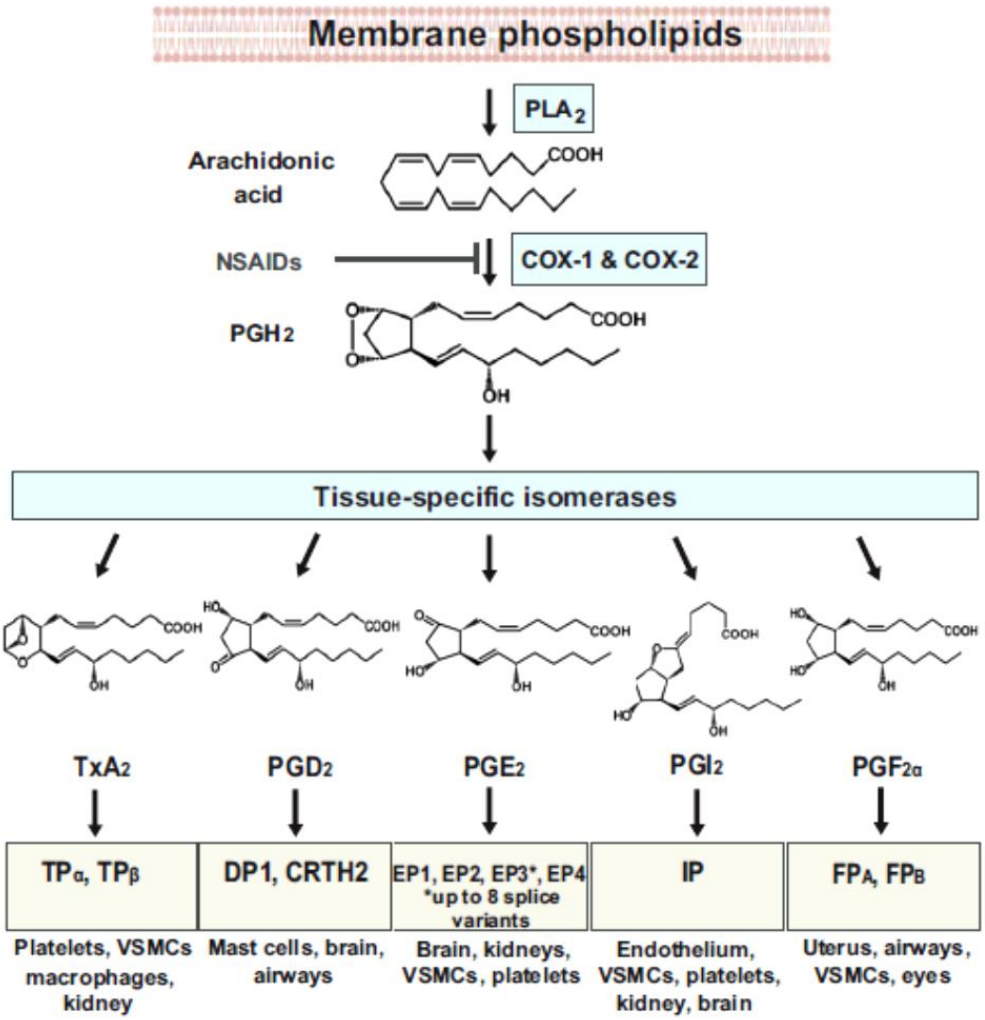

Figure 7.1. The biosynthetic pathway of PGs and Tx indicating the inhibitory activity of non-steroidal anti-inflammatory drugs on COXs (Ricciotti and FitzGerald, 2011).

Leukotrienes are produced by leukocytes, mast cells and macrophages by the oxidation of AA by a lipoxygenase (5-LO) in the presence of 5-lipoxygenase activating protein (FLAP) to 5-hydroperoxy-6,8,11,14-eicosatetraenoic acid (HPETE) and LTA_4 (Hammarström, 1983; Peters-Golden *et al.*, 2005). LTB_4 and LTC_4 are formed by the hydrolysis and conjugation of reduced glutathione, respectively. LTC_4 acts as the parent compound of cysteinyl LTs, known as LTD_4 and LTE_4 which are important in anaphylaxis and asthma (Peters-Golden *et al.*, 2005). LTs have a direct effect on chemotaxis and chemokinesis, by recruiting leukocytes to the site of inflammation. They are also responsible for enhanced phagocytosis and for increasing nitric oxide (NO) and reactive oxygen species (ROS). They are also partly responsible for the generation of other inflammatory mediators. The metabolites of 5-LO

promote the innate immunity responses by stimulating the amplification of cytokines (TNF-α, IL-8) and chemokines (MCP-1) (Peters-Golden *et al.*, 2005).

Histamine is one of the most important mediators of inflammation. It exerts its action by binding to its receptors (H1-H4) and causes vasodilation and increased vascular permeability as well as chemotaxis (MacGlashan, 2003).

Cytokines are inflammatory and immunomodulating proteins that are synthesized when the cell is stimulated in response to stress. They can be synthesized by almost every cell (Dinarello, 2000). The effect of any cytokine depends on the time of release, the local environment in which it acts, the presence of other molecules, availability of its receptors and tissue responsiveness (Abbas and Lichtman, 2005; Opal and DePalo, 2000). Proinflammatory cytokines include IL-1α/β, possibly IL-6, IL-12, TNF-α and IFN-γ and promote inflammation by upregulating gene expression for PLA_2 and COX as well as inducible NO synthase. IL-6 and -8 serve as secondary proinflammatory cytokines (Opal and DePalo, 2000).

Anti-inflammatory cytokines include IL-4, possibly IL-6, IL-10, IL-11, IL-13, TGF-β and cytokine inhibitors. These molecules exert their effect by downregulating the inflammatory response by the inhibition of synthesis of IL-1, TNF and other major proinflammatory cytokines (Opal and DePalo, 2000). The balance between pro- and anti-inflammatory cytokines is important in the onset and prevention of inflammation.

7.1.1. Inflammation and Cancer:

In 1863, Rudolf Virchow observed Leukocytes in neoplastic tissues and made the connection between cancer and inflammation. He suggested that the "lymphoreticular infiltrate" reflected the origin of cancer at sites of chronic inflammation (Balkwill and Mantovani, 2001). It is now well established with clinical and epidemiological studies that there is a strong association between chronic infection, inflammation and cancer (Lin and Karin, 2007). Conditions associated with chronic irritation of an organ such as cigarette smoke and asbestos to lungs, or alcohol abuse to the liver and pancreas, leads to inflammation at these sites and may ultimately lead to cancer of these organs. Chronic infections of microbes cause chronic inflammation and this may lead to cancer too (Rakoff-Nahoum, 2006, Lin and Karin, 2007).

Tumour-associated macrophages (TAMs) and T cells are the prominent leukocytes present in a tumour. Infiltrating immune cells in the microenvironment of the tumour can either promote tumour growth or exert anti-tumour effects. If chronic inflammation develops due to the overexposure of proinflammatory cytokines, it leads to the eradication of anti-tumour immunity and this enhances the growth of the tumour. This is illustrated in Figure 7.2 (Lin and Karin, 2007). The inflammatory cytokine network influences the survival, growth mutation, proliferation, differentiation and movement of tumour cells (Balkwill and Mantovani, 2001).

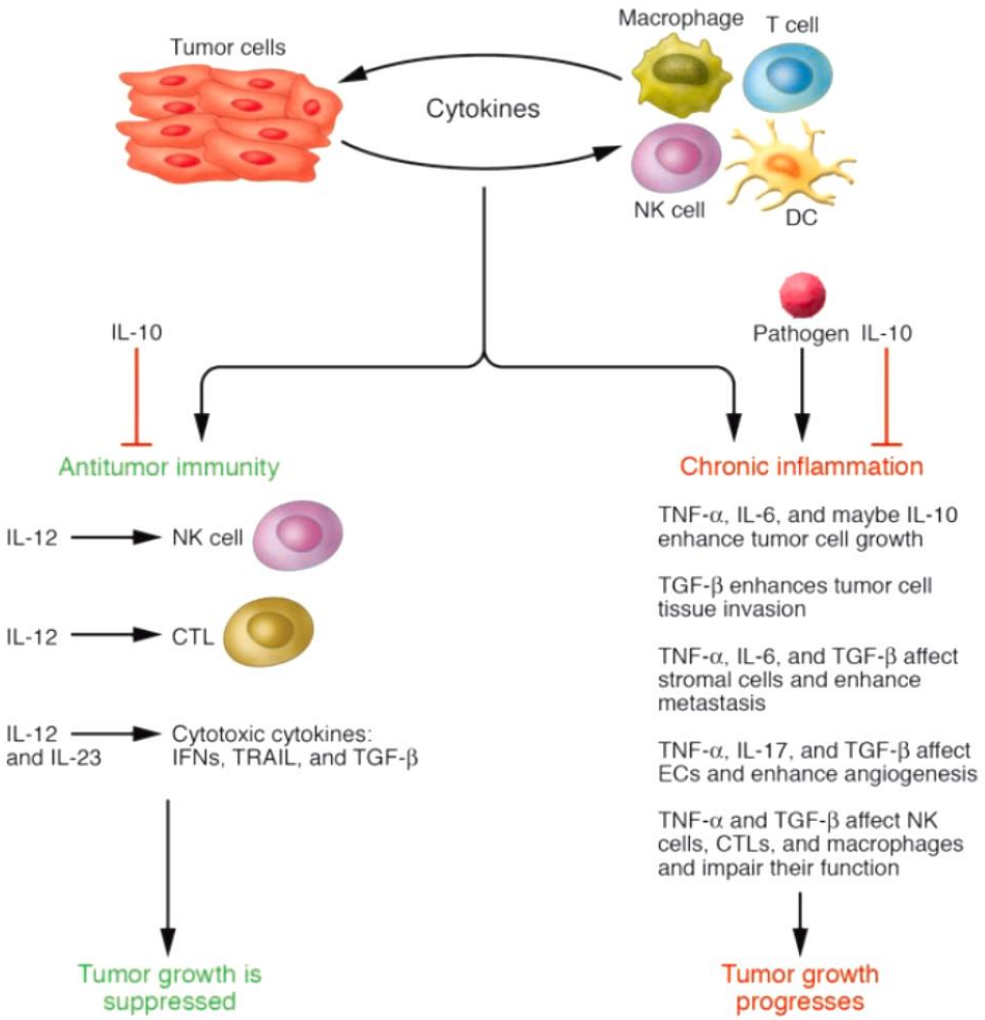

Figure 7.2. The interaction between tumour cells and inflammatory cytokines and immune cells which may enhance tumour growth by stimulating chronic inflammation or suppress tumour growth by directing anti-tumour activity in the microenvironment of the tumour cells (Lin and Karin, 2007).

An important molecular link between inflammation and cancer is the transcription factor, nuclear factor-κB (NF-κB) signalling pathway which is activated by proinflammatory cytokines. The identification of NF-κB as a key modulator is by way of its gene products, including TNF, IL-1, IL-6, chemokines, COX-2, 5-LO, matrix metalloproteases (MMPs) and vascular endothelial growth factors (VEGF) and adhesion molecules (Aggarwal and Gehlot, 2009) and it is also known that in most cancer cells, NF-κB is constitutively active and resides in the nucleus, thus maintaining a state of inflammation which has many benefits for cancer cells (Ravi and Bedi, 2004).

NF-κB promotes the expression of a diverse range of target genes (Lin and Karin, 2003; Ravi and Bedi, 2004; Lin and Karin, 2007; Aggarwal and Gehlot, 2009). These effects are illustrated in Figure 7.3 and are listed below:

- Suppression of tumour cell death by regulating apoptosis by enhancing the expression of most anti-apoptotic proteins that are implicated in the survival of tumours. These include bcl-1, bcl-xl, c-FLIP, the inhibitors of apoptosis (IAP) XIAP, IAP-1 and -2, TNF receptor associated factor 1 and 2 (TRAF1 and TRAF2) and survivin.
- Stimulation of tumour cell cycle progression and proliferation by regulating the gene expression of c-myc, cyclin D1 and COX-2.
- Enhancement of epithelial-to-mesenchymal transition for tumour invasion
- Provides inflammatory environment for the progression, invasion, angiogenesis and metastasis of cancer cells by controlling gene expression of adhesion molecules, MMPs and VEGFs.
- Transformation of cells and survival of cancer stem cells.

It has also been shown that NF-κB is activated in response to tobacco, stress, dietary agents, obesity, alcohol, infectious agents, irradiation and environmental stimuli.

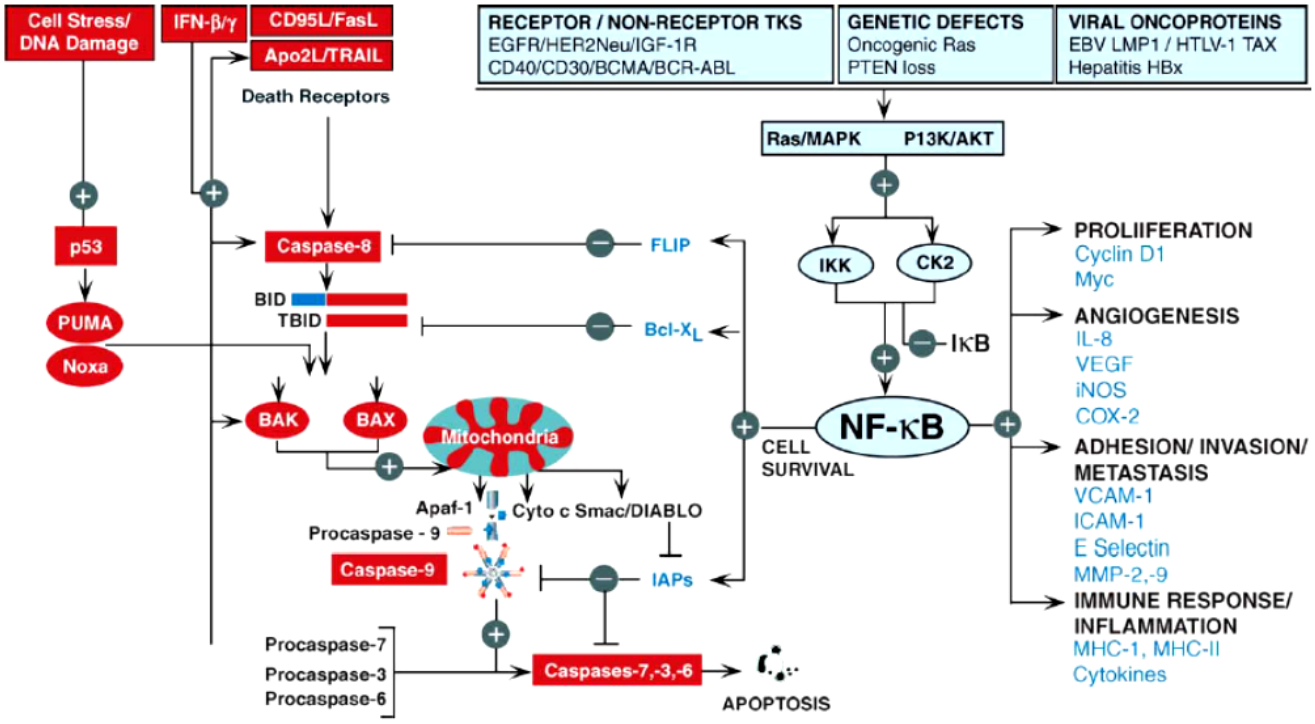

Figure 7.3. Molecular targets of NF-κB and its function in cancer (Ravi and Bedi, 2004).

7.1.2. Reported anti-inflammatory activity of *A. afra*:

No reported evidence of the *in vitro* anti-inflammatory activity of *A. afra* has been reported, although it is used for various respiratory conditions directly linked to inflammatory ailments (Chapter 1 and 2).

7.1.3. Reported anti-inflammatory activity of SLs:

SLs are known to have anti-inflammatory effects and have been suggested as promising lead compounds in the treatment of chronic inflammation. It has been shown that SLs interfere with several inflammatory processes. SLs inhibit DNA binding of NF-κB by alkylating cysteine residues in the DNA binding domain of the p65 subunit (Rüngeler *et al.*, 1999; Koch *et al.*, 2001). Because NF-κB regulates the expression of proinflammatory mediators, the inhibition of the activation of NF-κB is one of the main mechanisms of action of SLs for their anti-inflammatory and cytotoxic activities (Gertsch *et al.*, 2003).

The anti-inflammatory activity of alantolactone, the compound from which isoalantolactone is derived, has been reported (Chun *et al.*, 2012). Their study concluded that NO and PGE_2 levels were reduced due to the down-regulation of iNOS and COX-2 gene expression by treatment of RAW 264.7 cells with relatively low concentrations of alantolactone (1.25 – 10 μM range). It was found that inhibition of the expression of these enzymes was related to the inhibition of NF-κB, MAPK and AP-1 transcription factors via the MyD88 pathway. Isohelenin, a synonym for isoalantolactone, has shown to be a potent inhibitor of NF-κB at a low concentration of 5 μM (Bork *et al.*, 1997). In the same study by Bork *et al.* (1997), it was shown that isohelenin prevents the expression of inflammatory target genes of NF-κB and does not influence DNA-binding of the inducible transcription factor AP-1. Hehner *et al.* (1998) showed that isohelenin prevents the induced degradation of inhibitory proteins IκBα and IκBβ therefore interfering with the signalling cascade leading to the activation of NF-κB.

7.1.4. Aims:

As stated in 7.1.3, the anti-inflammatory activity of *A. afra* has hitherto not been reported and because SLs are known to exhibit anti-inflammatory activity and are major secondary metabolites of *A. afra*, this study sought to investigate the anti-inflammatory mechanism of *A. afra* as well as isoalantolactone. An investigation of NO production, COX-2 levels and active NF-κB in response to treatment of mouse macrophages (RAW 264.7) with *A. afra* crude extract and isoalantolatone was performed using the Griess reaction and immunochemistry, respectively.

7.2. Materials:

RAW 264.7 mouse macrophages were purchased from Highveld Biological (South Africa). Phospho-NF-κB p65 (Ser 536) (93H1) rabbit mAb, Cox2 (D5H5) XP Rabbit mAb, anti-rabbit IgG F(ab')2 fragment (Alexa fluor 488 conjugate) and rabbit IgG isotype controls (Alexa Fluor 488 conjugate) were all purchased from Cell Signaling Technology, Inc. (Danvers, MA, USA). Lipopolysaccharide (LPS) and Griess reagent were purchased from Sigma-Aldrich (St. Louise, MO, USA).

7.3. Methods:

7.3.1. Cell line maintenance:

The cell line selected for the study of the anti-inflammatory activity of *A. afra* and isoalantolactone were murine macrophages, RAW 264.7. RAW 264.7 were routinely maintained in 10 cm culture dishes in DMEM cell culture medium with 10% foetal bovine serum (FBS) (ThermoScientific, Logan, Utah, USA) in a humidified 5% CO_2 incubator at 37 ºC. No antibiotics were added to the medium.

7.3.2. IC_{50} determination of *A. afra* ethanol extract and isoalantolactone against RAW 264.7 cells:

Cytotoxicity of *A. afra* and isoalantolactone against RAW 264.7 cells was determined using the MTT assay. RAW 264.7 cells were seeded at 1 x 10^4 cells/mL in 200 µL aliquots in a 96 well plate. Cells were left overnight at 37°C. Cells were then treated with various concentrations of extract and compound independently. The respective concentration ranges were 3.9 – 250 µg/mL and 0.39 – 25 µg/mL. Cells were incubated for 24 hours. Medium containing the treatments was removed and fresh complete medium containing 0.5 mg/mL MTT was added to each well and further incubated for 3 hours. Thereafter, the blue formazan crystals were solubilised in DMSO and the absorbance was read at 540 nm. Dose response curves were plotted and IC_{50} values were determined using GraphPad Prism 4.0.

7.3.3. Production of nitric oxide (NO):

7.3.3.1. Background:

NO and reactive oxygen species (ROS) exert many effects on inflammation and play a key role in the regulation of the immune response. NO is formed when L-arginine is catalytically oxidized to L-citrulline by NOS. NO is constitutively produced by NO synthases (NOS) of the endothelium (eNOS) and neurons (nNOS) and in low concentrations, it inhibits expression of adhesion molecules, synthesis of cytokines and chemokines, leukocyte adhesion and transmigration. The molecular mechanisms involved in the physiological and pathophysiological functions of NO are directly associated with NO formed by eNOS and

nNOS (Guzik *et al.*, 2003). NO is rapidly oxidized to more active radicals such as peroxinitrite ($ONOO^-$) and nitrogen dioxide (N_2O_2) (Guzik *et al.*, 2003; Miller and Grisham, 1995).

Large amounts of NO is generally produced by inducible NO synthase (iNOS) and this can be toxic and proinflammatory. The activity of iNOS is regulated at the transcription level by NF-κB. Glucocorticosteroids and certain cytokines inhibit iNOS expression through the inhibition of NF-κB activation. The effects and actions of NO are not dependent only on its production by iNOS, but more importantly, on its concentration and the distance from the source and on the initial priming of immune cells (Guzik *et al.*, 2003).

NO has anti- and pro-apoptotic functions. The pro-apoptotic effects include:

- Loss of mitochondrial membrane potential and the increase of cyt-*c* release.
- Inducing p53 expression and accumulation.
- Activating members of the MAPK pathway leading to caspase -3 activation.

There are a number of ways to measure the levels of NO and its metabolites in biological samples (Archer, 1993). In this study, investigation of NO formation was done by the measurement of nitrite using the Griess reaction. In this reaction, sulfanilic acid is quantitatively converted to a diazonium salt by reacting with nitrite in an acidic solution. The diazonium salt is then coupled to *N*-(1-naphtyl) ethylenediamine (NED) forming an azo dye that is measured spectrophotometrically at an absorbance of 548 nm. This reaction (Figure 7.4) is known as the Griess diazotization reaction and was first described in 1879 by Peter Griess (Tsikas, 2007).

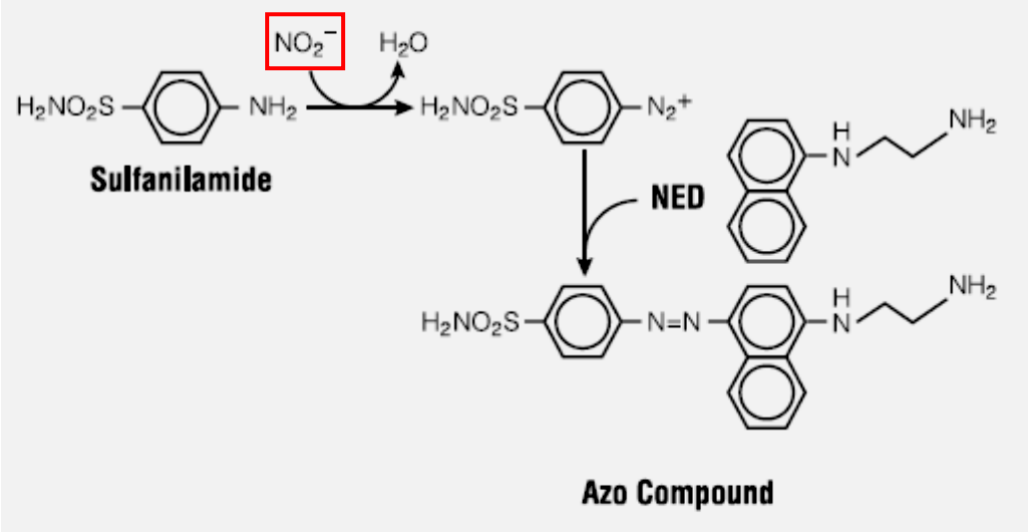

Figure 7.4. The Griess reaction used for the quantification of nitrite intermediates (red box) present in biological samples (adapted from www.promega.com).

7.3.3.2. Measurement of NO formation:

RAW 264.7 were seeded at 1 x 10^5 cells/mL in a 96 well plate in 100 µL aliquots. Cells were incubated at 37°C overnight to allow for attachment. Culture medium was then aspirated and cells were pre-treated for 2 hours with various concentrations of *A. afra* or isoalantolactone using IC_{50}, half IC_{50} and one fifth IC_{50}. Treatment was removed by centrifugation and medium was replaced with complete medium supplemented with LPS (1 µg/mL) for 18 and 36 hours to stimulate cells. After incubation, 100 µL aliquots of supernatant were removed and placed in a new 96-well plate and 100 µL of Griess reagent was added to it. The optical density was measured at 540 nm. A standard curve using sodium nitrate dissolved in medium (0 – 100 µM) was used to determine the concentration of NO in each sample. An MTT assay was performed on the cells to determine cytotoxic effects of the treatments and LPS. This was done by removal of the remaining medium and replacing with 200 µL complete medium containing 0.5 mg/mL MTT and incubated for 3 hours at 37°C. Thereafter the medium was removed and 200 µL DMSO was added to the wells for the solubilisation of the blue formazan crystals. Absorbance was read at 540nm using a BioTek® PowerWave XS spectrophotometer (Winooski, VT, USA).

7.3.4. COX-2 analysis:

7.3.4.1. Background:

COX isozymes catalyse a two-step reaction to form PGs which are then further converted to specific PGs by cell-type specific PG synthases. Collectively, these end products are known as prostanoids. The two isoforms of the enzyme is COX-1 and COX-2. COX-1-dependent production of PGs is thought to serve a number of "housekeeping" functions. It is responsible for the constitutive production of PGs and this is important for maintaining the integrity of the gastric mucosa, mediating normal platelet functions and regulating renal blood flow (Crofford, 1997; Rocca and FitzGerald, 2002). However, COX-1 expression can be regulated during development and by certain hormones and growth factors (Rocca *et al.,* 2002). COX-2 is virtually undetectable under resting conditions and its expression is induced by cytokines, endotoxins, growth factors and tumour promoters. It contributes to the local inflammatory and immunological responses by the production of PGs in response to external stimuli. However, it is constitutively expressed in the brain, reproductive tissues, kidneys and thymus (FitzGerald and Patrono, 2001; Rocca *et al.,* 2002). COX-2 has also been shown to play a role in cell proliferation (Rocca and FitzGerald, 2002).

The overexpression of COX-2 and the abundance of its product PGE_2 have key roles in the development of most cancers. It has been reported that there is a higher concentration of COX-2 in tumour tissue and in culture; growth can be inhibited by the use of COX activity. Overexpression of COX-2 has been implicated in leukaemia, gastrointestinal cancer genitourinary cancer, breast and gynaecological cancers as well as head and neck cancer (Aggarwal and Gehlot, 2009). The overexpression of COX-2 increases the production of PGE_2 and thus, increases the levels of anti-apoptotic proteins such as bcl-2 and reduces levels of the pro-apoptotic protein, Bax (Bakhle, 2001). Inhibitors of COX-2 such as aspirin and non-steroidal anti-inflammatory drugs (NSAIDs) have shown to induce apoptosis, indicating their effects on the enzyme (Gasparini *et al.,* 2003). The mechanism of apoptosis suppression and the increased expression of bcl-2 occurs via the Ras-MAPK/ERK pathway. It has been further shown that apoptosis suppression may be due to a number of different signalling pathways. These include the pro-survival pathways PI3K/AKT pathway, ERK signalling, cyclic adenosine monophosphate (cAMP)/protein kinase A signalling and the activation of epidermal growth factor receptor (EGFR) signalling as well as by indirectly transactivating

the nuclear peroxisome proliferator-activated receptor (PPAR)-δ via a PI3K/AKT dependent mechanism (Greenhough *et al.*, 2009).

7.3.4.2. Detection of change in levels of COX-2 in RAW 624.7 cells:

Detection of COX-2 levels in response to pre-treatment with *A. afra* and isoalantolactone followed by stimulation with LPS was done using flow cytometry. RAW 264.7 cells were seeded at $1x10^5$ cells/mL in 6 well culture plates, using 3 mL per well and left overnight to attach. Cells were then pre-treated with *A. afra* extract (4.4, 10.8 and 21.7 µg/mL) or isoalantolactone (1.25, 3 and 6 µM) for 2 hours and thereafter stimulated with LPS (0.5 µg/mL). Pre-treatment was not removed prior to addition of LPS. After addition of LPS, RAW 264.7 cells were incubated at 37 °C for 18 hours. After treatment, cells were trypsinised and harvested by centrifugation and then fixed and permeabilised using the IntraPrep kit. Cells were washed three times by resuspension in DPBS containing 0.5% BSA and centrifugation at 500 xg for 5 minutes. Cells were then blocked using 0.5% BSA for 10 minutes. COX-2 primary antibody was added to the cells at recommended working dilution (1:200) and incubated for 1 hour at 37°C. After incubation, cells were centrifuged at 500 xg for 5 minutes and thereafter washed as previously described. Conjugated secondary antibody (1:1000), anti-rabbit IgG F(ab') 2 fragment (Alexa fluor 488 conjugate), was added to the cells and incubated for 30 minutes at 37°C in the dark. Cells were washed as previously described to eliminate unbound secondary antibody. Cell samples were analyzed within 30 minutes using flow cytometry (3.3.10) and data was recorded in FL1.

7.3.5. NF-κB analysis:

7.3.5.1. Background:

The activation of NF-κB occurs either via the classical or alternative pathways, which are triggered by proinflammatory cytokines and bacterial and viral infections and TNF family of proteins. The two pathways both lead to the transcription of different genes and thus mediate different immune responses and functions.

The NF-κB family of transcription factors are heterodimeric and belong to a group of proteins known as the Rel proteins. They play an important role in determining the fate of a cell during immune, inflammatory and stress responses (Zhang and Fuller, 1997; Ravi and Bedi, 2004). The family includes 5 members in mammals. These are NF-κB1 (p105/p50), NF-κB2 (p100/p52), Rel A (p65), Rel B and c-Rel. The Rel proteins share a highly conserved N-terminal domain known as the Rel homology domain (RHD) and it is responsible for DNA binding, dimerisation and interaction with inhibitory proteins (IκB).

The precursor proteins p105 and p100 are both proteolytically processed by the proteosome to produce the p50 and p52 mature products, respectively. Rel proteins bind to the mature products and forms dimers that bind DNA. The major NF-κB complex in most cells is the p50/Rel A (p65) heterodimer.

The function of NF-κB dimers is regulated by the NF-κB inhibitory proteins known as the IκBs. These are IκBα, IκBβ, IκBε, IκBγ, bcl-3 and the precursor molecules p105 and p100. When the dimers are bound to IκB, they are sequestered in the cytoplasm. In order for activation of NF-κB to occur, degradation of IκB is required to allow the translocation of NF-κB dimers to the nucleus. In the classic (or canonical) pathway, heterodimers of p50/Rel A (p65) are sequestered in the cytoplasm through their assembly with IκBα. When cells are activated by extracellular stimuli, phosphorylation of two critical serine residues in the N-terminal regulatory domain of IκB (Ser32 and 36 in IκBα and Ser19 and 23 in IκBβ) occurs. This targets it for rapid degradation in an ubiquitin-mediated proteosome process. Phosphorylation is mediated by the IκB kinase (IKK) which is a multi-subunit enzyme consisting of 2 catalytic subunits (IKKα and IKKβ) responsible for phosphorylation and a regulatory subunit known as IKKγ [also known as NEMO (NF-κB essential modifier/modulator) or IKKAP1]. IKK activity is largely dependent on the integrity of IKKγ and IKKβ. The C-terminus of IKKγ serves as a docking site for upstream signals and the N-terminal half binds to IKKβ. This results in the phosphorylation of Ser177 and 181 in the T-loop of the catalytic domain of IKKβ. This pathway is important in innate immunity.

In the alternative (or non-canonical) pathway, NF-κB2p100 is bound to Rel B which renders it inactive. Members of the TNF family such as B-cell activating factor and CD40, selectively activate NF-κB inducing kinase (NIK) and IKKα. This leads to the phosphorylation of NF-κB2p100 and subsequent polyubiquitination and ultimately leads to its degradation by

proteolytic processing. This yields the p52 subunit and allows the release of Rel B. The dimer p52/Rel B is now able to translocate to the nucleus. This pathway plays an important role in adaptive immunity (Chen and Greene, 2004; Ravi and Bedi, 2004; Abbas and Lichtman, 2005; Rangan *et al.*, 2009).

In the nucleus, recruitment and regulation of transcriptional activation by NF-κB is mediated by phosphorylation and acetylation of the Rel subunit of the dimer. Phosphorylation is carried out by protein kinases including PKA, PKC and casein kinase II. Their respective targets are Ser276, Ser311 and Ser529 of p65 (Rel A). PI3-K/Akt and NIK phosphorylate IKK which in turn phosphorylates p65 at Ser536. Acetylation of p65 is mediated by histone acetyltransferases (HATs) p300/CBP and P/CAF, specifically targeting Lys residues 218, 221 and 310. This allows for the activation of target gene transcription. Deacetylation of p65 is mediated by histone deacetylases (e.g. HDAC3) and this in turn promotes the binding of IκBα (Ravi and Bedi, 2004; Mohan, 2012). NF-κB activation pathways are shown in Figure 7.4.

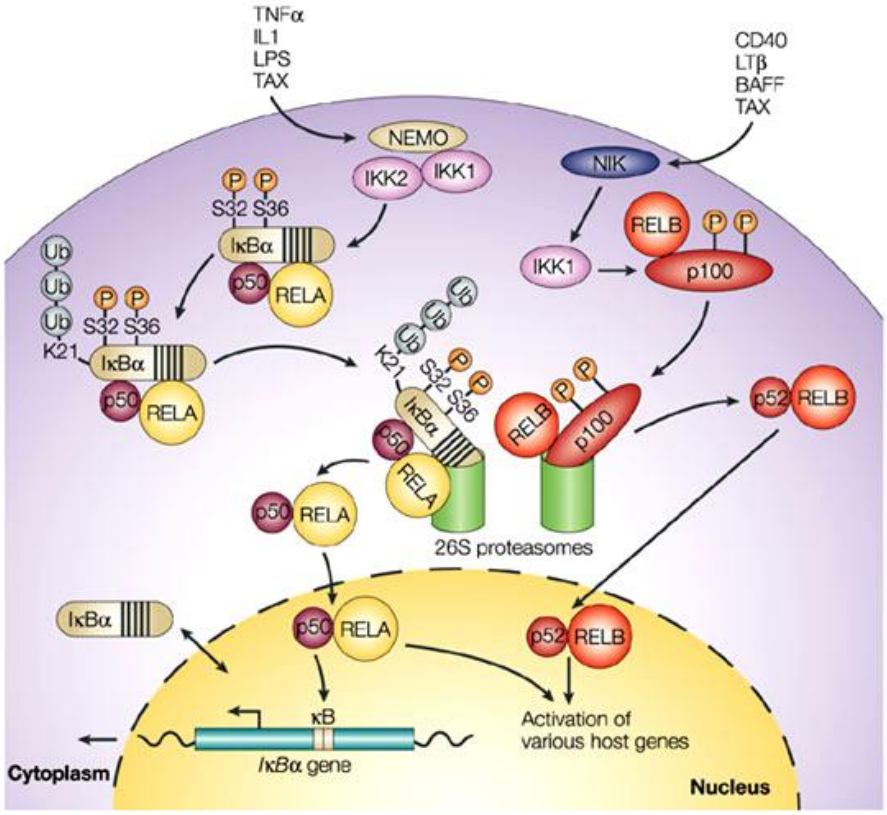

Figure 7.5. The activation pathways leading to NF-κB-dependent transcription of various host genes as described in text (Chen and Greene, 2004).

7.3.5.2. Detection of change in levels of phospho-NF-κB p65 (Ser536) in RAW 624.7 cells:

RAW 264.7 cells were seeded and treated the same way as for the analysis of COX-2 levels (7.3.2.2). Detection of phospho-NF-κB p65 (Ser536) was performed using a monoclonal antibody (1:250) and a conjugated secondary antibody, anti-rabbit IgG F(ab') 2 fragment (Alexa fluor 488 conjugate). Cell samples were analyzed within 30 minutes using flow cytometry (3.3.10) and data was recorded in FL1.

7.3.6. Statistical analysis:

All treatments of RAW 264.7 were conducted in triplicate. Histogram overlays are one representation of each experiment. Standard deviation (SD) was calculated for each experiment independently. For each assay, the Student two-tailed *t*-test was performed to determine significance. $p<0.05$ was considered significant, indicated by *, $p<0.005$ is indicated by **. For all flow cytometry assays, a minimum of 10 000 events were recorded for each sample.

7.4. Results:

7.4.1. IC_{50} determination of *A. afra* ethanol extract and isoalantolactone:

Dose response assays were carried out to determine the IC_{50} concentrations (Figure 7.6). An IC_{50} of 21.70 ± 2.08 µg/mL and 6.23 ± 1.05 µg/mL was achieved for *A. afra* and isoalantolactone. When considering the molecular mass of isoalantolactone, its IC_{50} value is converted to 26.84 µM.

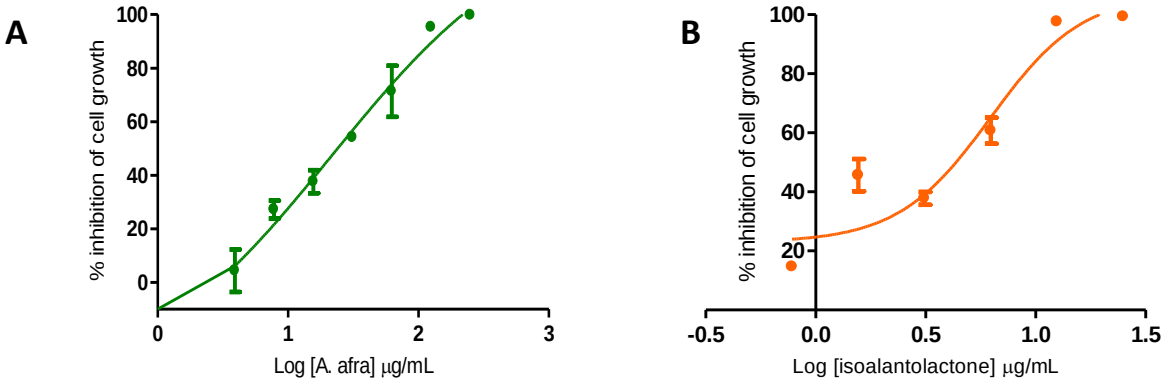

Figure 7.6: Cytotoxic effect of *A. afra* ethanol extract (A) and isoalantolactone (B) against RAW 264.7 mouse macrophages after 24 hours of exposure. Cell viability was determined using the MTT assay. Error bars indicate SD of 3 replicate values.

7.4.2. Measurement of NO formation:

After 18 hours of stimulation, after removal of treatment or in the presence of treatment, the formation of NO and the subsequent decrease in NO species was determined using the Griess method. A standard curve using 1 mM stock $NaNO_2$ was used for concentration calculation (Appendix A, Figure A3).

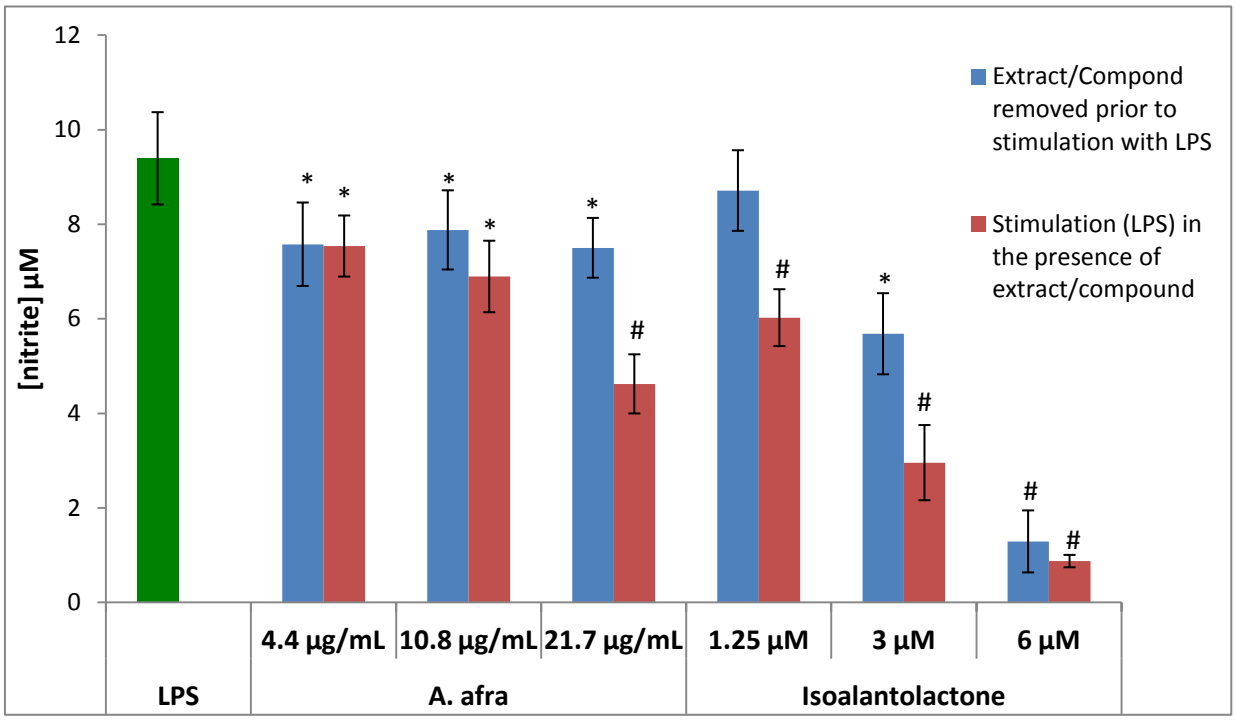

Figure 7.7: The effect of *A. afra* and isoalantolactone on NO production in RAW 264.7 cells. Treatments were carried out in triplicate (n=3), error bars indicate the SD of the mean. Significance was determined using Student *t*-test: *p < 0.05 and #p < 0.005.

An MTT assay was done to determine the viability of the cells after treatment and stimulation. The results showed that all treatments did not significantly affect the viability of the cells (Figure 7.8). Decreases in NO levels in the presence of treatments were therefore not as a result of different cell numbers.

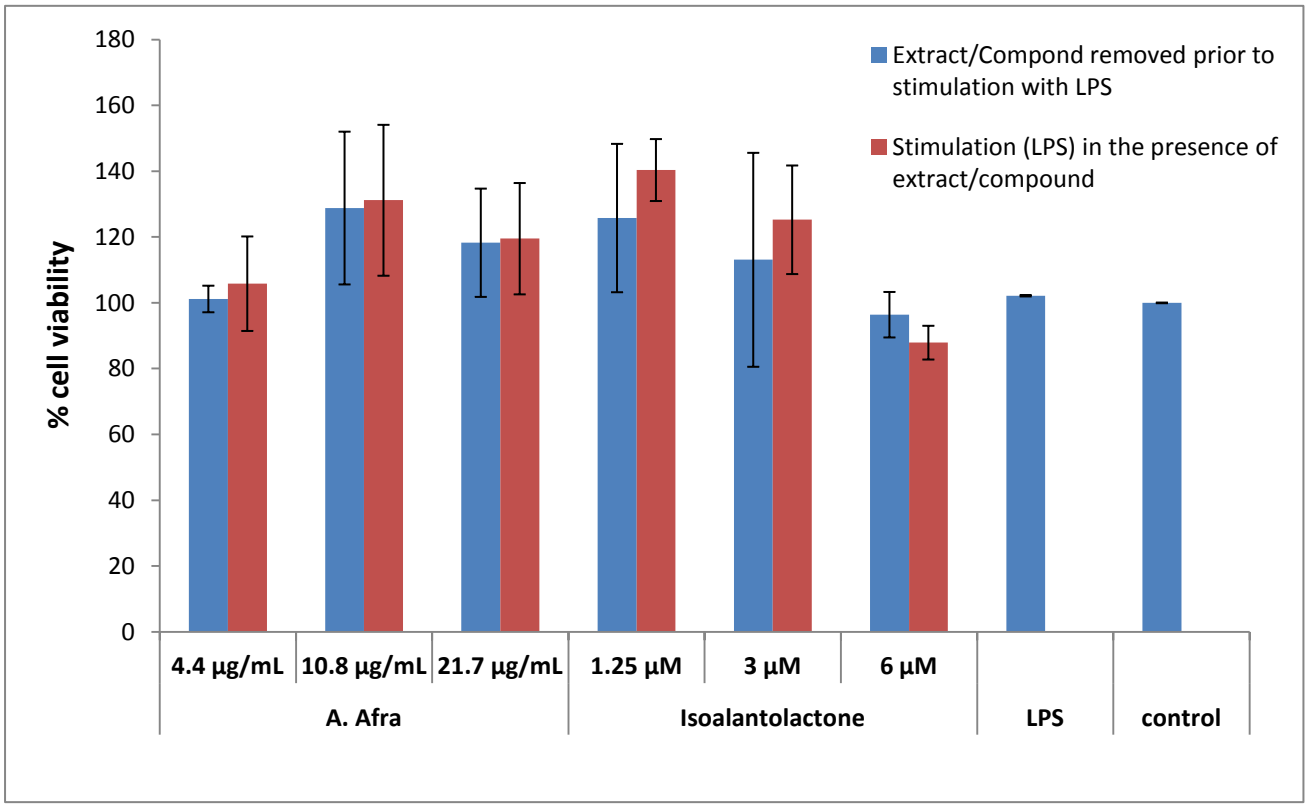

Figure 7.8: Determination of cell viability after NO production analysis. Treatments were performed in triplicate, error bars indicate SD and significant variance was determined using Student *t*-test.

7.4.3. COX-2 analysis:

COX-2 analysis was performed using flow cytometry. Figure 7.9 shows the resultant histogram overlays from the experiment and Figure 7.10 is a summary of the results. A slight, but significant decrease in the percentage cells that stained positive for COX-2 was evident after treatment and stimulation in RAW 264.7 cells. From the histograms it can also be seen that the amount of COX-2 per cell decreased in the presence of extract and isoalantolactone.

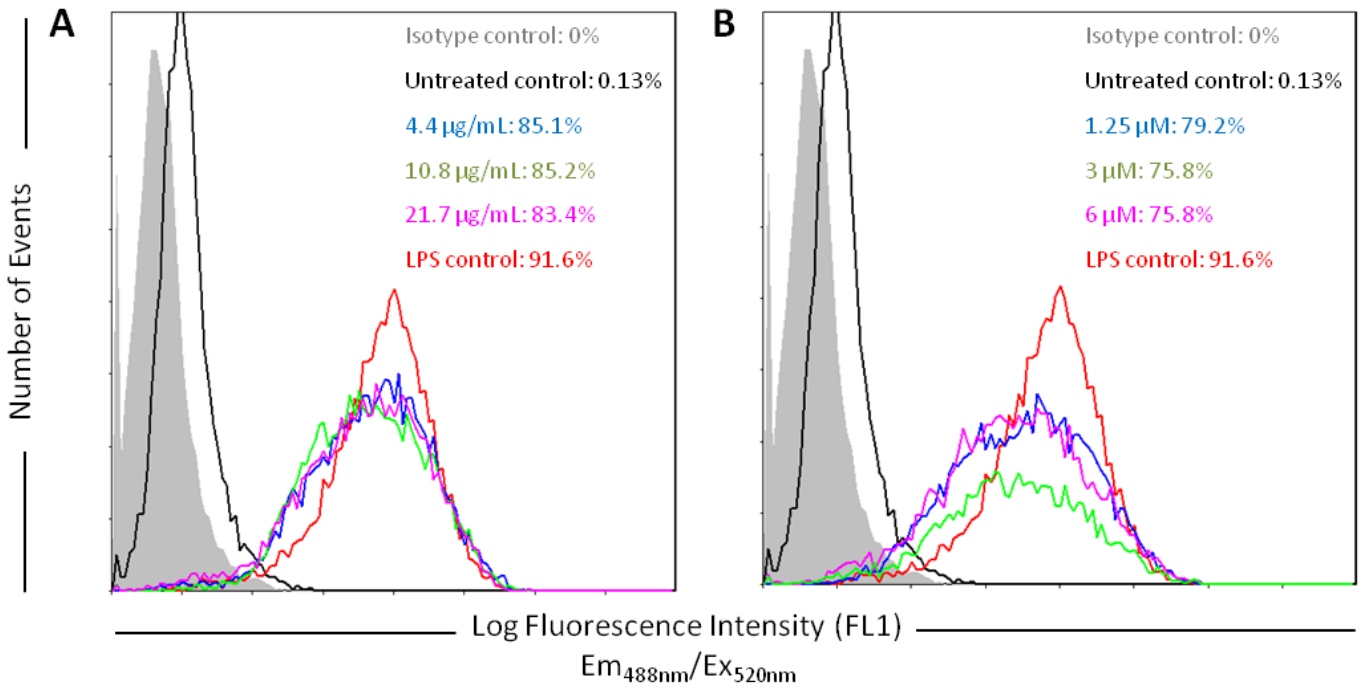

Figure 7.9: **Analysis of COX-2 protein levels after treatment with three different concentrations of *A. afra* (A) and isoalantolactone (B) as indicated. Control cells were not activated with LPS. For all other treatments, cells were pre-exposed to treatments for 2 hours before addition of LPS and further incubation for another 18 hours. Histogram overlay is one representative for an experiment carried out in triplicate.**

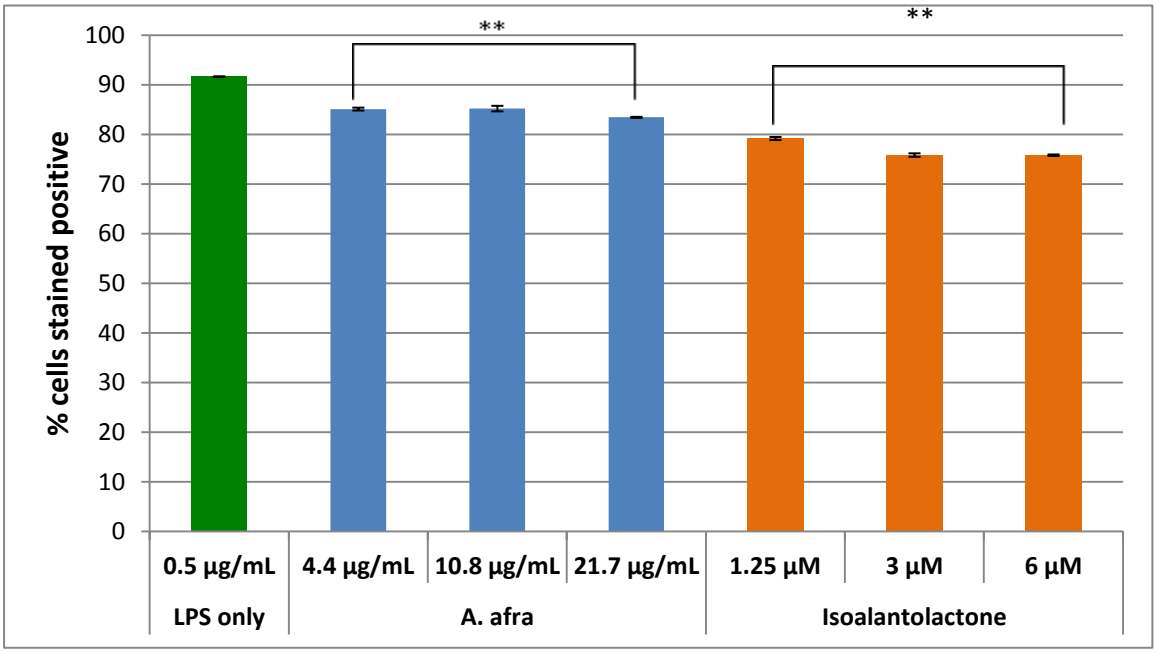

Figure 7.10: **The effect of *A. afra* (blue) and isoalantolactone (orange) on COX-2 protein levels in RAW 264.7 cells. Treatments were carried out in triplicate (n=3), error bars indicate SD of the mean. Significance was determined against LPS only control using the Student *t*-test: **p < 0.005.**

7.4.3. NF-κB analysis:

The effects of *A. afra* and isoalantolactone on the activation of NF-κB when stimulated with LPS were detected using a monoclonal antibody against phosphorylated NF-κB at Ser 536. Figure 7.11 shows the resulting histogram overlay plots of RAW 264.7 cells treated with 3 different concentrations of *A. afra* (A) and isoalantolactone (B). A shift in the histograms at each concentration for both *A. afra* and isoalantolactone indicates changes in levels of NF-κB p65 (Ser536). In Figure 7.11 A and B, increases in FL1 are noticed, however, the presence of increased isoalantolactone concentration results in a decrease in FL1 Figure 7.12 shows a summary of the results.

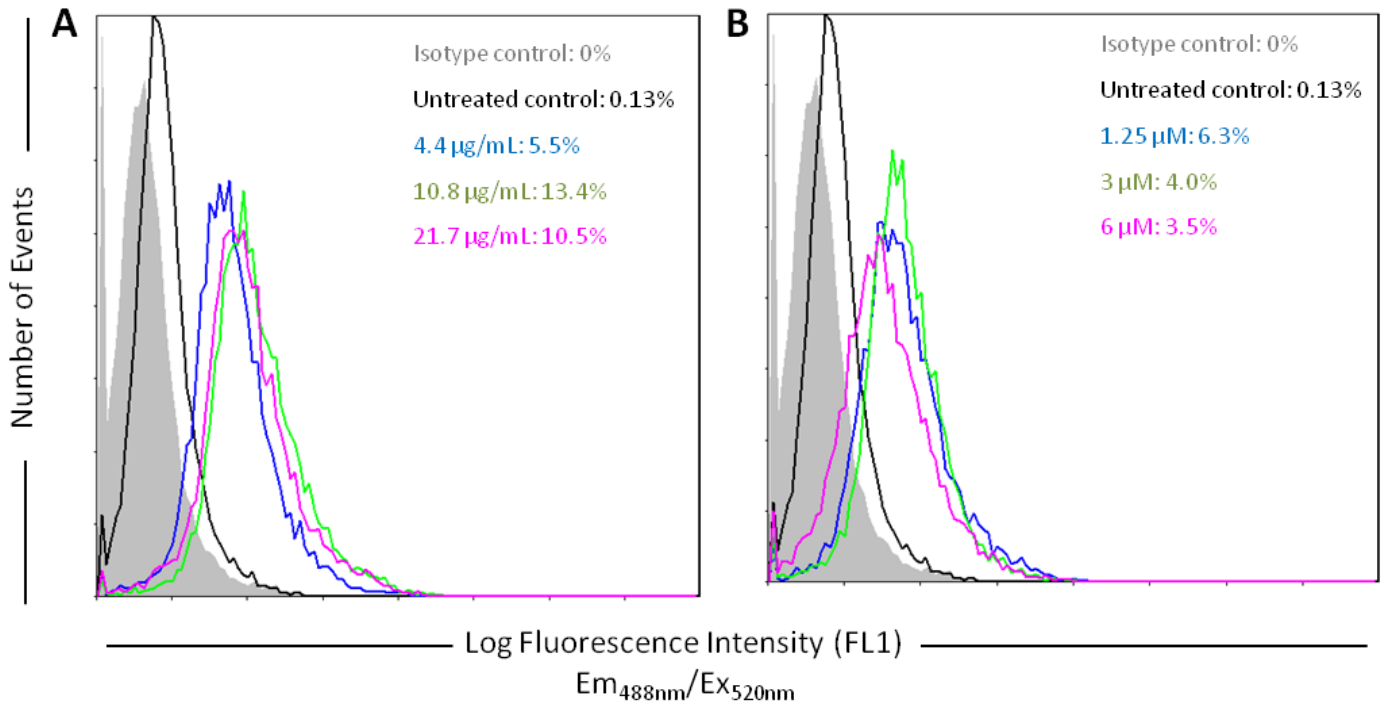

Figure 7.11: Histogram overlays of phospho-NF-κB p65 (Ser536) detected after treatment with *A. afra* (A) and isoalantolactone (B), stimulated using LPS. Control cells were not activated with LPS. For all other treatments, cells were pre-exposed to treatments for 2 hours before addition of LPS and further incubation for another 18 hours. Histogram overlay is one representative for an experiment carried out in triplicate.

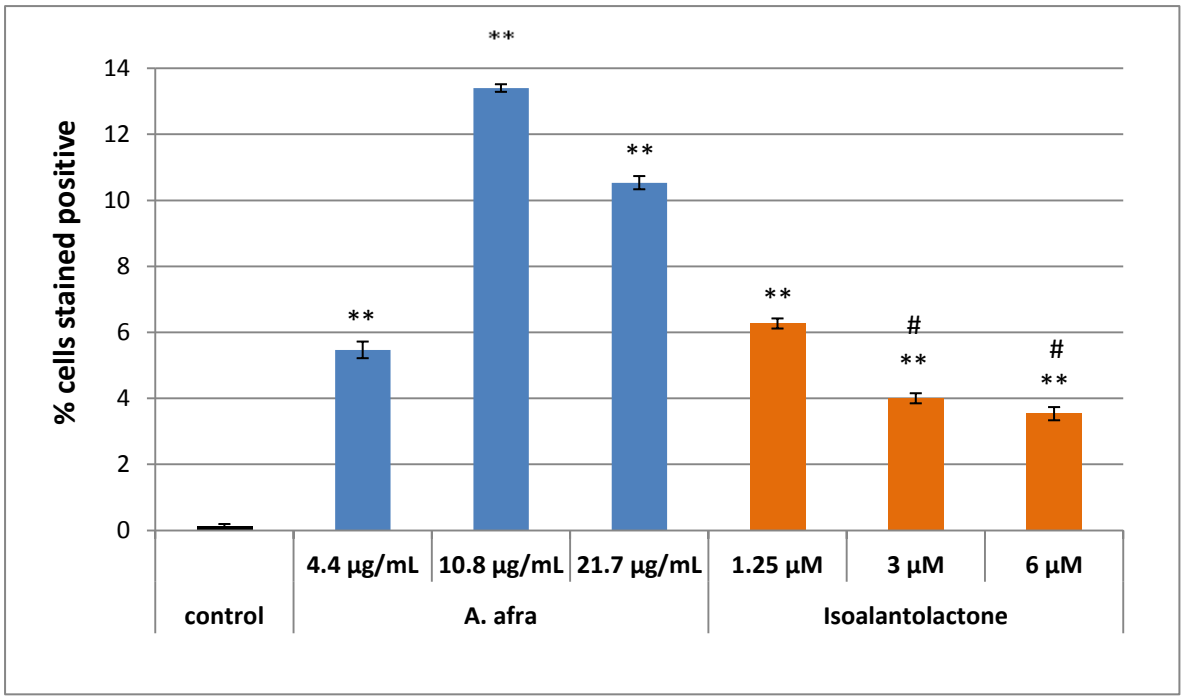

Figure 7.12: The effect of *A. afra* (blue) and isoalantolactone (orange) on phospho-NF-κB (Ser536) protein levels in RAW 264.7 cells. Control cells were not activated with LPS. For all other treatments, cells were pre-exposed to treatments for 2 hours before addition of LPS and further incubation for another 18 hours. Treatments were carried out in triplicate (n=3), error bars indicate SD of the mean. Significance was determined using Student *t*-test: *p < 0.05 and **p < 0.005. # indicates significant decrease (p<0.005) when compared to *A. afra* treatments.

7.5. Discussion and conclusion:

Three bioassays were performed to determine the anti-inflammatory activity of *A. afra* ethanol extract and isoalantolactone. RAW 264.7 murine macrophages were used for this study. Cytotoxicity of *A. afra* and isoalantolactone were determined and dose-response curves were plotted. IC_{50} values of 21.70 µg/mL and 6.23 µM for *A. afra* and isoalantolactone resulted, respectively.

NO formation was detected using the Griess method. Cells were pre-treated for 2 hours with either *A. afra* or isoalantolactone. Thereafter, medium containing plant extract or compound was removed and cells stimulated using 0.5 µg/mL LPS or LPS was added directly to the well containing the treatment. Cells were treated with three concentrations of extract or compound to determine whether the reduction in NO was dose dependent. After 18 hours of

stimulation, significant decreases in the concentration of NO were evident for both treatments in a dose dependent manner. Figure 7.6 indicates that pre-treatment with *A. afra* and the subsequent removal of the extract has a less drastic effect in the decrease of NO and the response in NO formation was not dose-dependent. Decreases from 9.39 μg/mL (LPS control) to 7.58, 7.88 and 7.5 μg/mL in NO for 4.4, 10.8 and 21.7 μg/mL *A. afra* was evident for this experiment. When LPS was added directly to pre-treated cells without the removal of the extract, decreases in NO from 9.39 μg/mL (LPS control) to 7.53, 6.89 and 4.62 μg/mL for the respective concentrations of *A. afra* was evident, indicating that exposure to the plant extract for longer than 2 hours is essential for significantly more drastic decreases in the NO formation. It also showed to be dose-dependent.

Pre-treatment with isoalantolactone and the removal of the compound after 2 hours showed to have the same effect on NO formation as when the compound was not removed from the cells However, with the longer exposure to the compound, formation of NO was significantly less than for cells only treated for 2 hours for 1.25 and 3 μM treatments.

The results of the NO assay indicate that both *A. afra* and isoalantolactone have inhibitory effects on the production of NO. However, pre-treatment with *A. afra* for 2 hours, and its subsequent removal, showed that a longer exposure time to the plant extract is required to have an inhibitory effect. An MTT cytotoxicity assay on cells was done after exposure to extract or compound and LPS to determine the effects of treatment on the viability of the cells and it showed that no cytotoxic effect resulted.

For the detection of changes in levels of COX-2 and phospho-NF-κB p65, cells were pre-treated with *A. afra* or isoalantolactone and LPS was directly added to the cells without the removal of the plant extract or compound.

COX-2 is responsible for the production of prostaglandins and is an important target for anti-inflammatory molecules for this reason. COX-2 expression is inhibited by anti-inflammatory cytokines as well as NSAIDs and thus inhibits the production of PGs (Gasparini *et al.*, 2003). The effect of *A. afra* and isoalantolactone on COX-2 protein levels was determined. A slight but significant decrease in the levels of COX-2 was evident for both plant extract and compound. In this assay, it was seen that COX-2 levels decreased from 91.6% in the LPS control to 85.1, 85.2 and 83.2% for the increasing concentrations of *A. afra.* The percentage

values indicated here suggest that the decrease in COX-2 levels is not dependent on the concentration of the extract. This was also shown in cells treated with isoalantolactone. The decrease in the levels of COX-2 was significantly lower than that of the crude extract, suggesting that pro-inflammatory compounds present in the plant extract contribute to an antagonistic effect thus, a higher percentage of COX-2 positive cells.

Alantolactone, the compound from which isoalantolactone is derived, has shown to inhibit COX-2 expression in a dose-dependent manner using a concentration range from 0.5 μM to 10 μM. This was shown using Western blot analysis and mRNA relative expression after 6 hours of stimulation with LPS (Chun *et al.*, 2012). In the same way, the effects *A. afra* and isoalantolactone can also be determined using expression analysis.

The transcription factor NF-κB is responsible for expression of as much as 150 target genes in response to inflammation, infections and other cellular stresses and thus induces the inflammatory response. The effect of *A. afra* and isoalantolactone on the activation of NF-κB was investigated by detecting the levels of the active p65 subunit. Once p65 is activated by phosphorylation of Ser536, it translocates to the nucleus where it interacts with DNA and permits the transcription of its target genes. In this study, it was shown that the levels of activated NF-κB p65 increased significantly from 4.4 to 10.8 μg/mL. This suggests that at the higher concentration, 10.8 μg/mL, inflammation is stimulated by the extract as LPS concentration remained constant for all treatments. When using 21.7 μg/mL of the ethanol extract, the level of activated NF-κB p65 decreased from 13.4% in 10.8 μg/mL treated cells to 10.5% in 21.7 μg/mL treated cells. This suggests that at the highest concentration of the plant extract, anti-inflammatory compounds within the extract dominate the inflammatory pathway. From the results for *A. afra* it can also be deduced that at the lowest concentration, possible pro-inflammatory compounds are less active than at the higher concentrations of the plant extract as the lowest activated NF-κB p65 levels were detected. Crude plant extracts contain many active compounds that interact with targets differently and the synergy between the compounds play an important role in the outcome of a bioactivity assay. In saying this, a shorter incubation time might have given a more accurate reflection of the inhibition of this pathway as NF-κB is a transcription factor responsible for activation of target genes such as iNOS and COX-2. Transcription of genes is a consequence of the activation of NF-κB and thus, analysis of NO production and levels of COX-2 was conducted after 18 hours of treatment and stimulation. Activation of the signal transduction pathway will occur

immediate in response to stimuli but the effects on iNOS and COX-2 levels are delayed due to the need for transcription and translation to take place first. Thus, inhibition of NF-κB activation will occur immediately (upstream) as a result of treatment with anti-inflammatory agents and therefore detection of inhibition should be conducted as early as 30 minutes after treatment and stimulation.

SLs have shown to directly interact with NF-κB by selectively alkylating cysteine sulfhydryl groups in the p65 subunit mediated by α,β- or α,β,γ-unsaturated carbonyl structures such as α-methylene-γ-lactones or α, β-unsubstituted cyclopentenones. These functional groups are known to react with nucleophiles in a Michael-type addition (García-Pineres *et al.,* 2001). Thus, SLs are known to possess anti-inflammatory activity. The results obtained in this study shows that when RAW 264.7 macrophages are stimulated with LPS, the presence of isoalantolactone mediates anti-inflammatory responses by decreasing the levels of activated p65 NF-κB. It is also evident that the decrease in protein levels is dose-dependent (Figure 7.11). This is in line with previously reported data that alantolactone (Chun *et al.,* 2012) and isohelenin (Bork *et al.,* 1997) decreases the transcriptional activity of NF-κB. It was also shown by Chun *et al.* (2012) that alantolactone inhibits the NF-κB pathway by inhibition of phosphorylation of IκBα and the suppression of phosphorylation of IKK as quick as 10 minutes after LPS stimulation in RAW 264.7 cells.

From this anti-inflammatory study, it can be concluded that *A. afra* and isoalantolactone possess anti-inflammatory activity, as expected. Both the plant extract and the compound show to decrease the production of NO and therefore it can be concluded that down-regulation of iNOS is experienced by the cell as a function of plant or compound exposure. The same is true for COX-2. COX-2 is an inducible cyclooxygenase and thus is only expressed in response to inflammation. Due to the exposure of RAW 264.7 cells to LPS, COX-2 expression is induced and levels of protein increases. When stimulated RAW 264.7 cells are simultaneously treated with *A. afra* and the stimulant or isoalantolactone and the stimulant, a slight decrease in COX-2 levels is indicated. This too suggests that the expression of the protein is suppressed due to the presence of *A. afra* and isoalantolactone. NF-κB p65 was shown to be activated in response to exposure to LPS. In the presence of isoalantolactone, a significant decrease in activated NF-κB p65 levels was evident. The results for *A. afra* were not as expected for this assay. A large increase was evident with the increase in the concentration of the extract and thereafter a decrease was detected. However,

this can be explained by the fact that crude plant extracts consist of many active compounds that work together or against one another to produce a biological effect. Decrease in activated NF-κB p65 levels will lead to the down-regulation of iNOS and COX-2 expression and this is evident in the results presented here. The study also suggests that the compound present in the plant extract, isoalantolactone, is partly responsible for the anti-inflammatory activity and it can be concluded that other compounds in the plant extract contribute to the less potent inhibition of inflammation as compared to isoalantolactone.

CHAPTER 8: Concluding remarks and recommendations for future work.

Extensive research has been done on the South Africa plant *A. afra* as outlined in Chapter 1. *A. afra* seems to have its fingers in all the pies, in terms of known biological activity. This study demonstrated the anticancer, anti-mitotic and anti-inflammatory activity upon treatment of cancer cells with *A. afra* and a new SL isolated from the plant, isoalantolactone. A schematic representation of this study and its findings is shown in Figure 8.1.

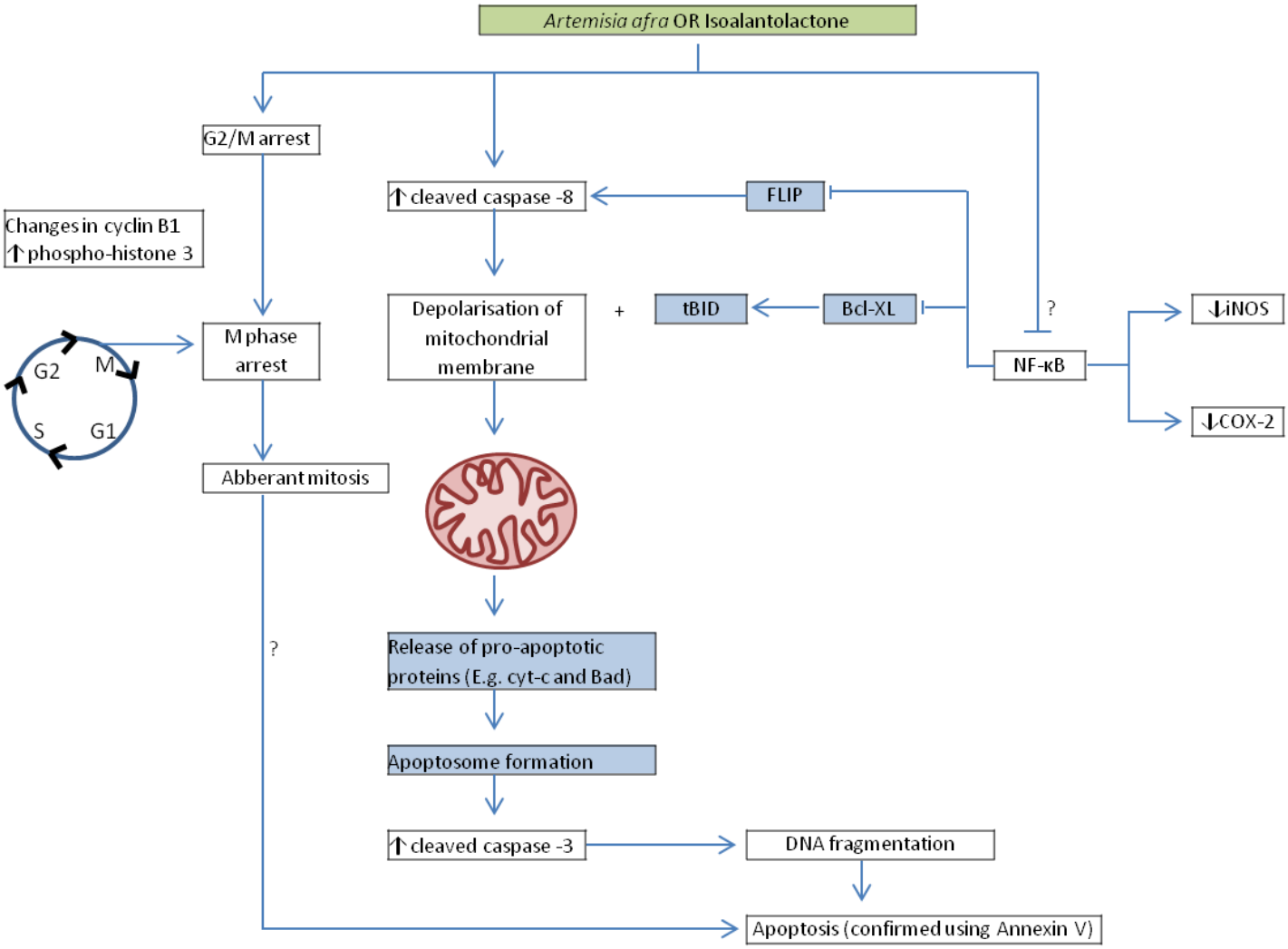

Figure 8.1: A schematic summary of the results of this study indicating the mechanisms of induced biological activity. White boxes indicate observations from the present study. Blue boxes indicate aspects that link observed activity that has not yet been studied.

Little research has been done on the cytotoxicity and anticancer properties of the plant although it is known to treat inflammatory ailments and with a well established molecular link between cancer and inflammation, the anticancer potential of the plant does not seem far-fetched. Thus, the main aim of the study was to determine the anticancer potential of *A. afra* by determining the mechanism of action of cell death in two cancer cell lines, namely HeLa and U937 cancer cells. This study was the first to describe this biological activity *in vitro.* It was found and reported (Chapter 3) that the ethanol extract of *A. afra* was cytotoxic against both HeLa and U937 cells exhibiting low, physiologically relevant IC_{50} values of ~30 µg/mL and ~20 µg/mL, respectively. Dose-response analysis against control cell lines Chang liver and Vero cells showed that the ethanol extract were not cytotoxic up to a concentration of 250 µg/mL, although a previous report indicated an IC_{50} value of ~ 113.0 µg/mL on Vero cells. The aqueous extract proved not to be cytotoxic against HeLa and U937 cells.

A. afra induces both the extrinsic and intrinsic pathways of apoptosis and this was shown by the significant increased levels of caspase -8 and the decrease in mitochondrial membrane potential, respectively. Increased levels of caspase -3 were also observed. Apoptosis induction was confirmed by the analysis of PS translocation using Annexin V and by the analysis of DNA fragmentation using the TUNEL assay. Thus, it was concluded that the ethanol extract of *A. afra* induces apoptosis in a caspase-dependent and mitochondria-dependent manner. After 12 hours of treatment, a large, significant increase of 4N DNA of the G2/M phase of the cell cycle was evident. This was shown in both HeLa and U937 cells. An article entitled "Caspase-dependent apoptosis is induced by *Artemisia afra* Jacq. ex Willd in a mitochondria-dependent manner after G2/M arrest" was published in a peer-reviewed journal, South African Journal of Botany.

Isolation and identification of the active compounds for an observed effect or activity is important not only for explaining biological activity of a plant, but also for the identification of possible new lead chemical compounds for the possible enhancement of a compound to be used in a treatment regime. The observed cytotoxic activity of *A. afra* led to the investigation of possible responsible (partly or wholly) cytotoxic compound(s). This was done by carrying out bioassay-guided fractionation of the ethanol extract using a hexane/ethylacetate and ethylacetate/methanol stepwise gradient. Further TLC purification of the most active fraction led to the isolation of one cytotoxic compound. Analytical and spectral analysis led to its identification as isoalantolactone, a eudesmanolide from *A. afra.* Glaucolides and

guaianolides are known sesquiterpene lactones from *A. afra*. This exciting identification of a new sesquiterpene lactone proves that plants harbour many unknown and/or unidentified compounds with biological prospects. In order to determine whether isoalantolactone contributes to the anticancer potential of *A. afra*, the same *in vitro* assays used for *A. afra* were performed for the compound. This study led to the conclusion that isoalantolactone does indeed contribute to this observation. An article entitled "Isoalantolactone, a newly isolated sesquiterpene lactone from *Artemisia afra* Jacq. ex Willd and its *in vitro* mechanism of induced cell death in HeLa cells" has been submitted to the Phytomedicine for peer-review.

Six other fractions also showed to be cytotoxic against HeLa cells. These fractions have been stored at 4°C and further purification and analytical procedures can be done to identify the compound(s) present in those fractions. This proves that *A. afra* has many compounds that contribute to its cytotoxic activity and warrants further investigation.

Upon inspection of HeLa cells after 24 hours incubation with *A. afra*, multinucleated cells were evident. Multinucleation is associated with G2/M arrest as cells have synthesized DNA in the S phase and newly formed nuclei have segregated but have not been able to undergo cytokinesis and thus nuclei containing full copies of DNA accumulate in one cell. Because G2/M arrest and multinucleation is one of the main morphological features of mitotic catastrophe, a special mode of apoptosis or cell death, it was hypothesised that mitotic catastrophe plays a role in the onset of apoptosis in HeLa and U937 cells. This led to a study of the mechanism of cell cycle arrest investigating the main players of the G2/M checkpoint, namely cyclin B1, Cdc2 and Cdc25. The state of H3 and the effect of *A. afra* on tubulin polymerisation were also investigated. Because G2/M arrest was also evident after treatment of HeLa cells with isoalantolactone, this study included the treatment of HeLa and U937 cells with isoalantolactone to determine its anti-mitotic effects as well. The results from these data showed that both *A. afra* and isoalantolactone arrest cells in the M phase due to the decrease in cyclin B1 levels after 12 hours of exposure in HeLa cells and thereafter an increase in cyclin B1 protein as well as the significant increase in phosphorylated H3 at Ser10. The rate of tubulin polymerisation increased significantly in the presence of both the plant extract and isoalantolactone. Confocal microscopy confirmed these findings by the evidence of the increase of mitotic cells when treated with *A. afra*. However, the same was not evident when HeLa cells were treated with isoalantolactone. It is thought that the compound may act faster than the crude plant extract and mitotic cells may be evident earlier than 12 hours as

membrane blebbing is seen at 12 hours whereas this morphological feature is prominent only at 24 hours of exposure to the plant extract as well as paclitaxel. From the results, it is proposed that *A. afra* and isoalantolactone possess anti-mitotic potential by acting as mitotic inhibitors causing hyperpolymerisation of MT and the subsequent dismantling of the MT network as apoptosis sets in and cell division is hindered resulting in aberrant mitosis and cell death. A draft for the publication of the anti-mitotic potential of *A. afra* and isoalantolactone is in preparation.

Inflammation and cancer are linked on a molecular level by the NF-κB pathway. The transcription factor regulates the transcription of many genes responsible for the physiological response of the immune system to cause inflammation. A three assay study was performed using murine macrophages (RAW 264.7) to establish the anti-inflammatory activity of *A. afra* and isoalantolactone. It is well known that SLs possess anti-inflammatory activity and due to the prevalence of these compounds in high amounts in plants of the Asteraceae family, *A. afra* was expected to possess this bioactivity. Results from this study indicated that RAW 264.7 cells treated with *A. afra* and stimulated with LPS down-regulates the expression of iNOS and COX-2 due to the evidence of decreased NO in a dose dependent manner and the decreased levels of COX-2 protein, respectively. This was also true for isoalantolactone.

SLs prevent the activation of the inflammatory pathways at different molecular levels and it seems as though the target of a particular SL is structure related. Eupatolide, a germacranolide SL has been shown to suppress the activation of NF-κB, AP-1 and MAPKs as well as Akt by preventing phosphorylation and degradation of IκBα. It has also been shown to affect inflammation further upstream, by inducing proteosomal degradation and polyubiquitination of TNFR-associated factor 6 (TRAF6). Thapsigargin, a guaianolide SL has shown to stimulate MAPKs (Krueger *et al.,* 2012). The SL parthenolide has been well studied for its anti-inflammatory activity. It has been reported that parthenolide inhibits inflammatory responses by directly interacting with the active p65 subunit of NF-κB. It inhibits this subunits ability to bind to DNA by alkylating it at residue Cys38 (García-Pineres *et al.,* 2001; Krueger *et al.,* 2012) and thus the downstream target genes such as iNOS, COX-2, IL-1β, IL-6, IL-8 and TNF as well as VEGF are not transcribed. In a study by Chun *et al.* (2012), alantolactone suppresses iNOS and COX-2 by down-regulation of NF-κB, MAPK and AP-1. The way in which alantolactone inhibits NF-κB is by inhibiting phosphorylation

and degradation of IκBα and thereby the translocation of both the p50 and p65 subunit to the nucleus. The results also suggested that alantolactone does not alkylate Cys38 and inhibit DNA binding like parthenolide, it acts further upstream. Because isoalantolactone is a derivative of alantolactone, it is likely that this compound will act in the same way, but more studies need to be conducted to confirm this.

Because isoalantolactone was isolated from *A. afra*, it can be assumed that the plant extract will behave in the same way. However, this plant might also contain other SLs (germacranolides and guaianolides) which may contribute to a different mechanism of anti-inflammatory activity. In saying this, the qualitative study here provides a yes/no answer for the anti-inflammatory activity of *A. afra* by the down-regulation of iNOS and COX-2 expression mediated by disruption of NF-κB activity in some way. This information has not been previously reported. A more mechanistic study can be conducted to determine molecular targets of the crude plant extract and hence its downstream effect. This will also provide an even more detailed mechanism of induced cell death to add to the reported data of this study as the inflammatory pathway and cell death is intimately linked as shown in Figure 7.3 of Chapter 7. Bioassays can include detection of changes in IκB subunit, the activity of IKK, the quantification of p65 in the nucleus versus its accumulation in the cytoplasm by separating cytosolic and nuclear cellular fractions using lysis and centrifugation techniques as described by Chun *et al.* (2012). A reporter gene assay such as the Cignal Reporter assay for NF-κB (Qiagen) can also be done and also provide information on the activity of NF-κB. In this assay, cells are transfected with a reporter GFP construct and will monitor the increase or decrease in the activity of NF-κB. This is a more accurate and sensitive method and will provide quantitative information. This information will provide complete data for a proposed mechanism of anti-inflammatory activity of *A. afra* which will too be submitted for publication.

In conclusion, this study shows that although a lot of information may exist in terms of biological activity of extracts from a specific plant as well as its constituents, new and more information as well as the isolation of new compounds from a plant can be obtained which can lead to the identification of pathways that can be exploited/inhibited in the treatment of various diseases. This again proves the usefulness of studying the biological activity of plants and their compounds.

REFERENCES:

Abad, M.J., Bedoya, L.M., Apaza, L., Bermejo, P. (2012). The Artemisia L. Genus: A review of Bioactive Essential Oils. Molecules 17: 2542 – 2566.

Abbas AK and Lichtman AH (2005). Cellular and Molecular Immunology. Fifth Edition. Elsevier Inc, Philadelphia, USA. Pp 277 – 280.

Abdool Karim, S.S., Ziqubu-Page, T.T., Arendse, R. (1994). Bridging the Gap: Potential for a health care partnership between African traditional healers and biomedical personnel in South Africa. SAMJ. 84, s1-s16.

Adams, J.M., Cory, S. (1998). The Bcl-2 protein family: arbiters of cell survival. Science. 281, 1322–1326.

Aggarwal, B.B., Gehlot, P. (2009). Inflammation and cancer: how friendly is the relationship for cancer patients? Curr. Opin. Pharmacol. 9: 351 – 369.

Aubry, J.P., Blaecke, A., Lecoanet – Henchoz, S., Jeannin, P., Herbault, N., Caron, G., Moine, V., Bonnefoy, J.Y. (1999). Annexin V used for measuring apoptosis in the early events of cellular cytotoxicity. Cytometry 37: 197 – 204.

Bakhle, Y.S. (2001). COX-2 and cancer: a new approach to an old problem. Br. J. Pharmacol. 134: 1137 – 1150.

Balkwill, F., Mantovani, A. (2001). Inflammation and Cancer: back to Virchow? Lancet 357: 539 – 545.

Balunas, M.J. and Kinghorn, A.D. (2005). Drug discovery from medicinal plants. Life Sciences 78: 431 - 441.

Beekman, A.C., Woerdenbag, H.J., van Uden, W., Pras, N., Konings, A.W., Wikström, H.V., Schmidt, T.J. (1997). Structure–cytotoxicity relationships of some helenanolide-type sesquiterpene lactones. J. Nat. Prod. 60: 252 – 257.

Bhakuni, R.S., Jain, D.C., Sharma, R.P., Kumar, S. (2001). Secondary metabolites of *Artemisia annua* and their biological activity. Current Science 80: 35 – 48.

Bohlmann, F., Mahanta, P.K., Jakupovic, J., Rastogi, R.C., Natu, A.A. (1978). New sesquiterpene lactones from *Inula* species. Phytochemistry 17: 1165 – 1172.

Bork, P.M., Lienhard Schmitz, M., Kuhnt, M., Escher, C., Heinrich, M. (1997). Sesquiterpene lactone containing Mexican Indian medicinal plants and pure sesquiterpene lactones as potent inhibitors of transcription factor NF-κB. FEBS Letters 402: 85-90.

Bremer, E., van Dam, G., Kroesen, B.J., de Leij, L., Helfrich, W. (2006). Targeted induction of apoptosis for cancer therapy: current progress and prospects. TRENDS Mol. Med. 12: 382 – 393.

Bruno, M., Rosselli, S., Raccuglia, R.A., Bastow, K.F., Lee, K.H. (2005). Cytotoxic activity of some natural and synthetic guaianolides. J. Nat. Prod. 68: 1042 – 1046.

Bucher, N., Britten, C.D. (2008). G2 checkpoint abrogation and checkpoint kinase – 1 targeting in the treatment of cancer. Br. J. Cancer 98: 523 – 528.

Busino, L., Chiesa, M., Draetta, G.F., Donzelli, M. (2004). Cdc25A phosphatase: combinatorial phosphorylation, ubiquitylation and proteolysis. Oncogene. 23, 2050–2056.

Castedo, M., Perfettini, J-L., Roumier, T., Andreau, K., Medema, R., Kroemer, G. (2004). Cell death by mitotic catastrophe: a molecular definition. Oncogene 23: 2825 – 2837.

Chadwick, M., Trewin, H., Gawthrop, F., Wagstaff, C. (2013). Sesquiterpene lactones: Benefit to plants and people. Int. J. Mol. Sci. 14: 12780 – 12805.

Chancerelle, Y., Mathieu, J., Kergonou, J.F. (1994). Recognition and elimination of senescent erythrocytes: Implication of antibodies specific for malonic dialdehyde-protein adducts, as demonstrated by flow cytometry. Biochem. Mol. Biol. Int. 34:.1259–1270.

Chaturvedi, D. (2011). Sesquiterpene lactones: Structural diversity and their biological activities. Opportunity, Challenge and Scope of Natural Products in Medicinal Chemistry: 313 – 334.

Chen, L-F., Green, W.C. (2004). Shaping the nuclear action of NF-κB. Nature Rev. Mol Cell Biol. 5: 392 – 401.

Chin, Y-W., Balunas, M.J., Chai, H.B., Kinghorn, A.D. (2006). Drug Discovery from Natural Sources. The AAPS Journal 8: E239 - E253.

Christensen, S.B., Skytte, D.M., Denmeade, S.R., Dionne, C., Møller, J.V., Nissen, P., Isaacs, J.T. (2009). A trojan horse in drug development: targeting of thapsigargins towards prostate cancer cells. Anticancer Agents Med. Chem. 9: 276 – 294.

Chun, J., Choi, R.J., Khan, S., Lee, D-S., Kim, Y-C., Nam, Y-J., Lee, D-U., Kim, Y.S (2012). Alantolactone suppresses inducible nitric oxide synthase and cyclooxygenase-2 expression by down-regulating NF-κB, MAPK and AP-1 via the MyD88 signaling pathway in LPS-activated RAW 264.7 cells. Int. Immunopharmacol. 14: 375 – 383.

Cho, R.J., Campbell, M.J., Winzeler, E.A., Steinmetz, L., Conway, A., Wodicka, L., Wolfsberg, T.G., Gabrielian, A.E., Landsman, D., Lockhart, D.J., Davis, R.W. (1998). A genome-wide transcriptional analysis of the mitotic cell cycle. Mol. Cell. 2: 65 – 73.

Clarkson, C., Maharaj, V.J., Crouch, N.R., Grace, O.M., Pillay, P., Matsabisa, M.G., Bhagwandin, N., Smith, P.J., Folb, P.I., 2004. *In vitro* antiplasmodial activity of medicinal plants native to or naturalised in South Africa. J. Ethnopharmacol. 92: 177 – 191.

Coates, J. (2000). Interpretation of Infrared Spectra, a practical approach in *Encyclopedia of Analytical Chemistry.* John Wiley and Sons Ltd, Chichester. Pp 10815 – 10837.

Cohen, G.M. (1997). Caspases: the executioners of apoptosis. Biochem. J. 326: 1 – 16.

Coller, H.A., Sang, L., Roberts, J.M. (2006) A new description of cellular quiescence. PLoS Biol 4: e38.

Collins, J.A., Schandl, C.A., Young, K.K., Vesely, J., Willingham, M.C. (1997a). Major DNA fragmentation is a Late Event in Apoptosis. The Journal of Histochemistry and Cytochemistry 45: 923 – 934.

Collins, K., Jacks, T., Pavletich, N.P. (1997b). The cell cycle and cancer. PNAS 94: 2776 – 2778.

Connor, J., Pak, C.C., Schroit, A.J. (1994). Exposure of phosphatidylserine in the outer leaflet of human red blood cells. J. Biol. Chem. 269: 2399 – 2404.

Crabbé, P (1971). An Introduction to the Chiroptical methods in Chemistry. Impresos Offisali, Col. Del Valle, Mexico. Pp 41 – 44.

Cragg, G.M., and Newman, D.J. (2005). Plants as a source of anti-cancer agents. J. Ethnopharmacol. 100: 72–79.

Crofford, L.J. (1997). COX-1 and COX-2 tissue expression: implications and predictions. J. Rheumatol Suppl. 49: 15 – 19.

Debatin, K.M., Stahnke, K., Fulda, S. (2003). Apoptosis in haematological disorders. Semin. Cancer Biol. 13: 149 – 158.

Dey, A., Tergaonkar, V., Lane, D.P. (2008). Double-edged swords as cancer therapeutics: simultaneously targeting p53 and NF-κB pathways. Nat Rev Drug Discovery 7: 1031 – 1040.

Dinarello, C.A. 2000. Pro-inflammatory cytokines. CHEST 118: 503-508.

DiPaola, R.S. (2002). To arrest or not to G_2-M cell-cycle arrest. Clin Cancer Res. 3311 – 3314.S

Elmore, S. (2007). Apoptosis: a review of programmed cell death. Toxicol. Pathol. 35, 495-516.

Fabricant, D.S., Farnsworth, N.R. (2001). The value of Plants used in Traditional Medicine for Drug Discovery. Environmental Health Perspectives 109: 69 – 75.

Fadok, V.A., Voelker, D.R., Campbell, P.A., Cohen, J.J., Bratton, D.L., Henson, P.M. (1992). Exposure of phosphatidylserine on the surface of apoptotic lymphocytes triggers specific recognition and removal by macrophages. J. Immunol. 148: 2207 – 2216.

Fadok, V.A., Laszlo, D.J., Noble, P.W., Weinstein, L., Riches, D.W., Henson, P.M. (1993). Particle digestibility is required for induction of the phosphatidylserine recognition mechanism used by murine macrophages to phagocytose apoptotic cells. J Immunol 151: 4274 – 4285.

Fischer, N.K., Weidenhamer, J.D., Riopel, J.L., Quijano, L., Menelaou, M.A. (1990). Stimulation of witchweed germination by sesquiterpene lactones: a structure-activity study. Phytochemistry 29: 2479 – 2483.

Fisher, R.P. (1997). CDKs and cyclins in transition(s). Curr. Opin. Genetics Dev. 7: 32 – 38.

FitzGerald, G.-A. & Patrono, C. (2001). The coxibs, selective inhibitors of cyclooxygenase-2. N. Engl. J. Med. 345: 433–442.

Fouche, G., Cragg, G.M., Pillay, P., Kolesnikova, N., Maharaj, V.J., Senabe, J. (2008). In vitro anticancer screening of South African plants. J. Ethnopharmacol. 119: 455–461.

Friesen, C., Fulda, S., Debatin, K.M. (1997). Deficient activation of the CD95 (APO-1/Fas) system in drug-resistant cells. Leukemia 11: 1833 – 1841.

Fulda, S., Debatin, K-A. (2006). Extrinsic versus intrinsic apoptosis pathways in anticancer chemotherapy. Oncogene 25: 4798 – 4811.

Gallagher Jr., B.M. (2007). Microtubule-stabilizing natural products as promising cancer therapeutics. Curr. Med. Chem. 14: 2959 – 2967.

García-Pineres, A.J., Castro, V., Mora, G., Schmidt, T.J., Strunk, E., Pahl, H.L., Merfort, I. (2001). Cysteine 38 in p65/NF-κB plays a crucial role in DNA binding inhibition by sesquiterpnen lactones. J. Biol. Chem 276: 39713 - 39720.

Gasparini, G., Longo, R., Sarmiento, R., Morabito, A. (2003). Inhibitors of cyclo-oxygenase 2: a new class of anticancer agents? Lancet Oncol. 4: 605-616.

Geissman, T. A. (1970): Sesquiterpene Lactones of *Artemisia – A. verlotorum and A. vulgaris.* Phytochem. 9: 2377 – 2381.

Gertsch, J., Sticher, O., Schmidt, T., Heilmann, J. (2003). Influence of helenanolide-type sesquiterpene lactones on gene transcription profiles in Jurkat T cells and human peripheral blood cells: anti-inflammatory and cytotoxic effects. Biochem. Pharmacol. 66: 2141 – 2153.

Gertsch, J. (2009). How scientific is the science of ethnopharmacology? Historical perspectives and epistemological problems. J. Ethnopharmacol. 122: 177-183.

Ghantous, A., Gali-Muhtasib, H., Vuorela, H., Saliba, N.A., Darwiche, N. (2010): What made sesquiterpene lactones reach cancer clinical trials? Drug Discovery Today 15: 668 – 678.

Gogvadze, V., Orrenius, S., Zhivotovsky, B. (2009). Mitochondria as targets for cancer chemotherapy. Semin. Cancer. Biol. 19: 57 – 66.

Gonzalez, R.J., Tarloff, J.B. (2001) Evaluation of hepatic subcellular fractions for Alamar blue and MTT reductase activity. Toxicol. In Vitro. 15: 257 – 259.

Green, J.A., Vistica, D.T., Young, T.C., Rogam, A.M., Ozols, R.F. (1984). Potential of melphalan cytotoxicity in human ovarian cancer cell lines by glutathione depletion. Cancer Res. 44: 5427 – 5431.

Greenhough, A., Smartt, H.J.M., Moore, A.E., Roberts, H.R., Williams, A.C, Paraskeva, C., Kaidi, A. (2009) The COX-2/PGE2 pathway: key roles in the hallmarks of cancer and adaptation to the tumour microenvironment. Carcinogenesis 30: 377 – 386.

Guantai, A.N., Addae-Mensah, I. (1999). Cardiovascular effect of Artemisia afra and its constituents. Pharmaceut. Biol. 37: 351 – 356.

Gurib-Fakim, A. (2006). Medicinal plants: Traditions of yesterday and drugs of tomorrow. Mol. Aspects Med. 27: 1-93.

Guzik, T.J., Korbut, R., Adamek-Guzik, T. (2003). Nitric oxide and superoxide in inflammation and immune regulation. J. Physiol. Pharmacol. 54: 469-487.

Guzman, M.L., Rossi, R.M., Karnischky, L., Li, X., Peterson, D.R., Howard, D.S., Jordan, C.T. (2005). The sesquiterpene lactone parthenolide induces apoptosis of human acute myelogenous leukemia stem and progenitor cells. Blood 105: 4163 – 4169.

Hagel, J.M., Yeung, E.C., Facchini, P.J. (2008). Got milk? The secret life of laticifers. Trends Plant Sci. 13: 631 – 639.

Hall, I.H., Lee, K.H., Starenes, C.O., Eigebaly, S.A., Ibuka, T., Wu, Y.S., Kimura, T., Haruna, M. (1978). Antitumor agents XXX: Evaluation of alpha-methylene gamma-lactone-containing agents for inhibition of tumor growth, respiration, and nucleic acid synthesis. J. Pharm. Sci. 67: 1235 – 1239.

Hall, I.H., Lee, K.H., Starenes, C.O., Sumida, Y., Wu, R.Y., Waddell, T.J., Cochran, J.W., Gerhart, K.G. (1979). Anti-inflammatory activity of sesquiterpene lactones and related compounds. J. Pharm. Sci. 68: 537 – 542.

Hammarström S. (1983). Leukotrienes. Ann. Rev. Biochem. 52: 355.

Hanahan, D., Weinberg, R.A. (2000). The hallmarks of cancer. Cell. 100: 57 - 70.

Harmatha, J., Nawrot, J. (1984). Comparison of the feeding detterent activity of some sesquiterpene lactones and a lignin lactone towards selected insect storage pests. Biochem. Sys. Ecol. 12: 95 – 98.

Harrison, J.C., Haber, J.E. (2006). Surviving the breakup: the DNA damage checkpoint. Annu. Rev. Genet 40: 209 - 235

Haworth, O., Buckley, C.D. (2007). Resolving the problem of persistence in the switch from acute to chronic inflammation. PNAS 104: 20647 – 20648.

Hehner, S.P., Heinrich, M., Bork, P.M., Vogt, M., Ratter, F., Lehmann, V., Schulze-Osthoff, K., Dröge, W., Lienhard Schmitz, M. (1998). Sesquiterpene lactones specifically inhibit activation of NF-κB by preventing the degradation of IκBα and IκBβ. J. Biol. Chem. 273: 1288 – 1297.

Holst-Hansen, C., Brünnner, N. (1998). MTT-cell proliferation assay. In: Celis, J. E., ed. Cell biology: a laboratory handbook, 2nd Ed. San Diego, California: Academic Press; pp 16-18.

Hong, S.H., Seo, S.H., Lee, J.H., Choi, B.T. (2004) The aqueous extract from Artemisia capillaris Thunb. Inhibits lipopolysaccharide-induced inflammatory response through preventing NF-kappaB activation in human hepatoma cell line and rat liver. Int J Mol Med. 13: 717 – 20.

Hutchings, A., Scott, A.H., Lewis, G., Cunningham, A.B. (1996). Zulu Medicinal Plants – An Inventory. University of Natal Press, Pietermaritzburg.

Huo, Y., Shi, H., Li, W., Wang, M., Li, X., (2010). HPLC determination and NMR structural elucidation of sesquiterpene lactones in *Inula helenium*. J. Pharmaceut. Biomed. 51: 942–946.

Hwang, A., Muschell R.J. (1998). Radiation and the G2 phase of the cell cycle. Radiat. Res. 150: S52- S59.

Institute of Natural Resources (2003). Indigenous medicinal plant trade, sector analysis. Investigative report no. 248.

Iranshashi, M., Emami, S. A., Mahmoud-Soltani, M. (2007). Detection of sesquiterpene lactones in ten Artemisia species population of Khorasan provinces. IJBMS 10: 183 – 188.

Irwin, M. A., Geissman, T.A. (1973). Rupicolin – A and –B, Rupin – A and – B and Cumambrin – B oxide from Artemisia tripartite spp rupicola. Phytochem. 12: 863 – 869.

Jabeen, N., Shawl, A.S., Dar, G.H., Jan, A., Sultan, P. (2007). Micropropagation of Inula racemosa Hook.f. A valuable medicinal plant. International Journal of Botany 3: 296–301.

Jakupovic, J., Chau-Thi, T.V., Warning, U., Bohlmann, F., Greger, H. (1986). 11β,13-dihydrogauianoldes from *Artemisia douglasiana* and a thiophene acetylene from *A. schidtiana*. Phytochem. 25: 1663 – 1667.

Jakupovic, J., Klemeyer, H., Bohlmann, F., Graven, E. H. (1988). Glaucolides and guaianolides from *Artemisia afra*. Phytochem. 27: 1129 – 1133.

Jakupovic, J., Tan, R. X., Bohlmann, F., Jia, Z. J., Huneck, S. (1991). Sesquiterpene lactones from *Artemisia rutifolia*. Phytochem. 30: 1714 – 1716.

Jennet-Siems, K., Köhler, I., Kraft, C., Beyer, G., Melzig, M.F., Eich, E. (2002). Cytotoxic constituents from *Exostema mexicanum* and *Artemisia afra*, two traditionally used plant remedies. Pharmazie. 57, 351-352.

Jeong, Y.S., Cho, S., Park, J.S., Ko, Y., Kang, Y-K. (2010). Phosphorylation of serine-10 of histone H3 shields modified lysine-9 selectively during mitosis. Genes cells 15: 181 – 192.

Jin, Z., McDonald, E.R., Dicker, D.T., El-Deiry, W.S. (2004). Deficient Tumor Necrosis Factor-related Apoptosis-inducing Ligand (TRAIL) Death Receptor Transport to the Cell Surface in Human Colon Cancer Cells Selected for Resistance to TRAIL-induced Apoptosis J. Biol. Chem 279: 35829 – 35839.

Johnson, L.V., Walsh, M.L., Chen, L.B. (1980). Localization of mitochondria in living cells with rhodamine 123. PNAS 77: 990 - 994.

Jordan, M.A., Wilson, L. (1998). Microtubules and actin filaments: dynamic targets for cancer chemotherapy. Curr. Opin. Cell. Biol. 10: 123 – 130.

Kantari, C., Walczak, H. (2011). Caspase – 8 and Bid: Caught in the act between death receptors and mitochondria. Biochim. Biophys. Acta 1813: 558 – 563.

Kasibhatla, S., Tseng, B. (2003). Why target apoptosis in cancer therapy? Mol. Cancer Ther. 2: 573 – 580.

Kaufmann, S.H.E., Dorhoi, A. (2013). Inflammation in tuberculosis: interactions, imbalances and interventions. Curr. Opin. Immunol. 25: 441 – 449.

Kelly, S.M., Price, N.C. (2000). The use of circular dichroism in the investigation of protein structure and function. Curr. Protein Pept. Sci. 1: 349 – 384.

Kelly, S.M., Jess, T.J., Price, N.C. (2005). How to study proteins by circular dichroism. Biochim. Biophys. Acta. 1751: 119 – 139.

Kerr, J.F.R., Wyllie, A.H., Currie, A.R. (1972). Apoptosis: A basic biological phenomenon with wide-ranging implications in tissue kinetics. Br. J. Cancer 26: 239 – 257.

Khan, M., Ding, C., Rasul, A., Yi, F., Li, T., Gao, H., Gao, R., Zhong, L., Zhang, K., Fang, X., Ma, T. (2012). Isoalantolactone Induces Reactive Oxygen Species Mediated Apoptosis in Pancreatic Carcinoma PANC-1 Cells. Int. J. Biol. Sci. 8: 533 – 547.

King, K. L. and Cidlowski, J. A. (1995). Cell cycle and apoptosis: Common pathways to life and death. J. Cell. Biochem., 58: 175–180.

Kitada, S., Pedersen, I.M., Schimmer, A.D., Reed, J.C. (2002). Dysregulation of apoptosis genes in hematopoietic malignancies. Oncogene 21: 3459 – 3474.

Koch, E., Klaas, C.A., Rungeler, P., Castro, V., Mora, G., Vichnewski, W., Merfort, I. (2001). Inhibition of inflammatory cytokine production and lymphocyte proliferation by structurally different sesquiterpene lactones correlates with their effect on activation of NF-κB. Biochem. Pharmacol. 62: 795 – 801.

Koopman, G., Reutelingsperger, C.P., Kuijten, G.A., Keehnen, R.M., Pals, S.T., van Oers, M.H. (1994). Annexin V for flow cytometric detection of phosphatidylserine expression on B cells undergoing apoptosis. Blood 84, 1415 – 1420.

Kraft, C., Jenett-Siems, K., Siems, K., Jakupovic, J., Mavi, S., Bienzle, U., Eich, E. (2003). In vitro antiplasmodial evaluation of medicinal plants from Zimbabwe. Phytother. Res. 17: 123 – 128.

Krueger A, Baumann S, Krammer PH, Kirchhoff S. (2001). FLICE-inhibitory proteins: regulators of death receptor-mediated apoptosis. Mol Cell Biol 21: 8247 – 8254.

Krueger, M.R.O., Grootjans, S., Biavatti, M.W., Vandenabeele, P., D'Herde, K. (2012). Sesquiterpene lactones as drugs with multiple targets in cancer treatment: focus on parthenolide. Anticancer Drugs: 1 – 14.

Krishan A. (1975). Rapid flow cytofluorometric analysis of cell cycle by propidium iodide staining. J. Cell Biol. 66: 188 – 193.

Kristjánsdóttir, K., Rudolph, J. (2004). Cdc25 phosphatases and cancer. Chem. Biol. 11: 1043 – 1051.

Kroemer, G., Galluzzi, L., Vandenabeele, P., Abrams, J., Alnemri., Baehrecke, E.H., Blagosklonny, M.V., El-Deiry, W.S., Golstein, P., Green, D.R., Hengartner, M., Knight, R.A., Kumar, S., Lipton, S.A., Malorni, W., Nunez, G., Peter, M.E., Tschopp, J., Yuan, J., Piacentini, M., Zhivotovsky, B., Melino, G. (2009). Classification of cell death: recommendations of the Nomenclature Committee on Cell Death 2009. Cell Death and Differentiation 16: 3 – 11.

Kühne, A., Tzvetkov, M.V., Hagos, Y., Lage, H., Burckhardt, G., Brockmöller, J. (2009). Influx and efflux transport as determinants of melphalan cytotoxicity: Resistance to melphalan in *MDR1* overexpressing tumor cell lines. Biochem. Pharmacol. 78: 45 – 53.

Kupchan, S.M., Eakin, M.A., Thomas, A.M. (1971). Tumor inhibitors. 69. Structure–cytotoxicity relationships among the sesquiterpene lactones. J. Med. Chem. 14: 1147 – 1152.

Lee, K.H. and Geissman, T.A. (1970). Sesquiterpene lactones of *Artemisia* constituents of *A. ludoviciana* spp. *mexicana*. Phytochemistry 9: 403 – 408.

Lee, K-H., Huang, E-S., Piantadosi, C., Pagano, J.S., Geissman, T.A. (1971). Cytotoxicity of Sesquiterpene Lactones. Cancer Research 31: 1649 – 1654.

Lees, E. (1995). Cyclin dependent kinase regulation. Curr. Opin. Cell Biol. 7: 773 – 780.

Liebmann, J.E., Cook, J.A., Lipschultz, C., Teague, D., Fisher, J., Mitchell, J.B. (1993). Cytotoxic studies of paclitaxel (Taxol) in human tumour cell lines. Br. J. Cancer. 68: 1104 – 1109.

Lin, W-W., Karin, M. (2003). NF-κB in cancer: a marked target. Semin. Cancer Biol. 13: 107 – 114.

Lin, W-W., Karin, M. (2007). A cytokine-mediated link between innate immunity, inflammation and cancer. J. Clin. Invest. 117: 1175 – 1183.

Liu, C., Mishra, A.K., Bing, H., Tan, R. (2001). Antimicrobial activities of isoalantolactone, a major sesquiterpene lactone of *Inula racemosa*. Chinese Science Bulletin 46: 1 – 4.

Liu, N.Q., Van der Kooy, F., Verpoorte, R. (2009). *Artemisia afra*: A potential flagship for African medicinal plants? South African Journal of Botany 75: 185 – 195.

Liu, N.Q, Cao, M., Frederich, M., Choi, Y.H., Verpoorte, R., van der Kooy, F. (2010). Metabolomic investigation of the ethnopharmological use of Artemisia afra with NMR spectroscopy and multivariate data analysis. J. Ethnopharmacol 128: 230 – 235.

Louw, C.A.M., Regnier, T.J.C., Korsten, L. (2002). Medicinal bulbous plants of South Africa and their traditional relevance in the control of infectious diseases. J. Ethnopharmacol. 82: 147-154.

Luo, X., Budihardjo, I., Zou, H., Slaughter, C., Wang, X. (1998). Bid, a Bcl2 interacting protein, mediates cytochrome c release from mitochondria in response to activation of cell surface death receptors. Cell. 94: 481 – 490.

Ma, Y., Zhao, D-G., Gao, K. (2013). Structural Investigation and Biological Activity of Sesquiterpene Lactones from the Traditional Chinese Herb *Inula racemosa*. J. Nat. Prod. 76: 564 - 570.

MacGlashan, D. Jnr. (2003). Histamine: A mediator of inflammation. J. Allergy Clin. Immunol. 112: S53 – S59.

Marco, J. A., Sanz, J. F., Sancenon, F., Rustaiyan, A., Saberi, M. (1993). Sesquiterpene lactones from Artemisia species. Phytocem. 32: 460 – 462.

Marini, M., Musiani, D., Sestili, P., Cantoni, O. (1996). Apoptosis of human lymphocytes in the absence or presence of internucleosomal DNA cleavage. Biochem. Biophys. Res. Commun. 229: 910 - 915.

Martin, S.J., Reutelingsperger, C.P., McGahon, A.J., Rader, J.A., van Schie, R.C., LaFace, D.M., Green, D.R. (1995). Early redistribution of plasma membrane phosphatidylserine is a general feature of apoptosis regardless of the initiating stimulus: inhibition by overexpression of Bcl-2 and Abl. J. Exp. Med. 182: 1545 – 1556.

Matthews, D. (2006). Dissecting the roles of Chk1 and Chk2 in mitotic catastrophe using chemical genetics. Eur. J. Cancer Suppl 4: 107

Mativandlela, S.P.N., Meyer, J.J.M., Hussein, A.A., Houghton, P.J., Hamilton, C.J., Lall, N. (2008). Activity against Mycobacterium smegmatis and M. tuberculosis by extract of South African medicinal plants. Phytother Res. 22: 841–845.

McGaw, L.J., Eloff, J.N. (2008). Ethnoveterinary use of southern African plants and scientific evaluation of their medicinal properties. J. Ethnopharmacol. 119: 559-574.

McMurry, J. (2008). Organic Chemistry, 7th Ed. Thomson Brooks/Cole. U.S.A. Pp 408 – 467.

Miller, M.J.S, Grisham, M.B. (1995). Nitric oxide as a mediator of inflammation? – You had better believe it. Mediators Inflamm. 4: 387 – 396.

Mohan, C. (2012). Signal Transduction. A short overview of its role in health and disease. 2nd Ed. Merck. Pp 103 – 106.

Mukinda, J.T., Syce, J.A. (2007). Acute and chronic toxicity of the aqueous extract of *Artemisia afra* in rodents. J. Ethnopharmacol. 112: 138 – 144.

Nabha, S.M., Mohammad, R.M., Dandashi, M.H., Coupaye-Gerard, B., Aboukameel, A., Pettit, G.R., Al-Katib, A.M. (2002). Combretastatin-A4 Prodrug Induces Mitotic Catastrophe in Chronic Lymphocytic Leukemia Cell Line Independent of Caspase Activation and Poly(ADP-ribose) Polymerase Cleavage. Clin. Cancer Res: 8, 2735–2741.

Nagaki, M. (1984): Two sesquiterpene lactones from Artemisia species. Phytochem. 23: 462 – 464.

Nagata, S. (2000): Apoptotic DNA fragmentation. Exp. Cell Res. 256: 12-18.

Nelson, D.L., Cox, M.M.. (2000). Lehninger: Principles of Biochemistry 3rd Ed. Worth Publishers. New York, USA. Pp 1152.

Newman, D.J. and Cragg, G.M. (2012). Natural Products as Sources of New Drugs over the 30 years from 1981 to 2010. J. Nat. Prod. 75: 311 – 335.

Nielsen, N.D., Sandager, M., Stafford, G.I., van Staden, J., Jäger, A.K. (2004). Screening of indigenous plants from South Africa for affinity to the serotonin reuptake transport protein. J. Ethnopharmocol. 94: 159 – 163.

Nojima, H. (2004). G1 and S-phase checkpoints, chromosome instability, and cancer. Methods Mol. Biol. 280: 3 – 49.

Nowak, S.J., Corces, V.G. (2004). Phosphorylation of histone 3: a balancing act between chromosome condensation and transcriptional activation. Trends Genet 20: 214-220.

Ntutela, S., Smith, P., Matika, L., Mukinda, J., Arendse, H., Allie, N., Estes, D.M., Mabusela, W., Folb, P., Steyn, L., Johnson, Q., Folk, W.R., Syce, J., Jacobs, M. (2009). Efficacy of Artemisia afra phytotherapy in experimental tuberculosis. Tuberculosis 89: S33 – S40.

Nxumalo, N., Alaba, O., Harris, B., Chersich, M., Goudge, J. (2011). Utilization of traditional healers in South Africa and costs to patients: Findings from a national household survey. J Public Health Pol. 32: S124 – S136.

O'Brien, J., Wilson, I., Orton, T., Pognan, F. (2000). Investigation of the Alamar Blue (resazurin) fluorescent dye for the assessment of mammalian cell cytotoxicity. Eur. J. Biochem. 267: 5421 – 5426.

Opal, S.M., DePalo, V.A. (2000). Anti-inflammatory cytokines. CHEST 117: 1162 – 1172.

Pagliuca, F.W., Collins, M.O., Choudhary, J.S. (2011). Coordinating cell cycle progression via cyclin specificity. Cell Cycle 10: 4195 – 4196.

Pan, L., Chai, H-B., Kinghorn, A.D. (2013). Discovery of new anticancer agents from higher plants. Frontiers in Bioscience 4: 142 – 156.

Parness, J., Horwitz, S.B. (1981). Taxol binds to polymerized tubulin in vitro. J. Cell. Biol. 91: 479 – 487.

Patil, G.V., Dass, S.K., Chandra, R. (2011). *Artemisia afra* and Modern Diseases. Pharmacogenomics and Pharmacoproteomics 2: 105 (1 - 22).

Peltzer, K. (2009). Utilization and Practice of Traditional/Complementary/Alternative medicine (TM/CAM) in South Africa. Afr. J. Trad. CAM 6: 175 – 185.

Peters-Golden, M., Canetti, C., Mancuso, P., Coffey, M.J. (2004). Leukotrienes: underappreciated mediators of innate immune responses. J. Immunol. 173: 589-594.

Pitti, R.M., Marsters, S.A., Lawrence, D.A., Roy, M., Kischkel, F.C., Dowd, P. Huang, A., Donahue, C.J, Sherwood, S.W., Baldwin, D.T., Godowski, P.J., Wood, W.I., Gurney, A.L., Hillan, K.J., Cohen, R.L., Goddard, A.D., Botstein, D., Ashkenazi. (1998). Genomic amplification of a decoy receptor for Fas ligand in lung and colon cancer. Nature 396: 699 - 703.

Planchais, S., Glab, N., Inzé, D., Bergounioux, C. (2000). Chemical inhibitors: a tool for plant cell cycle studies. FEBS Letters 476: 78 – 83.

Prigent, C., Dimitrov, S. (2003). Phosphorylation of serine 10 in histone H3, what for? J. Cell. Sci. 116: 3677 – 3685.

Rakoff-Nahoum, S. (2006). Why cancer and inflammation? Yale J. Biol. Med. 79: 123 – 130.

Rangan, G., Wang, Y., Harris. (2009). NF-kappaB signalling in chronic kidney disease. Front. Biosci. 14: 3496 – 3522.

Rao, S., Orr, G.A., Chaudhary, A.G., Kingston, D.G.I., Horwitz, S.B. (1995). Characterization of the Taxol binding site on the microtubule. J. Biol. Chem. 270: 20235 – 20238.

Rasul, A., Di, J., Millimouna, F.M., Malhi, M., Tsuji, I., Ali, M., Li, J., Li, X. (2013). Reactive oxygen species mediate isoalantolactone-induced apoptosis in human prostate cancer cells. Molecules 18: 9382 – 9396.

Ravi, R., Bedi, A. (2004). NF-κB in cancer – a friend turned foe. Drug Resist Updates 7: 53 – 67.

Reed, J.C., Pellecchia, M. (2005). Apoptosis-based therapies for hematologic malignancies. Blood 106: 408 – 418.

Reers, M., Smith, T.W., Chen, L.B. (1991). J-Aggregate Formation of a Carbocyanide as a Quantitative Fluorescent Indicator of Membrane Potential. Biochemistry 30: 4480 – 4486.

Rees, S.B., Harborne, J.B. (1985). The role of sesquiterpene lactones and phenolics in the chemical defence of the chicory plant. Phytochemistry 24: 2225 – 2231.

Riciotti, E., FitzGerald, G.A. (2011). Prostaglandins and Inflammation. Arterioscler. Thromb. Vasc. Biol. 31: 986 – 1000.

Richter, M. (2003). Traditional medicines and traditional healers in South Africa. Discussion paper prepared for the Treatment Action Campaign and AIDS Law Project. 29 Pages. Available online: http://www.tac.org.za/Documents/ResearchPapers/Traditional_Medicine_briefing.pdf

Roberts, M., (1990). Indigenous healing plants. Southern Book Publishers, Halfway House, Pp. 226–228.

Rocca, B., FitzGerald, G.A. 2002. Cyclooxygenase and prostaglandins: shaping up the immune response. Int. Immunopharmacol. 2: 603-630.

Rocca, B, Secchiero, P., Ciabattoni, G., Ranelletti, F.O., Catani, L., Guidotti, L., Melloni, E., Maggiano, N., Zauli, G., Patrono, C. (2002). Cyclooxygenase-2 expression is induced during human megakaryopoiesis and characterizes newly formed platelets. PNAS 99: 7634 – 7639.

Roninson, I.B., Broude, E.V., Chang, B-D. (2001) If not apoptosis, then what? Treatment-induced senescence and mitotic catastrophe in tumor cells. Drug Resist Updat. 4: 303 – 313.

Roth, W., Isenmann, S., Nakamura, M., Platten, M., Wick, W., Kleihues, P. Bähr, M., Ohgaki, H., Ashenazi, A., Weller, M. (2001). Soluble decoy receptor 3 is expressed by malignant gliomas and suppresses CD95 ligand-induced apoptosis and chemotaxis. Cancer Res. 61: 2759 – 2765.

Rowinsky, E.K., Donehower, R.C. (1995). Paclitaxel (Taxol). N. Engl. J. Med 332: 1004 – 1014.

Rüngeler, P., Castro, V., Mora, G., Goren, N., Vichnewski, W., Pahl, H.L., Merfort, I., Schmidt, T.J. (1999). Inhibition of transcription facto NF-κB by sesquiterpene lactones: a proposed molecular mechanism of action. Bioorg. Med. Chem. 7: 2343 – 2352.

Rybicki, E.P., Chikwamba, R., Koch, M., Rhodes, J.I., Groenewald, J-H. (2012). Plant-made therapeutics: An emerging platform in South Africa. Biotechnol Adv 30: 449 – 459.

Saelens, X., Festjens, N., Van de Walle. L., van Gurp, M., van Loo, G., Vandenabeele, P. (2004). Toxic proteins released from mitochondria in cell death. Oncogene 23: 2861–2874

Schafer, K.A. (1998). The cell cycle: A review. Vet Pathol. 35: 461 – 478.

Scott, G., Springfield, E.P., Coldrey, N. (2004). A Pharmacognostical study of 26 South Africa plant species used as Tradtional Medicines. Pharm. Biol. 42: 186 – 213.

Scotti, M.T., Fernandes, M.B., Ferreira, M. J. P., Emerenciano, V. P. (2007): Quantitative structure-activity relationship of sesquiterpene lactones with cytotoxic activity. Bioorg. Med. Chem. 15: 2927 – 2934.

Shah, M.A., Schwartz, G.A. (2001) Cell cycle-mediated drug resistance: an emerging concept in cancer therapy. Clin. Cancer Res. 7: 2168 – 2181 .

Sherr, C.H., Roberts, J.M. (2010). Living with or without cyclins and cyclin-dependent kinases. Genes Dev. 18: 2699 – 2711.

Shen, H.M., Tergaonkar, V. (2009). NF-κB signalling in carcinogenesis and as a potential molecular target for cancer therapy. Apoptosis 14: 348 – 363.

Silverton, R.M., Webster, F.X., Kiemle, D.J. (2005). Spectrometric identification of Organic compounds, 6th Ed. John Wiley and Sons, USA. Pp 72 – 284.

Sims, P. J., Waggoner, A. S., Wang, C-H., & Hoffmann, J.F. (1974). Studies on the mechanism by which cyanine dyes measure membrane potential in red blood cells and phosphatidylcholine vesicles. Biochemistry 13: 3315 - 3330.

Simstein, R., Burow, M., Parker, A., Weldon, C., Beckman, B. (2003). Apoptosis, chemoresistance, and breast cancer: insights from the MCF-7 cell model system. Exp. Biol. Med. 228: 995 - 1003.

Singh, R., George, J., Shukla, Y. (2010). Role of senescence and mitotic catastrophe in cancer therapy. Cell Div. 5: 1 – 12.

Sleath, P.R., Hendrickson, R.C., Kronhein, S.R., March, C.J., Black, R.A. (1990). Substrate specificity of the protease that processes human interleukin-1β. I. Biol. Chem. 265: 14526 – 14628.

Smiley, S.T., Reers, M., Mottola-Hartshorn, C., Lin, M., Chen, A., Smith, T.W., Steele, G.D., Chen, L.B. (1991). Intracellular heterogeneity in mitochondrial membrane potentials revealed by a J-aggregate-forming lipophilic cation JC-1. Cell Biology 88: 3671 – 3675.

Smith, I.C., Blandford, D.E. (1995). Nuclear magnetic resonance spectroscopy. Anal. Chem. 67: 509 – 518.

Spies, L., Koekemoer, T.C., Sowemimo, A.A., Goosen, E.D., van de Venter, M. (2013). Caspase-dependent apoptosis is induced by *Artemisia afra* Jacq. ex Willd in a mitochondria-dependent manner after G2/M arrest. S. Afr. J. Bot 84: 104 – 109.

Spite, M., Serhan, C.N. (2010). Novel lipid mediators promote resolution of acute inflammation: Impact of aspirin and statins. Circ. Res. 107: 1170 – 1184.

Stafford, G.I., Pedersen, M.E., van Staden, J., Jäger, A.K. (2008). Review on plants with CNS-effects used in traditional South African medicine against mental diseases. J. Ethnopharmacol. 119: 513 – 537.

Statistics South Africa (2011). Use of health facilities and levels of selected health conditions in South Africa: Findings from the General Household Survey, 2011. Report No. 03–00–05. Available online*:* www.statssa.gov.za/publications/Report-03.../Report-03-00-052011.pdf.

Stocklin, W., Waddell, T.G., Geissman, T.A. (1970). Circular discroism and optical rotator dispersion of sesquiterpene lactones. Tetrahedron 26: 2397 – 2410.

Suliman, S., van Vuuren, S.F., Viljoen, A.M. (2010) Validating the in vitro antimicrobial activity of Artemisia afra in polyherbal combinations to treat respiratory infections. S. Afr. J. Bot. 76: 655 - 661.

Sunmonu, T.O., Afolayan, A.J. (2010). Protective effect of *Artemisia afra* Jacq. on isoproterenol-induced myocardial injury in Wistar rats. Food Chem. Toxicol. 48: 1969 – 1972.

Sunmonu, T.O., Afolayan, A.J. (2013). Evaluation of Antidiabetic activity and associated toxicity of *Artemisia afra* aqueous extract in Wistar rats. Evidence-based Complementary and Alternative Medicine 2013: 1 – 8.

Sy, L-K., Brown, G.D. (2001): Deoxyarteannuin B, dihydro-deoxyarteannuin B and trans-5-hydroxy-2-isopropenyl-5-methylhex-3-en-1-ol from Artemisia anuua. Phytochem. 58: 1159 – 1166.

Sylvester, P.W. (2011). Optimization of the tetrazolium dye (MTT) colorimetric assay for cellular growth and viability. Methods Mol. Biol. 716: 157 – 168.

Tan, R.X., Tang, H.Q., Hu, J., Shuai, B. (1998). Lignans and sesquiterpene lactones from *Artemisia sieversiana* and *Inula racemosa.* Phytochemistry 49: 157 – 161.

Thornberry, N.A. (1998). Caspases: key mediators of apoptosis. Chem. Biol. 5: R97 – R103.

Thornberry, N.A., Lazebnik, Y. (1998). Caspases: enemies within. Science 281, 1312–1316.

Thring, T.S., Weitz, F.M. (2006). Medicinal plant use in the Bredasdorp/Elim region of the Southern Overberg in the Western Cape Province of South Africa. J. Ethnophol. 103: 261 – 275.

Toettcher, J.E., Loewer, A., Ostheimer, G.J., Yaffe, M.B., Tidor, B., Lahav, G. (2008). Distinct mechanisms act in concert to mediate cell cycle arrest. PNAS 106: 785 – 790.

Toyoshima-Morimoto, F., Taniguchi, E., Nishida, E. (2002). Plk1 promotes nuclear translocation of human Cdc25C during prophase. EMBO reports 3: 341 – 348.

Tsikas, D. (2007). Analysis of nitrite and nitrate in biological fluids by assays based on the Griess reaction: Appraisal of the Griess reaction in the L-arginine/nitric oxide area of research. J. Chromatogr. B. 851: 51 – 70.

Tsujimoto, Y., Finger, L.R., Yunis, J., Nowell, P.C., Croce, C.M. (1984). Cloning of the chromosome breakpoint of neoplastic B cells with the t(14;18) chromosome translocation. Science 226: 1097–1099.

Ullah, Z., Lee, C.Y., Lilly, M.A, DePamphilis, M.L. (2009). Developmentally programmed endoreduplication in animals. Cell Cycle 8: 1501 – 1509.

Vakifahmetoglu, H., Olsson, M., Zhivotovsky, B. (2008). Death through a tragedy: mitotic catastrophe. Cell Death Differ. 15: 1153–1162.

Van Engeland, M., Nieland, L.J.W., Ramaekers, F.C.S., Schutte, B., Reutelingsperger, C.P.M. (1998). Annexin V-affinity assay: a review on an apoptosis detection system based on phosphatidylserine exposure. Cytometry 31: 1-9.

van Noesel, M.M., van Bezouw, S., Salomons, G.S., Voute, P.A., Pieters, R., Baylin, S.B., Herman, J.G., Versteeg, R. (2002). Tumor-specific down-regulation of the tumor necrosis factor-related apoptosis-inducing ligand decoy receptors DcR1 and DcR2 is associated with dense promoter hypermethylation. Cancer Res. 62: 2157 – 2161.

van Wyk, B-E., van Oudtshoorn, B., Gerike, N. (1997). Medicinal Plants of South Africa. Briza Publications, Pretoria. pp. 142.

Van Wyk, B.-E. (2008). A broad review of commercially important southern African medicinal plants. J. Ethnopharmacol 119: 342 – 355.

Vermeulen, K., Berneman, Z.N., Van Bockstaele, D.R. (2003). Cell cycle and apoptosis. Cell Prolif. 36: 165 – 175.

Vermeulen, K., Berneman, Z.N., Van Bockstaele, D.R. (2005). Apoptosis: Mechanisms and relevance in cancer. Ann. Haemotol. 84: 626 - 639.

Viljoen, A.M., van Vuuren, S.F., Gwebu, T., Demirci, B., Hüsnü, K., Baser, C. (2006). The geographical variation and antimicrobial activity of African wormwood (*Artemisia afra* Jacq.) essential oil. JEOR 18: 19 - 25.

Wang, J., Lenardo, M.J. (2000). Roles of caspases in apoptosis, development, and cytokine maturation revealed by homozygous gene deficiencies. J. Cell Sci. 113: 753 – 757.

Wani, M. C., Taylor, H.L., Wall, M.E., Coggon, P., and McPhail, A.T. (1971). Plant antitumor agents. VI . The isolation and structure of taxol, a novel antileukemic and antitumor agent from *Taxus brevifolia*. J. Am. Chem. Soc. 93: 2325 – 2327.

Waterman-Storer, C. M. and Salmon, E. D. (1997). Microtubule dynamics: Treadmilling comes around again. Curr. Biol. 7: 369 – 372.

Watt, J., Breyer-Brandwijk, M.G. (1932). The medicinal and poisonous plants of southern and eastern Africa. Livingstone, Edinburgh.

Wei, Y., Mizzen, C.A., Cook, R.G., Gorovsky, M.A., Allis, C.D. (1998). Phosphorylation of histone H3 at serine 10 is correlated with chromosome condensation during mitosis and meiosis in Tetrahymena. Proc. Natl. Acad. Sci. 95: 7480 – 7484.

Wei, Y., Yu, L., Bowen, J., Gorovsky, M.A., Allis, C.D. (1999). Phosphorylation of histone H3 is required for proper chromosome condensation and segregation. Cell 97: 99 – 109.

Weller, M.G. (2012). A unifying review of bioassay-guided fractionation, effect directed analysis and related techniques. Sensors 12: 9181 – 9209.

Wilson, K., Walker, J. (2010). Principles and techniques of Biochemistry and Molecular biology, 7th Ed. Cambridge University Press. U.K. Pp 509 – 512.

Wolfender, J.-L., Rodriguez, S., Hostettmann, K. (1998). Liquid chromatography coupled to mass spectrometry and nuclear magnetic resonance spectroscopy for the screening of plant constituents. J. Chromatogr. 794: 299 – 316.

Wolffe, A.P., Hayes, J.J. (1999). Chromatin disruption and modification. Nucleic acid Res. 27: 711 – 720.

Zangemeister-Wittke, U., Simon, H.U. (2001). Apoptosis - Regulation and clinical implications. Cell Death Differ. 8, 537 – 544.

Zhang, Z., Fuller, G.M. (1997). The competitive binding of STAT3 and NF-κB on an overlapping DNA binding site.

Zhang, S., Won, Y-K., Ong, C-N., Shen, H-M. (2005). Anti-cancer potential of sesquiterpene lactones: bioactivity and molecular mechanisms. Curr. Med. Chem. – Anti-cancer Agents 5: 239-249.

www.beckmancoulter.com

www.biotek.com

www.cansa.org.za

www.cytoskeleton.com

www.promega.com

www.sigma.com

www.who.int

www.who.or.jp.

http://groundup.org.za

http://lcbim.epfl.ch/research

http://nccam.nih.gov.

APPENDIX A: Additional Results.

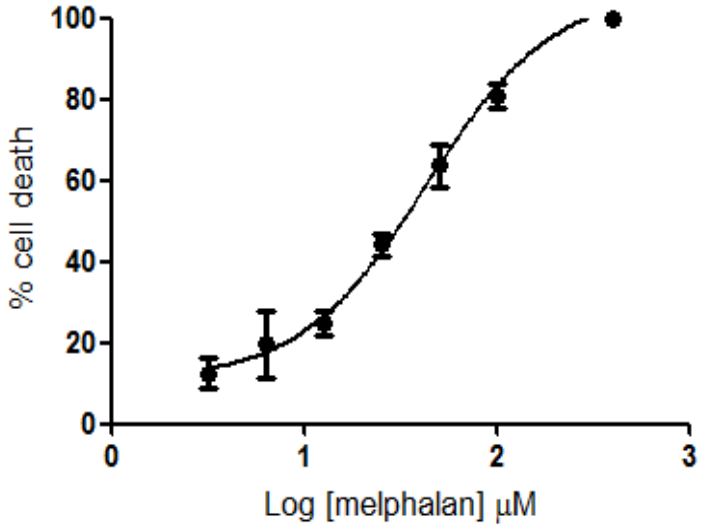

Figure A1: Cytotoxic effect of melphalan HeLa cancer cell lines after 48 hours of exposure. Cell viability was determined using the MTT assay for HeLa Error bars indicate SD of four replicate values of a single experiment.

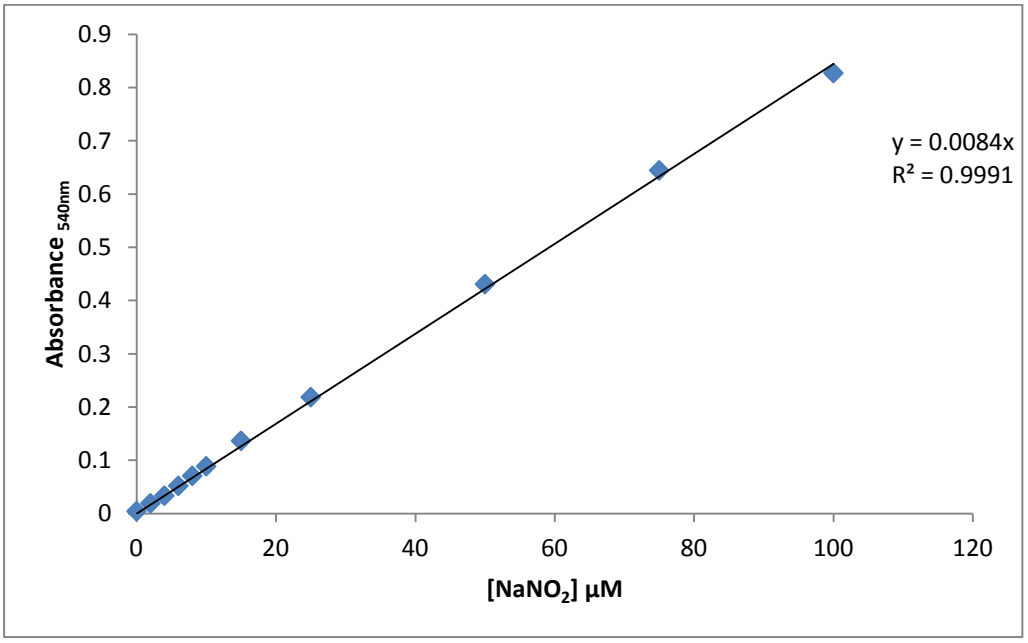

Figure A2: Standard curve of $NaNO_2$ (0 – 100 µM).

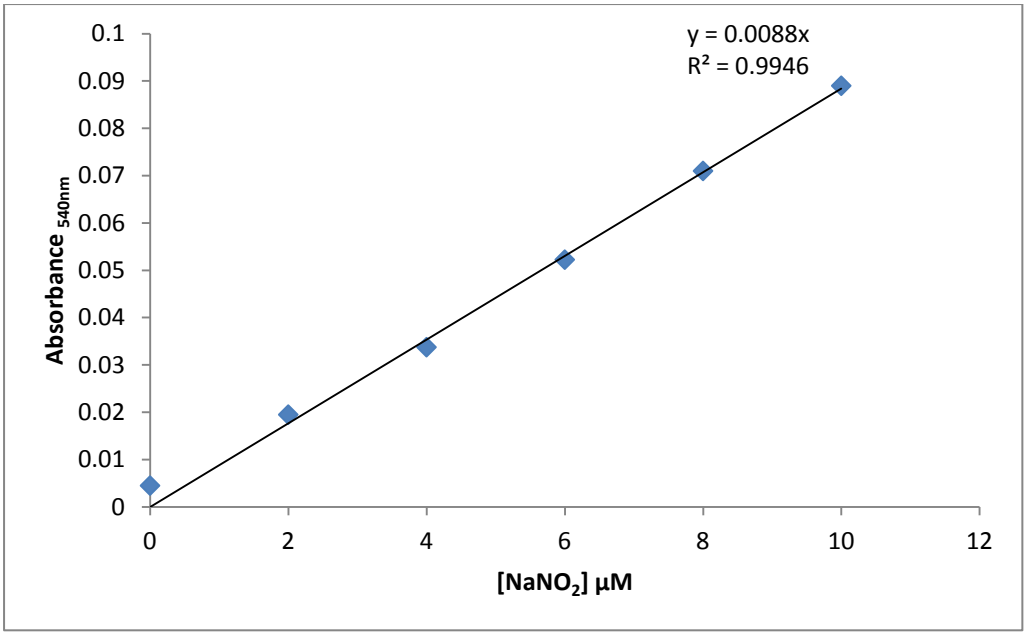

Figure A3: **Standard curve of $NaNO_2$ (0 – 10 µM).**

APPENDIX B: Project outputs.

Publication:

Spies, L., Koekemoer, T.C., Sowemimo, A.A., Goosen, E.D., van de Venter, M. (2013). Caspase-dependent apoptosis is induced by *Artemisia afra* Jacq. ex Willd in a mitochondria-dependent manner after G2/M arrest. S. Afr. J. Bot 84: 104 – 109.

See attached article.

Submitted publication:

A manuscript entitled "Isoalantolactone, a newly isolated sesquiterpene lactone from *Artemisia afra* and its *in vitro* mechanism of induced cell death in HeLa cells" has been submitted to Phytomedicine for peer-review.

See attached manuscript.

Conference outputs:

International conferences:

Poster presentations:

1. 59th International Congress and Annual Meeting of the Society for Medicinal Plant and Natural Product Research. Antalya, Turkey, 2011.
   Spies, L., Koekemoer, T.C., Sowemimo, A.A., and van de Venter, M. (2011). The anticancer potential of Artemisia afra. Planta Medica 77: PM 101.

2. International Symposium on Natural Products in Cancer Prevention and Therapy Naples, Italy, 2013.
   Venables, L., Koekemoer, T.C., Sowemimo, A.A., Goosen, E.D. and van de Venter, M. (2013). Isolation and in vitro cytotoxic mechanism of action of a sesquiterpene lactone from Artemisia afra.

National conference:

Oral presentation:

1. African Laser Centre (ALC) Student Symposium Stellenbosch, South Africa, 2011.
   Spies, L., Koekemoer, T.C., Sowemimo, A.A. and Van de Venter, M. (2011). The anticancer potential of Artemisia afra.

   The ALC Managers award was achieved for Best overall presentation at the Symposium.

Others:

The NMMU's Department of Biochemistry, Microbiology and Physiology conference days take place twice yearly where results are presented to fellow students, peers and academic staff.

South African Journal of Botany 84 (2013) 104–109

Contents lists available at SciVerse ScienceDirect

South African Journal of Botany

journal homepage: www.elsevier.com/locate/sajb

Caspase-dependent apoptosis is induced by *Artemisia afra* Jacq. ex Willd in a mitochondria-dependent manner after G2/M arrest

L. Spies [a], T.C. Koekemoer [a], A.A. Sowemimo [b], E.D. Goosen [c], M. Van de Venter [a,*]

[a] Department of Biochemistry and Microbiology, PO Box 77000, Nelson Mandela Metropolitan University, Port Elizabeth 6031, South Africa
[b] Department of Pharmacognosy, Faculty of Pharmacy, College of Medicine, University of Lagos, Nigeria
[c] Department of Pharmaceutical Chemistry, Rhodes University, Grahamstown, South Africa

ARTICLE INFO

Article history:
Received 29 May 2012
Received in revised form 2 October 2012
Accepted 29 October 2012
Available online 22 November 2012

Edited by LJ McGaw

Keywords:
A. afra
Cytotoxicity
Apoptosis
HeLa
U937

ABSTRACT

Artemisia afra is one of the oldest, most well known and widely used traditional medicinal plants in South Africa. It is used to treat many different medical conditions, particularly respiratory and inflammatory ailments (Liu et al., 2009). There is no reported evidence of its use for the treatment of cancer but due to its reported cytotoxicity (Fouche et al., 2008; Mativandlela et al., 2008), we investigated the mode of cell death induced by an ethanolic *A. afra* extract by using two cancer cell lines. IC_{50} values of 18.21 and 31.88 μg/mL of ethanol extracts were determined against U937 and HeLa cancer cells, respectively. An IC_{50} value of the aqueous extract was greater than 250 μg/mL. The effect of the cytotoxic ethanolic *A. afra* extract on U937 and HeLa cells and their progression through the cell cycle, apoptosis and mitochondrial membrane potential were investigated. Melphalan was used as a positive control. After 12 h of treatment with *A. afra* a delay in G2/M phase of the cell cycle was evident. Apoptosis was confirmed by using the TUNEL assay for DNA fragmentation, as well as fluorescent staining with annexin V-FITC. Apoptosis was evident with the positive control and *A. afra* treatment at 24 and 48 h. JC-1 staining showed a decrease in mitochondrial membrane potential at 24 h. The results obtained suggest that *A. afra* potentially has medicinal anticancer properties.

1. Introduction

A large percentage of the African population depends on medicinal plants for health care. Africa is one of the continents with the richest biodiversity in the world, however little effort has been devoted to development of chemotherapeutic agents from medicinal plants. It is estimated that only 15% of the world's plants have been screened for their therapeutic values (Louw et al., 2002; McGaw and Eloff, 2008).

The World Health Organization (WHO) has recognized that 80% of the African population makes use of traditional medicine (Gurib-Fakim, 2006) and in sub-Saharan Africa, the ratio of traditional healers to the rest of the population is 1:500, compared to the ratio of medical doctors to the rest of the population, which is 1:40,000 (Abdool Karim et al., 1994). Thus, it is clear that traditional healers play an important role in the lives of African people and have the potential to serve as crucial components of a comprehensive health care strategy.

Cancer is a class of disease in which a group of cells grow and divide uncontrollably and do not die. Normal cells in the body follow an orderly pattern of cell division, growth and death, known as the cell cycle. The event of programmed cell death, known as apoptosis, does not occur in cancer cells and thus the cells continue to divide and grow and cancer begins to form (Schafer, 1998).

Apoptosis is initiated by extracellular or intracellular signals in which a complex machinery is activated to start a cascade of events ultimately leading to the degradation of nuclear DNA and dismantling of the cell. The event of cell suicide needs to be regulated as too little apoptosis may result in cancer, autoimmune or chronic inflammatory diseases; too much apoptosis may lead to stroke-induced neuronal damage and neurodegenerative disorders (Zangemeister-Wittke and Simon, 2001).

Apoptosis is characterized by morphological changes such as membrane blebbing, cytoplasmic and chromatin condensation as well as apoptotic body formation. It is also characterized by biochemical changes including cysteine-dependent aspartate-directed proteases (caspase) activation, DNA fragmentation and phosphatidyl serine translocation (Elmore, 2007). Caspases are responsible for the proteolytic cleavage of cellular proteins leading to the characteristic apoptotic features (Vermeulen et al., 2005).

Plants have played an important role as a source of anticancer agents and it is reported that over 60% of anticancer agents are derived from natural products such as plants, marine organisms and microorganisms (Cragg and Newman, 2005). *Artemisia afra* is one of the oldest, most well known and widely used traditional medicinal plants in South Africa. It is commonly referred to as the African wormwood and it is used to

* Corresponding author. Tel.: +27 41 504 2813; fax: +27 41 504 2814.
E-mail address: maryna.vandeventer@nmmu.ac.za (M. Van de Venter).

0254-6299/$ – see front matter © 2012 SAAB. Published by Elsevier B.V. All rights reserved.
http://dx.doi.org/10.1016/j.sajb.2012.10.007

treat many different medical conditions, particularly respiratory and inflammatory ailments. The plant is prepared in many different ways, traditionally, for specific uses. An infusion of leaves and roots are used for the treatment of diabetes in the Eastern Cape region of South Africa. The leaves are boiled and the vapors are inhaled to treat respiratory conditions. For the treatment of colic, a tincture of leaves wetted with brandy is used. Leaves are also added to boiling water and allowed to draw for 10 min and this infusion is strained and drank for relief of flu type conditions (Liu et al., 2009). Mativandlela et al. (2008) showed cytotoxicity of *A. afra* in Vero cells and Fouche et al. (2008) reported that a dichloromethane:methanol (1:1) extract of *A. afra* induced cytotoxicity against renal and breast cancer cells as well as melanoma cells. Thus we investigated the mode of cell death caused by an ethanolic extract of *A. afra* on HeLa cervical cancer cells and a promonocytic leukemia cell line, U937.

2. Materials and methods

2.1. Materials, chemicals and reagents

Cervical (HeLa) cancer and human promonocytic leukemia U937 cells were purchased from Highveld Biological, South Africa. Cleaved caspase-3 (Asp175) and caspase 8 (Asp391) antibodies were purchased from Cell Signaling Technology, Inc. (Danvers, MA, USA). The Coulter® DNA Prep ™ reagents kit, goat anti-rabbit IgG (H + L chain specific) and rabbit IgG isotype, both labeled with fluorescein (FITC) conjugate and IsoFlow™ EPICS™ sheath fluid, were purchased from Beckman Coulter (CA, USA). MEBSTAIN apoptosis kit direct and IntraPrep™ permeabilizing reagent were purchased from Immunotech (Marseille, France). Annexin V-FITC/PI kit was purchased from MACS Miltenyi Biotec (Auburn, USA). 3-(4,5-dimethyl-2-thiazolul)-2,5-diphenyl-2H-tetrazolium bromide (MTT), 5,5′,6,6′tetrachloro-1,1′,3,3′-tetraethylbenzimidazol-carbocyanine iodide (JC-1), trypan blue and melphalan were purchased from Sigma (St. Louis, MO, USA). CellTiter-Blue® reagent was purchased from Promega (Madison, WI, USA). RPMI 1640 cell culture medium containing 25 mM Hepes, 2 mM glutamine and fetal bovine serum was purchased from ThermoScientific (Logan, Utah, USA).

2.2. Methods

2.2.1. Extraction

Herbarium specimen voucher number *A. afra* 15487 was deposited in the Nelson Mandela Metropolitan University Herbarium, Botany Department, South Campus. Leaves of the plant were dried at 80 °C and thereafter ground by using a blender. Aqueous and ethanol extracts were prepared by submerging the ground leaves in deionized water and 80% ethanol, respectively. The submerged leaves were incubated in the dark at room temperature overnight. After incubation, the liquid was filtered through Whatman filter paper (1.1 μm). The aqueous extract was freeze dried and the ethanol extract concentrated to dryness by evaporating ethanol by using a rotary evaporator (Buchi) and further freeze dried. The extracts were stored separately in a desiccator at 4 °C in the dark.

2.2.2. Cell culture conditions

The adherent cancer cell line, HeLa cells, and the suspension U937 cells were used for the experimental procedures. The cells were routinely maintained in 10-cm culture dishes and flasks, respectively, without antibiotics in RPMI 1640 cell culture medium containing 25 mM Hepes, 2 mM glutamine, supplemented with 10% fetal bovine serum and incubated in a humidified 5% CO_2 incubator at 37 °C. Trypan blue was used to determine cell viability and cell number. Counting of cells was done by using an improved Neubauer hemocytometer and cell densities (number of cells per mL) were altered according to the number of cells required for each experiment.

2.2.3. Cytotoxicity

HeLa and U937 cells were seeded in 200 μL and 100 μL aliquots, respectively, at 3×10^4 cells/mL in 96 well plates and HeLa cells were left overnight to attach. U937 cell were also incubated overnight at 37 °C before treatment. The medium was replaced with fresh medium containing varying concentrations (1.25–250 μg/mL) of aqueous and ethanolic extracts. One hundred microliter aliquots of fresh medium containing double the appropriate extract concentration was added to the respective wells for treatment of U937 cells. Both cell lines were incubated at 37 °C in a humidified 5% CO_2 incubator for 48 h. The medium containing *A. afra* extract was removed prior to addition of MTT to HeLa cell. Cytotoxicity assays were performed by using CellTiter-Blue® and MTT (5 mg/mL) for U937 and HeLa respectively. Melphalan (40 μM) was used as a positive control for all experiments. Absorbance was read at 540 nm by using a BioTek® PowerWave XS spectrophotometer (Winooski, VT, USA) for HeLa cells and fluorescence was read at $544_{Ex}/590_{Em}$ by using a Fluoroskan Ascent FL fluorometer (ThermoLabsystems, Finland) for U937 cells.

2.2.4. Cell cycle analysis

U937 cells were seeded at 1×10^5 cells/mL in culture flasks and HeLa cells were seeded at 5×10^4 cells/mL in 10 mL aliquots in 10 cm culture dishes and treated with 20 μg/mL and 30 μg/mL of ethanolic *A. afra* extract, respectively. Cells were incubated for 12, 24 and 48 h. After the appropriate incubation period, HeLa cells were trypsinized for 10 min, resuspended in phosphate buffered saline (PBS) and transferred to polypropylene tubes. U937 cells did not require trypsinization. The Coulter® DNA Prep™ reagents kit was used for DNA cell cycle analysis, as per manufacturer's instructions. Briefly, 100 μL lysis reagent was added to each tube and incubated for 5 min at room temperature. Thereafter 500 μL propidium iodide (50 μg/mL) was added and tubes were incubated for 15 min at 37 °C. Flow cytometric analysis was performed directly after incubation. A Beckman Coulter Cytomics FC500 was used for all flow cytometry analysis.

2.2.5. Phosphatidylserine translocation

U937 cells were seeded at 1×10^5 cells/mL in culture flasks and HeLa cells were seeded at 5×10^4 cells/mL in 6 well culture plates, by using 3 mL per well, and treated with 20 μg/mL and 30 μg/mL of ethanolic *A. afra* extract, respectively. Cells were incubated for 24 h at 37 °C. After treatment and incubation, HeLa cells were washed with ice-cold Dulbecco's Modified Eagle's Medium (DMEM). Accutase was used to detach the HeLa cells from the culture plate. Cells were incubated for 10 min with accutase and then resuspended in PBS. Cells were transferred to polypropylene tubes and centrifuged at 500 ×*g* for 5 min at room temperature and washed with PBS to remove accutase. U937 cells did not require the detachment step. Cells were then stained according to Annexin V-FITC/PI kit protocol (MACS Miltenyi Biotec). In brief, after centrifugation, the supernatant was discarded and cell pellets resuspended in ice-cold 1× binding buffer. Annexin V-FITC (1 μL; 25 μg/mL) and PI (5 μL; 250 μg/mL) were added to each tube. Compensation control tubes contained cells with Annexin V-FITC only, PI only and a combination of Annexin V-FITC and PI. Tubes were gently mixed and incubated on ice for 15 min in the dark. Samples were read within 30 min on a Beckman Coulter Cytomics FC500.

2.2.6. Mitochondrial membrane potential (MMP) analysis

U937 and HeLa cells were seeded and treated as described for phosphatidylserine translocation analysis. Cells were incubated for 24 and 48 h. After the incubation periods, cells were transferred to polypropylene tubes and cells collected by centrifuging at 500 ×*g* for 5 min at room temperature. After treatment and incubation, HeLa cells were washed with Ca^{2+} and Mg^{2+} free PBS, trypsinized for 10 min and resuspended in PBS. Cells were centrifuged at 500 ×*g* for 5 min at room temperature and washed with PBS to remove trypsin. U937 cells

did not require the trypsinization step. Thereafter, a lipophilic cation dye, JC-1, was added to a final concentration of 2 μg/mL. JC-1 was used to determine a change in the mitochondrial membrane potential. Cells were incubated for 10 min at room temperature in the dark. The cells were washed by using 500 μL PBS and centrifuged at 500 ×g for 5 min. The wash step was repeated three times before the flow cytometric analysis.

2.2.7. Caspase 8 and 3 activation

Cells were seeded and treated as described for MMP analysis. Cells were fixed and permeabilized by using the IntraPrep kit (Beckman Coulter). Cleaved caspase 8 (Asp 391) and cleaved caspase 3 (Asp 175) monoclonal antibodies (Cell Signaling) were used to determine the activation of caspase 8 and caspase 3 respectively. Cells were first blocked by using PBS containing 0.5% BSA and thereafter incubated with the antibodies separately (1:100 for caspase 8 and 1:50 for caspase 3) for 1 h at 37 °C. Cells were washed and incubated with the conjugated secondary antibody (1:1000) for 30 min at 37 °C in the dark. This step was not required for caspase 3 analysis as the antibody contains a conjugated FITC fluorophore. Cells were then analyzed by using flow cytometry.

2.2.8. DNA fragmentation

Cells were seeded, treated, fixed and permeabilized as described for caspase analysis. The MEBSTAIN apoptosis kit (Immunotech) was then used as per the manufacturer's instructions to determine the effect of *A. afra* on DNA fragmentation.

2.2.9. Statistical analysis

IC_{50} values of *A. afra* extracts were determined by using the GraphPad Prism Version 4.0 (GraphPad Software, San Diego, USA). Statistical significance was determined by using the two-tailed Student's *t*-test and $p<0.05$ was considered significant. For flow cytometry, a minimum of 10,000 events were recorded for each sample. Cell cycle analysis results were analyzed by using a Multicycle version 4.0 software.

3. Results

3.1. Cytotoxicity

The cytotoxic effects of the aqueous and ethanol *A. afra* extracts were determined by using the MTT assay and Cell Titre Blue assay for HeLa and U937 cancer cells respectively. The aqueous extract yielded IC_{50} values of greater than 250 μg/mL and thus was considered non-toxic (results not shown). Cytotoxicity was also determined by using confluent Chang liver cells and an IC_{50} value greater than 250 μg/mL was achieved for both extracts. The IC_{50} values obtained for the ethanolic extract against HeLa and U937 cancer cell lines were 31.88 ± 1.09 μg/mL and 18.21 ± 0.9 μg/mL, respectively (Fig. 1). From these results, the concentration of the ethanolic extract to be used for further experiments was fixed at 30 μg/mL for HeLa and 20 μg/mL for U937 cells.

3.2. Cell cycle analysis

DNA cell cycle analysis was performed on HeLa and U937 cancer cells after 12, 24 and 48 h of exposure to *A. afra* ethanol extract. After 12 h of exposure, an arrest of the cell cycle in the G2/M phase was noticed in HeLa cells (Fig. 2C) and U937 cancer cells (Fig. 2F). This was still evident after 24 and 48 h (data not shown).

3.3. Phosphatidylserine translocation

To determine the effect of *A. afra* exposure on the integrity of the cell membrane, Annexin-V FITC and PI staining was performed. HeLa and U937 cells were stained positive for Annexin-V and negative for PI after 24 h of exposure (Fig. 3A–C and 5D–F, respectively). A significant increase in the percentage of cells undergoing apoptosis was evident after 24 h of exposure to *A. afra* ethanol extract in both HeLa and U937 cancer cells. An increase from $5.83 \pm 1.33\%$ to $37.53 \pm 2.68\%$ ($p<0.005$) of apoptotic cells was recorded in HeLa cells and an increase from $4.73 \pm 0.38\%$ to $15.23 \pm 0.57\%$ ($p<0.005$) was recorded in U937 cancer cells.

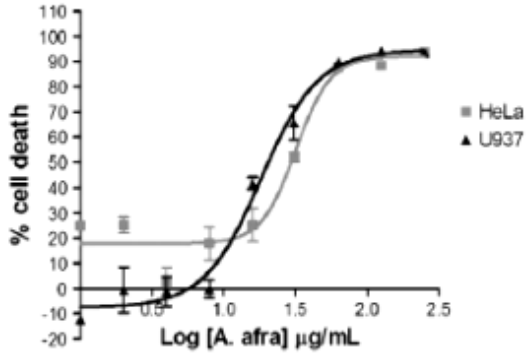

Fig. 1. Cytotoxic effect of *Artemisia afra* ethanol extract after 48 h of exposure. Cell viability was determined by using the MTT assay for HeLa and CellTitre Blue assay for U937 cells. Error bars indicate SD of four replicate values.

3.4. Mitochondrial membrane potential analysis

To determine the involvement of the mitochondria in the cell death pathway induced by *A. afra*, the mitochondrial potential was measured by using a lipophilic cationic dye, JC-1. This dye reversibly changes color from green to orange as the membrane potential increases. This property is due to the reversible formation of JC-1 aggregates upon membrane polarization. An increase in the mean green fluorescence intensity indicates a decrease in the mitochondrial membrane potential, suggesting that the mitochondria are involved in the onset of apoptosis (Table 1). Depolarization of the mitochondrial membrane is often associated with apoptosis by the release of pro-apoptotic proteins, such as cytochrome *c*, from the mitochondria and the formation of a pro-apoptotic complex (Adams and Cory, 1998; Vermeulen et al., 2005).

An increase in the mean green fluorescence intensity is noticed after 24 and 48 h of exposure to *A. afra*, thus the depolarization of the mitochondrial membrane. This suggests that the mitochondria are involved in the onset of apoptosis.

3.5. Caspase 8 and 3 activation

The caspase cascade plays a central role in the execution of apoptosis. Caspase 8 is an initiator caspase which forms part of the death inducing signaling complex (DISC) once a death signal is received by the cell. The formation of this complex allows for the autocatalytic cleavage of procaspases into active caspases. Activated caspases allow for the activation of the effector caspases, including caspase 3. Caspase 3 is known to be the main executioner of apoptosis by facilitating DNA fragmentation (Thornberry and Lazebnik, 1998; Vermeulen et al., 2005; Zangemeister-Wittke and Simon, 2001).

An increase in the log mean fluorescence value when compared to the untreated cell sample (control) indicates the presence of cleaved, or activated, caspase 8 or -3. A significant increase in both activated caspase 8 and -3 in HeLa and U937 (data not shown) cells was noticed after 24 h and 48 h of exposure to *A. afra*, respectively (Table 2).

3.6. DNA fragmentation

DNA fragmentation is characteristic of late apoptosis and was investigated in HeLa and U937 cancer cells (Fig. 4). Significant increases in

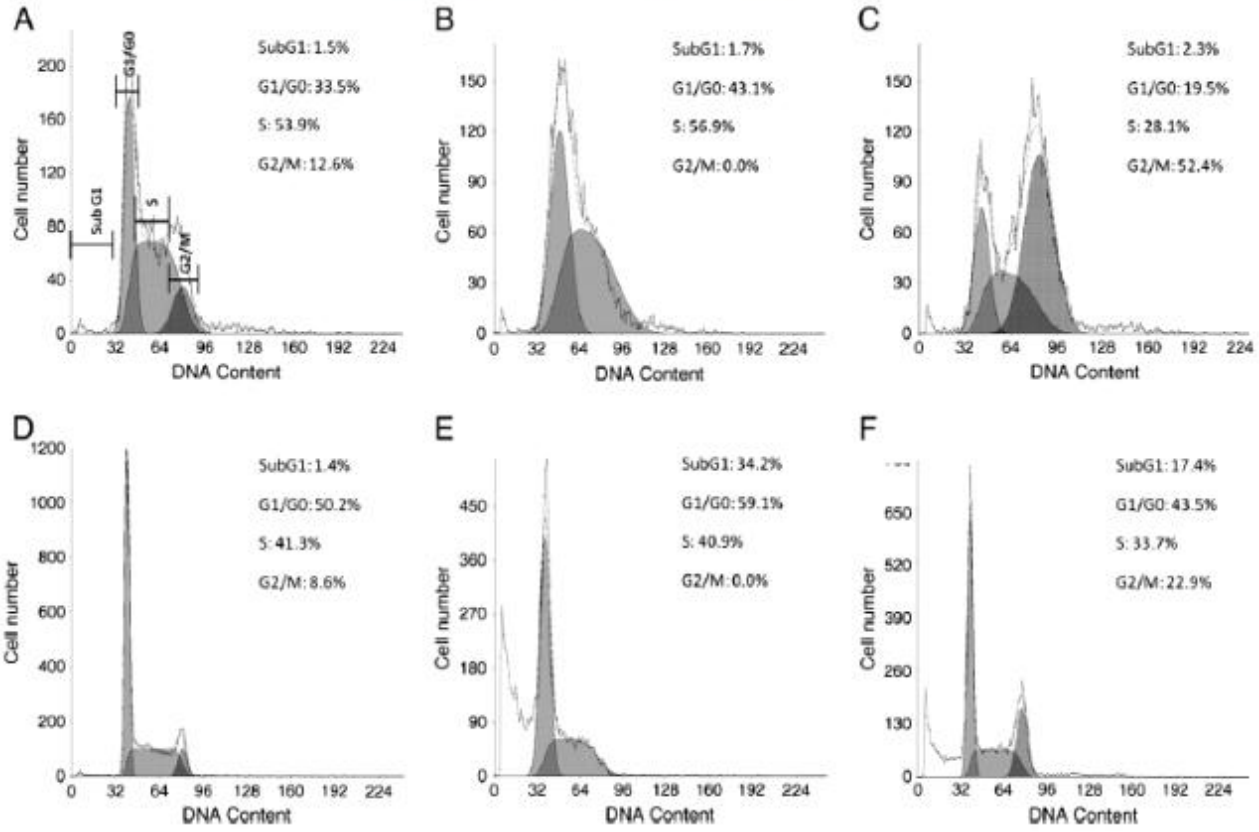

Fig. 2. Histograms representing DNA cell cycle analysis after 12 h of treatment in HeLa cells (A–C) and U937 cells (D–F). HeLa cells were treated with 40 μM melphalan (B) and 30 μg/mL *Artemisia afra* (C). U937 cells were treated with 40 μM melphalan (E) and 20 μg/mL *A. afra* (F). Control cell populations are represented by histograms A and D for HeLa and U937 cells respectively. Cell cycle analysis was done on a Beckman Coulter Cytomics FC500 after PI staining of DNA. Ten thousand events were recorded for each sample.

the amount of fragmented DNA were evident after 24 and 48 h in both cell lines.

4. Discussion

A. afra is known to be used to treat many different ailments and possesses antiviral, antibacterial and anti-inflammatory activities (Liu et al., 2009). Many different preparations of the plant including infusions, decoctions, brewing a tea and preparing a tincture by using the leaves and brandy are used to treat various symptoms. There is no reported evidence of its use for the treatment of cancer, but there has been reported evidence of its cytotoxicity (Fouche et al., 2008; Mativandlela et al., 2008).

Dose–response assays were performed by using the MTT assay for HeLa cells and the CellTitre Blue assay for U937 cells. An IC_{50} value of 113.0 ± 2.05 μg/mL against Vero cells was previously reported (Mativandlela et al., 2008). Vero cells are a continuous and non-tumor cell line and are used as a model for non-cancerous cells. The IC_{50} values achieved for both U937 and HeLa cells are promising as they are 3 to 5 times lower than that of the reported IC_{50} value obtained by using Vero cells for the ethanolic extract of *A. afra*. The IC_{50} value reported here for the Chang liver cells is >250 μg/mL, indicating that the ethanol extract is not toxic to this non-tumor cell line. Gertsch (2009) stated that extracts used at concentrations >200 μg/mL are likely to display artificial results in in vitro assays, despite their being reproducible and questions whether extracts used at concentrations >50 μg/mL are physiologically meaningful. Here, we achieved IC_{50} values below 50 μg/mL and displayed reproducible bioassay results.

A DNA cell cycle analysis was performed in order to determine if and which phase of the cell cycle the cells arrest in. Fig. 2C shows a cell cycle arrest in the G2/M phase of HeLa and U937 cells after 12 h of exposure to *A. afra*. Upon treatment of the cells with melphalan (40 μM), cells arrest in the S phase of the cell cycle (Fig. 2B). The mechanism of this G2/M arrest cannot be deduced from the PI cell cycle analysis and more than one possibility exists. The phosphatases Cdc25B and Cdc25C are regulators of the progression of the cell cycle from the G2 phase through the M phase. These proteins regulate the progression by its activity on Cdc2/cyclinA and Cdc2/cyclinB complexes (Busino et al., 2004). DNA damage causes G2/M arrest by the inhibition of the activation of Cdc2 (Hwang and Muschell, 1998). Active Cdc2 complexed to cyclin B1 is required for the progression from the G2 phase to the M phase of the cell cycle. Cdc25C dephosphorylates the active site of Wee1, which increases the activity of Cdc2. When DNA damage occurs, Chk1 is activated and deactivates Cdc25C. This results in the phosphorylation and inactivity of Cdc2/cyclinB complex and the cell arrests in the G2/M phase. G2/M arrest can also be associated with problems in the formation of the mitotic spindle resulting in mitotic catastrophe. G2/M arrest is an early event as it is apparent after 12 h of exposure to *A. afra*. Other apoptotic markers investigated here were evident later. This suggests that G2/M arrest may be the primary event occurring upon treatment with *A. afra* and apoptosis results in response to the mitotic catastrophe (Vakifahmetoglu et al., 2008).

The negatively charged phospholipid phosphatidylserine (PS) is located on the inner side of the plasma membrane lipid bilayer in most normal cells. During apoptosis, PS is translocated from the inner surface to the outer surface of the plasma membrane. Annexin V has a high affinity for PS and thus is used to determine the presence of PS on the surface of the cells. After 24 h of treatment with *A. afra*, a significant increase in the percentage of cells stained positive for Annexin-V was evident, confirming the occurrence of apoptosis. Propidium iodide was also used in the staining procedure to detect necrotic and/or late apoptotic cells (the latter also referred to as

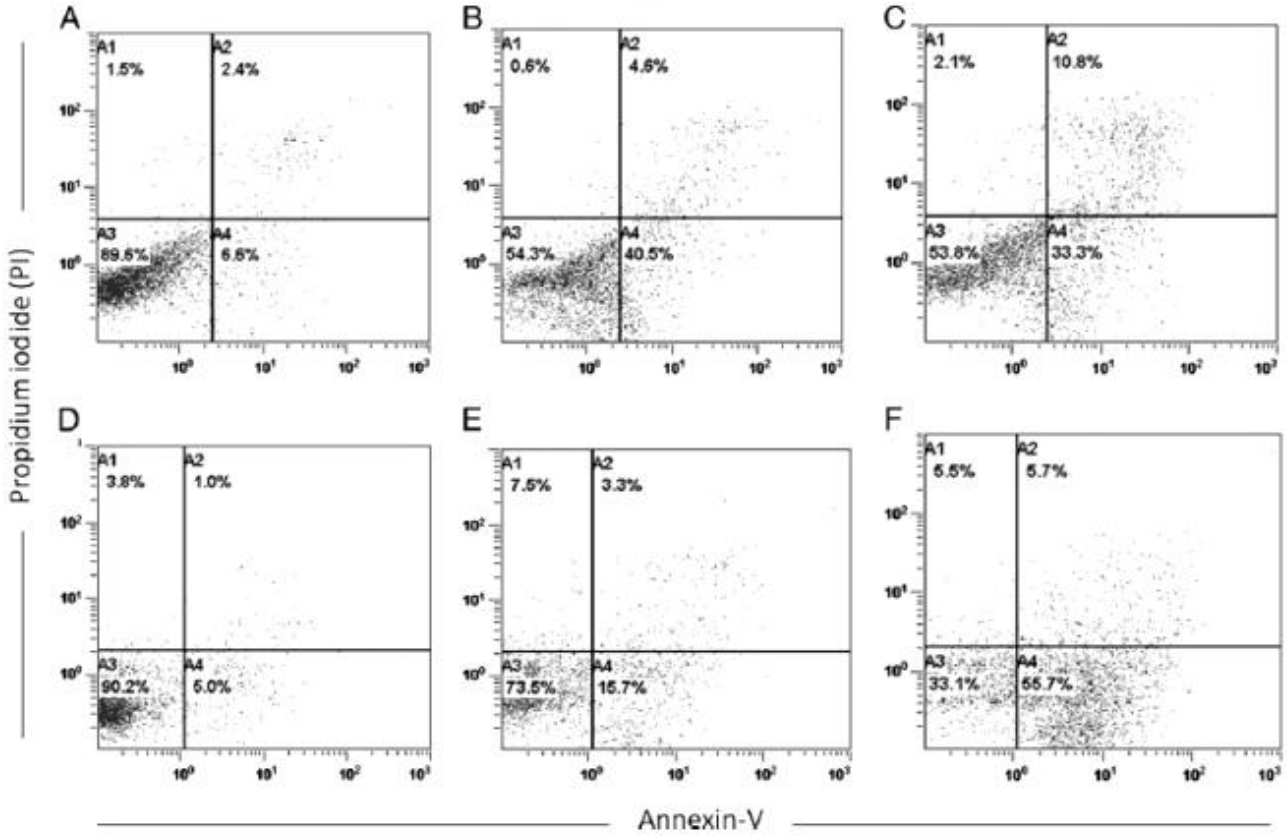

Fig. 3. Dot plots of Annexin V-FITC stained HeLa cells (A, B and C) and U937 cells (D, E and F) after 24 h exposure to medium only (A, D), 30 μg/mL and 20 μg/mL *Artemisia afra* (B, E; respectively) and 40 μM melphalan (C, F). Four quadrants represent unstained/live cells (A3: Annexin V-negative; PI-negative), early apoptotic cells (A4: Annexin V-positive; PI-negative), late apoptotic cells (A2: Annexin V-positive; PI-positive) and necrotic cells (A1: Annexin V-negative; PI-positive). A minimum of 20,000 events were read (n = 3).

"secondary necrosis"). During early apoptosis the plasma membrane is still intact, but becomes leaky with the onset of late apoptosis or necrosis and an increase in PI positive cells will be evident (Koopman et al., 1994). No increase was observed in PI positive cells in this study, confirming that cell death was not due to necrosis.

In the intrinsic pathway of apoptosis, caspase activation is closely linked to the permeabilization of the outer mitochondrial membrane by pro-apoptotic proteins. Cytotoxic stimuli may induce outer membrane permeabilization resulting in depolarization of the mitochondria. A set of proteins normally found between the inner and outer membranes is released including cytochrome *c*, Smac/DIABLO, Omi/HtrA2, AIF and endonuclease G. Once released in the cytosol, these proteins promote caspase activation or may act as caspase-independent death effectors (Saelens et al., 2004). As mentioned, the lipophilic dye, JC-1 was used to determine the state of the mitochondrial membrane after the treatment of cancer cells with *A. afra* extract. A significant increase in the mean green fluorescence intensity was observed, suggesting the depolarization of the mitochondrial membrane. Thus it is deduced that the intrinsic pathway plays a role in the execution of apoptosis induced by *A. afra*. The intrinsic pathway can be activated in the presence of intracellular signals or in response to the activation of death receptors on the plasma membrane. Caspase 8 activation occurs when the death inducing signaling complex (DISC) is formed in response to an extracellular signal. Thus, the activation of caspase 8 in response to extract treatment would also suggest a cellular response to an external signal for cell death. Hence, activated caspase 8 can be used as a convenient indicator of involvement of the extrinsic death receptor pathway of apoptosis (Fulda and Debatin, 2006).

Caspase activation was determined by using immunochemistry. Antibodies against activated caspase 8 and caspase 3 were used. Caspase 8 is an initiator caspase which is first activated through a death signal, suggesting a cellular response to an external signal for cell death.

Table 1
Summary of results obtained for analysis of mitochondrial membrane potential after treatment with melphalan (40 μM) and *A. afra* ethanol extract.

Treatment		Mean green fluorescence intensity[a] for Hela cells	Mean green fluorescence intensity[a] for U937 cells
24 h	Control	19.03 ± 3.46	19.25 ± 3.46
	Melphalan	41.93 ± 0.21**	85.75 ± 0.21**
	A. afra	70.40 ± 0.92**	69.45 ± 0.92**
48 h	Control	9.99 ± 2.81	24.93 ± 1.44
	Melphalan	105.77 ± 9.62**	257.71 ± 16.40**
	A. afra	34.83 ± 0.97**	144.25 ± 4.29**

[a] Mean of green flourescence intensity. Depolarization is accompanied by an increase in green and a decrease in red flourescence.
** Significantly higher than control; p<0.005: significance was determined by using the two-tailed Student's *t*-test.

Table 2
Summary of results obtained for analysis of caspase 8 and caspase 3 activation in HeLa cells after treatment with melphalan (40 μM) and *A. afra*.

Treatment		Percentage (%) of control	
		Cleaved caspase 8	Cleaved caspase 3
12 h	Control	100.00 ± 5.324	100.00 ± 7.46
	Melphalan	127.79 ± 13.43	92.50 ± 13.72
	A. afra	105.36 ± 15.89	115.12 ± 22.99
24 h	Control	100.00 ± 4.76	100.00 ± 8.67
	Melphalan	157.47 ± 34.25**	161.80 ± 19.51**
	A. afra	189.28 ± 44.82**	153.38 ± 19.61**
48 h	Control	100.00 ± 5.83	100.00 ± 5.75
	Melphalan	288.89 ± 39.49**	331.77 ± 39.30**
	A. afra	143.07 ± 23.16*	285.15 ± 48.95**

Significance was determined by using the two-tailed Student's *t*-test: *p<0.05; **p<0.005 compared to control.

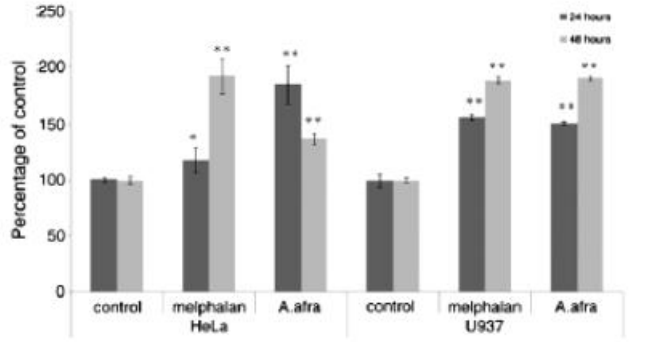

Fig. 4. DNA fragmentation in HeLa and U937 cells after 24 and 48 h of exposure to treatments. Cells were treated with 40 μM melphalan, 20 μg/mL *Artemisia afra* ethanolic extract (U937) or 30 μg/mL *A. afra* ethanolic extract (HeLa). Bar graph represents the average of two individual experiments each performed in triplicate. 10,000 events were recorded per sample. Significance was determined by using the two-tailed Student's *t*-test: *$p<0.05$; **$p<0.005$ compared to control.

Executioner caspases, including caspase 3, are in turn activated by the initiator caspases. The activation of both caspase-8 and caspase-3 is evident for both HeLa (Table 2) and U937 cells although the data for U937 cells are not shown. It is thus deduced that the cell death pathway induced by *A. afra* is caspase dependent and involves both the extrinsic and intrinsic pathways.

One of the later steps in apoptosis is the degradation or fragmentation of DNA by activated endonucleases and/or activated executioner caspases. Caspase-3 and caspase-7 are executioner caspases responsible for the degradation of the chromatin structure into fragments of ~300 kb and then into smaller fragments of ~50 kb. In order to detect the DNA fragments, the TUNEL (terminal deoxynucleotidyltransferase dUTP nick end labeling) method was used. FITC-labeled dUTP DNA fragments were detected by using flow cytometry and a significant increase in the amount of fragmented DNA was noticed after 48 h of exposure to *A. afra* in both HeLa and U937 cell lines confirming the involvement of apoptosis in the cytotoxic mechanism of *A. afra* (Fig. 4).

Taken together our results demonstrate for the first time that *A. afra* has potential anti-cancer properties despite the absence of ethnobotanical reports. However, *A. afra* is used to treat inflammation associated with various diseases (Liu et al., 2009). This study has shown that upon treatment of HeLa and U937 cells with an ethanol extract of *A. afra*, apoptosis is induced. The mechanism of induction of cell death upon treatment with an ethanolic extract of *A. afra* is accompanied by G2/M cell cycle arrest and depolarization of the mitochondrial membrane. Caspase-8 and caspase-3 are both activated resulting in the fragmentation of the DNA, a characteristic of late apoptosis. Since these studies were conducted on a crude extract, we cannot rule out the possibility that different primary cell death mechanisms were activated due to the multicomponent nature of the extract. Jennet-Siems et al. (2002) identified sesquiterpene lactones as the cytotoxic compounds of *A. afra*. Studies are currently underway to identify/confirm the active component(s) and to characterize the precise mechanism of action of cytotoxicity induced by *A. afra*.

References

Abdool Karim, S.S., Ziqubu-Page, T.T., Arendse, R., 1994. Bridging the gap: potential for a health care partnership between African traditional healers and biomedical personnel in South Africa. South African Medical Journal 84, s1–s16.

Adams, J.M., Cory, S., 1998. The Bcl-2 protein family: arbiters of cell survival. Science 281, 1322–1326.

Busino, L., Chiesa, M., Draetta, G.F., Donzelli, M., 2004. Cdc25A phosphatase: combinatorial phosphorylation, ubiquitylation and proteolysis. Oncogene 23, 2050–2056.

Cragg, G.M., Newman, D.J., 2005. Plants as a source of anti-cancer agents. Journal of Ethnopharmacology 100, 72–79.

Elmore, S., 2007. Apoptosis: a review of programmed cell death. Toxicologic Pathology 35, 495–516.

Fouche, G., Cragg, G.M., Pillay, P., Kolesnikova, N., Maharaj, V.J., Senabe, J., 2008. In vitro anticancer screening of South African plants. Journal of Ethnopharmacology 119, 455–461.

Fulda, S., Debatin, K.-A., 2006. Extrinsic versus intrinsic apoptosis pathways in anticancer chemotherapy. Oncogene 25, 4798–4811.

Gertsch, J., 2009. How scientific is the science of ethnopharmacology? Historical perspectives and epistemological problems. Journal of Ethnopharmacology 122, 177–183.

Gurib-Fakim, A., 2006. Medicinal plants: traditions of yesterday and drugs of tomorrow. Molecular Aspects of Medicine 27, 1–93.

Hwang, A., Muschell, R.J., 1998. Radiation and the G2 phase of the cell cycle. Radiation Research 150, S52–S59.

Jennet-Siems, K., Köhler, I., Kraft, C., Beyer, G., Melzig, M.F., Eich, E., 2002. Cytotoxic constituents from *Exostema mexicanum* and *Artemisia afra*, two traditionally used plant remedies. Pharmazie 57, 351–352.

Koopman, G., Reutelingsperger, C.P., Kuijten, G.A., Keehnen, R.M., Pals, S.T., Van Oers, M.H., 1994. Annexin V for flow cytometric detection of phosphatidylserine expression on B cells undergoing apoptosis. Blood 84, 1415–1420.

Liu, N.Q., Van der Kooy, F., Verpoorte, R., 2009. *Artemisia afra*: a potential flagship for African medicinal plants? South African Journal of Botany 75, 185–195.

Louw, C.A.M., Regnier, T.J.C., Korsten, L., 2002. Medicinal bulbous plants of South Africa and their traditional relevance in the control of infectious diseases. Journal of Ethnopharmacology 82, 147–154.

Mativandlela, S.P.N., Meyer, J.J.M., Hussein, A.A., Houghton, P.J., Hamilton, C.J., Lall, N., 2008. Activity against *Mycobacterium smegmatis* and *M. tuberculosis* by extract of South African medicinal plants. Phytotherapy Research 22, 841–845.

McGaw, L.J., Eloff, J.N., 2008. Ethnoveterinary use of southern African plants and scientific evaluation of their medicinal properties. Journal of Ethnopharmacology 119, 559–574.

Saelens, X., Festjens, N., Van de Walle, L., Van Gurp, M., Van Loo, G., Vandenabeele, P., 2004. Toxic proteins released from mitochondria in cell death. Oncogene 23, 2861–2874.

Schafer, K.A., 1998. The cell cycle: a review. Veterinary Pathology 35, 461–478.

Thornberry, N.A., Lazebnik, Y., 1998. Caspases: enemies within. Science 281, 1312–1316.

Vakifahmetoglu, H., Olsson, M., Zhivotovsky, B., 2008. Death through a tragedy: mitotic catastrophe. Cell Death and Differentiation 15, 1153–1162.

Vermeulen, K., Berneman, Z.N., Van Bockstaele, D.R., 2005. Apoptosis: mechanisms and relevance in cancer. Annals of Hematology 84, 626–639.

Zangemeister-Wittke, U., Simon, H.U., 2001. Apoptosis — regulation and clinical implications. Cell Death and Differentiation 8, 537–544.

Isoalantolactone, a newly isolated sesquiterpene lactone from *Artemisia afra* Jacq. ex Willd and its *in vitro* mechanism of induced cell death in HeLa cells.

Luanne Venables[a], *Trevor. C. Koekemoer*[a], *Maryna van de Venter*[a,*] *and Eleonora.D Goosen*[b].

[a] Department of Biochemistry and Microbiology, PO Box 77000, Nelson Mandela Metropolitan University, Port Elizabeth 6031, South Africa.

[b] Division of Pharmaceutical Chemistry, Faculty of Pharmacy, Rhodes University, Grahamstown, South Africa.

[*] Corresponding author. Tel: +27 41 504 2813; Fax: +27 41 504 2814; E-mail address: maryna.vandeventer@nmmu.ac.za (M. van de Venter)

Keywords: *A. afra*, isoalantolactone, NMR spectroscopy, cytotoxicity, apoptosis.

ABSTRACT:

Isoalantolactone is a sesquiterpene lactone (SL) that has not yet been isolated from *Artemisia afra*, a South African plant that is commonly used in the Eastern Cape Province as a traditional remedy for inflammation and respiratory ailments. Recently, an ethanol extract of *A. afra* has shown to induce caspase-dependent apoptosis in a mitochondrial-dependent manner. In the current study, bio-assay guided fractionation was used to isolate isoalantolactone from *A. afra*. Structural elucidation was done by IR, 1D and 2D NMR, CD and mass spectrometry. HeLa cancer cells were treated with isoalantolactone and cytotoxicity was exhibited in a dose-dependent manner. A low IC_{50} value of 8.15 ± 1.16 µM was achieved. In this study, we show that after 24 hours of treatment of HeLa cells with 8.62 µM Isoalantolactone, a delay in G2/M phase of the cell cycle was evident accompanied by a decrease in mitochondrial membrane potential. Apoptosis was confirmed using the TUNEL assay to detect DNA fragmentation and phosphatidylserine translocation was detected using Annexin-V/FITC staining after 24 hours of exposure to this compound. In summary, we show that cytotoxic isoalantolactone isolated from *A. afra* induces apoptosis in a mitochondrial and caspase-dependent manner and thus contributes to cytotoxicity induced by *A. afra*.

INTRODUCTION:

Plants are a rich source of natural products for the treatment of many medical conditions and have played an important role as a source of anti-cancer agents (Cragg and Newman, 2005). Plant derived drugs used for cancer treatment include vinblastine, vincristine, camptothecin derivatives, topotecan, irinotecan, etoposide and paclitaxel. A number of new plant derived agents are in clinical development and sesquiterpene lactones (SLs) are no exception. SLs are a stable class of terpenoids and have been isolated from a number of plant families, but the greatest number of SLs has been isolated from the Asteraceae (Compositae) family with over 300 reported different structures (Ghantous *et al.,* 2010; Chaturvedi, 2011). It is known that SLs possess cytotoxic activity against various cell lines (Ghantous *et al.,* 2010; Zhang *et al.,* 2005; Schmidt and Heilmann, 2002). QSAR studies have indicated that the biological activities, including cytotoxicity, are mediated chemically by moieties such as the α-methylene-γ-lactone group present in Isoalantolactone (Schmidt and Heilmann, 2002).

Artemisia afra, a South African plant also belonging to the Asteraceae family, is used traditionally for the treatment of various ailments, including inflammation, respiratory diseases and colon conditions. The plant is prepared in different ways for its specific use (Liu *et al.,* 2009). A large number of SLs have been isolated from the *Artemisia* genus (Geissman, 1970; Irwin and Geissman, 1973; Nagaki, 1984; Jakupovic *et al.,* 1986; Jakupovic *et al.,* 1986; Marco *et al.,* 1993; Sy and Brown, 2001; Iranshashi *et al.,* 2007); and glaucolides and guaianolides have been isolated from *A. afra* (Jakupovic *et al.,* 1998). Recently, an ethanol extract of *A. afra* has been shown to induce cell death via mitochondrial- and caspase-dependent apoptosis after a delay in the G2/M phase of the cell cycle in both HeLa and U937 cancer cells (Spies *et al.,* 2013). Thus, it was our objective to isolate and identify the compound(s) in this extract responsible for the induction of this cell death pathway. The SL, isoalantolactone (compound **1**) was isolated and identified as one of the major cytotoxic compounds in the *A. afra* ethanol extract.

Isoalantolactone is known to be a major sesquiterpene lactone found in the roots of the *Inula* species. *I. racemosa* and *I. helenium* are plants that are used as traditional medicine in India, China and Europe for the treatment of abdominal pain, acute enteritis, asthma, lung disorders, tuberculosis, bacillary dysentery and infectious and helminthic diseases (Huo *et al.,* 2010). It has recently been shown that commercial, synthetic isoalantolactone induces apoptosis via a reactive oxygen species mediated pathway and its mechanism of cytotoxicity has been well characterized in pancreatic cancer cells (Khan *et al.,* 2012; Rasul *et al.,* 2013). Here we describe, for the first time, the isolation of isoalantolactone from *A. afra* and show that it is one of the main compounds responsible for apoptosis induction of *A. afra* in HeLa cells.

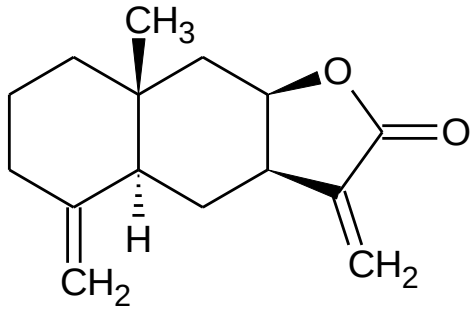

1

MATERIALS AND METHODS:

General experimental procedures: Column chromatography was on performed silica gel (0.063 mm – 0.200 mm, Merck 7754) and preparative TLC on a 0.2mm silica gel, aluminium backed plate (Merck Art. 5554). Leaves of *A. afra* were collected from Port Elizabeth, South Africa, in April 2011. The plant was identified by the Botany Department at Nelson Mandela Metropolitan University and herbarium specimen voucher number *Artemisia afra* 15487 was deposited in the Nelson Mandela Metropolitan University Herbarium, Botany Department, South Campus. Fresh leaves were ground using a blender and submerged in 80% ethanol and left overnight in the dark. The extract was filtered through a Whatman filter paper (1.1 µm), the ethanol was removed by evaporation under nitrogen and the remaining aqueous solution freeze dried. The extract was stored in a desiccator at 4°C in the dark. Column chromatography of 2.204 g of the dried extract was performed using a 1cm diameter gravity column collecting 10ml fractions using a hexane/ethylacetate stepwise gradient. 56.8 mg of the cytotoxic fraction 8 was further purified by preparative TLC using 50% hexane/ethylacetate as eluent and yielded 14.8 mg Isoalantolactone, (3a*R*,4a*S*,8a*R*,9a*R*)-decahydro-8a-methyl-3,5-dimethylidenenaphtho[2,3-b]furan-2(3H)-one), (Rf=0.65) TLC visualisation was done at 254nm. IR spectra were recorded on a Perkin Spectrum 400 FT-IR/FT-FIR spectrometer with an ATR sampling accessory. 1D and 2D NMR experiments were obtained on a Brucker Avance II 600Mhz spectrometer using standard pulse sequences. ^{1}H and ^{13}C NMR experiments were recorded in $CDCl_3$ (Merck S5536220) at 600.03 and 150.89 MHz, respectively, using residual solvent signals as internal references. The GC/ EI MS was obtained on an Agilent Technologies MS system (6890N) and the CD spectrum recorded in methanol on an Applied Photophysics Chirascan Plus spectrometer at 293 K with a path length of 10mm.

Cell culture conditions: The adherent cancer cell line, HeLa cells, was used for the experimental procedures. The cells were routinely maintained in 10 cm culture dishes without antibiotics in RPMI 1640 cell culture medium containing 25 mM Hepes, 2 mM glutamine, supplemented with 10% foetal bovine serum and incubated in a humidified 5% CO_2 incubator at 37°C. Trypan blue was used to determine cell viability and cell number. Counting of cells was done using an improved Neubauer haemocytometer and cell densities (number of cells per mL) were altered according to the number of cells required for each experiment.

Cytotoxicity: Fractions were tested for cytotoxic activity using concentrations of 3.0, 30.0 and 100.0 µg/mL. HeLa cells were seeded in 200 µL aliquots at $3x10^4$ cells/mL in 96 well plates and left overnight to attach. The medium was replaced with fresh medium containing a particular fraction at a particular concentration and incubated at 37°C in a humidified 5% CO_2 incubator for 48 hours. Cytotoxicity assays were performed using MTT (5 mg/mL). The medium was removed prior to addition of MTT to HeLa cells. Melphalan (40 µM) was used as a positive control for all experiments. Absorbance was read at 540 nm using a BioTek® PowerWave XS spectrophotometer (Winooski, VT, USA).

Cell cycle analysis: HeLa cells (5×10^4 cells/mL) in a 10 cm culture dish were treated with 2 µg/mL isoalantolactone for 12 hours. Cells were trypsinized and harvested and resuspended in PBS and transferred to polypropylene tubes. DNA cell cycle analysis was performed using the Coulter® DNA Prep™ reagents kit as per manufacturer's instructions. Briefly, cells were incubated with 100 µL lysis buffer for 5 minutes at room temperature. Thereafter, 500 µL propidium iodide (50 µg/mL) was added and cells were incubated for 15 minutes at 37°C. Cells were analysed using flow cytometry immediately after incubation. A Beckman Coulter Cytomics FC500 was used for all flow cytometry analysis.

Phosphatidylserine translocation: HeLa cells were seeded in a 6 well plate at a cell density of 5×10^4 cells/mL using 3 mL aliquots. Cells were treated with 2 µg/mL (8.62µM) isoalantolactone and incubated for 24 hours at 37°C. After treatment, HeLa cells were washed with ice-cold Dulbecco's Modified Eagle's Medium (DMEM). Cells were detached from the plate using accutase and thereafter transferred to polypropylene tubes and centrifuged at 500 xg for 5 minutes at room temperature. Cells were washed with PBS to remove accutase. Cells were stained according to Annexin V-FITC/PI Kit protocol (MACS Miltenyi Biotec, USA). Briefly, cell pellets were resuspended in ice-cold 1x binding buffer. Annexin V-FITC (1 µL; 25µg/mL) and PI (5 µL; 250 µg/mL) were added to each tube. Compensation control tubes were prepared containing cells stained with Annexin V-FITC only, PI only and combination of Annexin V-FITC and PI. Tubes were gently mixed and incubated on ice for 15 min in the dark. Samples were read within 30 min on a Beckman Coulter Cytomics FC500.

Mitochondrial membrane potential (MMP) analysis: HeLa cells were seeded and treated as described for analysis of phosphatidylserine translocation. Cells were incubated for 12 and 24 hours. After incubation, cells were collected and transferred to polypropylene tubes by centrifugation at 500 xg for 15 minutes at room temperature. Cells were washed using PBS. Thereafter, a lipophilic cationic dye, 5,5',6,6'tetrachloro-1,1',3,3'-tetraethylbenzimidazol-carbocyanine iodide JC-1, was added to each tube to a final concentration of 2 µg/mL and incubated for 10 minutes at room temperature in the dark. Cells were then washed thoroughly using 500 µL PBS and centrifuged at 500 xg for 5 minutes to remove unwanted JC-1. This wash step was repeated three times before flow cytometric analysis.

Caspase -8 and -3 activation: Cells were seeded and treated as described for MMP analysis. Cells were fixed and permeabilized using the IntraPrep kit. Cleaved caspase -8 (Asp 391) and cleaved caspase -3 (Asp 175) monoclonal antibodies were used to determine the presence of cleaved caspase 8 and caspase 3 respectively, i.e. activated caspases. Cells were first blocked using PBS containing 0.5 % BSA and thereafter incubated with the antibodies separately (1:100 for caspase 8 and 1:50 for caspase 3) for 1 hour at 37°C. Cells were washed and incubated with the conjugated secondary antibody (1:1000) for 30 minutes at 37°C in the dark. This step was not required for caspase 3 analysis as the antibody contains a conjugated FITC fluorophore. Cells were then analyzed using flow cytometry.

DNA fragmentation: HeLa cells were seeded, treated, fixed and permeabilized as described for caspase analysis. Cells were incubated for 24 hours. The Apo-Direct DNA Fragmentation kit was used as per manufacturer's instructions. In brief, cells were resuspended in 1 mL wash buffer and centrifuged at 500 xg for 5 minutes. DNA labelling solution was prepared using reaction buffer, TdT enzyme, FITC dUTP and distilled water. The DNA solution was prepared as per manufacturer's instructions. Cells were incubated in 50 µL DNA labelling solution for 60 minutes at 37°C and thereafter washed with 1 mL rinse buffer and centrifuged as described. This rinse step was repeated twice. Cells were then analysed using flow cytometry.

Statistical analysis: IC_{50} values were determined using GraphPad Prism Version 4.0 (GraphPad Software, San Diego, USA). Each treatment was performed in triplicate (n=3) and each experiment was conducted three independent times. SD represents standard

deviation of the mean of all experimental data. Statistical significance was determined using the two-tailed student's *t*-test and $p<0.05$ was considered significant. For flow cytometry, a minimum of 10 000 events were recorded for each sample. Cell cycle analysis results were analysed using Multicycle version 4.0 software.

RESULTS AND DISCUSSION:

Isolation and structural elucidation of isoalantolactone (1) from A. afra: Bio-assay guided fractionation of an ethanol extract of *A. afra* using column chromatography and TLC resulted in the isolation of isoalantolactone (**1**), a sesquiterpene lactone that has hitherto not been reported to have been isolated from this plant. The structure of isoalantolactone was elucidated by spectroscopic methods including, IR, 1D and 2D NMR techniques as well as EI-MS and were congruent with previously reported data (Miller and Nash, 1974; Bohlmann *et al.,* 1978). The negative Cotton effect at 257 nm confirmed the absolute configurations at carbons eight and nine as 8*R* and 9*R,* leading to a *cis*-fused lactone ring. This was also congruent with previously reported X-ray data (Cantrell *et al.,* 2010). All spectral data is provided in Supporting Information.

Cytotoxicity of fractions and IC_{50} determination of isoalantolactone against HeLa cells: Bio-assay guided fractionation of an ethanol extract of *A. afra* using column chromatography resulted in the production of 16 fractions. Fractions 7 to 16 were tested for cytotoxicity using HeLa cancer cells and the MTT cytotoxicity assay (Figure S2, Supporting Information). Fraction 8 showed to be the most cytotoxic and further purification resulted in the isolation of a single compound identified as isoalantolactone. A dose-dependent cytotoxicity assay yielded an IC_{50} value of 1.89 ± 0.11 µg/mL after 48 hours of treatment with isoalantolactone (Figure 1). When considering the molecular mass of this compound, 232.15 g/mol (Supporting Information, S13), this IC_{50} value can be converted to a Molar value of 8.15 ± 1.16 µM. Khan *et al.* (2012) reported an IC_{50} value for isoalantolactone of 40, 43 and 48 µM against PANC-1 (pancreas/duct cancer), BxPC3 (pancreatic cancer) and HPAC (pancreatic adenocarcinoma epithelial) cells, respectively. In a study using prostate cancer cells, isoalantolactone induced cell death using IC_{50} values of 27.84, 33.84 and 29.84 µM for LNCap (androgen-responsive prostate cancer), PC-3 and DU-145 (androgen-insensitive prostate cancer) cells (Rasul *et al.,* 2013). A review article by Gertsch (2009)

implies that this value is too high for a pure compound to have clinical significance. In our study, we show isoalantolactone isolated from *A. afra* to have an IC_{50} value of 8.15 µM against HeLa cells, which is considered more meaningful. However, dose-response assays were conducted for a 24 hour exposure time for the above mentioned studies where the IC_{50} determined here was determined after 48 hours of exposure. IC_{50} value obtained here is in line with the data presented by Ma *et al.* (2013) where HepG2 cells were treated with isoalantolactone and an IC_{50} value of 7.65 µM was achieved using the CCK-8 method and exposing the cells to isoalantolactone for 72 hours.

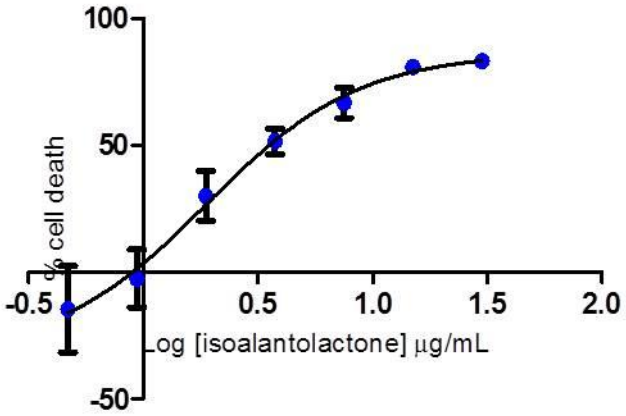

Figure 1: Dose-response curve of isoalantolactone tested using HeLa cells after 48 hours of exposure. Cell viability was tested using MTT. Error bars indicate SD values of quadruplicate readings.

G2/M cell cycle arrest was evident after 12 hours of exposure to isoalantolactone: DNA cell cycle analysis was performed in order to determine in which phase of the cell cycle the cells arrest in, if any. Table 1 shows a significant increase in the amount of DNA in the G2/M phase of the cell cycle. This is consistent with the findings of Rasul *et al.* (2013), where prostate cancer cells were treated with isoalantolactone. However, cell cycle analysis of pancreatic cancer cells showed an arrest in the S phase of the cell cycle after 24 hours of treatment (Khan *et al.*, 2012). From the cell cycle analysis results obtained here, one cannot determine whether the delay is observed in the G2 phase or the M phase of the cell cycle and further investigation needs to be done in order to determine exactly which phase it is. In saying this, a number of possibilities exist. The progression of the cell cycle from the G2 phase through the M phase is regulated by the phosphatase Cdc25B and Cdc25C. The

physiological substrates for these enzymes are the cyclin-dependent kinases known as Cdk's, which are complexed with cyclins. Cdk's are the inactive catalytic subunit and requires association with a positive regulatory subunit, the cyclin. In order for the complex to be active, phosphorylation of the catalytic subunit and dephosphorylation of threonine 14 and tyrosine 15 of Cdk is required (Kristjánsdóttir and Rudolph, 2004). Active Cdc2 complexed to cyclin B1 is required for the progression from the G2 phase to the M phase of the cell cycle. Cdc25C dephosphorylates the active site of Cdc2, which increases its activity. When DNA damage occurs, Chk1 is activated and deactivates Cdc25C. This results in the phosphorylation and inactivity of cdc2/cyclinB complex and the cell arrests in the G2/M phase (Castedo *et al.,* 2004). G2/M arrest can also be associated with problems in the formation of the mitotic spindle resulting in mitotic catastrophe. An investigation into the state of cdc2 and cyclin B1, as well as the mitotic spindle is being conducted to determine whether cells are progressing into the M phase of the cell cycle.

Table 1: The average percentage cells present in the various indicated stages of the cell cycle after 12 hours of treatment in HeLa cells.

Treatment	sub G1	G0/G1	S	G2/M
Untreated control	1.33 ± 0.55	50.23 ± 3.25	20.1 ± 2.49	16.3 ± 0.98
isoalantolactone (2 µg/mL)	6.3 ± 1.1 *	51.97 ± 2.7	10.73 ± 3.42 *	21.53 ± 1.21 *

* Significance determined using Student ttest: $p<0.05$

Apoptosis in HeLa cells is induced by treatment with isoalantolactone: Phosphatidylserine translocation is a biochemical feature of apoptosis and is often used as a marker of apoptosis. The negatively charged phospholipid phosphatidylserine (PS) is located on the inner side of the plasma membrane lipid bilayer of most normal cells. During apoptosis, this phospholipid is translocated to the outside of the membrane and can be detected by Annexin V. Annexin V has a high affinity for PS (Koopman *et al.,* 1994). Propidium iodide is also used in the staining procedure to detect late apoptotic or necrotic cells. Figure 2 indicates a significant increase in the percentage of cells in the A4 quadrant of the dot plots. This quadrant correlates with cells undergoing early apoptosis and is said to be Annexin V positive and PI negative. An increase in late apoptotic cells is also evident. This

too is consistent with previous reports of apoptosis induction by isoalantolactone (Khan *et al.*, 2012; Rasul *et al.*, 2013) and also with reported evidence that ethanolic *A. afra* induces apoptosis (Spies *et al.*, 2013). However, lower percentage of apoptotic cells is evident here when considering published data. Khan *et al.* (2012) and Rasul *et al.* (2013) used 20 µM and 40 µM isoalantolactone, at least double the µM concentration used in this study. This can explain the difference in the percentage of cells undergoing early and late apoptosis. A greater cell population stained positive for PI and negative for Annexin V is also evident in the result published for PS translocation by Rasul *et al.*, (2013). This is an indication of necrotic cell death. This result was not evident when treating HeLa cells with 8.62 µM isoalantolactone for 24 hours.

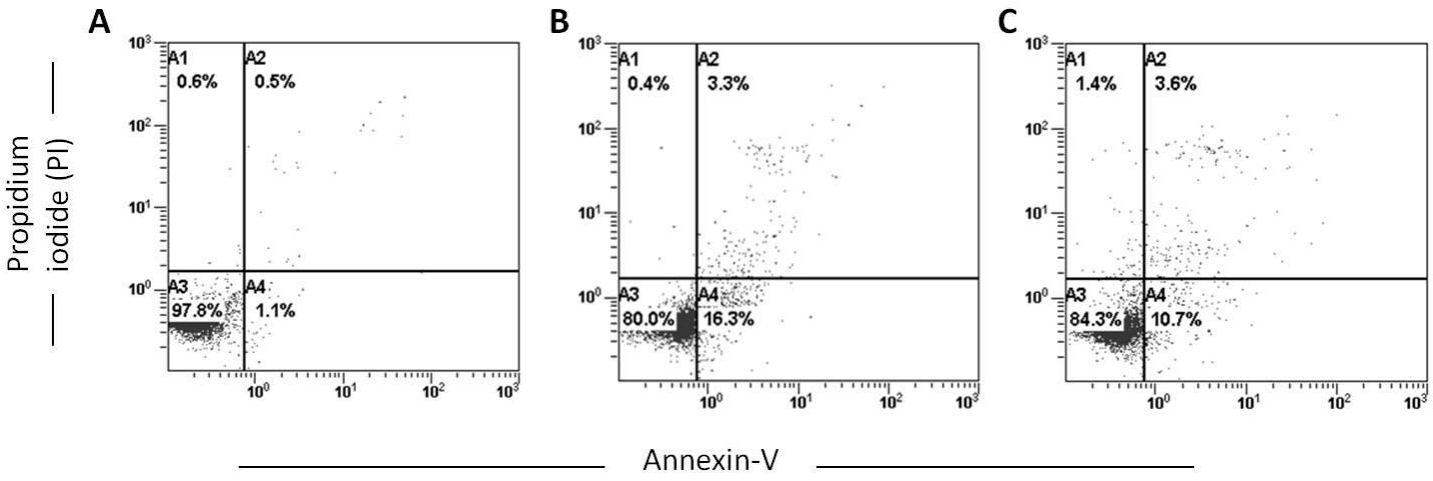

Figure 2: Dot plots of Annexin V-FITC stained HeLa cells (A, B and C). A; control population, B; cells treated with 30 µg/mL *A. afra,* C; cells treated with 2 µg/mL isoalantolactone. Four quadrants represent unstained/live cells (A3: Annexin V-negative; PI-negative), early apoptotic cells (A4: Annexin V-positive; PI-negative), late apoptotic cells (A2: Annexin V-positive; PI-positive) and necrotic cells (A1: Annexin V-negative; PI-positive). A minimum of 20 000 events were read (n=3).

Isoalantolactone treatment causes mitochondrial membrane depolarization and caspase activation: In the intrinsic pathway, apoptosis is initiated within the cell. It is usually in response to cellular signals resulting from DNA damage, a defective cell cycle, detachment from the extracellular matrix, hypoxia and severe cell stress (Vermeulen *et al.*, 2005). This pathway involves the release of pro-apoptotic proteins from the mitochondria which, in turn,

results in the activation of caspases, which ultimately leads to apoptosis. The execution of the intrinsic pathway of apoptosis is dependent on the balance of activity between pro- and anti-apoptotic proteins in the cell (Saelens *et al.*, 2004). Upon release of pro-apoptotic proteins, the mitochondrial membrane will experience depolarization (Vermeulen *et al.*, 2005). As mentioned, JC-1 dye was used to determine the state of the mitochondrial membranes after treatment of cancer cells with isoalantolactone. A significant increase in the mean green fluorescence intensity was observed (Table 2), suggesting depolarization of the mitochondrial membranes. Previous studies have also indicated a decrease in mitochondrial membrane potential. In conjunction with this evident MMP decrease, apoptotic regulatory proteins associated with the mitochondria have also been investigated. It has been shown that treatment of pancreatic cancer cells with isoalantolactone, 20 µM, results in increased expression of Bax, a decreased expression of Bcl-2 accompanied by the release of cyt-*c*, which in turn activates caspase -3 (Khan *et al*, 2012).

Table 2: Mitochondrial membrane depolarization of HeLa cells after 24 hours of treatment.

Treatment	Mean green fluorescence intensity
Untreated	1.39 ± 0.13
isoalantolactone (2µg/mL)	9.78 ± 0.56 **
melphalan (µM)	22.90 ± 1.36 **

Significance determined using Student ttest: *p<0.05, **p<0.005

Caspase -8, the major initiator caspase, is activated when the death inducing signalling complex (DISC) is formed in response to external stimuli and is first activated through a death signal, suggesting a cellular response to an external signal for cell death. Thus, caspase -8 is used as a marker for the extrinsic mode of apoptosis. Caspase -3, the major executioner caspase, is in turn activated by initiator caspases (Thornberry and Lazebnik, 1998; Kantari and Walczak, 2011). Immunochemistry was used to determine caspase activation in this study. Figure 3 shows that both caspase -8 and -3 are activated upon treatment with isoalantolactone, thus it is deduced that both the intrinsic and extrinsic pathways of apoptosis is induced by this compound due to the decrease in MMP and the activation of caspase -8, respectively. The cleavage of caspase -8 in response to isoalantolactone exposure has as of yet not been reported.

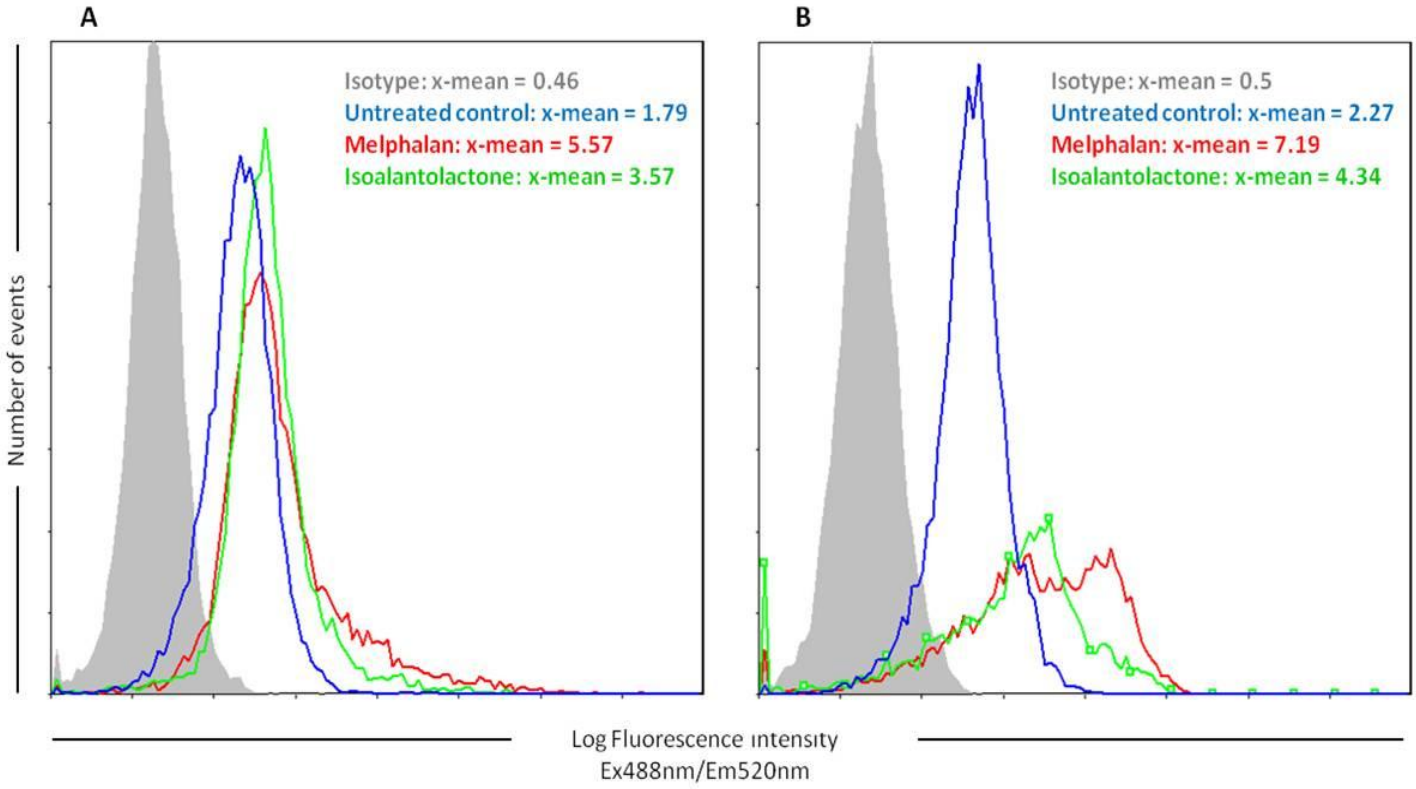

Figure 3: Histogram overlays representing activated caspase 8 (A) and activated caspase 3 (B) in HeLa cells after 24 hours of exposure to treatments. 10 000 events were recorded. X-mean values indicate the mean of fluorescence intensity of cells staining positive for active caspase 3 (One representation for two individual experiments, n=3).

DNA fragmentation results after caspase -3 activation: DNA fragmentation is one of the later steps in apoptosis. It is a process which results from the activation of endonucleases during the onset of apoptosis. These nucleases degrade the higher order of chromatin structure into small ~300 kb of DNA and then degrade these fragments further (Marini *et al.*, 1996; Nagata, 2000). The Apo-Direct assay labels these DNA fragments with FITC labeled dUTPs catalyzed by the TdT enzyme. This way, flow cytometric analysis will enable the observation of DNA fragmentation. The histogram overlay of Figure 4 indicates the increase in green fluorescence intensity (FL1) as a result of DNA fragmentation.

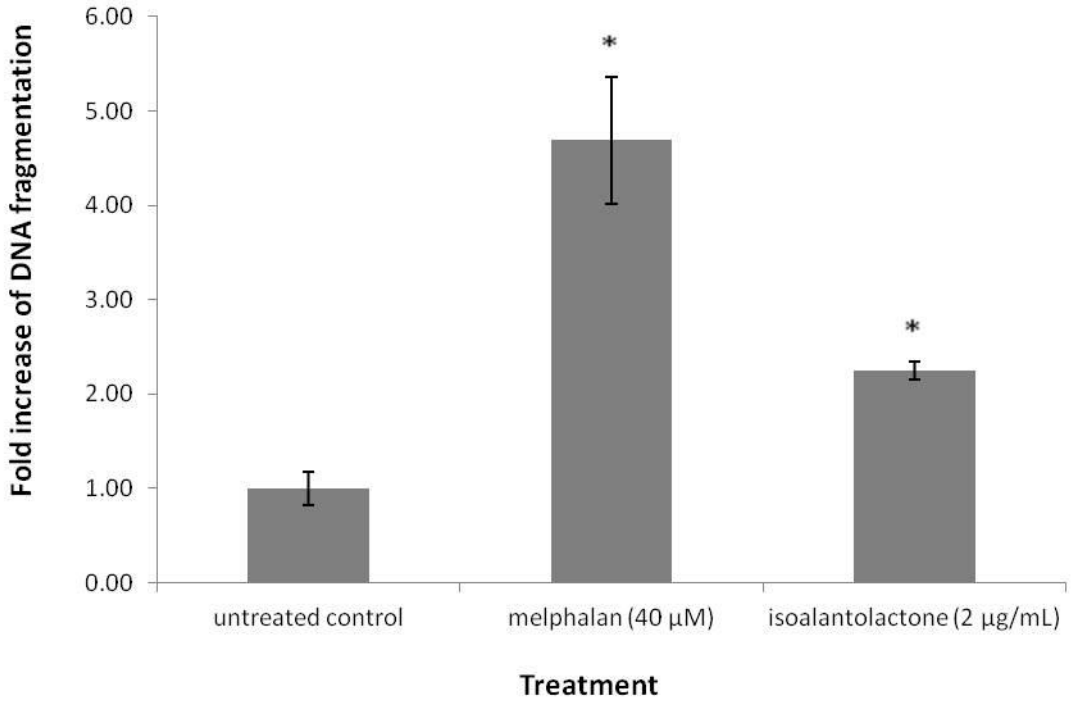

Figure 4: DNA fragmentation in HeLa cells after 24 hours of exposure to treatments. 10000 events were recorded. Significance was determined using the two-tailed Student's *t*-test: *p<0.05.

CONCLUSION:

This study has led to the isolation of isoalantolactone from *A. afra*. An ethanol extract of *A. afra* leaves has shown to induce apoptosis (Spies *et al.*, 2013). Previous studies have shown apoptosis induction and cell cycle arrest by commercial isoalantolactone, however, the present study revealed additional mechanistic information and a few interesting differences in cervical cancer cells as compared to the previous reports on pancreatic (Khan *et al.*, 2012) and prostate cancer cells (Rasul *et al.*, 2013). Here we report that isoalantolactone from *A. afra* induces apoptosis in HeLa cells by the indication of phosphatidylserine translocation, after G2/M arrest of the cell cycle. It was also evident that apoptosis was mediated by caspases, as both caspase -8 and caspase -3 were activated after 24 hours of exposure to the compound. The results also suggest the involvement of the mitochondria due to the depolarization of the mitochondrial membrane after exposure to isoalantolactone. Therefore, we can conclude that isoalantolactone present in *A. afra* contributes to the observed cytotoxicity induced by an ethanol extract of this plant as reported by Spies *et al.* (2013).

Results presented here and the studies conducted by Khan *at al.* (2012) and Rasul *et al.* (2013) provide clues as to how cell death is induced by isoalantolactone, however, more studies can be done to determine the exact mode of apoptosis induced by isoalantolactone. G2/M cell cycle arrest was evident in cervical cancer cells, as reported here, and in prostate cancer cells (Rasul *et al.*, 2013); however, S phase arrest in pancreatic cancer cells was reported by Khan *et al.* (2012). This suggests that cell cycle arrest is cell type specific and thus more studies of the mechanism of cell cycle arrest can be conducted. These studies can include the possible onset of mitotic catastrophe in cervical and prostate cancer cells.

ACKNOWLEDGEMENTS:

This work is based on the research supported in part by the National Research Foundation of South Africa (Grant number: 81780), Nelson Mandela Metropolitan University, Horace Alfred Taylor trust and the African Laser Center.

REFERENCES:

Bohlmann, F., Mahanta, P.K., Jakupovic, J., Rastogi, R.C., Natu, A.A. (1978). New sesquiterpene lactones from *Inula* species. Phytochemistry 17: 1165 – 1172.

Cantrell, C.L., Pridgeon, J.W., Fronczek, F. And Becnel, J.R. (2010). Structure-activity relationship studies on derivatives of eudesmanolides from *Inula helenium* as toxicants against *Aedes aegypti* larvae and adults. Chemistry and Biodiversity 7, 1681 – 1697.

Castedo, M., Perfettini, J-L., Roumier, T., Andreau, K., Medema, R., Kroemer, G. (2004). Cell death by mitotic catastrophe: a molecular definition. Oncogene 23: 2825 – 2837.

Chaturvedi, D. (2011). Sesquiterpene lactones: Structural diversity and their biological activities. Opportunity, Challenge and Scope of Natural Products in Medicinal Chemistry: 313 – 334.

Cragg, G.M., and Newman, D.J. (2005). Plants as a source of anti-cancer agents. J. Ethnopharmacol. 100: 72–79.

Ghantous, A., Gali-Muhtasib, H., Vuorela, H., Saliba, N.A., Darwiche, N. (2010): What made sesquiterpene lactones reach cancer clinical trials? Drug Discovery Today 15: 668 – 678.

Geissman, T. A. (1970): Sesquiterpene Lactones of *Artemisia – A. verlotorum and A. vulgaris.* Phytochem. 9: 2377 – 2381.

Huo, Y., Shi, H., Li, W., Wang, M., Li, X., (2010). HPLC determination and NMR structural elucidation of sesquiterpene lactones in *Inula helenium*. J. Pharmaceut. Biomed. 51: 942–946.

Iranshashi, M., Emami, S. A., Mahmoud-Soltani, M. (2007). Detection of sesquiterpene lactones in ten Artemisia species population of Khorasan provinces. IJBMS 10: 183 – 188.

Irwin, M. A., Geissman, T.A. (1973). Rupicolin – A and –B, Rupin – A and – B and Cumambrin – B oxide from Artemisia tripartite spp rupicola. Phytochem. 12: 863 – 869.

Jakupovic, J., Chau-Thi, T.V., Warning, U., Bohlmann, F., Greger, H. (1986). 11β,13-dihydrogauianoldes from *Artemisia douglasiana* and a thiophene acetylene from *A. schidtiana*. Phytochem. 25: 1663 – 1667.

Jakupovic, J., Klemeyer, H., Bohlmann, F., Graven, E. H. (1988). Glaucolides and guaianolides from *Artemisia afra*. Phytochem. 27: 1129 – 1133.

Jakupovic, J., Tan, R. X., Bohlmann, F., Jia, Z. J., Huneck, S. (1991). Sesquiterpene lactones from *Artemisia rutifolia*. Phytochem. 30: 1714 – 1716.

Kantari, C., Walczak, H. (2011). Caspase – 8 and Bid: Caught in the act between death receptors and mitochondria. Biochim. Biophys. Acta 1813: 558 – 563.

Khan, M., Ding, C., Rasul, A., Yi, F., Li, T., Gao, H., Gao, R., Zhong, L., Zhang, K., Fang, X., Ma, T. (2012). Isoalantolactone Induces Reactive Oxygen Species Mediated Apoptosis in Pancreatic Carcinoma PANC-1 Cells. Int. J. Biol. Sci. 8: 533 – 547.

Koopman, G., Reutelingsperger, C.P., Kuijten, G.A., Keehnen, R.M., Pals, S.T., van Oers, M.H. (1994). Annexin V for flow cytometric detection of phosphatidylserine expression on B cells undergoing apoptosis. Blood 84, 1415 – 1420.

Kristjánsdóttir, K., Rudolph, J. (2004). Cdc25 phosphatases and cancer. Chem. Biol. 11: 1043 – 1051.

Liu, N.Q., Van der Kooy, F., Verpoorte, R. (2009). *Artemisia afra*: A potential flagship for African medicinal plants? South African Journal of Botany 75: 185 – 195.

Ma, Y., Zhao, D-G., Gao, K. (2013). Structural Investigation and Biological Activity of Sesquiterpene Lactones from the Traditional Chinese Herb *Inula racemosa*. J. Nat. Prod. 76: 564 - 570.

Marco, J. A., Sanz, J. F., Sancenon, F., Rustaiyan, A., Saberi, M. (1993). Sesquiterpene lactones from Artemisia species. Phytocem. 32: 460 – 462.

Marini, M., Musiani, D., Sestili, P., Cantoni, O. (1996). Apoptosis of human lymphocytes in the absence or presence of internucleosomal DNA cleavage. Biochem. Biophys. Res. Commun. 229: 910 - 915.

Miller, R.B., Nash, R.D. (1974) A highly stereoselective total synthesis of (±)-isoalantolactone. Tetrahedron 30: 2961 – 2965.

Nagaki, M. (1984): Two sesquiterpene lactones from Artemisia species. Phytochem. 23: 462 – 464.

Nagata, S. (2000): Apoptotic DNA fragmentation. Exp. Cell Res. 256: 12-18.

Rasul, A., Di, J., Millimouna, F.M., Malhi, M., Tsuji, I., Ali, M., Li, J., Li, X. (2013). Reactive oxygen species mediate isoalantolactone-induced apoptosis in human prostate cancer cells. Molecules 18: 9382 – 9396.

Saelens, X., Festjens, N., Van de Walle. L., van Gurp, M., van Loo, G., Vandenabeele, P. (2004). Toxic proteins released from mitochondria in cell death. Oncogene 23: 2861–2874

Schmidt, T.J. and Heilmann, J. (2002). Quantitative Structure-Cytotoxicity Relationships of Sesquiterpene Lactones derived from partial charge (Q)-based fractional Accessible Surface Area Descriptors (QfrASAs). Quant. Struct.-Act. Relat. 21: 276 – 287.

Spies, L., Koekemoer, T.C., Sowemimo, A.A., Goosen, E.D., van de Venter, M. (2013). Caspase-dependent apoptosis is induced by *Artemisia afra* Jacq. ex Willd in a mitochondria-dependent manner after G2/M arrest. S. Afr. J. Bot 84: 104 – 109.

Sy, L-K., Brown, G.D. (2001): Deoxyarteannuin B, dihydro-deoxyarteannuin B and trans-5-hydroxy-2-isopropenyl-5-methylhex-3-en-1-ol from Artemisia anuua. Phytochem. 58: 1159 – 1166.

Thornberry, N.A., Lazebnik, Y. (1998). Caspases: enemies within. Science 281, 1312– 1316.

Vermeulen, K., Berneman, Z.N., Van Bockstaele, D.R. (2005). Apoptosis: Mechanisms and relevance in cancer. Ann. Haemotol. 84: 626 - 639.

Zhang, S., Won, Y-K., Ong, C-N., Shen, H-M. (2005). Anti-cancer potential of sesquiterpene lactones: bioactivity and molecular mechanisms. Curr. Med. Chem. – Anti-cancer Agents 5: 239-249.